

CERTIFICATE OF MAILING BY "FIRST CLASS MAIL"

I hereby certify that this correspondence is being deposited with the United States Postal Service as first class mail in an envelope addressed to:
Assistant Commissioner for Patents, Washington, D.C. 20231, on June 4, 2001.

Jami M Procopio



IN THE UNITED STATES PATENT AND TRADEMARK OFFICE

In the application of:

Terry P. Snutch, *et al.*

Serial No.: 09/030,482

Filing Date: 25 February 1998

For: NOVEL HUMAN CALCIUM
CHANNELS AND RELATED PROBES,
CELL LINES AND METHODS

Examiner: Nirmal S. Basi

Group Art Unit: 1646

EXPEDITED PROCEDURE --
EXAMINING GROUP 1646

#22
D. B. J.
6/13/01

DECLARATION OF DR. TERRANCE SNUTCH

Assistant Commissioner for Patents
Washington, D.C. 20231

Dear Sir:

I, Terrance Snutch, declare as follows:

1. I am a co-inventor of the subject matter claimed in the above-referenced application and have been practicing in the field of molecular biology, and specifically in the field of ion channels, for over 15 years. A copy of my *curriculum vitae* is attached hereto as Exhibit A. I have published many papers on the structure and function of calcium channels and am considered one of the leading researchers in this field.

2. The nucleotide sequence set forth as SEQ. ID. NO: 18 encodes about 85% of the total amino acid sequence, starting at the exact N-terminus, of a member of a family of voltage-gated ion channels that contain four homologous structural domains (domains I, II, III and IV). All of the identified members of this four-domain class of ions channels are either voltage-gated

calcium or sodium ion channels. In each case, each of the four homologous domains contains structural elements necessary for channel function. Each contains six transmembrane segments including a transmembrane segment called the S4 region that acts as the voltage sensor of the channel. Also contained in each homologous domain is a region called the P-loop or Pore region that contains specific amino acid residues responsible for ion selectivity. Voltage-gated sodium and calcium channels can easily be distinguished from each other based upon their overall degree of sequence conservation and by the specific amino acid residues that constitute the Pore region responsible for ion flux (see below).

3. I have concluded that SEQ. ID. NO: 18 encodes virtually the entire amino acid sequence of a major branch of the calcium channel family that represents a T-type channel. The calcium channel family and the evolutionary relationships between its members are shown in Figure 1. The construction of the family is based on sequence homology in the genes encoding the various members. As seen in Figure 1, a closely related branch of the family is represented by several types designated P/Q, N and R; this major branch is more distantly related to another branch which is represented by various L-type channels. The nucleotide sequence set forth in the present invention as SEQ. ID. NO: 18 has characteristics which place it in this general family, but it is relatively distantly related to the two branches represented by the α_1 subunits A, B, E and α_1 subunits S, C and D. My conclusion that Figure 1 represents an accurate characterization of SEQ. ID. NO: 18 is based on the reasoning set forth in paragraphs 4-6 below.

4. Over the past 30 years native calcium channels have been classified into high-threshold (L-type, N-type, P/Q-type and R-type) or low threshold subtypes (T-type), as illustrated in Figure 1. The placement of the high-voltage types is based on evolutionary analysis of already cloned calcium channels. This shows that the P/Q-type, N-type and R-type calcium channel α_1 subunits constitute one branch of calcium channels while the L-type subunits α_1C , α_1D and α_1S constitute a second evolutionary branch. The only class of calcium channel not accounted for is the third branch which would thus include the T-type. Comparison of SEQ. ID. NO: 18 deduced amino acid with that of the other α_1 subunits clearly indicates that it forms a third evolutionary class of calcium channel, which based upon physiological and pharmacological criteria must represent the T-type channel.

5. Examination of the Pore region of SEQ. ID. NO: 18 compared to the high threshold calcium channels and also sodium channels indicates that SEQ. ID. NO: 18 encodes a novel type

of calcium channel. In all high threshold calcium channels, the pore region of each domain (I, II, III, and IV) contains a glutamate residue (E) that is responsible for the selective flux of calcium through the channel (Yang, *et al.*, 1993, "Molecular Determinants of Ca Selectivity and Ion Permeation in L-type Ca Channels," *Nature* 366:158-161). In contrast, sodium channels possess other amino acids in the analogous positions (domain I = aspartate (D), domain II = glutamate (E), domain III = lysine (K). Mutation of the domain III lysine (K) of sodium channels to the corresponding glutamate (E) found in the high threshold calcium channels results in the flux of calcium and indicates that the domain III pore region is critical to defining ion flux (Heinemann, *et al.*, 1992, "Calcium Channel Characteristics Conferred on the Sodium Channel by Single Mutations," *Nature* 356:441-443). It is known from the behavior of the calcium channels whose genes had not yet been cloned that these "T-type" calcium channels possess distinct permeation properties compared to high-threshold calcium channels. In general, while high-threshold calcium channels flux barium at a higher rate than calcium, T-type channels flux calcium at a similar or higher rate than that for barium (for review, see Huguenard, 1996, "Low-Threshold Calcium Currents in the Central Nervous System Neurons" *Annu. Rev. Physiol.* 58:329-348). Examination of the Pore region of SEQ. ID. NO: 18 shows that in domain III it contains the substitution of an aspartate residue (D) for the glutamate residue (E) that is absolutely conserved in all of the high threshold calcium channels. A comparison of the relevant positions in the Pore regions of domains I, II and III of the known calcium channels, the sodium channel, and SEQ. ID. NO: 18 is shown in Figure 2. Since the domain III glutamate (E) residue of the high threshold calcium channels is critical for ion flux (Yang, *et al.*, 1993, *supra*), one can conclude that the substitution of D for E in SEQ. ID. NO: 18 contributes to the unique permeation properties of the T-type channel.

6. The intracellular linker region separating domains I and II of all high threshold calcium channels contains a high-affinity binding site for the calcium channel β subunit. The consensus β subunit binding site found in the N-type, P/Q-type, L-type and R-type channels is: QQ-E—L-GY—WI---E and is a defining characteristic of high threshold calcium channels (Pragnell, *et al.*, 1994 "Calcium Channel β -Subunit Binds to a Conserved Motif in the I-II Cytoplasmic Linker of the α_1 Subunit," *Nature* 368:67-70). It is known that T-type calcium channels do not contain or bind to the β subunit of high threshold calcium channels. The amino

acid sequence encoded by SEQ. ID. NO: 18 does not possess the consensus β subunit binding sequence. This is consistent with SEQ. ID. NO: 18 encoding a T-type calcium channel.

7. For the reasons set forth in paragraphs 4-6, I am certain that SEQ. ID. NO: 18 encodes a T-type calcium ion channel α_1 subunit. To summarize, as set forth in paragraph 4, a comparison of the deduced amino acid sequence in SEQ. ID. NO: 18 with that of other known four-domain voltage gated channels shows that it is relatively distantly related from the calcium channels whose genes have already been cloned and amino acid sequences deduced and thus belongs to the low-threshold subtype (T-type) which had not heretofore been cloned; paragraph 5 demonstrates that the critical amino acids in the Pore region verify that it is a calcium ion channel rather than a sodium ion channel and that it is distinct from the already cloned high-threshold channels, and paragraph 6 demonstrates that as expected, the deduced amino acid sequence lacks a β subunit binding sequence. The coding sequence is not entirely complete (approximately 85%), but it is sufficient both to (1) verify its nature as encoding a T-type calcium ion channel subunit and (2) to provide sufficient information to permit supplementation with additional nucleotide sequence to encode a functional T-type channel without retrieving a full length clone.

8. SEQ. ID. NO: 18 contains an ATG start codon that precedes three complete homologous structural domains I, II and III, and up to the S1 transmembrane segment of domain IV. Each of the domains I through III possesses an intact voltage sensor segment (S4) as well as a complete Pore region. Since structural domains II, III and IV result from the evolutionary duplication of domain I, SEQ. ID. NO: 18 contains sufficient information to construct a complete domain IV and thus a functional T-type calcium channel α_1 subunit. The nature of the amino acid sequence in domain IV can be surmised from the amino acid sequence of domain III. Of course, means to construct a nucleotide sequence extending the nucleotide sequence of SEQ. ID. NO: 18 to include a nucleotide sequence encoding this deduced amino acid sequence are routine.

9. In summary, one of ordinary skill in the art given the information set forth in SEQ. ID. NO: 18

(a) would understand that it encodes about 85% of a functional T-type calcium channel α_1 subunit starting at the N-terminus,

(b) would be able to design an amino acid sequence representing the missing C-terminal portion based on homology to the three domains encoded by SEQ. ID. NO: 18, and

(c) would be able to construct an expression system containing a nucleotide sequence encoding a functional T-type calcium ion channel α_1 subunit without obtaining a full length clone.


10. In addition to the foregoing demonstration that the application discloses the essential features of a T-type calcium channel, I further provide information regarding the nexus between all T-type calcium channels and identified conditions which can be treated with compounds that interact with T-type calcium channels. There are several T-type calcium channels found in a single individual which vary slightly in structure and demonstrably in terms of their distribution among various tissues. The particular T-type calcium channel involved in a particular condition may depend on its tissue distribution; for instance, T-type channels found in the neuronal system are associated with epilepsy and neurological diseases in general where spastic convulsions are involved. However, it is not necessary to understand which particular T-type calcium channel is being used in a screen for compounds that would be useful in treating, for example, these convulsive conditions because of the similarity in the binding specificity of all T-type channels. In very simple terms, compounds which are found to inhibit the activity of neuronal T-type channels will also inhibit the activity of T-type channels found in other tissues. Thus, any arbitrarily chosen T-type channel could be expressed in a cell line for use in screening assays to identify antagonists and the antagonists would be useful in treating the conditions associated with any T-type channel. As noted in the accompanying response, abnormal T-type activity is associated with a number of cardiac conditions, with hypertension, with neurological diseases involving spastic convulsions, and with impaired fertility. An antagonist identified with regard to any T-type channel would be useful in all of these conditions.

11. The pattern of similar binding activity among all T-type channels can be analogized to such a pattern among L-type channels. All of the T-type channels have similar behaviors in that they activate at low membrane potential, have small single channel conductance, have negative steady state inactivation properties, and contribute to spike firing patterns and rhythmic bursting processes. Analogous to the T-type channel another type of channel linked by similar behaviors is the L-type. There are several α_1 subunits associated with various L-type channels - *i.e.*, α_{1S} , α_{1C} , and α_{1D} and each is encoded by a distinct gene and exhibits a distinct distribution

pattern. For example, α_{1S} is in skeletal muscle; α_{1C} is in neurons and cardiac and smooth muscle; and α_{1D} is found in neurons and endocrine cells. They can be discriminated from all other types of calcium channels by their common sensitivity to 1,4-dihydropyridines. Thus, any one of these genes could be used to generate an L-type calcium channel for use in a cell-based assay to identify antagonists. These identified antagonists would bind to all of these L-type channels and thus would be useful in treating conditions related to any one of them.

I declare that all statements made herein of my own knowledge are true and that all statements made on information and belief are believed to be true; and further, that these statements are made with the knowledge that willful, false statements and the like so made are punishable by fine or imprisonment or both, under Section 1001 of Title 18 of the United States Code and that such willful false statements may jeopardize the validity of the application or any patent issued thereon.

Executed at VANCOUVER, BC on 29 May 2001.



Terrance Snutch



CURRICULUM VITAE

Terrance Preston SNUTCH

Date of Birth: November 21, 1957

Place of Birth: Preston, Ontario, Canada

Citizenship: Canadian

EDUCATION

<u>Dates</u>	<u>Degree</u>	<u>Institution</u>	<u>Major</u>
1975 - 1979	B.Sc.	Simon Fraser University	Biochemistry
1980 - 1984	Ph.D.	Simon Fraser University	Molecular Genetics

Ph.D. : A Molecular and Genetic Analysis of the Heat Shock Response of
Caenorhabditis Elegans

Supervisor: Professor David L. Baillie

AWARDS and FELLOWSHIPS

High School

1975 Chilliwack Medical Society University Entrance Scholarship

1975 Government of B.C. University Entrance Scholarship

University

1982 - 1983 Simon Fraser University Open Graduate Scholarship

1983 - 1984 Natural Sciences & Engineering Research Council of
Canada Postgraduate Scholarship

Postdoctoral

- 1985 - 1987 American Heart Association Postdoctoral Fellowship
- 1985 - 1986 Natural Sciences and Engineering Research Council of Canada Postdoctoral Fellowship
- 1987 - 1988 American Heart Association Advanced Postdoctoral Fellowship
- 1986 - 1987 American Heart Association GLAA, Lievre Family Award (Top Application)
- 1987 - 1988 American Heart Association GLAA, Lievre Family Award (Top Application)

Faculty

- 1991 *Killam Research Prize* (personal award: CDN\$ 10,000)
- 1991 - 1993 *Alfred P. Sloan Research Foundation Fellowship in Neuroscience* (research support US\$ 30,000)
- 1991 - 1996 *Howard Hughes Medical Institute International Research Scholar* (research support: US\$ 500,000)
- 1992 *PMAC Keynote Address*, Canadian Federation of Biological Societies
- 1994 *Outstanding Academic Alumni Award*, Simon Fraser University
- 1995 - 2000 *MRC Scientist*, Medical Research Council of Canada (salary support: CDN\$ 300,000)
- 1996 *International Albrecht Fleckenstein Award*
- presented by Bayer AG, Germany, for novel and significant research in the field of calcium channel pharmacology and modulation (personal award: CDN\$ 45,000)
- 1997 *Steacie Prize*, Steacie Memorial Fund
Canada's most prestigious award for young scientists and engineers (personal award: CDN\$ 10,000)
- 1999 *Keynote Address*, UCSF Annual Neuroscience Retreat, Asilomar, CA
- 2000 – 2005 *CIHR Senior Scientist Award*, Canadian Institutes of Health Research

SOCIETIES

American Association for the Advancement of Science
Society for Neuroscience

EXPERIENCE

Teaching

Jan 1990 - present **Instructor**, Univ. British Columbia, Biol 437, Biol 455, NeuroSci 500

June 7 - 27, 1991 **Instructor and Course Organizer**: Cold Spring Harbor Laboratory Course
Molecular Approaches to Ion Channel Function and Expression

June 8 - 28, 1990 **Instructor and Course Organizer**: Cold Spring Harbor Laboratory Course
Molecular Approaches to Ion Channel Function and Expression

June 9 - 29, 1989 **Instructor and Course Organizer**: Cold Spring Harbor Laboratory Course
Molecular Approaches to Ion Channel Function and Expression

June 3 - 23, 1988 **Instructor and Course Organizer**: Cold Spring Harbor Laboratory Course
Molecular Approaches to Ion Channel Function and Expression

Aug. 10 - 14, 1987 **Instructor**: Hopkins Marine Station, Stanford University:
Ion Channels in Natural and Model Membranes

June 5 - 25, 1987 **Instructor and Course Organizer**: Cold Spring Harbor Laboratory Course
Molecular Approaches to Ion Channel Function and Expression

June 4 - 24, 1986 **Instructor and Course Organizer**: Cold Spring Harbor Laboratory Course
Single Channel Methods: Expression and Recording

1980 - 1982 Teaching Assistant, Simon Fraser University

Research

July 2000 – present **CIHR Senior Scientist**, Univ. British Columbia

July 1996 – present **Professor**, Biotechnology Laboratory and Departments
Psychiatry and Zoology, University of British Columbia

July 1995 – present **MRC Scientist**, Univ. British Columbia

July 1994 – June 1996 **Associate Professor** (with tenure), Biotechnology
Laboratory and Departments of Psychiatry and Zoology,
University of British Columbia

Feb. 1989 - June 1994

Assistant Professor
and Departments of
University of British Columbia

Sept. 1987 - Jan. 1989

Senior Research Fellow, Divis
California Institute of Technology
Supervisors: Professors Norman Davidson, Lester

Aug. 1984 - Aug. 1987

Research Fellow, Division of Chemistry
California Institute of Technology
Supervisor: Professor Norman Davidson

EXTERNAL SCHOLARLY ACTIVITIES

Scientific Review Panel: Genome B.C. (2000 - present)
Board of Directors, BIRC Corporation (2000 - present)
Editorial Board, Journal of Biological Chemistry (2000 - present)
Grant Review Panel (Neurosciences B): Medical Research Council of Canada (2000 - ad hoc)
Advisory Board, Steacie Institute for Molecular Sciences, Ottawa (1998 - present)
Reviewing Panel, Peter Wall Institute for Advanced Studies (1997 - 2000)
Green College, Academic Board Member (1996 - 1999)
Evaluation Panel, Current Drugs (1996 - 2000)
Advisory Panel, Journal Molecular Membrane Biology (1995 - present)
Scientific Advisory Committee, Amyotrophic Lateral Sclerosis Society of Canada (1995 - 1997)
Simon Fraser University Alumni Association Awards Committee (1995 - 1997)
Chair, Calcium Channel Session, Society for Neuroscience, San Diego (1995)
Grant Review Panel (Neurosciences B): Medical Research Council of Canada (1994 - 1997)
Chair, Calcium Channel Session, Society for Neuroscience, Miami (1994)
Grant Review Panel (Established Investigator): B.C. Health Care Research Foundation (1994)
National Institutes of Health, Physiology Study Section (1993)
University of B.C. High School Connect Program (1993, 1994, 1995, 1997)
Grant Review Panel (Basic Sciences): B.C. Health Care Research Foundation (1991-1993)
Editorial Board: GENETICA: International Journal of Genetics (1990-1992)
American Heart Association GLAA Fellowship Committee (1988)

Grant Peer Reviews (1990 - present)

Alberta Heritage Foundation for Medical Research
Amyotrophic Lateral Sclerosis Society

B.C. Health Research Foundation
 Canadian Institutes for Health Research
 Cystic Fibrosis Foundation of Canada
 Heart and Stroke Foundation of Canada
 Hong Kong Research Grants Council
 Medical Research Council of Canada
 Natural Sciences and Engineering Research Council of Canada
 National Institutes of Health, USA
 National Science Foundation, USA

Scientific Journal Peer Reviews (1990 - present)

European Journal of Pharmacology
 FEBS Letters
 Journal of Biological Chemistry
 Journal of Membrane Biology
 Journal of Neuroscience
 Molecular Pharmacology
 Nature Neuroscience
 Neuron
 Neuroscience
 Proceedings of the National Academy of Science (USA)
 Receptors and Channels
 Science
 Trends in Neuroscience
 Trends in Pharmacological Sciences

GRANT SUPPORT

	Total Funding	Term
Canadian Institutes for Health Research (operating grant)	\$1,225,000	2000 - 2005
Medical Research Council of Canada (operating grant)	\$944,929	1989 - 2000
B.C. Health Care Research Foundation (operating grant)	\$79,300	1990 - 1992
Parkinson Foundation of Canada (with S.R. Vincent, Dept. of Psychiatry)	\$117,000	1990 - 1993
Howard Hughes Medical Institute International Research Scholar Award	US\$ 500,000	1991 - 1996

Alfred P. Sloan Research Foundation Research Fellowship in Neuroscience	US\$ 30,000	1991 - 1993
National Centres of Excellence on Neuronal Regeneration and Functional Recovery	\$100,000	1991 - 1993
Neurex Corp.	US\$ 30,000	1992 - 1993
Pfizer Inc.	US\$ 30,000	1992 - 1993
SmithKline Beecham Pharma	\$940,000	1993 - 1996

INVITED LECTURES (accepted 1989 - present)

Department of Pharmacology and Biophysics, University of Cincinnati, Cincinnati
 Cystic Fibrosis: Beyond The Gene- Special Conference, Toronto, Ontario (symposia)
 Department of Medical Genetics, University of British Columbia
 Department of Physiology, Colorado State University, Fort Collins, Colorado
 Department of Physiology, University of Colorado, Denver, Colorado
 Department of Medicine, University of British Columbia
 Department of Ophthalmology, Vancouver General Hospital
 Department of Pharmacology, University of California, San Diego, California
 Salk Institute of Biotechnology, La Jolla, California
 March of Dimes Clinical Conference, Vancouver (symposia)
 Department of Pharmacology, University of California, Los Angeles, California
 Neurex Corporation, Menlo Park, California
 Society for Neuroscience Satellite Symposium on Calcium Channels, New Orleans (symposia)
 Division of Molecular Immunology and Neuroscience, Mount Sinai Hospital, Toronto
 Playfair Neurosciences Unit, University of Toronto, Toronto, Ontario
 Canadian Federation of Biological Sciences PMAC Keynote Address, Victoria (symposia)
 '92 FASEB Conference on Calcium and Cell Function, Saxton River, Vermont (symposia)
 Department of Zoology, University of Alberta, Edmonton, Alberta
 Department of Microbiology, University of British Columbia
 Department of Pharmacology, University of Washington, Seattle, Washington
 Division of Neuroscience, Neuroscience Discussion Group, University of British Columbia
 Department of Physiology, University of North Carolina, Chapel Hill, North Carolina
 Department of Medical Physiology, University of Calgary, Calgary, Alberta
 National Centres of Excellence Network for Protein Engineering, Edmonton, Alberta (symposia)

International Union of Physiological Sciences, XXXII Congress, Glasgow Scotland (symposia)
 Calcium Channels and Cell Signalling, Neuropharmacology Satellite Symposium, Wash. DC
 (symposia)

Mexican Physiological Society, Cancun, Mexico (symposia)

'94 FASEB Conference on Calcium and Cell Function, Saxton River, Vermont (symposia)

'94 Howard Hughes Medical Institute, Bethesda, Maryland (symposia)

Vollum Institute for Advanced Biomedical Research, Oregon Health Sciences University,
 Portland, Oregon

Fifth Colloque Sur Les Canaux Ioniques, Marseille, France (symposia)

'95 Howard Hughes Medical Institute, Bethesda, Maryland (symposia)

Department of Biophysics, University of Iowa, Iowa City

'95 International Brain Research Organization, Kyoto, Japan (symposia)

Canadian Congress of Neurological Sciences, Victoria (symposia)

'95 Cold Spring Harbor Laboratory, Ion Channel Course, Cold Spring Harbor, NY

Voltage-Gated Ion Channels, IBC Conference, Philadelphia PA (symposia)

'96 Winter Conference on Brain Research, Snowmass Colorado (symposia)

SmithKline Beecham, Division of Biophysical Sciences, Harlow, United Kingdom

'96 Howard Hughes Medical Institute, Bethesda, Maryland (symposia)

'96 Cold Spring Harbor Laboratory, Ion Channel Biology Course, Cold Spring Harbor, NY

Bayer AG, Leverkusen, Germany (symposia)

'96 Gordon Conference on Ion Channels, Tilton, New Hampshire (symposia)

Department of Physiology & Biophysics, Case Western Reserve University, Cleveland

Special Meeting on T-type Calcium Channels, sponsored by F. Hoffman-La Roche AG,
 Montpellier, France (symposia)

'97 Biophysical Society Meeting, New Orleans (symposia)

'97 Gordon Conference: Second Messengers and Protein Phosphorylation, Meriden, NH
 (symposia)

'97 Cold Spring Harbor Laboratory, Ion Channel Biology Course, Cold Spring Harbor, NY

Department of Biochemistry, University of Manitoba, Winnipeg

Keynote Speaker, '97 Neuroscience Day, University of Calgary

'98 European Winter Brain Conference, ARC 2000, France (symposia)

'98 New York Academy of Sciences Conference: Ion Channels & Receptors (symposia)

'98 Cold Spring Harbor Laboratory, Ion Channel Biology Course, Cold Spring Harbor, NY

Advances in Ion Channel Research, San Francisco, Mar. 14-17, 1999 (symposia)

Department of Pharmacology, Yale University, May 6, 1999

Neurobiology Seminar Series, University of Illinois at Chicago, May 14, 1999

UCSF Graduate Program in Neuroscience, Alisomar, Sep. 27, 1999 (symposia)
 Montreal Neurological Institute, Montreal, Nov. 16, 1999
 Ion Channels: From structure to physiopathology, Universidad de Colima, Mexico, Nov. 26-29/2000 (symposia)
 Department of Physiology, University of Colorado, Feb. 8, 2001
 Pharmacology Vancouver 2001, Mar. 28, 2001 (symposia)
 Canadian Pain Society Annual Conference, Montreal, May 12, 2001 (symposia)

GRADUATE STUDENTS SUPERVISED

Heather Guthrie, M. Sc. (in progress)
 Kevin Hamming, Ph. D. (in progress)
 Eleanor Mathews, Ph. D. (2000)
 Carola Ibe, M. Sc. (1991)

POSTDOCTORAL FELLOWS SUPERVISED

Emmanuel Bourinet, Ph.D. (CNRS, Montpellier, France)
 Deidre Brink, Ph.D. (University of Oregon)
 Arik Hasson, Ph.D. (Hebrew University, Jerusalem)
 *John McRory, Ph.D. (University of Victoria)
 Donald Nelson, Ph.D. (Simon Fraser University)
 *Celia Santi, M.D./PhD. (UNAM, Mexico)
 Anthony Stea, Ph.D. (McMaster University)
 Terence Starr, Ph.D. (Simon Fraser University)
 Tuck Wah Soong, Ph.D. (University of Singapore)
 Kathy Sutton, Ph.D. (University of London, UK)
 *Colin Thacker, Ph.D. (University of Utah)
 John Willoughby, Ph.D. (University of London, UK)
 Gerald Zamponi, Ph.D. (University of Calgary)

* currently at UBC in Snutch lab

PDF Fellowships Awarded

EMBO, INSERM
 Epilepsy Canada
 Human Frontiers
 MRC
 NSERC
 Human Frontiers
 NSERC, MRC
 NSERC, MRC
 Univ. Singapore PDF
 Killam Foundation

Wellcome Trust Foundation
 NSERC, MRC, Alberta Heritage

MAJOR RESEARCH INTEREST

The study of the molecular mechanisms of signal transduction in the mammalian central nervous system and the relationship to neurological disorders. The research concentrates on using a multidisciplinary approach to characterize various aspects of the molecular, electrophysiological, genetic, pharmacological and biochemical properties of ion channels and neurotransmitter receptors.

PUBLICATIONS - Refereed, Full-length (Total = 72)

72. Feng Z-P, J Hamid, C. Doering, SE Jarvis, GM Bosey, E Bourinet, TP SNUTCH and GW Zamponi (2000) **Amino acid residues outside of the pore region contribute to N-type calcium channel permeation.** Journal of Biological Chemistry, in press.
71. SNUTCH, TP, KG Sutton and GW Zamponi (2000) **Voltage-dependent calcium channels — Beyond dihydropyridine antagonists.** Current Opinion in Pharmacology, in press.
70. McRory, JE, CM Santi, KSC Hamming, J Mezeyova, KG Sutton, DL Baillie, A Stea and TP SNUTCH (2000) **Molecular and functional characterization of a family of rat brain T-type calcium channels.** Journal of Biological Chemistry, in press.
69. Tam, T, E Mathews, TP SNUTCH and WR Schafer (2000) **Voltage-gated calcium channels direct neuronal migration in *Caenorhabditis elegans*.** Developmental Biology 226: 104-117.
68. Ertel, E, KP Campbell, MM Harpold, F Hofmann, Y Mori, E Perez-Reyes, A Schwartz, TP SNUTCH, T Tanabe, L Birnbaumer, RW Tsien and WA Catterall (2000) **Nomenclature of voltage-gated calcium channels.** Neuron 25: 533-5.
67. Walker, D, D Bichet, S Geib, E Mori, V Cornet, TP SNUTCH, Y Mori and M De Waard (1999) **A new β subtype-specific interaction in α_{1A} subunit controls P/Q-type Ca^{2+} channel activation.** Journal of Biological Chemistry 274: 12383-12390.
66. Jimenez, C, Bourinet, V Leuranguer, S Richard, TP SNUTCH and J Nargeot (1999) **Determinants of voltage-dependent inactivation affect mibefradil block of calcium channels.** Neuropharmacology 39: 1-10.
65. Sutton, KG, JE McRory, H Guthrie, TH Murphy and TP SNUTCH (1999) **P/Q-type Ca^{2+} channels mediate the activity dependent feedback of syntaxin-1A.** Nature 401: 800-804.
64. Kamatchi, GL, CK Chan, TP SNUTCH, ME Durieux and C Lynch III (1999) **Volatile anesthetic inhibition of neuronal Ca channel currents expressed in *Xenopus* oocytes.** Brain Research 831: 85-96.
63. Lewis, Jr., BA, LP Jones, S Dubel, TW Soong, TP SNUTCH and DT Yue (1999) **Identification and characterization of two dihydropyridine-insensitive calcium channels in frog sympathetic neurons.** Submitted.
62. Bourinet, E, TW Soong, K Sutton, S Slaymaker, E Mathews, A Monteil, GW Zamponi, J Nargeot and TP SNUTCH (1999) **Phenotypic variants of P- and**

Q-type calcium channels are generated by alternative splicing of the $\alpha 1A$ subunit gene. Nature Neuroscience 2: 407-415.

61. Hamid, J, D Nelson, R Spaetgens, SJ Dubel, TP SNUTCH and GW Zamponi (1999) **Identification of an integration centre for PKC and G protein modulation of N-type calcium channels.** Journal of Biological Chemistry 274: 6195-6202.
60. Stea, A, SJ Dubel and TP SNUTCH (1999) **α_{1B} N-type calcium channel isoforms with distinct biophysical properties.** Annals of the New York Academy of Sciences 868: 118-130.
59. Zamponi, GW and TP SNUTCH (1998) **Decay of prepulse facilitation during G-protein inhibition of N-type calcium channels involves binding of a single $G_{\beta\gamma}$ subunit.** Proc. Natl. Acad. Sci. USA 95: 4035-4039.
60. Zamponi, GW and TP SNUTCH (1998) **Modulation of voltage-dependent calcium channels by G proteins.** Current Opinion in Neurobiology 8: 351-356.
58. Bourinet, E, GW Zamponi, J Nargeot and TP SNUTCH (1998) **The permeation properties of α_{1E} Ca channels are similar to a subset of low threshold calcium channels.** In Low-Voltage-Activated T-type Calcium Channels. Edited by Tsien, Clozel and Nargeot. p. 92-98.
57. Zamponi, GZ, E Bourinet and TP SNUTCH (1998) **Limitations of nickel ions as a tool for discrimination between high and low threshold calcium channels.** In Low-Voltage-Activated T-type Calcium Channels. Edited by Tsien, Clozel and Nargeot. p. 251-257.
56. Sutton, K, C Siok, A Stea, G Zamponi, S Heck, RA, Volkmann, M Ahljianian and TP SNUTCH (1998) **Differential inhibition of neuronal calcium channels by a novel peptide spider toxin, DW 13.3.** Molecular Pharmacology 54: 407-418.
55. Zamponi, GW, E Bourinet, D Nelson, J Nargeot and TP SNUTCH (1997) **Crosstalk between G-proteins and protein kinase C mediated by the calcium channel $\alpha 1$ subunit.** Nature 385: 442-446.
54. Ray, JM, PE Squires, RM Meloche, DW Nelson, TP SNUTCH and AMJ Buchan (1997) **L-type calcium channels regulate gastrin release from human antral G cells.** American Journal of Physiology 273: 281-288.
53. El-Husseini, AED, H Guthrie, TP SNUTCH and SR Vincent (1997) **Molecular cloning of a mammalian homologue of the yeast vesicular transport protein vps45.** Biochimica et Biophysica Acta 1325: 8-12.
52. TP SNUTCH and MM Gilbert (1997) **Structure and Function of Ca^{2+} Channels.** Trends in Pharmacological Sciences, Receptor and Ion Channel Supplement.
51. Brody, DL, PG Patil, JG Mulle, TP SNUTCH and DT Yue (1997) **Bursts of action potential waveforms relieve G-protein inhibition of recombinant**

- P/Q-type Ca^{2+} channels in HEK 293 cells.** Journal of Physiology 499: 637-644.
50. Jones, LP, PG Patil, **TP SNUTCH** and DT Yue (1997) **G-protein modulation of N-type calcium channel gating current in human embryonic kidney cells.** Journal of Physiology 498: 601-610.
49. Patil, PG, M de Leon, RR Reed, SJ Dubel, **TP SNUTCH** and DT Yue (1996) **Elementary events underlying voltage-dependent G-protein inhibition of N-type calcium channels.** Biophysical Journal 71: 2509-2521.
48. Bourinet, E, GW Zamponi, A Stea, TW Soong, BA Lewis, LP Jones, DT Yue and **TP SNUTCH** (1996) **The α_{1E} calcium channel exhibits permeation properties similar to low-voltage-activated calcium channels.** Journal of Neuroscience 16: 4983-4993.
47. Rettig, J, ZH Sheng, DK Kim, CD Hodson, **TP SNUTCH** and WA Catterall (1996) **Isoform-specific interaction of the α_{1A} subunits of brain Ca^{2+} channels with the presynaptic proteins syntaxin and SNAP-25.** Proc. Natl. Acad. Sci. USA 93: 7363-7368.
46. Zamponi, GW, E Bourinet and **TP SNUTCH** (1996) **Nickel block of a family of neuronal calcium channels: subtype and subunit-dependent action at multiple sites.** Journal of Membrane Biology 151: 77-90.
45. Zamponi, GW and **TP SNUTCH** (1996) **Evidence for a specific site for modulation of calcium channel activation by external calcium.** Pflugers Archiv - European Journal of Physiology 431: 470-472.
44. Zamponi, GW, TW Soong, E Bourinet and **TP SNUTCH** (1996) **β subunit coexpression and the α_1 subunit domain I-II linker affect piperidine block of neuronal calcium channels.** Journal of Neuroscience 16: 2430-2443.
43. Bourinet, E, A Stea, TW Soong and **TP SNUTCH** (1996) **Determinants of the G-protein-dependent opioid modulation of neuronal calcium channels.** Proc. Natl. Acad. Sci. USA 93: 1486-1491.
42. de Leon, M, L Jones, E Perez-Reyes, X Wei, TW Soong, **TP SNUTCH** and DT Yue (1995) **An essential Ca^{2+} -binding motif for Ca^{2+} -sensitive inactivation of L-type Ca^{2+} channels.** Science 270: 1502-1506.
41. Stea, A, TW Soong and **TP SNUTCH** (1995) **Determinants of PKC-dependent modulation of a family of neuronal calcium channels.** Neuron 15: 929-940.
40. Yokoyama, CT, RE Westenbroek, JW Hell, TW Soong, **TP SNUTCH** and WA Catterall (1995) **Biochemical properties and subcellular distribution of the neuronal class E calcium channel α_1 subunit.** Journal of Neuroscience 15: 6419-6432.
39. Westenbroek, RE, T Sakurai, EM Elliott, JW Hell, TVB Starr, **TP SNUTCH** and WA Catterall (1995) **Immunochemical identification and subcellular**

- distribution of the $\alpha 1$ subunit of neuronal class A calcium channels.** Journal of Neuroscience 15: 6403-6418.
38. Bourinet, E, P Charnet, WJ Tomlinson, A Stea, TP SNUTCH and J Nargeot (1994) **Voltage-dependent facilitation of a neuronal α_{1C} L-type calcium channel.** EMBO Journal 21: 5032-5039.
37. Charnet, P, E Bourinet, SJ Dubel, TP SNUTCH and J Nargeot (1994) **Calcium currents recorded from a neuronal α_{1C} L-Type calcium channel.** FEBS Lett. 344: 87-90.
36. Stea, A, WJ Tomlinson, TW Soong, E Bourinet, SJ Dubel, SR Vincent and TP SNUTCH (1994) **The localization and functional properties of a rat brain α_{1A} calcium channel reflect similarities to neuronal Q- and P-type channels.** Proc. Natl. Acad. Sci. USA 91: 10576-10580.
35. Stea, A, TW Soong and TP SNUTCH (1994) **Voltage-gated calcium channels.** In: Handbook on Ion Channels. RA North (ed), CRC Press, p.113-151.
34. Birnbaumer, L, KP Campbell, WA Catterall, MM Harpold, F Hofmann, WA Horne, Y Mori, A Schwartz, TP SNUTCH, T Tanabe and RW Tsien (1994) **The naming of voltage-gated calcium channels.** Neuron 13: 505-506.
33. Pragnell, M, M De Waard, Y Mori, T Tanabe, TP SNUTCH and KP Campbell (1994) **Calcium channel β subunit binds to a conserved motif in the I-II cytoplasmic linker of the $\alpha 1$ subunit.** Nature 368: 67-70.
32. Hell, JW, RE Westenbroek, C Warner, MK Ahljianian, W Prystay, MM Gilbert, TP SNUTCH and WA Catterall (1993) **Identification and differential subcellular localization of the neuronal class C and class D L-type calcium channel $\alpha 1$ subunits.** Journal of Cell Biology 123: 949-962.
31. Tomlinson, WJ, A Stea, E Bourinet, P Charnet, J Nargeot and TP SNUTCH (1993) **Functional properties of a neuronal class C L-type calcium channel.** Neuropharmacology 32: 1117-1126.
30. Stea, A, SJ Dubel, M Pragnell, JP Leonard, KP Campbell and TP SNUTCH (1993) **A β subunit normalizes the electrophysiological properties of a cloned N-type Ca^{2+} channel $\alpha 1$ subunit.** Neuropharmacology 32: 1103-1116.
29. Soong, TW, A Stea, CD Hodson, SJ Dubel, SR Vincent and TP SNUTCH (1993) **Structure and functional expression of a member of the low voltage-activated calcium channel family.** Science 260: 1133-1136.
28. Catterall, WA, K De Jongh, E Rotman, J Hell, R Westenbroek, S Dubel and TP SNUTCH (1993) **Molecular properties of calcium channels in skeletal muscle and neurons.** Annals N.Y. Acad. Sci. 681: 342-355.
27. Hell, JW, CT Yokoyama, ST Wong, C Warner, TP SNUTCH and WA Catterall (1993) **Differential phosphorylation of two size forms of the neuronal class C calcium channel $\alpha 1$ subunit.** Journal Biol. Chem. 68: 19451-19457.

26. SNUTCH, TP and PB Reiner (1992) **Calcium channels: diversity of form and function.** Current Opinion in Neurobiology 2: 247-253.
25. Dubel, SJ, TVB Starr, J Hell, MK Ahljianian, JJ Enyeart, WA Catterall and TP SNUTCH (1992) **Molecular cloning of the alpha-1 subunit of an omega-conotoxin-sensitive calcium channel.** Proc. Natl. Acad. Sci. (USA) 89: 5058-5062.
24. Oguro-Okano, M, GE Griesmann, ED Wieben, SJ Slaymaker, TP SNUTCH and VA Lennon (1992) **Molecular diversity of neuronal-type calcium channels identified in small cell lung carcinoma.** Mayo Clinic Proceedings 67: 1150-1159.
23. Westenbroek, RE, JW Hell, C Warner, SJ Dubel, TP SNUTCH and WA Catterall (1992) **Biochemical properties and subcellular distribution of an N-type calcium channel $\alpha 1$ subunit.** Neuron 9: 1099-1115.
22. SNUTCH, TP and G Mandel (1992). **Tissue RNA as a source of exogenous ion channels and receptors.** Methods in Enzymology 207: 297-309.
21. Starr TVB, W Prystay and TP SNUTCH (1991) **Primary structure of a calcium channel that is highly expressed in the rat cerebellum.** Proc. Natl. Acad. Sci., (USA) 88: 5621-5625.
20. SNUTCH, TP, WJ Tomlinson, JP Leonard and MM Gilbert (1991) **Distinct calcium channels are generated by alternative splicing and are differentially expressed in the mammalian CNS.** Neuron 7: 45-57.
19. Yu, L, H Nguyen, H Lee, LJ Bloem, CA Kozak, BJ Hoffman, TP SNUTCH, HA Lester, N Davidson and H Lubbert (1991) **The mouse 5-HT_{1C} receptor contains eight hydrophobic domains and is X-linked.** Molecular Brain Research 11: 143-149.
18. Drinnan, SL, BT Hope, TP SNUTCH and SR Vincent (1991). **Golf in the basal ganglia.** Molecular and Cellular Neurosciences 2: 66-70.
17. Leonard, JP and TP SNUTCH. (1991) **Expression of neurotransmitter receptors and ion channels in *Xenopus* oocytes.** In: Molecular Neurobiology: A Practical Approach. IRL Press, pp. 161-182.
16. SNUTCH TP, JP Leonard, MM Gilbert, HA Lester and N Davidson (1990) **Rat brain expresses a heterogeneous family of calcium channels.** Proc. Natl. Acad. Sci. (USA) 87: 3391-3395.
15. Lester HA, TP SNUTCH, JP Leonard, J Nargeot, N Dascal, BM Curtis and N Davidson (1989) **Expression of mRNA encoding voltage-dependent Ca channels in *Xenopus* oocytes.** Annals N.Y. Acad. Sci. 560: 174-182.

14. Lester HA, TP SNUTCH, JP Leonard, J Nargeot and N Davidson (1988)
Expression of mRNA encoding rat brain Ca channels in *Xenopus* oocytes.
In: The Calcium Channel: Structure, Function and Implications. Edited by
M Morad, WG Nayler, S Kazda and M Schramm, Springer, p. 272-280.
13. SNUTCH TP, MFP Heschl and DL Baillie (1988) **The *Caenorhabditis elegans*
hsp70 gene family: a molecular genetic characterization.** Gene 64: 241-255.
12. SNUTCH TP, JP Leonard, J Nargeot, H Lubbert, N Davidson and HA Lester
(1987) **Characterization of voltage-gated calcium channels in *Xenopus*
oocytes after injection of RNA isolated from electrically excitable tissues.**
In: Cell Calcium and Membrane Transport. Edited by L Mandel and D
Eaton, Society of General Physiologists Series, Vol. 42, Rockefeller
University Press, p. 153-166.
11. Krafte DS, TP SNUTCH, JP Leonard, N Davidson and HA Lester (1988)
**Evidence for the involvement of more than one mRNA species in
controlling the inactivation process of rat and rabbit brain Na channels
expressed in *Xenopus* oocytes.** Journal of Neurosci. 8: 2859-2868.
10. SNUTCH TP (1988) **The use of *Xenopus* oocytes to probe synaptic
communication.** Trends in Neurosci. 11: 250-256.
9. Lubbert H, BJ Hoffman, TP SNUTCH, T van Dyke, AJ Levine, PR Hartig, HA
Lester and N. Davidson (1987) **cDNA cloning of a serotonin 5HT-1C
receptor using electrophysiological assay of mRNA injected *Xenopus*
oocytes.** Proc. Natl. Acad. Sci. (USA) 84: 4332-4336.
8. Lubbert H, TP SNUTCH, N Dascal, HA Lester and N Davidson (1987) **Rat
brain 5HT-1C receptors are encoded by a 5-6 kb mRNA size class and
functionally expressed in *Xenopus* oocytes.** Journal of Neurosci. 7: 1159-
1165.
7. Leonard JP, J Nargeot, TP SNUTCH, N Davidson and HA Lester (1987)
**Calcium channels induced in *Xenopus* oocytes by injection of rat brain
mRNA.** Journal of Neurosci. 7: 875-881.
6. Goldin AL, TP SNUTCH, H Lubbert, A Dowsett, J Marshall, V Auld, W
Downey, RC Fritz, HA Lester, R Dunn, WA Catterall and N Davidson
(1986) **mRNA coding for only the alpha subunit of the rat brain Na
channel is sufficient for expression of functional channels in *Xenopus*
oocytes.** Proc. Natl. Acad. Sci. (USA) 83: 7503-7507.
5. Dascal N, TP SNUTCH, H Lubbert, N Davidson and HA Lester (1986)
**Expression and modulation of voltage-gated calcium channels after RNA
injection in *Xenopus* oocytes.** Science 231: 1147-1150.
4. Dascal N, C Ifune, R Hopkins, TP SNUTCH, H Lubbert, N Davidson, MI Simon
and HA Lester (1986) **Involvement of a GTP-binding in mediation of the**

serotonin and acetylcholine responses in *Xenopus* oocytes injected with rat brain mRNA. Molecular Brain Research 1: 201-209.

3. Rose AM and TP SNUTCH (1984) **Isolation of the closed circular form of the transposable element, Tc1, in *Caenorhabditis elegans*. Nature 311: 485-486.**
2. SNUTCH TP and DL Baillie (1984) **A high degree of DNA strain polymorphism associated with the major heat shock gene of *Caenorhabditis elegans*. Molecular and General Genetics 195: 329-335.**
1. SNUTCH TP and DL Baillie (1983) **Alterations in the pattern of gene expression following heat shock in *Caenorhabditis elegans*. Can. J. Biochem. Cell Biol. 61: 480-487.**

Published Abstracts and Notes - Since 1989 (Total = 72)

1. SNUTCH T.P., M.M. Gilbert, J.P. Leonard, H.A. Lester and N. Davidson (1989) **Cloning of a family of putative calcium channels from rat brain.** Society for Neuroscience Abstracts 15: 652.
2. Tomlinson W.J., M.M. Gilbert and T.P. SNUTCH (1990) **Distinct rat brain class-C calcium channels are generated by alternative splicing.** Society for Neuroscience Abstracts 16: 1957.
3. Dubel S.J. and T.P. SNUTCH (1990) **Primary structure and expression of the rat brain class-B calcium channel.** Society for Neuroscience Abstracts 16: 1173.
4. Starr T.V.B., W.A. Prystay and T.P. SNUTCH (1990) **Primary structure and expression of the rat brain class-A calcium channel.** Society for Neuroscience Abstracts 16: 1174.
5. Tomlinson, W.J. , S.R. Vincent and T.P. Snutch (1991) **In situ localization of calcium channel mRNA.** Society for Neuroscience Abstracts 17: 773.
6. Leonard, J.P., T.V.B.Starr, B.P. Schmidt, M. Pragnell, S.B. Ellis, M. Williams, M.M. Harpold, K.P. Campbell and T.P. SNUTCH (1991) **Functional expression of a rat brain calcium channel in *Xenopus* oocytes.** Society for Neuroscience Abstracts 17: 773.
7. Dubel, S.J., W.J. Tomlinson, T.V.B. Starr, S.R. Vincent, and T.P. SNUTCH (1992) **Cloning and regional distribution of a brain calcium channel alpha2-subunit.** Society for Neuroscience Abstracts 18: 1139.
8. Soong, T.W. and T.P. SNUTCH (1992) **Molecular cloning and characterization of a calcium channel highly expressed in the hippocampus.** Society for Neuroscience Abstracts 18: 1139.
9. Westenbroek, R.E., J.W. Hell, S.J. Dubel, T.P. SNUTCH and W.A. Catterall (1992) **Distribution of omega conotoxin-sensitive calcium channels in the adult rat brain.** Society for Neuroscience Abstracts 18: 971.
10. Williams, L.A., C.D. Hodson, T.P. SNUTCH and S.R. Vincent (1992) **Golf expression in the brain: Molecular cloning, *in situ* hybridization and immunohistochemistry.** Society for Neuroscience Abstracts 18: 1004.
11. SNUTCH, T. P. (1992) **Molecular Properties of Neuronal Voltage-gated Calcium Channels.** Howard Hughes Medical Institute Annual Scientific Report 1991-1992 p. 533-534.

12. Westenbroek, R.E., Hell, J.W. Sakurai, T., T.P. SNUTCH and W.A. Catterall (1993) **Immunocytochemical localization of class A calcium channels in adult rat brain.** Society for Neuroscience Abstracts 19: 1334.
13. Stea, A., T.W. Soong, C.D. Hodson, S.J. Dubel, W.J. Tomlinson and T.P. SNUTCH (1993) **Electrophysiological and pharmacological comparison of a family of neuronal calcium channels.** Society for Neuroscience Abstracts 19: 1330.
14. Soong, T.W., A. Stea, C.D. Hodson, S.R. Vincent and T.P. SNUTCH (1993) **Expression and localization of a calcium channel which is a member of the low voltage-activated family.** Society for Neuroscience Abstracts 19: 1331.
15. Charnet, P., E. Bourinet, W.J. Tomlinson, T.P. SNUTCH and J. Nargeot (1993) **Pharmacological characterisation of class C L-type calcium channel.** International Union of Physiological Sciences XXXII Congress 205.5.
16. SNUTCH T.P., S.J. Dubel, C.D. Hodson, T.W. Soong, W.J. Tomlinson and A. Stea (1993) **Molecular properties of neuronal calcium channels, structure, function and cellular distribution.** International Union of Physiological Sciences XXXII Congress 147.1.
17. Stea, A., W.J. Tomlinson, S.J. Dubel and T.P. SNUTCH (1993) **Electrophysiological and pharmacological characterization of cloned neuronal N-type and L-type calcium channels.** Biophysical Society Abstracts 64: A6.
18. SNUTCH, T. P. (1993) **Molecular Properties of Neuronal Calcium Channels.** Howard Hughes Medical Institute Annual Scientific Report 1992-1993 p. 524-526.
19. SNUTCH, T.P. (1993) **Molecular Studies on Neuronal Calcium Channels** Howard Hughes Medical Institute Research in Progress 1992-1993 p. 529-530.
20. Brody, D.L., S.J. Dubel, T.P. SNUTCH and D.T. Yue (1994) **No current-dependent inactivation of cloned N-type Ca channels transiently expressed in mammalian cells.** Biophysical Society Abstract 66: A16.
21. Charnet, P., E. Bourinet, W.J. Tomlinson, T.P. SNUTCH and J. Nargeot (1994) **Voltage-dependent regulation of class C L-type Ca Channels.** Biophysical Society Abstracts 66: A321.
22. Kondo, A., T.W. Soong, D.N. Mbungu, Olivera, B.M., T.P. SNUTCH and M.E. Adams (1994) **Pharmacological profile of the rat α_{1E} calcium channel**

- subunit expressed in *Xenopus* oocytes.** Society for Neuroscience Abstracts 20: 72.
23. Dubel, S.J., A. Stea and T.P. SNUTCH (1994) **Two cloned rat brain N-type calcium channels have distinct kinetics.** Society for Neuroscience Abstracts 20: 631.
24. Bourinet, E., A. Stea, T.W. Soong and T.P. SNUTCH (1994) **Neuronal α_{1E} calcium channels display permeation characteristics similar to low voltage activated channels.** Society for Neuroscience Abstracts 20: 70.
25. Stea, A., T.W. Soong, S.J. Dubel, W.J. Tomlinson and T.P. SNUTCH (1994) **Activation of PKC selectively up-regulates both α_{1E} and α_{1B} calcium channels.** Society for Neuroscience Abstracts 20: 1468.
26. Soong, T.W., E. Bourinet, S. Slaymaker, E. Mathews, S.J. Dubel, S.R. Vincent and T.P. SNUTCH (1994) **Alternative splicing generates rat brain α_{1A} calcium channel isoforms with distinct electrophysiological properties.** Society for Neuroscience Abstracts 20: 70.
27. Mathews, E., P.B. Reiner and T.P. SNUTCH (1994) **Molecular cloning and genomic organization of a calcium channel α_1 subunit from *Caenorhabditis elegans*.** Society for Neuroscience Abstracts 20: 69.
28. Yokoyama, C.T., R.E. Westenbroek, J.W. Hell, T.P. SNUTCH and W.A. Catterall (1994) **Biochemical characterization and immunohistochemical localization of the class E calcium channel from rat brain.** Society for Neuroscience Abstracts 20: 72.
29. SNUTCH, T. P. (1994) **Molecular Properties of Neuronal Calcium Channels.** Howard Hughes Medical Institute Annual Scientific Report 1993-1994 p. 546-548.
30. SNUTCH, T.P. (1994) **Molecular Studies on Neuronal Calcium Channels** Howard Hughes Medical Institute Research in Progress 1994, p. 597-599.
31. SNUTCH, T.P., E. Bourinet, T.W. Soong and A. Stea (1995) **Molecular Mechanisms of calcium Channel Modulation.** IBRO, in press.
32. De Leon, M., L. Jones, E. Perez-Reyes, X. Wei, T.W. Soong, T.P. SNUTCH and D.T. Yue (1995) **An essential structural domain for Ca-sensitive inactivation of L-type Ca channels.** Biophysical J. 68: A13.

33. Patil, P., M. de Leon, R. Reed, S. Dubel, T.P. SNUTCH and D.T. Yue (1995) **Regulation of recombinant N-type Ca channels by G-proteins and voltage.** Biophysical J. 68: A348.
34. Zamponi, G.W., E. Bourinet and T.P. SNUTCH (1995) **High and low affinity local anesthetic binding sites on neuronal calcium channels.** Biophysical J. 68: A349.
35. Lewis, B.A., S. Dubel, T.W. Soong, T.P. SNUTCH and D.T. Yue (1995) **Elementary properties of two non-L-type Ca^{2+} channels in frog sympathetic neurons.** Biophysical J. 68: A361.
36. Bourinet, E., T.W. Soong, A. Stea, S.J. Dubel, L. Yu and T.P. SNUTCH (1995) **The β subunit contributes to the direct G-protein-dependent inhibition of neuronal calcium channels.** Society for Neuroscience Abstracts 21: 515.
37. Stea, A., E. Bourinet, T.W. Soong and T.P. SNUTCH (1995) **Differential coupling of neuronal $\alpha 1B$ and $\alpha 1E$ calcium channels to a metabotropic glutamate receptor.** Society for Neuroscience Abstracts 21: 340.
38. Mathews, E. and T.P. SNUTCH (1995) **Molecular cloning of a class D L-type calcium channel with an elongated carboxyl terminus.** Society for Neuroscience Abstracts 21: 1574.
39. Zamponi, G.W., E. Bourinet, S.J. Dubel and T.P. SNUTCH (1995) **Nickel modulates two distinct effects on neuronal calcium channels: block and inhibition of activation-gating.** Society for Neuroscience Abstracts 21: 1753.
40. Ahljianian, M.K., L.D. Artman, A. Stea, R.D. Williams, L.F. Lanyon, M.J. Welch, S. Heck, R. Ronau, T.P. SNUTCH and R.A. Volkman (1995) **DW 13.3, a peptide toxin from the spider *Filistata*, is a novel calcium channel blocker.** Society for Neuroscience Abstracts 21: 338.
41. SNUTCH, T. P. (1995) **Molecular Properties of Neuronal Calcium Channels.** Howard Hughes Medical Institute Annual Scientific Report 1994-1995 p. 638-640.
42. SNUTCH, T.P. (1995) **Molecular Studies on Neuronal Calcium Channels** Howard Hughes Medical Institute Research in Progress 1995, p. 617-618.

43. Patil, P., M. de Leon, R. Reed, S. Dubel, T.P. SNUTCH and D.T. Yue (1996) **Elementary events underlying voltage-dependent G-protein inhibition of N-type Ca channels.** Biophysical J. 70: A28.
44. Bourinet, E., T.W. Soong, G.W. Zamponi, A. Stea and T.P. SNUTCH (1996) **Alternative splicing in the domain I-II linker alters α_{1A} Ca channel gating and modulation by G-proteins.** Society for Neuroscience Abstracts 22: 343.
45. Sutton, K.G., A. Stea, L.D. Artman, S. Heck, R.A. Volkman, M.K. Ahljianian and T.P. SNUTCH (1996) **DW13.3, a peptide toxin from the spider *Filistata*, differentially blocks transiently expressed neuronal calcium channels.** Society for Neuroscience Abstracts 22: 343.
46. Brody, D.L., T.P. SNUTCH and D.T. Yue (1996) **Gating of recombinant A-class calcium channels during action potential-shaped voltage waveforms.** Society for Neuroscience Abstracts 22: 1242.
47. Patil, P.G., T.P. SNUTCH and D.T. Yue (1996) **Reconstituted muscarinic inhibition and prepulse facilitation of recombinant A-class calcium channels in HEK 293 cells.** Society for Neuroscience Abstracts 22: 1745.
48. SNUTCH, T. P. (1996) **Molecular Properties of Neuronal Calcium Channels.** Howard Hughes Medical Institute Annual Scientific Report 1995-1996 p. 623-625.
49. SNUTCH, T.P. (1996) **Molecular Studies on Neuronal Calcium Channels** Howard Hughes Medical Institute Research in Progress 1996, p. 739-740.
50. Patil, P.G., D.L. Brody, T.P. SNUTCH and D.T. Yue (1997) **β -subunit modulation of G-protein inhibition and voltage-dependent inactivation of P/Q-type (A-Class) calcium channels.** Biophysical J. 72: A22.
51. Zamponi, G.W., E. Bourinet, D. Nelson, J. Nargeot and T.P. SNUTCH (1997) **Crosstalk between PKC-dependent upregulation and direct G-protein inhibition of N-type Ca channels is mediated by the Ca channel domain I-II linker.** Biophysical J. 72: A22.
52. Kamatchi, G., M.E. Durieux, C. Chan, T.P. SNUTCH and C. Lynch III (1997) **Volatile anesthetic depression of Ca channels expressed in oocytes.** Biophysical J. 72: A256.

53. Brody, D.L., P.G. Patil, J.G. Mulle, T.P. SNUTCH and D.T. Yue (1997) **Bursts of action potential-shaped voltage waveforms can relieve G-protein inhibition of recombinant A-class Ca^{2+} channels.** Biophysical J. 72: A22.
54. Jones, L.P., Patil, P., T.P. SNUTCH and D.T. Yue (1997) **G-protein modulation of N-type Ca^{2+} channel gating currents.** Biophysical J. 72: A22.
55. Mathews, E., G. Mullen, D. Brink, D.G. Moerman and T.P. SNUTCH (1997) **Structural and functional analysis of the calcium channel $\alpha 1$ subunit encoded by the *C. elegans unc-2* gene.** Society for Neuroscience Abstracts 23: 2015
56. Brink, D., H. Guthrie, D. Nelson, I. Kovesdi and T.P. SNUTCH (1997) **Analysis of T-type Ca currents in CNS neurons using an adenovirus based antisense strategy.** Society for Neuroscience Abstracts 23: 2015.
57. Mathews, E., G. Mullen, D. Moerman and T.P. SNUTCH (1997) **Structural and functional analysis of the calcium channel $\alpha 1$ subunit encoded by the *C. elegans unc-2* gene.** International meeting on *C. elegans*. in press
58. Pietrobon, D., Tottene, A., Hivert, B., Rizzuto, R. and T.P. SNUTCH (1997) **Correlation between native neuronal calcium channels and cloned calcium channel subunits.** Society for Neuroscience Abstracts 23: 2012.
59. Bourinet, E., Leuranguer, V., Richard, S., Snutch, T.P. and Nargeot, J. (1997) **Mibefradil block of recombinant calcium channels: modulation by the nature of their β subunit.** Society for Neuroscience Abstracts 23: 1193.
60. Chan, C.K., J.J. Pancrazio, T.P. SNUTCH, M.E. Durieux, C. Lynch and Y.I. Kim (1998) **Lambert-Eaton syndrome antibodies inhibit recombinantly expressed P/Q-type calcium channels.** Society for Neuroscience Abstracts 24: 187.5
61. Sutton, K.G., G.W. Zamponi, E. Bourinet, T.W. Soong and T.P. SNUTCH (1998) **Alternative splicing of the α_{1A} gene generates distinct P-type or Q-type sensitivity to ω -agatoxin IVA.** Society for Neuroscience Abstracts 24: 16.1
62. Guthrie, H., K. Hamming and T.P. SNUTCH (1998) **Identification of a novel protein that interacts with the N-type calcium channel.** Society for Neuroscience Abstracts 24: 407.2
63. Hasson, A. and T.P. SNUTCH (1998) **Bi-phasic modulation of N-type calcium channels by phorbol esters.** Society for Neuroscience Abstracts 24: 621.14

64. Hamid, J., D. Nelson, R. Spaetgens, T.P. SNUTCH and G.W. Zamponi (1998) **Mechanism of PKC modulation of N-type Ca^{++} channels.** Society for Neuroscience Abstracts 24: 694.6
65. McRory, J.E., J. Mezeyova, C.M. Santi, K. Hamming, K.G. Sutton and T.P. SNUTCH (1999) **Isolation and characterization of a family of T-type calcium channels.** Society for Neuroscience Abstracts 25: 79.2
66. Sutton, K.G., J.E. McRory, H. Guthrie, T.H. Murphy and T.P. SNUTCH (1999) **Calcium influx through P-type calcium channels mediates syntaxin-1A expression.** Society for Neuroscience Abstracts 25: 431.6
67. Feng, J.-P., G.R. Bosey, T.P. Snutch and G.W. Zamponi (1999) **A single amino acid substitution in the α_{1B} calcium channel domain III- S5-S6 linker increases affinity and reversibility for ω -conotoxin GVIA.** Society for Neuroscience Abstracts 25: 78.1
68. Santi, C.M., J.E. McRory, K.G. Sutton, J. Mezeyova, A. Hasson and T.P. Snutch (1999) **α_{11} : AT-type calcium channel with novel gating properties.** Society for Neuroscience Abstracts 25: 79.5
69. Sutton, K.G., J.E. McRory, H. Guthrie and T.P. Snutch (1999) **Ca influx through P/Q-type Ca channels mediates syntaxin-1A gene transcription.** British Neuroscience Association Mtg, Harrogate, UK.
70. Mathews, E.A., E. Garcia, C.M. Santi and T.P. Snutch (2000) **A point mutation in the carboxyl tail modifies P/Q-type channel biophysical properties.** Biophysical J., B308 .
71. McRory, J.E., K.G. Sutton, E. Garcia, D. Parker and T.P. Snutch (2000) **Alternatively spliced variants of the α_{1A} P/Q-type calcium channel differentially mediate the activity-dependent feedback of syntaxin-1A.** Biophysical J. 1566-Plat.
72. Feng, Z.P., J. Hamid, G.R. Bosey, T.P. Snutch and G.W. Zamponi (2000) **A single amino acid substitution in an external EF hand motif of the α_{1B} Ca channel domain III S5-S6 linker reduces Ba conductance and increases the sensitivity to ω -conotoxin GVIA.** Canadian Physiological Society, in press.

EVOLUTIONARY ANALYSIS INDICATES THAT SEQ ID NO:18 IS A T-TYPE CALCIUM CHANNEL

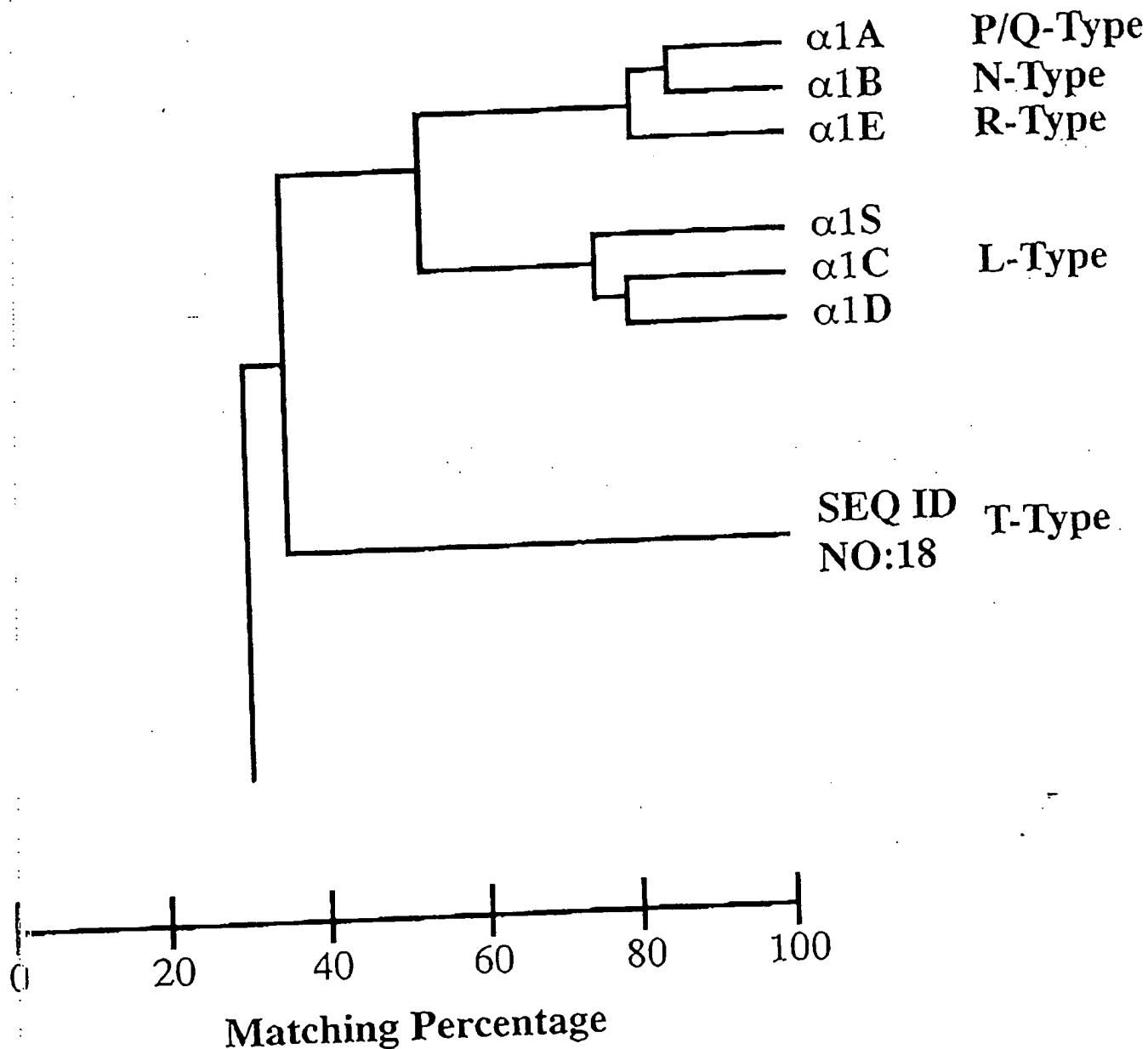


Figure 1

Comparison of the Pore Region

Domain I	Domain II	Domain III	
*	*	*	SEQ ID NO:18
QVITL E GWVEI	QILTO E DWNVV	VLASK D GWVNI	L-type Ca channel
QCITM E GWTDV	QLITG E DWNSV	TVSTF E GWPEL	P/Q-type Ca channel
QCITM E GWTDL	QILTG E DWNEV	TVSTG E GWPQV	sodium channel
RLMTQ D FWENL	RVLCG E WIETM	QVATF K GWMDI	

Figure 2

CONTRIBUTION OF TWO TYPES OF CALCIUM CURRENTS TO THE PACEMAKER POTENTIALS OF RABBIT SINO-ATRIAL NODE CELLS

By NOBUHISA HAGIWARA, HIROSHI IRISAWA
AND MASAKI KAMEYAMA

*From the National Institute for Physiological Sciences,
Myodaiji, Okazaki 444, Japan*

(Received 8 April 1987)

SUMMARY

1. Two types of calcium currents, the transient type and long-lasting type, were examined by both whole-cell and cell-attached patch-clamp modes in single isolated sino-atrial node cells of the rabbit.
2. In the whole-cell clamp mode, in response to a depolarizing pulse to -40 mV from a holding potential of -80 mV, a transient type calcium current with an amplitude of 2.1 ± 0.7 pA/pF (mean \pm s.d.; $n = 15$) was recorded. The threshold potential was approximately -50 mV.
3. Nickel ($40 \mu\text{M}$) and tetramethrin ($0.1 \mu\text{M}$) blocked the transient type calcium current without appreciable effects on the long-lasting type. Nifedipine and D600 blocked the long-lasting type, but did not affect the transient type. Cadmium ($20 \mu\text{M}$) and cobalt (2 mM) inhibited both types of calcium currents equally.
4. Both types of calcium currents showed an increased amplitude with increasing extracellular calcium concentration. The values of the Michaelis constant, K_m , were 0.95 mM for the transient type and 3.92 mM for the long-lasting type, indicating that these types represent two different classes of channels.
5. In the cell-attached patch-clamp mode, the single-channel conductance of the transient type calcium current was 8.5 pS, by using 100 mM -BaCl₂ in the pipette, whereas that of the long-lasting type was 16.0 pS, under the same conditions. Each of these values was similar to those found in other cells, respectively.
6. In the whole-cell clamp mode, the transient type current began to inactivate at -70 mV and was fully inactivated at -40 mV. The steady-state inactivation curve of the transient type current was approximately 50 mV negative to that of the long-lasting type. The overlap of the membrane potential between the activation and inactivation curves was small. The time constant of the inactivation shortened from 20 to 5 ms as the potential became progressively positive over the range from -80 to $+30$ mV.
7. Isoprenaline ($1 \mu\text{M}$) increased the amplitude of the long-lasting type Ca²⁺ current, but was not effective on the transient type, suggesting that the long-lasting type calcium current may be responsible for the positive chronotropic effect of isoprenaline.
8. While recording spontaneous electrical activity of the cell, application of $40 \mu\text{M}$ -nickel induced bradycardia and this effect was enhanced when the membrane was

constantly hyperpolarized. The bradycardia was caused mainly by a reduction in the rate of depolarization in the later phase of the pacemaker depolarization. The bradycardia elicited by nickel was due neither to blockade of the hyperpolarization-activated inward current nor to inhibition of the delayed rectifier potassium current.

9. It was concluded that the transient type calcium channel exists in the cardiac nodal cell and that the current participates in the later half of the slow diastolic depolarization.

INTRODUCTION

The slow diastolic depolarization of cardiac pacemaker cells is of vital importance in the generation of the rhythmic action potential of these cells. On the one hand it has been proposed that the decaying conductance of the K^+ outward current, which is activated by the preceding action potential, initiates the pacemaker depolarization and is the major component during further depolarization (Trautwein & Kassebaum, 1961; for review see Brown, 1982). On the other hand, however, it has been suggested that a calcium current, which is activated during the pacemaker depolarization, promotes depolarization further and finally leads to the upstroke of the following action potential (Yanagihara & Irisawa, 1980*b*; Noma, Kotake & Irisawa, 1980; Kokubun, Nishimura, Noma & Irisawa, 1982; Noma, Morad & Irisawa, 1983). The latter idea, however, has been challenged because the threshold for activation of the calcium current so far studied is around -40 mV, whereas the pacemaker depolarization occurs between -65 and -40 mV (Brown, 1982; Noble, 1984). It remains to be clarified, therefore, how extensively the calcium current contributes to the pacemaker depolarization. More recently, the presence of low-threshold type calcium channels has been detected in various excitable cells (Hagiwara, Ozawa & Sand, 1975; Llinás & Yarom, 1981*a, b*; Carbone & Lux, 1984; Fedulova, Kostyuk & Veselovsky, 1985), including cardiac atrial (Bean, 1985), ventricular (Nilius, Hess, Lansman & Tsien, 1985) and embryonic cells (Reuter, Kokubun & Prod'homme, 1986). Since the activation range of this current overlaps with the pacemaker potential (Bean, 1985; Armstrong & Matteson, 1985), the low-threshold, transient type calcium current ($I_{Ca,T}$) might contribute to the generation of the pacemaker current, if it exists in the nodal cell.

In the present study, we investigated the possible existence of $I_{Ca,T}$ in single pacemaker cells isolated from the sino-atrial node (SAN) of the rabbit by the whole-cell patch clamp as well as cell-attached patch-clamp method (Hamill, Marty, Neher, Sakmann & Sigworth, 1981). As a result, we found in the SAN cell a low-threshold Ca^{2+} current which closely resembled the $I_{Ca,T}$ of other cardiac cells in its electrophysiological and pharmacological properties. It will be shown that $I_{Ca,T}$ in the SAN cell plays a significant physiological role in the generation of the later half of the pacemaker potential. A preliminary report of this work has appeared previously (Hagiwara, Irisawa & Kameyama, 1987).

METHODS

Cell isolation procedure. Isolation of single cells from the SAN region was carried out according to the chopping method of DiFrancesco, Ferroni, Mazzanti & Tromba (1986), with some

modifications. In brief, albino rabbits weighing 1–1.5 kg were killed by intravenous injection of nembutal (40 mg/kg) under heparinization (300 units/kg). After exsanguination, the heart was isolated and immersed in normal Tyrode solution. The SAN region was excised under the dissection microscope and cut into small strips of about 0.5–1 mm in width. The SAN strips were further cut into pieces within the nominally Ca²⁺-free Tyrode solution (Table 1) and were incubated in 5 ml of the Ca²⁺-free Tyrode solution containing 0.1% collagenase (Sigma type 1) for 30–35 min at 37 °C. The specimens were then transferred to KB solution (Isenberg & Klöckner, 1982a) and stored at 4 °C for approximately 1 h before use. We employed single cells which, under a phase-contrast microscope, revealed a relatively smooth and shiny surface and a regular spontaneous contraction which could be arrested by adding 0.2 μ M-acetylcholine (ACh) to the bath. These criteria for viable cells were identical to those used by previous workers in our laboratory (Nakayama, Kurachi, Noma & Irisawa, 1984). The cell size was in the range of 10–25 μ m in length and 10–15 μ m in width.

TABLE 1. External solutions

	Tyrode	20 mM-Na ⁺	Na ⁺ -free	115 mM-Ba ²⁺
NaCl	136.9	20.0	—	—
KCl	5.4	5.4	5.4	—
CaCl ₂	1.8	0.5–10.0	2.5	—
MgCl ₂	0.5	0.5	0.5	—
NaH ₂ PO ₄	0.33	—	—	—
Glucose	5.0	5.0	5.0	5.0
HEPES	5.0	5.0	5.0	10.0
Tris-Cl	—	120.0	140.0	—
BaCl ₂	—	—	—	115.0
TTX	—	0.02	0.01	0.01

Concentrations are expressed in mM. The pH was adjusted to 7.4 in all solutions. Ca²⁺-free Tyrode solution was made simply by removing CaCl₂ from the Tyrode solution.

Whole-cell current and voltage clamp. The whole-cell patch-clamp mode (Hamill *et al.* 1981) was applied using glass pipette tip diameters of approximately 3–5 μ m and resistances in the range of 3–10 M Ω . A tight seal was established under superfusion with ACh solution. Because the pipette contained more than 100 mM-aspartate, we corrected the liquid junction potential (–10 mV) between the pipette solution and the bath solution in all the data.

The membrane capacitance was determined from the current amplitude in response to a voltage ramp pulse of 3.3 V/s, which was applied at the beginning of each whole-cell clamp experiment. In twenty-six cells, the average membrane capacitance was 35.4 ± 4.8 pF. All statistical data were expressed as the mean \pm s.d. In conjunction with this method, the surface area of the nodal cells was estimated from measurements of the minor and major axes under a microscope. In the twenty-six samples, the surface area was 1124.5 ± 382.8 μ m². The sizes of the cells employed in the present experiments were considerably smaller than those used previously in our laboratory (Nakayama *et al.* 1984). Current and voltage signals were stored on magnetic tape for computer analysis (NEC 98 series). The voltage drop across the electrode resistance (series resistance) which is produced by current flow was electrically compensated.

Single-channel current recordings. The cell-attached patch-clamp technique was the same as that reported by Hamill *et al.* (1981). The resistance of the patch electrode was in the range of 3–5 M Ω with 100 mM-BaCl₂ and the tip of the electrode was coated with Sylgard (Shin-Etsu Chemical Co., KE106). Data were stored on a video recorder (Victor, BR6400) using a PCM converter system (NF Electronic Circuit Design, Tokyo RP-880). The data were low-pass filtered employing a filter (NF, FV-625) with Bessel characteristics and analysed with an Hitachi E600 computer. The cut-off frequency of the filter defined at the –3 dB point was 1 kHz. The membrane potential of the patch was calculated as the difference between the resting potential and the pipette potential. All experiments were performed at 37 °C.

Solutions. The compositions of the external perfusates are shown in Table 1. In the whole-cell voltage clamp, the pipette contained (in mM): CsOH, 110; aspartic acid, 90; CsCl, 20; K₂ATP, 5;

potassium creatine phosphate, 5; EGTA, 10; MgCl_2 , 1; HEPES, 5; cyclic AMP, 0.05; and the pH was adjusted to 7.4 with CaOH . When isoprenaline was applied, cyclic AMP was omitted from the pipette solution. For the single-channel recording, the pipette solution contained (in mM): BaCl_2 , 100; HEPES, 10; tetrodotoxin (TTX), 0.01; and the pH was 7.4. Tetramethrin (3,4,5,6-tetrahydrophthalimidomethyl(IRS)-*cis,trans*-chrysanthemate), was a generous gift from Sumitomo Kagaku Kogyo K. K., Osaka.

RESULTS

Identification of two types of calcium currents in sino-atrial node cells

Separation of two types of calcium current by different holding potentials

In the following voltage-clamp experiments, the delayed K^+ outward current was eliminated with 130 mM- Cs^+ in the pipette solution and the Na^+ inward current was almost entirely blocked by 20 μM -TTX in Na^+ -depleted (20 mM) Tris Tyrode solution, containing 2.5 mM- Ca^{2+} . Under these conditions, we employed the method of Bean (1985) to induce the two types of Ca^{2+} currents, which was to use two different holding potentials.

In the experiment shown in Fig. 1, a series of depolarizing voltage-clamp pulses was applied from alternate holding potentials of -80 and -40 mV, to minimize the effect of the 'run-down' phenomenon of the channel during the course of the experiment. A rapidly decaying inward current was elicited at test potentials positive to -50 mV with the holding potential of -80 mV (Fig. 1A1). When the holding potential was -40 mV, the conventional slowly decaying inward current which is known as the slow inward current or the Ca^{2+} current appeared (Fig. 1A2). The former current was apparently larger and decayed faster than the latter especially at negative potentials. At the positive potentials, however, both the amplitude and the time course of the two currents were similar. The difference in the current traces between the two different holding potentials (Fig. 1A3) was relatively small in amplitude and inactivated quickly within 20 ms, similar to those reported as the transient type Ca^{2+} current by other workers. The current-voltage relations are illustrated in Fig. 1B. Currents elicited from the holding potential of -80 mV (\circ) were larger than those from -40 mV (\bullet) in the potential range between -50 and 20 mV. The two current-voltage curves were almost superimposable at more positive potentials than 20 mV (Fig. 1B). The difference current began to activate at -50 mV (Fig. 1C), and it peaked at -10 mV, which was 10–20 mV more negative than the peak of the conventional Ca^{2+} current. The difference current appeared to reverse at 30 mV.

To eliminate the possibility of participation of the Na^+ current in the current activated from -80 mV, the same protocol was repeated in 115 mM- Ba^{2+} solution (Fig. 2A) and in Na^+ -free Tyrode solution (replaced by Tris) containing 2.5 mM- Ca^{2+} (Fig. 2B). The onset time course and amplitude of the current were comparable between 115 mM- Ba^{2+} and 2.5 mM- Ca^{2+} solutions, but the rate of decay of the conventional type current was slower in Ba^{2+} solution than in Ca^{2+} solution. In 115 mM- Ba^{2+} solution, both types of currents disappeared within 5 min. Both types of inward currents measured in these experiments were insensitive to TTX, present in Na^+ -free solution. They were also carried by both Ba^{2+} and Sr^{2+} (not shown in the Figure) and were abolished by 2 mM- Co^{2+} (Fig. 2C). These findings indicate that the

inward currents recorded are indeed Ca^{2+} currents and not the Na^{+} current. We will therefore denote the difference current as the transient type Ca^{2+} current or $I_{\text{Ca,T}}$ and the current activated from the holding potential of -40 mV, or the conventional Ca^{2+} current, as $I_{\text{Ca,L}}$ (long-lasting type) in the following sections according to the notation of Nilius *et al.* (1985).

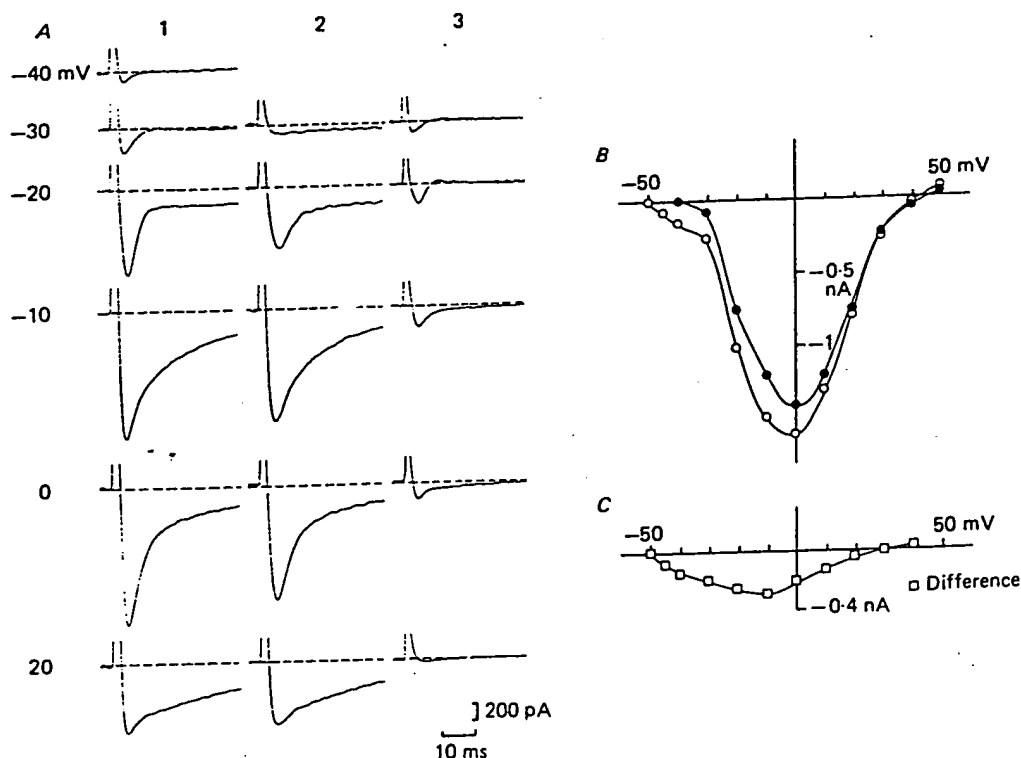


Fig. 1. Two components of calcium currents in an SAN cell separated by depolarizing pulses from two different holding potentials. A1, membrane currents were recorded at various test potentials from a holding potential of -80 mV in 2.5 mM- Ca^{2+} solution. The test potentials were varied from -40 to $+20$ mV, as indicated to the left of each trace. A2, currents in response to the test pulse from a holding potential of -40 mV, i.e. the long-lasting type Ca^{2+} current. A3, subtraction of the membrane currents in A2 from those in A1 gives the low-threshold, transient type Ca^{2+} current (A3). The dashed line in A indicates the zero current level. B, current-voltage relations of the calcium currents shown in A. \circ , currents elicited from a holding potential of -80 mV (A1); \bullet , currents obtained from a holding potential of -40 mV (A2). C, current-voltage relation of the difference in currents between the two different holding potentials shown in A3, which corresponds to the current-voltage relation of $I_{\text{Ca,T}}$.

In fifteen experiments, the amplitude of $I_{\text{Ca,T}}$ measured at -40 ± 4.2 mV was 88.3 ± 23.2 pA. The current density was 2.14 ± 0.74 pA/pF. The threshold potential, which was measured by averaging twenty successive current traces, was -47 ± 2.4 mV ($n = 5$). In ten examples, the peak amplitude of $I_{\text{Ca,T}}$ was $20.5 \pm 0.7\%$ of the peak $I_{\text{Ca,L}}$.

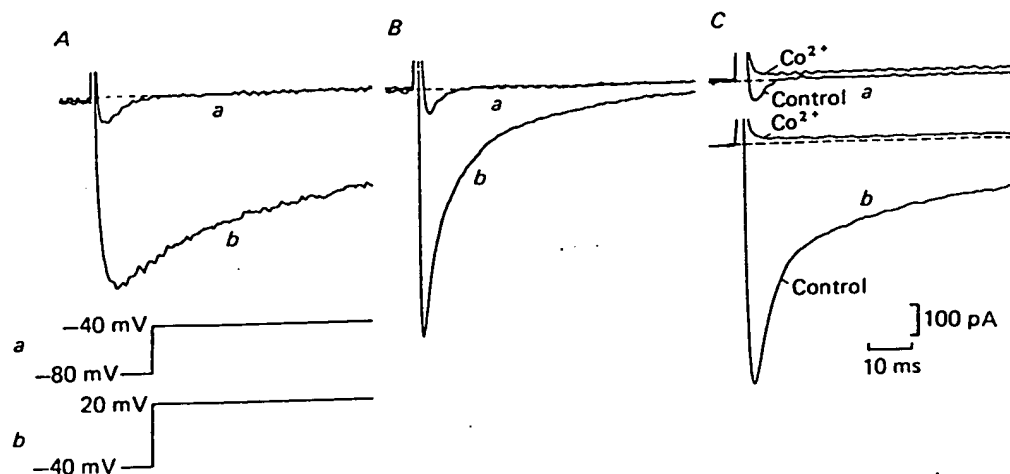


Fig. 2. Two types of calcium currents under various conditions. *A*, the top traces show two types of calcium currents obtained in 115 mM $BaCl_2$ solution. $I_{Ca,T}$ (a) was obtained with a depolarization test pulse to -40 mV from a holding potential of -80 mV. $I_{Ca,L}$ (b) was recorded with a depolarizing pulse to 20 mV from a holding potential of -40 mV. The bottom traces illustrate the voltage. *B*, $I_{Ca,T}$ (a) and $I_{Ca,L}$ (b) obtained in Na^+ -free Tyrode solution, where all the Na^+ in the Tyrode solution was removed and substituted with Tris chloride. The concentration of Ca^{2+} in the Tyrode solution was 2.5 mM. The same voltage conditions as in *A* apply. *C*, both $I_{Ca,T}$ (a, upper two traces) and $I_{Ca,L}$ (b, lower two traces) were abolished within 3 min after superfusion of 2 mM-cobalt solution. The dashed lines give the zero current levels in all the current traces.

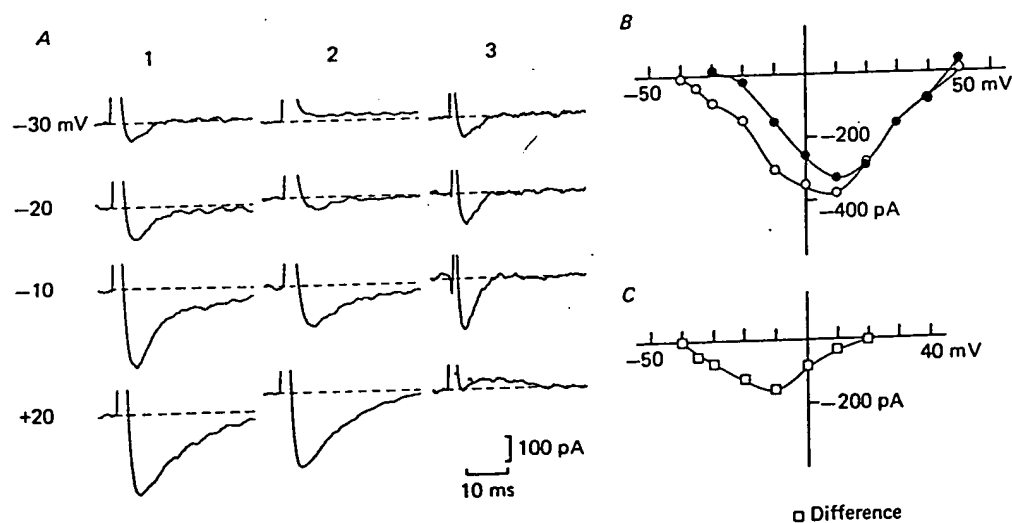


Fig. 3. Effect of 40 μM - Ni^{2+} on the two types of calcium currents. *A1* shows the current traces at various membrane potentials (indicated on the left) in control Tyrode solution. *A2* depicts those after administration of 40 μM -nickel. During nickel superfusion, no current was observed at -30 mV. The differences between the two traces are shown in *A3*. The holding potential was -80 mV. *B*, current-voltage relations of the Ca^{2+} current shown in *A1* in the control (○) and in *A2* during administration of 40 μM -nickel (●). *C*, current-voltage relation of the difference current in *A3* indicates that of $I_{Ca,T}$.

Blockers of the calcium current

Specific blockers of the transient type Ca^{2+} current. A low concentration of nickel has been found to block $I_{\text{Ca,T}}$ in neuroblastoma cells (Tsunoo, Yoshii & Narahashi, 1985). In SAN cells, $I_{\text{Ca,T}}$ recorded at a test pulse of -30 mV (Fig. 3A1, top panel) was abolished within 2 min after superfusion of the cell with $40 \mu\text{M-Ni}^{2+}$ (Fig. 3A2, top panel). The inward current remaining in the presence of Ni^{2+} was activated at potentials positive to -30 mV (Fig. 3B) and was sensitive to D600 and nifedipine.

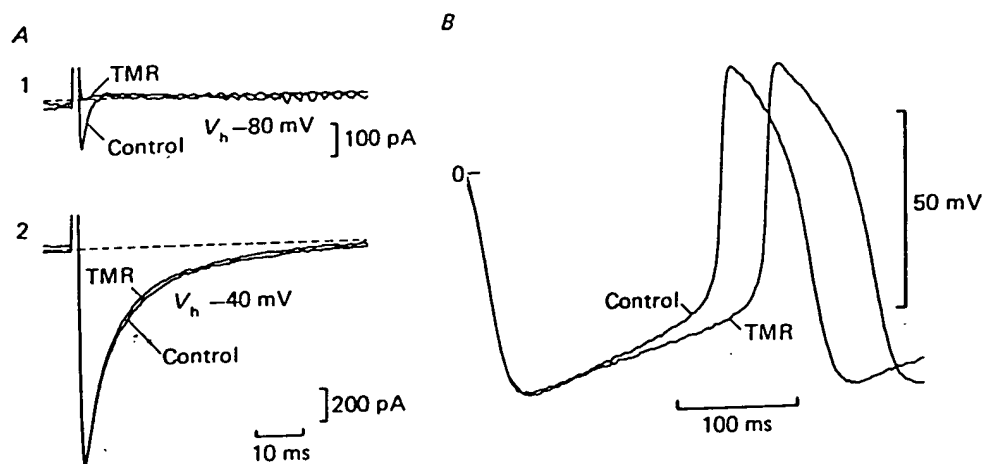


Fig. 4. *A*, superimposed records of $I_{\text{Ca,T}}$ (A1) and $I_{\text{Ca,L}}$ (A2). TMR indicates current records during superfusion of $0.1 \mu\text{M}$ -tetramethrin. The traces in A1 were elicited by depolarization from a holding potential of -80 mV to a test potential of -30 mV. The traces in A2 were obtained by depolarization from a holding potential of -40 mV to a test potential of 10 mV. The dashed lines indicate the zero current level. *B*, superimposed action potentials before (Control) and during the application of tetramethrin (TMR).

As a result, $I_{\text{Ca,L}}$ activated with a holding potential of -40 mV was unaffected by $40 \mu\text{M-Ni}^{2+}$ (Fig. 1A of Hagiwara *et al.* 1987). The difference between the currents in the presence and absence of $40 \mu\text{M-Ni}^{2+}$ would thus represent $I_{\text{Ca,T}}$, as shown in Fig. 3A3 and C. The peak amplitude of $I_{\text{Ca,T}}$ so estimated was 160 pA which was 40% of the peak $I_{\text{Ca,L}}$ in this example. The $I_{\text{Ca,L}}$ was decreased by about 30% in $80 \mu\text{M-Ni}^{2+}$ solution. Tsunoo *et al.* (1985) reported that in neuroblastoma cells, $50 \mu\text{M}$ -tetramethrin reduced the amplitude of the peak $I_{\text{Ca,T}}$ by 70 – 80% while it reduced $I_{\text{Ca,L}}$ by only 20 – 30% (Tsunoo *et al.* 1985). In the SAN cell, however, $50 \mu\text{M}$ -tetramethrin blocked both $I_{\text{Ca,L}}$ and $I_{\text{Ca,T}}$ completely, whereas a low concentration of tetramethrin ($0.1 \mu\text{M}$) abolished $I_{\text{Ca,T}}$ without affecting $I_{\text{Ca,L}}$ significantly (Fig. 4A). This specific action of tetramethrin on $I_{\text{Ca,T}}$ was confirmed in three other cells.

Specific blockers of the long-lasting type Ca^{2+} current. Superfusion of the cell with $2 \mu\text{M}$ -nifedipine did not change $I_{\text{Ca,T}}$ elicited from a holding potential of -80 mV (Fig. 5A1) but abolished $I_{\text{Ca,L}}$ elicited from -40 mV (Fig. 5A2). The current-voltage

relations obtained with the holding potential of -80 mV showed no change in the potential range between -50 and -30 mV, but there was a marked reduction at potentials positive to -30 mV, in the presence of nifedipine. In contrast, the current-voltage relations with the holding potential of -40 mV revealed complete block of the inward current (Fig. 5B) by nifedipine. Superfusion of cells with D600 ($1 \mu\text{M}$) yielded similar results in two cells. It can be concluded, therefore, that both nifedipine and D600 selectively block $I_{\text{Ca,L}}$ and have no effect on $I_{\text{Ca,T}}$.

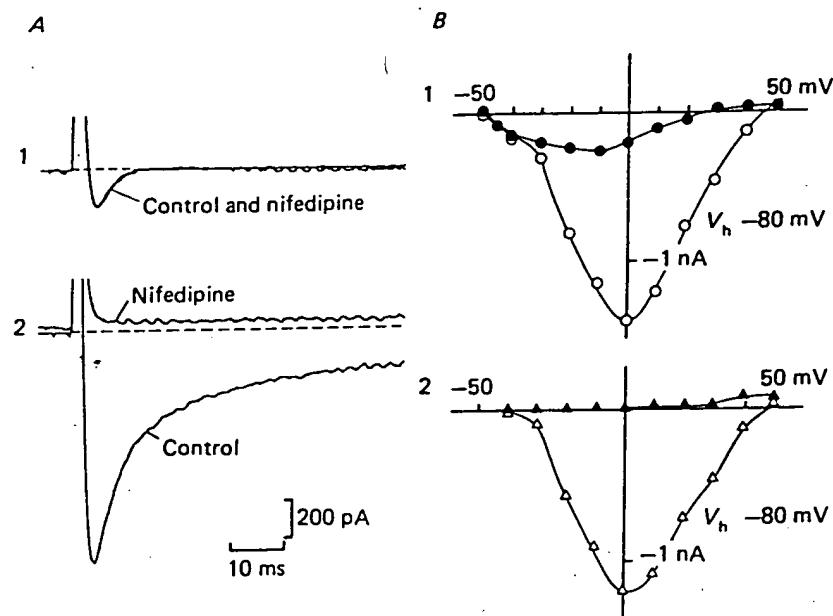


Fig. 5. Effect of nifedipine on the two types of the calcium currents. A1, a representative $I_{\text{Ca,T}}$ activated by a pulse to -40 mV from -80 mV. A2, $I_{\text{Ca,L}}$ in response to a depolarizing clamp pulse to 0 mV from -40 mV. The dashed lines indicate the zero current level. $I_{\text{Ca,T}}$ before and during administration of nifedipine were completely superimposable. Nifedipine abolished the $I_{\text{Ca,L}}$ after 5 min (A2). B1, current-voltage relations of the calcium current shown in A. \circ , the control before nifedipine superfusion. \bullet , in the presence of nifedipine ($2 \mu\text{M}$), which corresponded to $I_{\text{Ca,T}}$. B2 gives the current activated by depolarization from a holding potential of -40 mV. \triangle , the control $I_{\text{Ca,L}}$; \blacktriangle , in nifedipine.

Other blockers. As shown in Fig. 2C, 2 mM-Co^{2+} completely blocked both $I_{\text{Ca,T}}$ and $I_{\text{Ca,L}}$. Similarly, the blockade by cadmium (Cd^{2+}) was not selective between $I_{\text{Ca,T}}$ and $I_{\text{Ca,L}}$. Cadmium ion at $20 \mu\text{M}$ decreased $I_{\text{Ca,T}}$ by 62%, and $I_{\text{Ca,L}}$ by 83%. We obtained similar results in two other examples.

In conclusion, it can be said that there are two types of Ca^{2+} channel blockers: one is selective to either type of the Ca^{2+} channels and the other non-selective. Low concentrations of nickel and tetramethrin are selective blockers of $I_{\text{Ca,T}}$, whereas nifedipine and D600 are specific to $I_{\text{Ca,L}}$.

ange in the
duction at
ntrast, the
l complete
with D600
that both

mV

nV

nV

mV

entative
larizing
el. $I_{Ca,T}$
ossible.
of the
in the
activated
; ▲. in

h $I_{Ca,T}$ and
n $I_{Ca,T}$ and
e obtained

ockers: one
ctive. Low
T, whereas

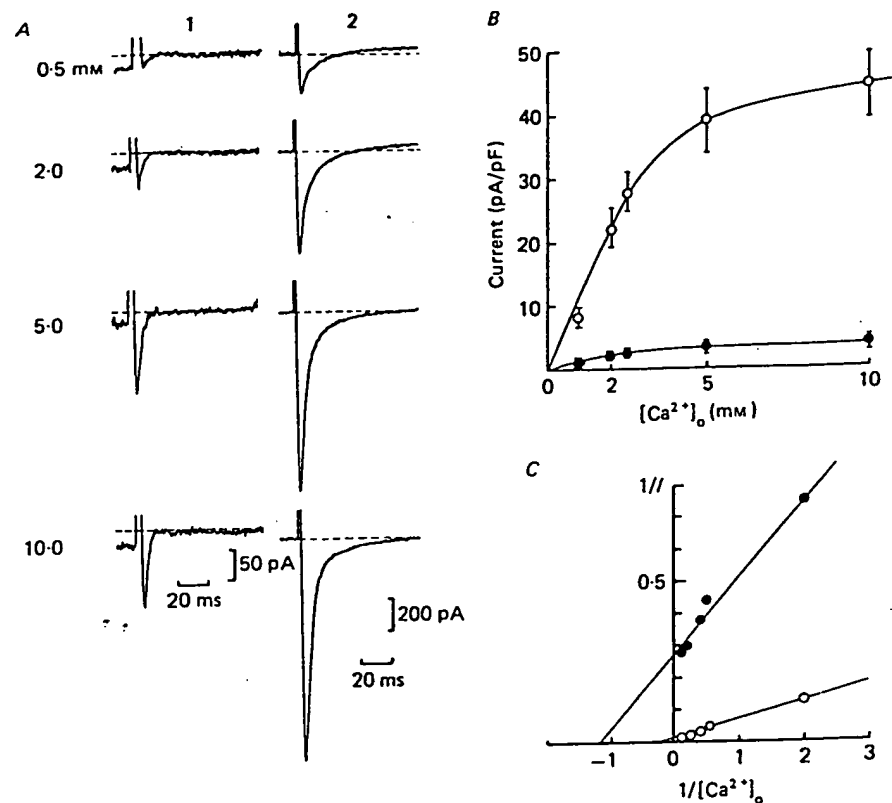


Fig. 6. *A*, effects of various concentrations of external calcium on $I_{Ca,T}$ and $I_{Ca,L}$. *A1* shows the current traces of $I_{Ca,T}$, and *A2* those of $I_{Ca,L}$. The numbers to the left of the current traces indicate the concentration of Ca^{2+} in the Tyrode solution in mM. The current traces shown in *A1* are the differences between responses to the test pulse of -10 mV from two different holding potentials (-80 and -40 mV), whereas those in *A2* are obtained in response to the test pulse of 0 mV from the holding potential of -40 mV. *B*, relation between concentration of Ca^{2+} and current density. The abscissa shows the concentration of Ca^{2+} in mM, and the ordinate is the amplitude of the Ca^{2+} current in pA/pF. ● refers to $I_{Ca,T}$; ○ refers to $I_{Ca,L}$. The number of experiments at 0.5, 2.0, 2.5, 5.0 and 10 mM was five, five, fourteen, eleven and five respectively. *C*, Lineweaver-Burk plot; this gives a K_m value of Ca^{2+} for $I_{Ca,T}$ as 0.95 mM and for $I_{Ca,L}$ as 3.92 mM. V_{max} for $I_{Ca,T}$ was 3.85 pA/pF and for $I_{Ca,L}$ was 55.6 pA/pF. These results suggest that the two types of Ca^{2+} currents represent different current systems.

Effect of various concentrations of extracellular Ca^{2+} on $I_{Ca,T}$ and $I_{Ca,L}$

To compare sensitivities of both $I_{Ca,T}$ and $I_{Ca,L}$ channels to the permeant ions, we varied the concentration of extracellular Ca^{2+} ($[Ca^{2+}]_o$). The amplitude of $I_{Ca,T}$ was increased from 20 to 125 pA (about a 6-fold increase) by increasing $[Ca^{2+}]_o$ from 0.5 to 5 mM, and it almost reached a maximum at 5.0 mM, while $I_{Ca,L}$ also increased approximately 6-fold with an increase in $[Ca^{2+}]_o$ from 0.5 to 5 mM and the further increase was only slight at 10 mM $[Ca^{2+}]_o$ (Fig. 6*A*). The amplitude of the peak

current was normalized by the cell capacitance and was plotted as a function of $[Ca^{2+}]_o$ in twenty-five cells (Fig. 6*B*). The data indicate that both $I_{Ca,T}$ and $I_{Ca,L}$ have saturation kinetics with $[Ca^{2+}]_o$, suggesting involvement of binding sites in the permeation of Ca^{2+} through these channels. A double-reciprocal plot of the data in Fig. 6*B* indicated that the Michaelis constant (K_m) of Ca^{2+} for $I_{Ca,T}$ and $I_{Ca,L}$ were 0.95 mM and 3.92 mM, respectively (Fig. 6*C*). The K_m value of $I_{Ca,L}$ was comparable to that reported by Hess & Tsien (1984).

These findings suggest that the structure of the pore in the channel may be different between the two types of Ca^{2+} channels.

Single-channel recordings

To obtain further evidence of the two distinct classes of Ca^{2+} channels in the SAN cell, single-channel currents were recorded in the cell-attached patch configuration.

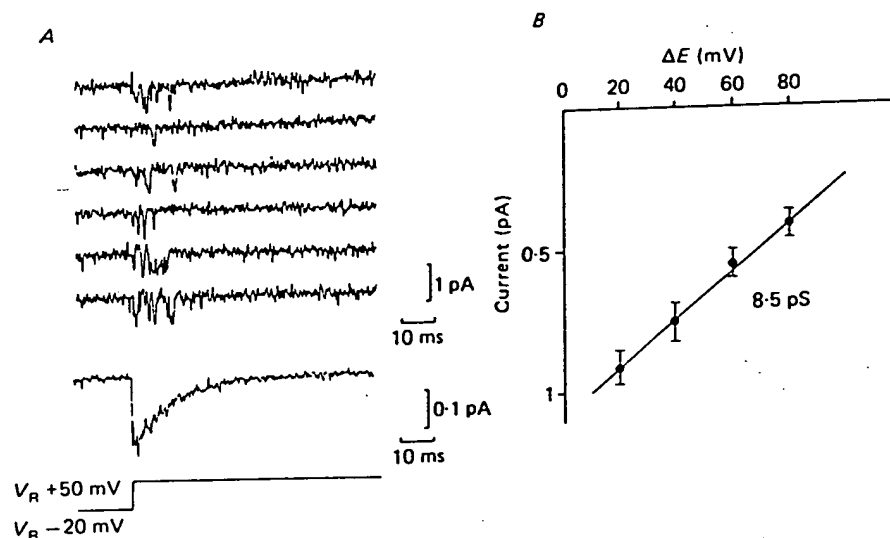


Fig. 7. Single-channel recordings of $I_{Ca,T}$. *A*, six successive traces of $I_{Ca,T}$ in response to the test pulse ($V_R + 50$ mV) from the holding potential (-20 mV from the resting potential, $V_R - 20$ mV). The electrode solution contained 100 mM-BaCl₂, 10 mM-HEPES and 10 μ M-TTX. The ensemble average of 550 traces is shown in the bottom panel with the command potential. *B*, the current-voltage curve of $I_{Ca,T}$ gives a slope conductance of 8.5 pS.

The recording pipette contained 100 mM-BaCl₂. One type of single-channel current was activated by depolarizing the membrane patch from $V_R - 20$ mV to $V_R + 100$ mV, where the resting membrane potential (V_R) was estimated to be -80 mV in the presence of ACh. The single-channel conductance was 16.0 pS (data not shown) and the activity was observed over the entire period of the depolarizing pulse of 300 ms, suggesting that this channel had slow inactivation kinetics. The open time of this current was prolonged by Bay K 8644, and the activity was reduced by nifedipine in the perfusate. These results led us to conclude that this channel represents $I_{Ca,L}$.

Another type of single-channel current was activated by pulses from $V_R - 20$ mV to potentials more positive than $V_R + 20$ mV. A single-channel current of 0.62 pA was elicited by 100 ms depolarizing pulses from $V_R - 20$ mV to $V_R + 50$ mV in the presence of $10 \mu M$ -nifedipine (Fig. 7A). The single-channel current activity was increased by shifting the holding potential to more negative potentials ($V_R - 40$ mV). The activity was seen only during the initial 30 ms of the test pulses in most cases. The ensemble average current revealed a peak current of 0.18 pA at 2 ms after the onset of the pulse and an inactivation with the time constant of 12 ms. The single-channel conductance was 8.5 ± 1.2 pS ($n = 4$) (Fig. 7B). This result is comparable to the whole-cell clamp data in Ba^{2+} . Since Ba^{2+} did not affect the inactivation of $I_{Ca,T}$ in the whole-cell clamp as shown in Fig. 2, we concluded that these single-channel events were Ba^{2+} currents through the transient type calcium channel.

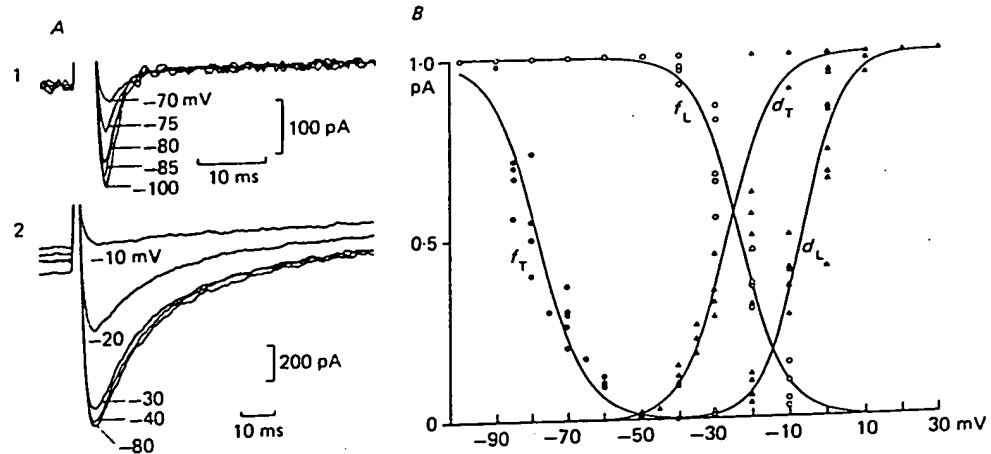


Fig. 8. Inactivation of $I_{Ca,T}$ and $I_{Ca,L}$. A1, superimposed traces of $I_{Ca,T}$. The currents were elicited by a test pulse of 2 s duration to -30 mV from various holding potentials. A2, superimposed traces of $I_{Ca,L}$. The currents were elicited at $+20$ mV by varying holding potentials. The numbers give the holding potentials in millivolts for both currents. A1 and A2 have different time and voltage calibrations. B, steady-state inactivation and activation curves of both $I_{Ca,T}$ and $I_{Ca,L}$. ● and ▲ indicate the steady-state inactivation and activation curves of $I_{Ca,T}$ respectively. ○ and △ indicate the steady-state inactivation and activation curves of $I_{Ca,L}$ respectively. The data were obtained from five different experiments. The continuous curves were drawn according to the equations described in the text.

Kinetic properties of the two types of Ca^{2+} currents

Voltage dependence of inactivation

The results of the above experiments suggest that $I_{Ca,T}$ is available in SAN cells with a holding potential of -80 mV but is inactivated with -40 mV. To quantify the degree of inactivation of $I_{Ca,T}$, the membrane potential was held at various levels between -100 and -70 mV and depolarizing test pulses of 200 ms were applied to -30 mV (Fig. 8A1). For $I_{Ca,L}$, the holding potential was varied between -80 and -10 mV and the test pulses to 20 mV were applied (Fig. 8A2). The peak amplitudes of both $I_{Ca,T}$ and $I_{Ca,L}$ were normalized and plotted against the membrane potentials (Fig. 8B). The degree of steady-state inactivation of $I_{Ca,T}$ and $I_{Ca,L}$ revealed a

sigmoidal relation to voltage (Fig. 8B). $I_{Ca,T}$ was completely inactivated at potentials positive to -40 mV. For descriptive purposes, we approximate the steady-state inactivation parameter (f_x) and the activation parameter (d_x) as follows. d_x was estimated from the peak conductance according to Isenberg & Klöckner (1982b) as:

$$d_x = g_{Ca}/\bar{g}_{Ca} = I_{Ca}/\bar{g}_{Ca}(V_m - E_{rev}),$$

where g_{Ca} is the peak conductance, \bar{g}_{Ca} the maximum value of g_{Ca} , I_{Ca} the peak Ca^{2+} current, and E_{rev} the reversal potential of the Ca^{2+} current. E_{rev} was assumed to be the zero-current potential in the current-voltage relations. Since E_{rev} for Ca^{2+} is an apparent one, the method of calculating the d_x curve may represent the activation of $I_{Ca,T}$ to the first approximation. The activation parameters so calculated are plotted in Fig. 8B. The continuous curves in the Figure were calculated according to:

$$y_x = ((1 + \exp(V_m - V_{0.5})/s)^{-1},$$

where y_x is either f_x or d_x , $V_{0.5}$ is the potential to give a half-value and s is the slope factor which determines the steepness of the curve. The inactivation and activation parameters were fitted well by a Hodgkin-Huxley type equation (Hodgkin & Huxley, 1952, applied by Reuter, 1973; Isenberg & Klöckner, 1982b). For $I_{Ca,T}$, the slope factor (s) of the steady-state inactivation curve was 6.6 mV and $V_{0.5}$ was -75 mV. $I_{Ca,T}$ activates at around -50 mV and saturates at 0 mV. The slope factor was 6.1 mV and $V_{0.5}$ was -23 mV. The steady-state activation and inactivation curves crossed at -50 mV and had a very small overlap.

$I_{Ca,L}$ revealed similar f_x and d_x curves to those reported by various authors (for review, see Carmeliet & Vereecke, 1979). The steady-state inactivation of $I_{Ca,L}$ was also expressed by a sigmoidal curve, having a slope factor of 6.0 mV and $V_{0.5}$ of -25 mV. The steady-state activation curve of $I_{Ca,L}$ had a slope factor of 6.6 mV and $V_{0.5}$ of -6.6 mV. The steady-state inactivation curve of $I_{Ca,T}$ was thus shifted by approximately 50 mV negative to that of $I_{Ca,L}$, whereas the activation curve of $I_{Ca,T}$ shifted by 20 mV negative to that of $I_{Ca,L}$.

Time course of inactivation

The time course of the inactivation was analysed in two ways: one was direct for the potentials positive to -40 mV and the other was an indirect way for the voltages negative to -50 mV. Firstly, $I_{Ca,T}$ was activated by various test pulses to the range between -40 and -10 mV from a holding potential of -80 mV, and the time course of the decaying phase of $I_{Ca,T}$ was measured. Figure 9A illustrates a representative experiment where the current decay was single exponential and its time constant was 3 ms at -30 mV. The time constant became smaller as the potential became more positive. Secondly, the time course of the inactivation between -100 and -50 mV was measured indirectly. As shown in the bottom trace of Fig. 9B, $I_{Ca,T}$ was activated by various initial conditioning pulses to between -100 and -50 mV from -90 mV with a variable duration, and then envelope curves of $I_{Ca,T}$ were obtained at the fixed test potential of -30 mV (dashed curves in Fig. 9B). The time constant of the envelope curves was 25 ms for a conditioning pulse of -60 mV and 9.5 ms for -50 mV. The time constant of inactivation of $I_{Ca,T}$ obtained in the two different ways is plotted against the membrane potential in Fig. 9C. The time constant of $I_{Ca,T}$ increased as the conditioning pulse became more negative. We calculated the

activated at
proximate the
eter (d_x) as
Isenberg &

he peak Ca^{2+}
ssumed to be
for Ca^{2+} is an
he activation
alculated are
ed according

s is the slope
nd activation
(Hodgkin &
For $I_{Ca,T}$, the
and $V_{0.5}$ was
e slope factor
inactivation

authors (for
of $I_{Ca,L}$ was
and $V_{0.5}$ of
of 6.6 mV and
us shifted by
curve of $I_{Ca,T}$

was direct for
the voltages
to the range
e time course
representative
constant was
became more
and -50 mV
B, $I_{Ca,T}$ was
-50 mV from
ere obtained
ime constant
nd 9.5 ms for
two different
e constant of
alculated the

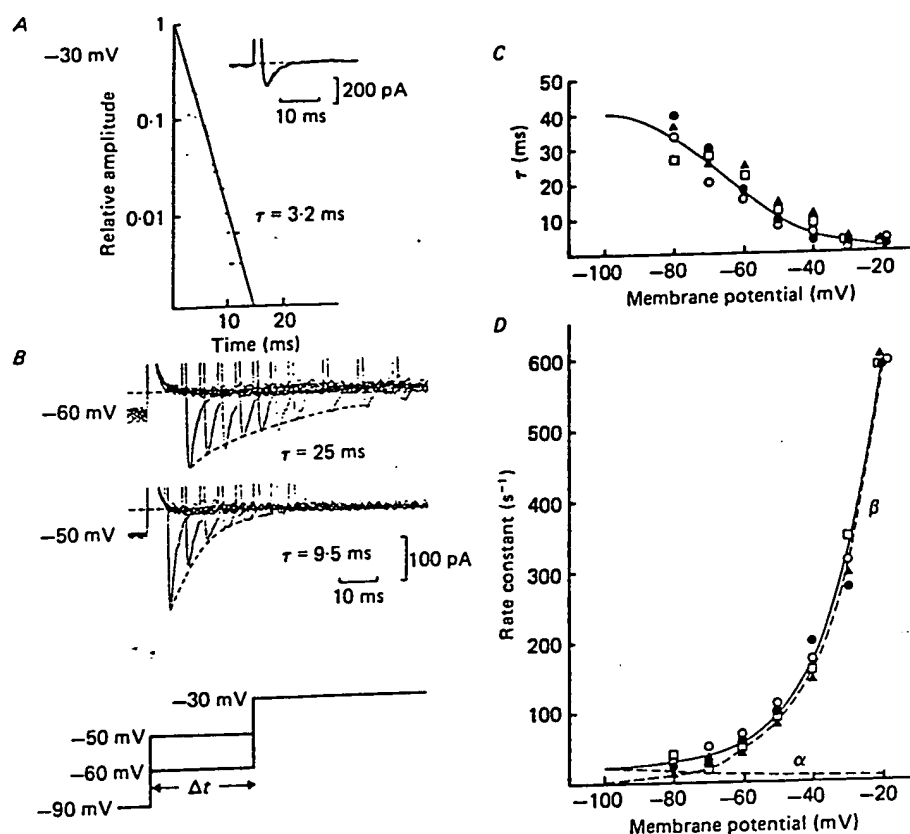


Fig. 9. Time course of inactivation of $I_{Ca,T}$. A, the inactivation time course of $I_{Ca,T}$ at -30 mV was fitted by a single-exponential curve, with a time constant of 3.2 ms. The inset shows the original current trace from which the computation was made. B, time course of inactivation of $I_{Ca,T}$ at -60 mV and -50 mV. The time courses of inactivation at these potentials were measured indirectly by using the two step pulses. The experimental paradigms are shown at the bottom. C, relation between the time constant of inactivation of $I_{Ca,T}$ and the membrane potential. Different symbols refer to different samples. The continuous curve was fitted to the equation $\tau = 1/(\alpha + \beta)$. D, rate constants of inactivation of $I_{Ca,T}$ at various membrane potentials. The symbols correspond to those in C. α and β were fitted by the empirical equations shown in the text.

rate constants of the inactivation, α_t and β_t , from the steady-state inactivation parameters and the time constant (Fig. 9D). The value of α_t and β_t could apparently be expressed by the following equation:

$$\alpha_t = 16.67 \exp(-0.012 (V + 75)),$$

$$\beta_t = 16.67 \exp(0.065 (V + 75)).$$

Recovery from the inactivation was also measured for $I_{Ca,T}$ and $I_{Ca,L}$ by applying a pair of pulses with a variable interval duration. The time constant of the recovery of $I_{Ca,T}$ was 144 ± 5.3 ms at -80 mV and that of $I_{Ca,L}$ was 225 ± 12.5 ms at -40 mV in three examples, suggesting that both $I_{Ca,T}$ and $I_{Ca,L}$ are available in the normal cardiac cycle.

Physiological significance of $I_{Ca,T}$ *Role of $I_{Ca,T}$ in the action potential*

Since $40 \mu\text{M-Ni}^{2+}$ specifically abolished $I_{Ca,T}$ (Fig. 3), its effect on the action potential was examined. Figure 10 *A* compares the spontaneous action potentials recorded from a single SAN cell before and in the presence of $40 \mu\text{M-Ni}^{2+}$. Nickel

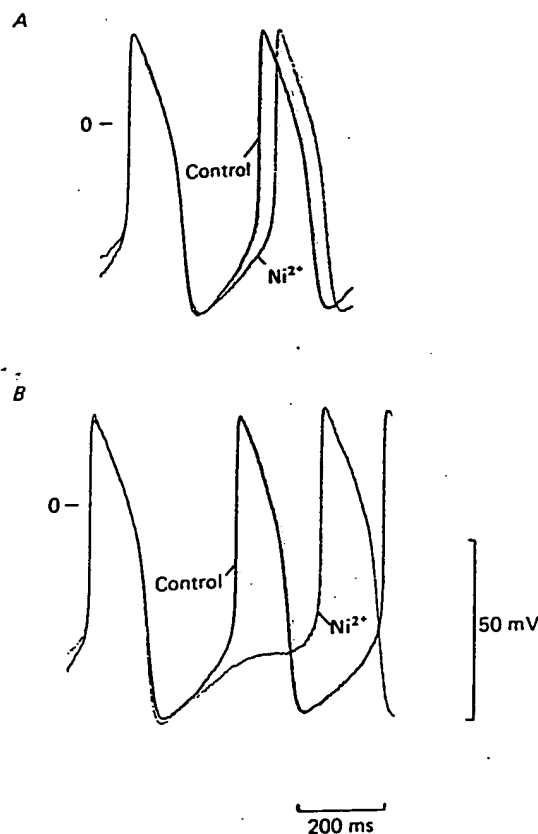


Fig. 10. Effect of a low concentration of nickel on the spontaneous action potentials in the SAN cell. *A*, superimposed action potentials before (Control) and after (Ni^{2+}) administration of $40 \mu\text{M-nickel}$. The slope of the slow diastolic depolarization was decreased. 0 is the zero membrane potential. *B*, superimposed action potential traces under the effect of a hyperpolarizing current for the control and during administration of $40 \mu\text{M-nickel}$ (Ni^{2+}). Marked prolongation of the latter phase of the diastolic depolarization is observed.

consistently produced a negative chronotropic effect (control interval, 296.4 ± 47.5 ms; after Ni^{2+} , 340.0 ± 55.9 ms; 14.4% prolongation, $n = 5$). This effect was more pronounced when the cell was hyperpolarized by injecting a constant current. As shown in Fig. 10 *B*, a constant hyperpolarizing current (20 pA) decreased the cycle length by only 9.9% in the absence of Ni^{2+} , whereas the same current produced obvious bradycardia in the presence of Ni^{2+} (60.7% prolongation of the pacemaker depolarization). This effect was confirmed in three other examples. The negative

E_L

(I_L
of
the
un
(F
not
con
blo

chronotropic effect of Ni^{2+} was due to slowing of the diastolic depolarization in the latter two-thirds of the pacemaker potential. These findings indicate that $I_{\text{Ca,T}}$ does indeed play an important role in the generation of the pacemaker potential, especially in the latter two-thirds of the diastolic phase.

The effects of tetramethrin, another specific blocker of $I_{\text{Ca,T}}$, on the spontaneous action potentials were also examined. As shown in Fig. 4B, the cycle length was 273.3 ± 10.2 ms in the control, whereas it was prolonged to 305.7 ± 19.0 ms (11.4% increase) in the presence of $0.1 \mu\text{M}$ -tetramethrin. The prolongation in this example occurred at the middle phase of the pacemaker depolarization. The effects of tetramethrin were thus consistent with that of nickel, indicating that $I_{\text{Ca,T}}$ is activated during the pacemaker depolarization.

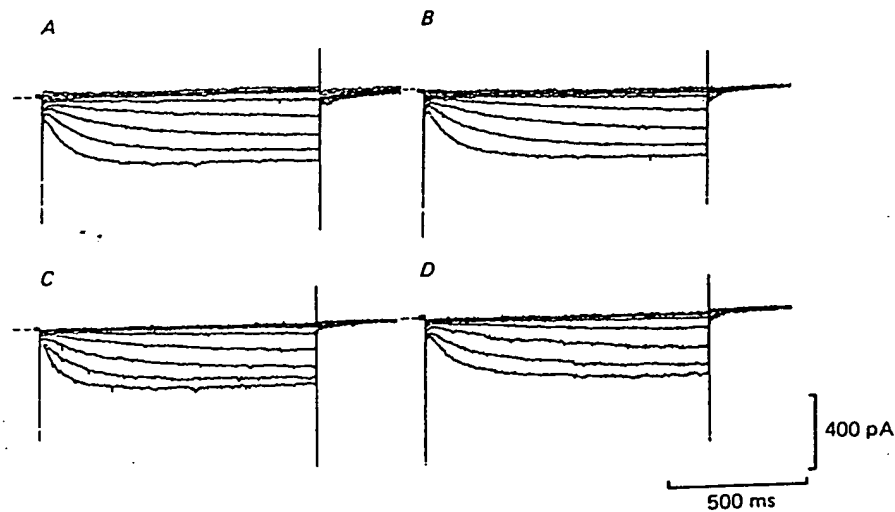


Fig. 11. Effect of $40 \mu\text{M}$ -nickel on the hyperpolarization-activated inward current. A, hyperpolarization-activated currents elicited by various test pulses to potentials between -50 and -120 mV from a holding potential of -40 mV before administration of $40 \mu\text{M}$ -nickel. B, hyperpolarization-activated currents at 10 min after administration of $40 \mu\text{M}$ -nickel. C, superfusion of 1 mM -nickel in the same cell. Although there was a small decrease in amplitude (run-down) during B and just before C, 1 mM -Ni caused no appreciable change. D, the currents after washing out the 1 mM -nickel. The result confirmed that the hyperpolarization-activated current was resistant to Ni^{2+} up to 1 mM .

Effect of Ni^{2+} on current systems other than $I_{\text{Ca,T}}$

If $40 \mu\text{M}$ -nickel also inhibited the hyperpolarization-activated inward current (I_h ; Yanagihara & Irisawa, 1980a; I_f ; DiFrancesco *et al.* 1986), then the small change of heart rate would be attributable to a decrease of I_f as well. The amplitude of I_f was therefore examined in the presence and absence of Ni^{2+} , but it was found to be unchanged by superfusion of $40 \mu\text{M}$ - or even 1 mM - Ni^{2+} for as long as 10 min (Fig. 11A-D). The Ni^{2+} neither changed the potassium current upon depolarization nor its tail current upon repolarization to -40 mV (data not shown). It was concluded, therefore, that the bradycardia produced by $40 \mu\text{M}$ -nickel was due to blockade of $I_{\text{Ca,T}}$ and not to a change in I_f or I_K .

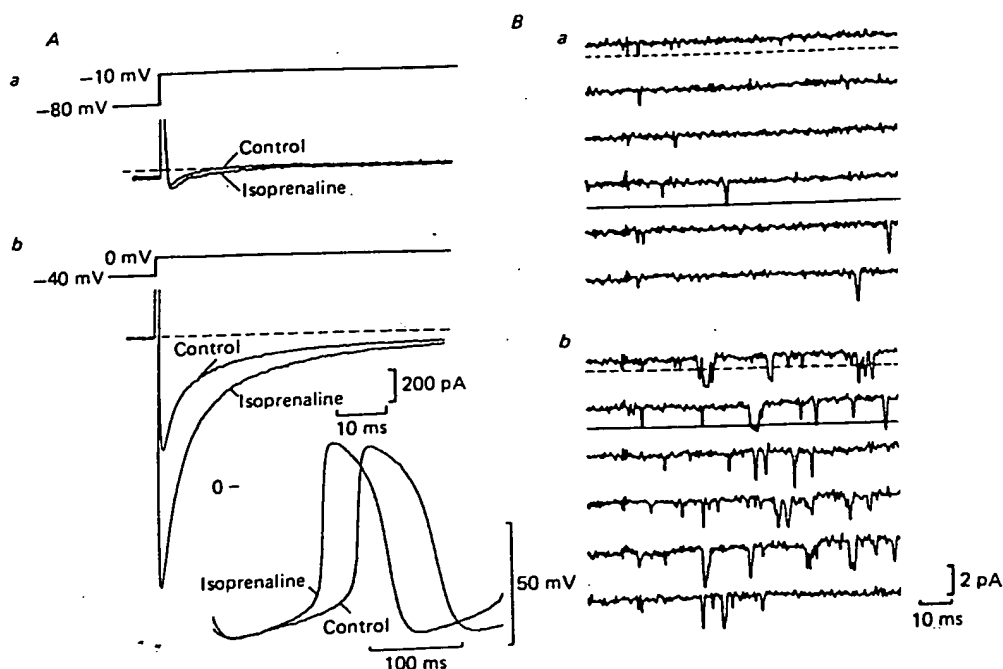


Fig. 12. Effect of isoprenaline on the two types of calcium currents. *A*, effect of isoprenaline on the two types of calcium currents. *a*, effect of isoprenaline on $I_{Ca,T}$. The upper trace shows the experimental paradigm and the lower trace gives the current records. $I_{Ca,T}$ was obtained through the subtraction procedure as shown in Fig. 1A3. 'Isoprenaline' is the current during $1 \mu\text{M}$ -isoprenaline superfusion. *b*, effect of isoprenaline on $I_{Ca,L}$. The upper trace shows the experimental paradigm, and the lower trace gives the current records. 'Isoprenaline' is the $I_{Ca,L}$ recorded at 5 min after superfusing $1 \mu\text{M}$ -isoprenaline solution. The inset to *Ab* illustrates the effect of isoprenaline on the spontaneous action potential. The slope of the slow diastolic depolarization was increased after administration of $1 \mu\text{M}$ -isoprenaline. *B*, effect of isoprenaline on the two types of single calcium current. *a*, current traces with 100 mM - Ba^{2+} in the pipette. This patch contained both types of channels. The patch membrane was depolarized from -80 to -30 mV . The dashed line below the top trace gives the detection level for the $I_{Ca,T}$. The continuous line below the fourth trace gives that for $I_{Ca,L}$. *b*, after administration of $1 \mu\text{M}$ -isoprenaline, the open probability of the $I_{Ca,L}$ was increased, but that for $I_{Ca,T}$ was insignificant. The dashed line and the continuous line mean the same as in panel *a*.

Effects of the β -adrenergic agonist, isoprenaline, on the two types of Ca^{2+} currents

In multicellular specimens, the positive chronotropic action of adrenaline has been attributed to an increase of the slow inward current (Noma *et al.* 1980). Is this increase in the slow inward current due to an increase in $I_{Ca,T}$ and/or $I_{Ca,L}$? In four out of five whole-cell voltage-clamp experiments, $I_{Ca,T}$ was not significantly increased ($4.8 \pm 3.4\%$) by $1 \mu\text{M}$ -isoprenaline, whereas $I_{Ca,L}$ was markedly enhanced ($103.0 \pm 33.0\%$; Fig. 12A).

To confirm this effect, isoprenaline was applied during the single-channel analysis in the cell-attached mode (Fig. 12B). As described previously the pipette contained

100 mM-BaCl₂ and the extracellular fluid contained 150 mM-potassium aspartate. When the patch membrane was depolarized from -80 to -30 mV, two kinds of Ca²⁺ currents were observed (Fig. 12*Ba*). There was a very small amount of opening of $I_{Ca,L}$ in the control, but after superfusing with isoprenaline the opening of $I_{Ca,L}$ at -30 mV increased considerably, therefore isoprenaline increases the probability of opening of $I_{Ca,L}$ (Fig. 12*Bb*). As for $I_{Ca,T}$, neither the single-channel conductance nor the open-state probability was affected by the β -adrenergic agonist. We repeated this experiment under the influence of 2 μ M-nifedipine where $I_{Ca,L}$ was blocked, and confirmed that the change in $I_{Ca,T}$ was insignificant. Changes in the action potential configuration were also examined (Fig. 12, inset to *Ab*). The frequency of the spontaneous action potential increased after administration of isoprenaline, mainly because the diastolic depolarization was accelerated. This finding suggests that an increase in $I_{Ca,L}$ is involved, at least partly, in the positive chronotropic action of the β -adrenergic agonist.

DISCUSSION

Presence of $I_{Ca,T}$ in sino-atrial node cells

Diversity of the Ca²⁺ channels in non-cardiac cells has been well established (Hagiwara *et al.* 1975; Fox & Krasne, 1984; Deitmer, 1984). In inferior olivary neurones, Llinás & Yarom (1981*a, b*) obtained evidence for two components of Ca²⁺ currents in the guinea-pig: one of them was activated at relatively negative membrane potentials and inactivated quickly, while the other required more depolarized potentials for activation and inactivated slowly. Evidence for two or three types of Ca²⁺ channels has also been presented for sensory neurones and pituitary cells (Carbone & Lux, 1984; Armstrong & Matteson, 1985; Fedulova *et al.* 1985; Nowycky, Fox & Tsien, 1985). In cardiac ventricular and atrial cells, the two types of Ca²⁺ channels, $I_{Ca,T}$ and $I_{Ca,L}$, were found by both the whole-cell voltage-clamp and cell-attached patch-clamp techniques (Bean, 1985; Nilius *et al.* 1985; Mitra & Morad, 1985, 1986; Reuter *et al.* 1986).

In the present study, we identified the two types of Ca²⁺ channels in rabbit SAN cells. The transient type current, denoted as $I_{Ca,T}$, is distinct from $I_{Ca,L}$ in its activation and inactivation kinetics, conductance properties and sensitivities to blockers. The $I_{Ca,T}$ channel is different from the Na⁺ channel since the current persists in the Na⁺-free condition, Ba²⁺ solution, as well as in TTX-containing solution. $I_{Ca,T}$ thus shares common properties with the transient type Ca²⁺ current found in other cells. Although the current is not TTX sensitive, it does resemble the Na⁺ current in several respects. Firstly, the potential ranges of activation and inactivation of $I_{Ca,T}$ are similar to those of the Na⁺ current. Secondly, the inactivation and activation curves of $I_{Ca,T}$ overlap very little. Thirdly, tetramethrin, a potent Na²⁺ channel blocker, is also effective. These similarities lead us to speculate that the $I_{Ca,T}$ channel might have some molecular structure in common with the Na⁺ channel.

Current density of $I_{Ca,T}$ in sino-atrial node cells

Bean (1985) found that the amplitude of I_{fast} (termed by him the transient type Ca²⁺ current) in the dog atrial cell in 5 mM-Ca²⁺ Tyrode solution was 24 ± 7 pA. He

2 pA
10 ms

effect of
 $I_{Ca,T}$. The
current
fig. 143.
isoprenaline
gives the
fig 1 μ M-
on the
increased
types of
is patch
-80 to
 $I_{Ca,T}$. The
ation of
 $I_{Ca,T}$ was
el a.

currents
ne has been
80). Is this
 $I_{Ca,L}$? In four
ificantly in-
y enhanced

nel analysis
e contained

stated that in cells isolated from the right ventricle, $I_{Ca,T}$ was either very small or absent. Since the average cell capacitance of the isolated atrial cells was 70 ± 3 pF (mean \pm S.E.M., $n = 71$; Bean, 1985), the average current density was 0.34 pA/pF. In SAN cells, however, the average cell capacitance was 35.4 ± 4.8 pF, and the current density of $I_{Ca,T}$ was 2.6 ± 0.8 pA/pF in 2.5 mM- Ca^{2+} Tyrode solution. Since the amplitude of $I_{Ca,T}$ increased approximately 1.3 times at 5 mM- Ca^{2+} compared to 2.5 mM- Ca^{2+} (Fig. 6), the current density of $I_{Ca,T}$ in the SAN cell would appear to be about ten times larger than that in atrial and ventricular cells. This conclusion is in good agreement with the finding that single-channel events were encountered more frequently in SAN cells than in guinea-pig ventricular myocytes (N. Hagiwara, unpublished observation). Since the current density of $I_{Ca,T}$ amounts to about 20% of $I_{Ca,L}$, $I_{Ca,T}$ may contribute more to the shape of the action potential in the SAN cell than other cells of the heart.

Threshold of activation of $I_{Ca,T}$ and time course of inactivation

The activation of $I_{Ca,T}$ in the SAN cell was at around -50 mV and the current peaked at around -20 to -10 mV. These values are similar to those reported for other excitable cells (Carbone & Lux, 1984; Bean, 1985; Mitra & Morad, 1986; Bossu & Feltz, 1986). In view of the fact that the foot of the activation curve extends to more negative potentials and the external solution contains 2.5 mM- Ca^{2+} , the current is probably activated at potentials more negative than -50 mV *in vivo*. Thus, in the single-channel recordings, $I_{Ca,T}$ could be recorded at approximately -60 mV. It would seem reasonable to infer, therefore, that the threshold potential of $I_{Ca,T}$ is -60 to -50 mV. The time course of inactivation and that of the recovery from inactivation were faster in this experiment than in those of other workers. In other cells, the time constant of inactivation ranged between 20 and 60 ms (Carbone & Lux, 1984; Bean, 1985; Nilius, 1986; Cognard, Lazdunski & Romey, 1986), whereas in the present experiment the value was less than 20 ms. One of the reasons for this discrepancy could be the higher temperature employed in our experiment (37°C) compared to a bath temperature of 12 – 22°C in all other experiments.

Effects of β -adrenergic agonist on $I_{Ca,T}$

In neural cells, $I_{Ca,T}$ is known to be unaffected by cyclic AMP or dibutyryl cyclic AMP (Tsunoo *et al.* 1985; Fedulova *et al.* 1985). In guinea-pig ventricular cells, Mitra & Morad (1986) observed an increase of $I_{Ca,T}$ by isoprenaline, whereas in canine atrial cells, Bean (1985) found that 4 μM -isoprenaline exerted no effect on $I_{Ca,T}$. In the present experiment, we applied 1 μM -isoprenaline in both the whole-cell and cell-attached patch-clamp modes. In the whole-cell clamp mode, we observed no significant increase in $I_{Ca,T}$ in four out of five cells. In the remaining cell, $I_{Ca,T}$ dissected by the different holding potentials, was increased by up to 40% at potentials where $I_{Ca,L}$ was activated. It is possible, therefore, that a small reduction in $I_{Ca,L}$ ($\sim 4\%$) during the dissection procedure resulted in an apparent increase in $I_{Ca,T}$ since the amplitude of $I_{Ca,L}$ was about ten times larger than that of $I_{Ca,T}$ in the presence of isoprenaline. In the single-channel analysis, we failed to observe any increase in either the single-channel conductance or the open-state probability of the $I_{Ca,T}$ channel under conditions of nifedipine treatment. On this

basis, we conclude that $I_{Ca,T}$ of the SAN cell is not sensitive to β -adrenergic stimulation.

Physiological significance of $I_{Ca,T}$

Using a brain stem slice preparation, Llinás & Yarom (1981*a*) found that the low-threshold Ca²⁺ spike contributes to the oscillatory behaviour of inferior olivary neurones. In cardiac tissues, although $I_{Ca,T}$ has previously been found in atrial and ventricular cells (Nilius *et al.* 1985; Bean, 1985; Mitra & Morad, 1985, 1986; Reuter *et al.* 1986), its precise physiological role in these cells remains to be clarified. Nilius (1986) suggested from his mathematical simulation model that $I_{Ca,T}$ plays an essential role in the pacemaker potential. In the present study, we demonstrated that the current density of $I_{Ca,T}$ in the SAN cell is higher than in atrial or ventricular cells and that its activation potential range coincided with the pacemaker potentials. Nickel and tetramethrin, selective blockers of $I_{Ca,T}$, prolonged the cardiac cycle significantly by slowing the rate of the pacemaker depolarization. This slowing appears to occur at -55 to -50 mV, which is consistent with the activation threshold for $I_{Ca,T}$. The initial phase of the pacemaker depolarization is not affected by blocking $I_{Ca,T}$. These findings lend further support to the view that the initial phase of the pacemaker potential is generated mainly by a decaying conductance of the delayed K⁺ current and that the latter phase is produced by an activation of the Ca²⁺ currents. This idea is clearly exemplified in the experiment illustrated in Fig. 10*B*. In this particular case, a hyperpolarizing current dissociates the pacemaker potential into two phases in the absence of $I_{Ca,T}$. The initial phase may be attributed to the K⁺ conductance decay and the latter phase to the activation of $I_{Ca,L}$. The evidence for this is illustrated by Fig. 10 where hyperpolarizing the cell alone did not cause a significant decrease of the rate of the electrical activity. The role of $I_{Ca,T}$ in the pacemaker mechanism is thus significant but rather like a stabilizer of the rate of depolarization. When the cell has a higher maximum diastolic potential, this current may contribute more to the pacemaker potential because the channel is less activated. It is interesting to speculate that the nodal tissue may be liable to be hyperpolarized by muscarinic stimulation unless $I_{Ca,T}$ is activated. $I_{Ca,L}$ triggers the upstroke of the action potential, and it appears that an increase of $I_{Ca,L}$ and not $I_{Ca,T}$ is involved in the positive chronotropic action of isoprenaline. Thus, the SAN cell seems to make use of both types of Ca²⁺ channels in different ways for pacemaking.

Dr J. Kimura made many helpful suggestions during the course of this work. N.H. is affiliated with the Department of Cardiovascular Division, Tokyo Women's Medical College, Shinjuku-ku, Tokyo. He wishes to thank Professor K. Hirose and Dr H. Kasanuki for providing him with the opportunity of conducting joint research at NIPS. The technical assistance of Mr M. Ohara and Mr O. Nagata is greatly appreciated. This study was supported by a research grant from the Ministry of Education, Science and Culture of Japan.

REFERENCES

- ARMSTRONG, C. M. & MATTESON, D. R. (1985). Two distinct populations of calcium channels in a clonal line of pituitary cells. *Science* **227**, 65-67.
 BEAN, B. P. (1985). Two kinds of calcium channels in canine atrial cells. Differences in kinetics, selectivity, and pharmacology. *Journal of General Physiology* **86**, 1-30.

- BOSSU, J. L. & FELTZ, A. (1986). Inactivation of the low-threshold transient calcium current in rat sensory neurones: Evidence for a dual process. *Journal of Physiology* 376, 341-357.
- BROWN, H. (1982). Electrophysiology of the sinoatrial node. *Physiological Reviews* 62, 505-530.
- CARBONE, E. & LUX, H. D. (1984). A low voltage-activated, fully inactivating Ca channel in vertebrate sensory neurones. *Nature* 310, 501-502.
- CARMELIET, E. & VEREECKE, J. (1979). Electrogenesis of the action potential and automaticity. In *Handbook of Physiology*, section 2: *The Cardiovascular System*, vol. 1, *The Heart*, ed. BERNE, R. M., SPERELAKIS, N. & GEIGER, S. R., pp. 269-334. Bethesda, MD: American Physiological Society.
- COGNARD, C., LAZDUNSKI, M. & ROMEY, G. (1986). Different types of Ca^{2+} channels in mammalian skeletal muscle cells in culture. *Proceedings of the National Academy of Sciences of the U.S.A.* 83, 517-521.
- DEITMER, J. W. (1984). Evidence for two voltage-dependent calcium currents in the membrane of the ciliate *Stylonychia*. *Journal of Physiology* 355, 137-159.
- DI FRANCESCO, D., FERRONI, A., MAZZANTI, M. & TROMBA, C. (1986). Properties of the hyperpolarizing-activated current (i_f) in cells isolated from the rabbit sino-atrial node. *Journal of Physiology* 377, 61-88.
- FEDULOVA, S. A., KOSTYUK, P. G. & VESELOVSKY, N. S. (1985). Two types of calcium channels in the somatic membrane of new-born rat dorsal root ganglion neurones. *Journal of Physiology* 359, 431-446.
- FOX, A. P. & KRASNE, S. (1948). Two calcium currents in *Neanthes arenaceodentatus* egg cell membranes. *Journal of Physiology* 356, 491-505.
- HAGIWARA, N., IRISAWA, H. & KAMEYAMA, M. (1987). Transient-type calcium current contributes to the pacemaker potential of rabbit sino-atrial node. *Journal of Physiology* 382, 104P.
- HAGIWARA, S., OZAWA, S. & SAND, O. (1975). Voltage-clamp analysis of two inward current mechanisms in egg cell membrane of a starfish. *Journal of General Physiology* 65, 617-644.
- HAMILL, O. P., MARTY, A., NEHER, E., SAKMANN, B. & SIGWORTH, F. J. (1981). Improved patch-clamp techniques for high-resolution current recording from cells and cell-free membrane patches. *Pflügers Archiv* 391, 85-100.
- HESS, P. & TSIEN, R. W. (1984). Mechanism of ion permeation through calcium channels. *Nature* 309, 453-456.
- HODGKIN, A. L. & HUXLEY, A. F. (1952). A quantitative description of membrane current and its application to conduction and excitation in nerve. *Journal of Physiology* 117, 500-544.
- ISENBERG, G. & KLÖCKNER, U. (1982a). Isolated bovine ventricular myocytes: Characterization of the action potential. *Pflügers Archiv* 395, 19-29.
- ISENBERG, G. & KLÖCKNER, U. (1982b). Calcium currents of isolated bovine ventricular myocytes are fast and of large amplitude. *Pflügers Archiv* 395, 30-41.
- KOKUBUN, S., NISHIMURA, M., NOMA, A. & IRISAWA, H. (1982). Membrane currents in the rabbit atrioventricular node cell. *Pflügers Archiv* 393, 15-22.
- LLINÁS, R. & YAROM, Y. (1981a). Electrophysiology of mammalian inferior olivary neurones in vitro: Different types of voltage-dependent ionic conductances. *Journal of Physiology* 315, 549-567.
- LLINÁS, R. & YAROM, Y. (1981b). Properties and distributions of ionic conductances generating electroresponsiveness of mammalian inferior olivary neurones in vitro. *Journal of Physiology* 315, 569-584.
- MITRA, R. & MORAD, M. (1985). Evidence of two types of calcium channels in guinea-pig ventricular myocytes. *Journal of General Physiology* 86, 22-23a.
- MITRA, R. & MORAD, M. (1986). Two types of calcium channels in guinea pig ventricular myocytes. *Proceedings of the National Academy of Sciences of the U.S.A.* 83, 5340-5344.
- NAKAYAMA, T., KURACHI, Y., NOMA, A. & IRISAWA, H. (1984). Action potential and membrane currents of single pacemaker cells of the rabbit heart. *Pflügers Archiv* 402, 248-257.
- NILIUS, B., HESS, P., LANSMAN, J. B. & TSIEN, R. W. (1985). A novel type of cardiac calcium channel in ventricular cells. *Nature* 316, 443-446.
- NILIUS, B. (1986). Possible functional significance of a novel type of cardiac Ca channel. *Biochimica et biophysica acta* 45, suppl. 8, K37-45.
- NOBLE, D. (1984). The surprising heart: a review of recent progress in cardiac electrophysiology. *Journal of Physiology* 353, 1-50.

- NOMA, A., KOTAKE, H. & IRISAWA, H. (1980). Slow inward current and its role mediating the chronotropic effect of epinephrine in the rabbit sinoatrial node. *Pflügers Archiv* 388, 1-9.
- NOMA, A., MORAD, M. & IRISAWA, H. (1983). Does the "pacemaker current" generate the diastolic depolarization in the rabbit SA node cells? *Pflügers Archiv* 397, 190-194.
- NOWYCKY, M. C., FOX, A. P. & TSIEN, R. W. (1985). Three types of neuronal calcium channel with different calcium agonist sensitivity. *Nature* 316, 440-443.
- REUTER, H. (1973). Divalent cations as charge carriers in excitable membrane. *Progress in Biophysics and Molecular Biology* 16, 1-43.
- REUTER, H., KOKUBUN, S. & PRODHOM, B. (1986). Properties and modulation of cardiac calcium channels. *Journal of Experimental Biology* 124, 191-201.
- TRAUTWEIN, W. & KASSEBAUM, D. G. (1961). On the mechanism of the spontaneous impulse generation in the pacemaker of the heart. *Journal of General Physiology* 45, 317-330.
- TSUNOO, A., YOSHII, M. & NARAHASHI, T. (1985). Differential block of two calcium channels in neuroblastoma cells. *Biophysical Journal* 47, 433a.
- YANAGIHARA, K. & IRISAWA, H. (1980a). Inward current activated during hyperpolarization in the rabbit sinoatrial node cell. *Pflügers Archiv* 385, 11-19.
- YANAGIHARA, K. & IRISAWA, H. (1980b). Potassium current during the pacemaker depolarization in rabbit sinoatrial node cell. *Pflügers Archiv* 388, 255-260.

T-Type Ca^{2+} Current Is Expressed in Hypertrophied Adult Feline Left Ventricular Myocytes

H. Bradley Nuss, Steven R. Houser

Macroscopic T-type Ca^{2+} currents, which are often observed in fetal and neonatal cardiac muscle cells, were not found in normal (0 of 17) adult feline ventricular myocytes. However, they were present in most (15 of 21) myocytes isolated from adult feline left ventricles with long-standing pressure-overload-induced hypertrophy. This is the first study to provide evidence in a large mammal, such as the cat, that T-type Ca^{2+} channels may be reexpressed in adults in association with hypertrophy resulting from slow progressive pressure overload. Importantly, this expression was stable for the duration of the hypertrophy process and was not associated with abrupt pressure overload. T-type Ca^{2+} currents were separated from L-type Ca^{2+} currents by exploiting the differences in their voltage dependence of steady-state inactivation. Depolarizations from -80 mV revealed a rapidly activating inward current that peaked in magnitude at -30 mV (-1.8 ± 0.9 [mean \pm SD] pA/pF) and fully inactivated within 100 milliseconds in 15 of 21 hypertrophied myocytes studied. Further depolarizations activated progressively less T-type Ca^{2+} current, so that at $+10$ mV the L-type Ca^{2+} current predominated. In the hypertrophied myocytes that demonstrated both T-type and L-type Ca^{2+} currents, two distinct peaks occurred in their current-voltage relations. T-type Ca^{2+} currents were not evident in any of the 17 normal adult feline left ventricular myocytes studied. The purpose of T-type Ca^{2+} currents in hypertrophy is unclear. However, their presence may make hypertrophied myocardium more prone to spontaneous action potentials and increase the likelihood for arrhythmias in partially depolarized hypertrophied myocardium. (*Circ Res.* 1993;73:777-782.)

KEY WORDS • T-type Ca^{2+} currents • cardiac hypertrophy • ventricular myocytes • patch clamp

Hemodynamic overloading, such as pressure overload, is one factor known to stimulate the adult heart to enter an active growth phase.¹ Slow progressive pressure overload produces severe hypertrophy of the myocytes that make up the overloaded ventricle.²⁻⁴ Associated with this hypertrophic growth is prolongation of the myocyte action potential duration⁴⁻⁶ and a propensity for arrhythmias.⁷ The membrane basis for the electrophysiological alterations of the hypertrophied myocyte has been examined. These studies have shown that, in general, small but significant alterations in L-type Ca^{2+} current ($I_{\text{Ca,L}}$),^{5,8} delayed rectifier K^+ current,^{6,9} and inward rectifier K^+ current⁹ contribute to the action potential prolongation of the hypertrophied myocyte. The putative role of the T-type Ca^{2+} current ($I_{\text{Ca,T}}$) in the electrical or mechanical changes during hypertrophy has not, to our knowledge, been studied to date. One possibility is that alterations in T-type Ca^{2+} channel density are involved in hypertrophy-related arrhythmias.

The objective of this study was to determine if the expression of $I_{\text{Ca,T}}$ is altered with hypertrophy. We have not previously observed $I_{\text{Ca,T}}$ in normal adult feline

ventricular myocytes.¹⁰ However, there is some evidence that T-type Ca^{2+} channels are developmentally regulated and that expression varies with cardiac cell type.¹¹⁻¹³ In support of this idea, the largest $I_{\text{Ca,T}}$ density has been recorded in embryonic chick ventricular cells.¹⁴ In addition, in mouse¹⁵ and rat¹⁶ skeletal muscle, $I_{\text{Ca,T}}$ decreases in a progressive manner during postnatal development. Since hypertrophy recapitulates the fetal phenotype,^{17,18} it seemed possible that $I_{\text{Ca,T}}$ might be altered in the hypertrophied heart. In the present study, we confirmed that $I_{\text{Ca,T}}$ was not present in normal adult feline ventricular myocytes and observed that it was present in a large percentage of hypertrophied myocytes.

Materials and Methods

Model of Left Ventricular Hypertrophy

The chronic feline model of left ventricular hypertrophy used in this study was recently described in detail² and was modified from a model of right ventricular hypertrophy described by Cooper et al.¹⁹ A band of fixed diameter was placed around the aorta of immature animals (1 kg) such that minimal constriction of the aorta occurred at the time of surgery. A slow progressive pressure overload developed on the left ventricle during the growth of the animals into adulthood.² This long-standing pressure overload resulted in severe cardiac hypertrophy, and myocytes isolated from these hearts exhibited alterations in both electrophysiological and contractile properties.^{2,8}

Received March 26, 1993; accepted June 30, 1993.

From the Department of Physiology, Temple University School of Medicine, Philadelphia, Pa.

Correspondence to Steven R. Houser, PhD, Temple University School of Medicine, Department of Physiology, 3420 N. Broad Street, Philadelphia, PA 19140.

Isolation of Ventricular Myocytes

Myocytes were disaggregated from feline hearts using cell isolation techniques developed in this laboratory²⁰ with slight modifications. On the day of study, the animal was given an intramuscular injection of ketamine (50 mg/kg) and acepromazine (0.5 mg/kg). The heart was then rapidly excised and rinsed in saline until the chambers were clear of blood. After cannulation of the aorta, the coronaries were perfused with nominally Ca^{2+} -free modified Krebs-Henseleit buffer²⁰ (KHB) until the coronary circulation was cleared of blood cells. Perfusion was continued with recirculating KHB containing collagenase (180 U/mL, type II, Worthington Biochemical Corp, Freehold, NJ) and gassed with 95% O_2 -5% CO_2 to maintain its pH at 7.4. The flow rate was adjusted to achieve an initial perfusion pressure of 80 to 100 mm Hg. After the perfusion pressure dropped and the heart tissue became flaccid, the left ventricle was dissected free from the rest of the heart. This tissue was minced in the remaining KHB solution containing collagenase and gently shaken for 5 minutes in a shaking water bath. The cells were filtered through 300- μm meshing, rinsed with KHB, centrifuged, and resuspended in KHB containing 1% serum albumin and 1 mmol/L Ca^{2+} . The cells were kept at room temperature (24°C) and gassed with 95% O_2 -5% CO_2 . All solutions used in the isolation procedure were maintained at 37°C. Only myocytes from the left ventricles of normal and aortic-banded cats were used in these experiments. All experiments were performed within 16 hours of isolation.

Solutions

A drop of cell-containing solution was placed in the experimental chamber. After the myocytes had settled to the bottom, perfusion was begun with a modified Tyrode's solution composed of (mmol/L) NaCl, 150; KCl, 5.4; MgCl_2 , 1.2; dextrose, 10; pyruvate, 2.5; HEPES, 5; and CaCl_2 , 1 (pH 7.4). The pipette filling solution was composed of (mmol/L) CsCl, 125; tetraethylammonium chloride (TEA-Cl), 20; EGTA, 10; HEPES, 10; and $\text{K}_2\text{-ATP}$, 5 (pH 7.3).

Upon the attainment of gigaohm seals, suction was used to disturb the patch of membrane enclosed by the pipette tip. Dialysis of the pipette filling solution occurred in 3 to 5 minutes using 2- to 3-M Ω pipettes as evidenced by depolarization of membrane potential from -70 mV to less than -40 mV. The cells were then superfused with the 0 Na^+ recording solution without developing contracture. Depolarizations from -80 to -40 mV were used to monitor the exchange of solutions. After the disappearance of the Na^+ current, an additional 3 minutes of continuous perfusion with the recording solution ensured that the removal of Na^+ from the bathing solution was complete. The recording solution was composed of (mmol/L) choline chloride, 140; CsCl, 5; dextrose, 5.5; HEPES, 5; MgCl_2 , 0.5; 4-aminopyridine, 2; and CaCl_2 , 5 (pH 7.4). All experiments were conducted at 35°C.

Whole-Cell Voltage Clamp

Whole-cell membrane currents were recorded by the patch-clamp method described by Hamill et al.²¹ Pipettes were fabricated from filament-containing glass

capillary tubes (1.5 mm outer diameter, World Precision Instruments, Sarasota, Fla) on a microelectrode puller (model P-87, Sutter Instruments Co, Novato, Calif) and then fire-polished. Pipettes had tip resistances of 2 to 3 M Ω when filled with the internal solution. The bath potential was recorded with a 3 mol/L KCl agar-Ag/AgCl reference electrode. Voltage clamp was achieved using the discontinuous switch clamp technique^{22,23} (Axoclamp-2 amplifier, Axon Instruments, Burlingame, Calif). Careful adjustment of capacity neutralization, steady-state gain, and phase shift produced capacity transients with time constants of less than 1 millisecond.^{5,23} The maximum peak voltage error produced when recording a peak current of 3 nA in a myocyte with an input capacitance of 250 pF was calculated to be in the range of 1 to 2 mV at a switching frequency of 10 to 15 kHz.^{5,22,23}

The voltage-clamp protocols were controlled using PCLAMP software (version 5.5.1, Axon Instruments) on an IMB-AT computer. Membrane currents were digitized on-line with 12-bit resolution using a Labmaster interface analog to digital converter (Axon Instruments) and stored on hard disk for off-line analysis.

Myocyte input capacitance was calculated from data obtained while in the current-clamp mode immediately after obtaining access to the cell.⁵ Briefly, the slope conductance (ratio of current to voltage) was calculated from a small hyperpolarizing current step and the resultant voltage change. The membrane time constant was calculated from the decay of voltage at the end of the current pulse. The input capacitance was given by the product of the slope conductance and the membrane time constant.

Data Analysis and Statistics

Peak current measurements and curve-fitting were accomplished using PCLAMP software (version 5.5.1, Axon Instruments). All measurements are reported as mean \pm SD. Student's *t* test was used to determine if measurements in hypertrophied myocytes were significantly different from measurements in normal myocytes.

Results

Hemodynamics and Cell Properties

The general characteristics of the animals used in this study have been reported previously.² In brief, there were large increases, more than 70 mm Hg, in the pressure gradient across the constricting band as the animals grew. In addition, the ratio of heart weight to body weight increased by more than 100%, documenting severe hypertrophy in response to this pressure overload. Myocytes isolated from these hearts had prolonged action potential and contractile durations characteristic of hypertrophied myocardium.^{2,8} Myocytes from these same hearts were used in the experiments described below.

Separation of $I_{\text{Ca,T}}$ and $I_{\text{Ca,L}}$

The voltage-clamp protocols were designed to identify with certainty macroscopic $I_{\text{Ca,T}}$ in normal and hypertrophied feline ventricular myocytes. Approximately 40 mV separates the voltage dependence of steady-state inactivation of $I_{\text{Ca,T}}$ and $I_{\text{Ca,L}}$.^{11,24-26} Preliminary experiments confirmed that conditioning pulses (7

seconds) to -80 mV removed inactivation from functional T-type Ca^{2+} channels when present. Conditioning pulses to -40 mV inactivated T-type Ca^{2+} channels, when present, without affecting L-type Ca^{2+} channel availability. Removal of Na^+ from the bath and internal solutions eliminated both tetrodotoxin-sensitive and tetrodotoxin-resistant Na^+ currents in feline ventricular myocytes.²⁷ Outward K^+ currents were minimized by the substitution of Cs^{2+} for K^+ in combination with internal TEA-Cl (20 mmol/L) and external 4-aminopyridine (2 mmol/L). Depolarizations from -80 mV could elicit both $I_{Ca,T}$ and $I_{Ca,L}$, whereas depolarizations from -40 mV would elicit only $I_{Ca,L}$. The difference in the current recordings obtained from the two conditioning potentials represents the $I_{Ca,T}$ elicited at that test potential.

Preliminary experiments indicated that small amounts of rundown of $I_{Ca,L}$ or small changes in the amount of leak current could hamper the identification of $I_{Ca,T}$ in the difference currents. In addition, a depolarized conditioning potential had to be selected so that $I_{Ca,L}$ was not partially inactivated.²⁶ To avoid these problems, the voltage was stepped to a given test potential first from a holding potential of -80 mV and 7 seconds later from -40 mV. The -40 -mV conditioning potential, used to inactivate $I_{Ca,T}$, did not inactivate any $I_{Ca,L}$ because the Ca^{2+} currents elicited after the -40 - and -80 -mV conditioning pulses were identical at 0 mV and more positive test potentials (Figs 1 and 3).

$I_{Ca,T}$ in Hypertrophied Myocytes

$I_{Ca,T}$ was not evident in any of the current recordings obtained from the 17 normal myocytes studied from eight different cats (Fig 1). The Ca^{2+} currents elicited after the -80 -mV conditioning pulse were measurably identical in peak magnitude to $I_{Ca,L}$ elicited from -40 mV at every test potential (Fig 2). On the basis of this negative finding and previous unpublished negative observations from this laboratory,¹⁰ we suggest that normal adult feline ventricles either lack or have a very low density of functional T-type Ca^{2+} channels.

Significant $I_{Ca,T}$ s were recorded in 15 of 21 hypertrophied ventricular myocytes studied (Fig 3). The remaining 6 hypertrophied myocytes did not have an obvious $I_{Ca,T}$. Hypertrophied myocytes were studied from nine different aortic-banded cats.

In the hypertrophied myocytes, $I_{Ca,T}$ first became evident on depolarization to -45 mV, peaked in magnitude at -30 mV, grew smaller with further depolarizations, and became undetectable by 0 mV (Fig 4). Peak $I_{Ca,T}$ in the hypertrophied myocytes measured -0.47 ± 0.25 nA ($n=15$) with 5 mmol/L external Ca^{2+} . $I_{Ca,T}$ magnitudes were measured as the difference between the peak current and the steady-state current at 500 milliseconds. The corresponding $I_{Ca,T}$ density was -1.8 ± 0.9 pA/pF ($n=14$) once normalized by myocyte input capacitance. $I_{Ca,T}$ inactivation at -30 mV was best fit by a single exponential decay with an inactivation time constant (τ) of 9.3 ± 1.8 milliseconds ($n=14$). This value is similar to those defined by others in previous studies.^{11,25,28} When myocytes were exposed to Cd^{2+} (50 to 200 μ mol/L $CdCl_2$), $I_{Ca,L}$ was eliminated, but a significant portion (approximately 50%) of $I_{Ca,T}$ remained (data not shown). The remaining $I_{Ca,T}$ could be eliminated by either Ni^{2+} (1 mmol/L $NiCl_2$) or removal of extracellular Ca^{2+} . These data show that the current

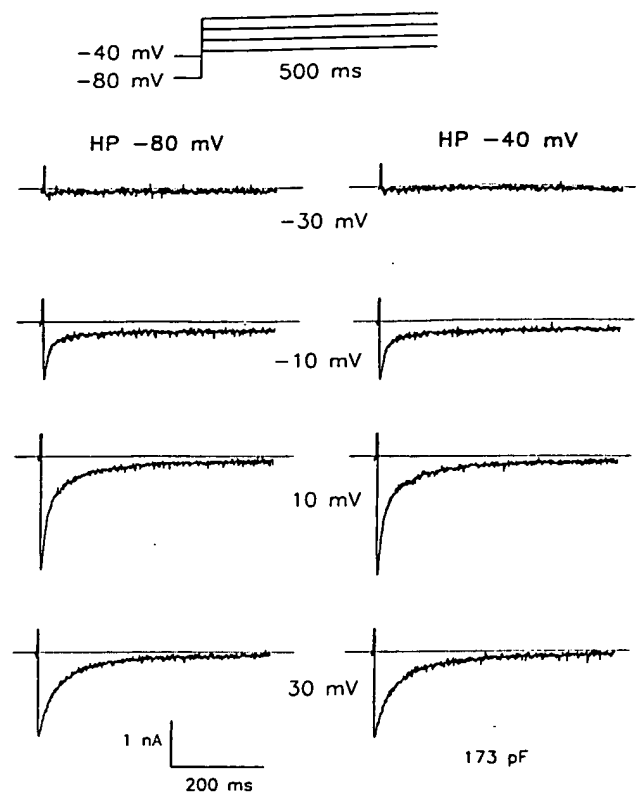


FIG 1. Raw current tracings are shown for a representative normal ventricular myocyte. Membrane potential was stepped to the test potentials indicated for 500 milliseconds. At each test potential, Ca^{2+} current was elicited first from a holding potential (HP) of -80 mV and 7 seconds later from an HP of -40 mV. Zero current level is indicated by the dotted line. Na^+ currents were eliminated by using a Na^+ -free recording solution. Outward currents were minimized by Cs^{2+} substitution of K^+ , internal tetraethylammonium chloride (20 mmol/L), and external 4-aminopyridine (2 mmol/L). The charge carrier was Ca^{2+} (5 mmol/L). Cell capacitance was 173 pF.

we observed in hypertrophied myocytes has properties similar to $I_{Ca,T}$ studied previously.^{11,24,29}

$I_{Ca,L}$ in Hypertrophied Myocytes

With 5 mmol/L Ca^{2+} as the charge carrier, peak $I_{Ca,L}$, elicited from -40 to $+10$ mV, in hypertrophied left ventricular myocytes (-2.8 ± 0.8 nA, $n=21$) was not different from normal myocytes (-2.8 ± 0.9 nA, $n=17$). However, after correction for individual myocyte input capacitance, peak $I_{Ca,L}$ density in hypertrophied myocytes (-11.3 ± 1.9 pA/pF, $n=19$) was significantly ($P < .01$) reduced to 77% of normal (-14.6 ± 3.3 pA/pF, $n=16$) at $+10$ mV. These data are summarized in Fig 5. Inactivation of $I_{Ca,L}$ at $+10$ mV was best described as a biexponential decaying process. The time course of both the fast and slow decay processes were slower for hypertrophied (τ_{fast} , 14.4 ± 2.7 milliseconds; τ_{slow} , 80.5 ± 14.1 milliseconds; $n=21$) than normal (τ_{fast} , 10.4 ± 1.7 milliseconds; τ_{slow} , 78.1 ± 9.9 milliseconds; $n=17$) myocytes. Only the fast component was slowed significantly ($P < .01$). The magnitude of the slow and maintained components of $I_{Ca,L}$ were reduced significantly in hypertrophied myocytes (see the Table). These results are similar to those we have observed previous-

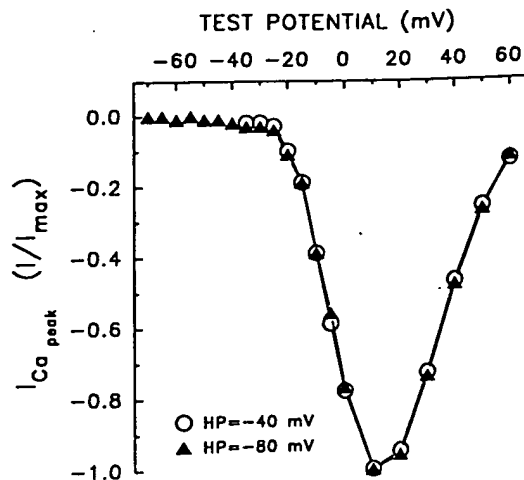


FIG 2. Graph shows normalized peak Ca^{2+} current (normalized $I_{\text{Ca,peak}} [I_{\text{max}}]$)–voltage relation for the representative normal myocyte shown in Fig 1. Currents were alternately elicited from holding potentials (HPs) of -80 mV (\blacktriangle) and -40 mV (\circ). There is no evidence of T-type Ca^{2+} current in the -80 -mV current-voltage relation at negative test potentials.

ly.^{5,8} They show that peak $I_{\text{Ca,L}}$ density is reduced in severely hypertrophied myocytes. Total Ca^{2+} influx via L-type Ca^{2+} channels may not be significantly altered because $I_{\text{Ca,L}}$ inactivation is slowed.

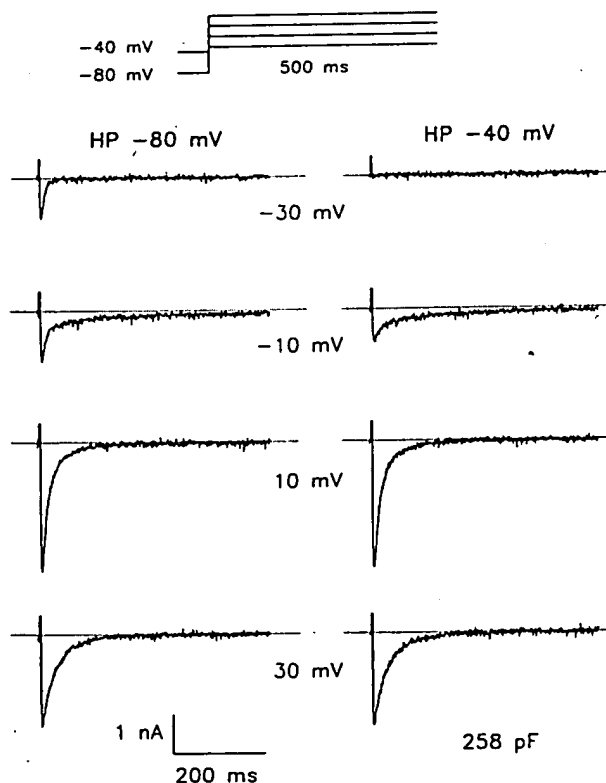


FIG 3. Raw current tracings are shown for a representative hypertrophied ventricular myocyte. HP indicates holding potential. T-type Ca^{2+} current is evident in the current elicited at -30 mV from -80 mV by comparison with the current tracing obtained from -40 mV. Voltage-clamp protocol and solutions are as described in Fig 1. Cell capacitance was 258 pF.

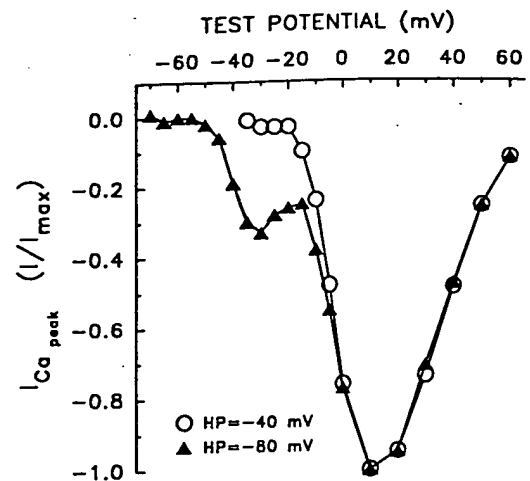


FIG 4. Graph shows normalized peak Ca^{2+} current (normalized $I_{\text{Ca,peak}} [I_{\text{max}}]$)–voltage relation for the representative hypertrophied myocyte shown in Fig 2. HP indicates holding potential. Currents were alternately elicited from -80 mV (\blacktriangle) and -40 mV (\circ). The difference in the current-voltage relations at negative test potentials is due to the maximal activation of the T-type Ca^{2+} current at potentials (-30 mV) where the L-type Ca^{2+} current is minimally activated.

Discussion

The present study shows that slow progressive pressure overload of the feline left ventricle induces severe hypertrophy that is associated with a reduction in $I_{\text{Ca,L}}$ and the appearance of $I_{\text{Ca,T}}$. Although the physiological role of T-type Ca^{2+} channels is not clear at present, the largest $I_{\text{Ca,T}}$ densities have been recorded in embryonic¹⁴ and neonatal²⁸ ventricular myocytes. Increases in $I_{\text{Ca,T}}$ have also been observed in myocytes from growth hormone-stimulated rats.³⁰ Thus, $I_{\text{Ca,T}}$ has been associ-

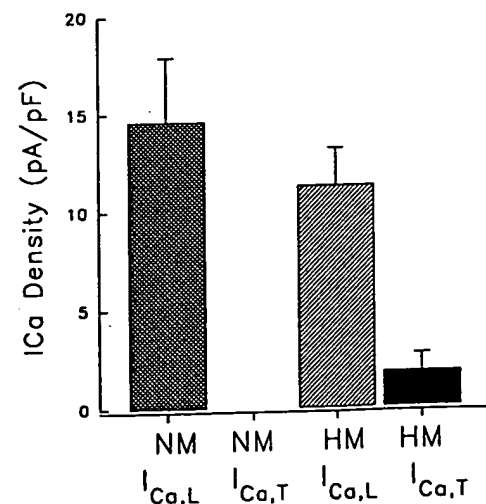


FIG 5. Bar graph compares Ca^{2+} current (I_{Ca} , T-type [$I_{\text{Ca,T}}$] and L-type [$I_{\text{Ca,L}}$]) densities in normal myocytes (NM) and hypertrophied myocytes (HM). $I_{\text{Ca,L}}$ density is significantly ($P < .01$) reduced in HM (-11.3 ± 1.9 pA/pF, $n = 19$) to 77% of that measured in NM (-14.6 ± 3.3 pA/pF, $n = 16$) at $+10$ mV. Mean $I_{\text{Ca,T}}$ density equaled -1.8 ± 0.9 pA/pF in 15 of 21 HM studied and was not present (or unmeasurably small) in NM ($n = 17$). Data are indicated as mean \pm SD.

Inactivation Parameters of L-Type Ca^{2+} Current

	τ_{fast} , ms	τ_{slow} , ms	Amp_{fast} , nA	Amp_{slow} , nA	SS, nA
NM	10.4 ± 1.7	78.1 ± 9.9	-1.8 ± 0.6	-1.0 ± 0.2	-0.2 ± 0.1
HM	$14.4 \pm 2.7^*$	80.5 ± 14.1	-1.8 ± 0.5	$-0.7 \pm 0.2^*$	$-0.1 \pm 0.1^*$

τ_{fast} and τ_{slow} indicate fast and slow time constants of inactivation, respectively; Amp_{fast} and Amp_{slow} , fast and slow amplitudes, respectively; SS, maintained (steady-state) component; NM, normal myocytes; and HM, hypertrophied myocytes. Values are mean \pm SD.

The inactivation of the L-type Ca^{2+} current in 17 NM and 21 HM was fit as a biexponential decaying process.

* $P < .01$ vs NM.

ated with active growth phases, suggesting that it is developmentally regulated. The present results suggest that the cell-signaling process that produces hypertrophy also results in a reduced density of one type of Ca^{2+} channel (L-type) and an increased density of another type (T-type), implying differential regulation.

Gene Expression in Hypertrophy

A number of previous studies support the idea that an increase in hemodynamic loading in adults signals a general reexpression of fetal phenotypes (see References 17 and 31). Pressure or volume overloading of the adult rat heart induces β -myosin heavy chain messenger RNA and β -myosin heavy chain proteins, which comprise V_3 myosin.³²⁻³⁴ The V_3 myosin isozyme predominates in embryonic ventricle,³⁵ is replaced by V_1 myosin in the young adult, but is reexpressed in hypertrophied adult ventricles.^{32,33} The idea that hypertrophy induces genes encoding fetal proteins has recently been reviewed.^{17,31} The fact that I_{CaT} predominates over I_{CaL} in embryonic ventricles,¹⁴ is small or absent in adult ventricular myocytes, and then reemerges in hypertrophied adult feline ventricles is consistent with the idea that the T-type Ca^{2+} channel gene(s) is developmentally regulated.

 I_{CaT} -Mediated Ca^{2+} Influx in Hypertrophy

The mean I_{CaT} density recorded in hypertrophied feline ventricular myocytes (-1.8 ± 0.9 pA/pF) is comparable to that found in rabbit sinoatrial node cells (-2.1 pA/pF)²⁹ and canine Purkinje cells (-1.7 and -2.9 pA/pF).^{11,25} Smaller I_{CaT} densities have been recorded in rat atrial (-0.4 pA/pF)³⁰ and guinea pig ventricular (-0.6 pA/pF)²⁶ myocytes. Larger I_{CaT} densities have been recorded only in chick embryonic (-4.2 pA/pF)¹⁴ and cultured neonatal rat (-3.0 pA/pF)²⁸ ventricular myocytes.

Our finding of I_{CaT} in hypertrophied ventricular myocytes but not in normal adult ventricular myocytes (at least with the approach we used) suggests that Ca^{2+} influx via T-type Ca^{2+} channels might be associated with cell growth. Xu and Best³⁰ found that growth hormone-secreting tumors, which result in volume overload and cardiac hypertrophy, increase I_{CaT} in rat atrial myocytes. Furukawa et al²⁸ found that the vasoconstrictive peptide endothelin-1, which induces hypertrophy and increased DNA and protein synthesis,³⁶ increases I_{CaT} in cultured neonatal rat ventricular myocytes. The regulation of I_{CaT} expression and its precise link to the growth that occurs in cardiac hypertrophy cannot be fully studied at pres-

ent because the gene(s) encoding this membrane protein has not, to our knowledge, yet been cloned.

Expression of T-Type Ca^{2+} Channels in Hypertrophy

We have found evidence that T-type Ca^{2+} channels are expressed during hypertrophy in the adult feline ventricle, where there is normally no measurable I_{CaT} , and that the expression of these channels is stable throughout long-standing hypertrophy. The expression of T-type Ca^{2+} channels in the adult feline ventricle may be intimately associated with its reentry into an active growth phase during pressure-overload hypertrophy. In addition to being involved in growth and development, I_{CaT} could also influence basic electrophysiological characteristics of the hypertrophied ventricle, thereby making hypertrophied hearts more prone to arrhythmias.

Acknowledgments

This study was supported by National Institutes of Health Grant RO1 HL-33921 to Dr Houser.

References

- Morgan HE, Baker KB. Cardiac hypertrophy: mechanical, neural, and endocrine dependence. *Circulation*. 1991;83:13-25.
- Bailey BA, Houser SR. Calcium transients in feline left ventricular myocytes with hypertrophy induced by slow progressive pressure overload. *J Mol Cell Cardiol*. 1992;24:365-373.
- TenEick RE, Bassett AL, Robertson LL. Possible electrophysiological basis for decreased contractility associated with myocardial hypertrophy in the cat: a voltage clamp approach. In: Alpert NR, ed. *Perspectives in Cardiovascular Research: Myocardial Hypertrophy and Failure*. New York, NY: Raven Press, Publishers; 1983;7: 245-259.
- Hemwall EL, Duthinh V, Houser SR. Comparison of slow response action potentials from normal and hypertrophied myocardium. *Am J Physiol*. 1984;246:H675-H682.
- Kleiman RB, Houser SR. Calcium currents in normal and hypertrophied isolated feline ventricular myocytes. *Am J Physiol*. 1988; 255:H1434-H1442.
- Nuss HB, Houser SR. Reduced delayed rectifier potassium current causes action potential prolongation in hypertrophied feline left ventricular myocytes. *Circulation*. 1990;82(suppl 3):III-522. Abstract.
- January CT, Riddle JM, Salata JJ. A model for early afterdepolarizations: induction with the Ca^{2+} channel agonist Bay K 8644. *Circ Res*. 1988;62:563-571.
- Nuss HB, Houser SR. Voltage dependence of contraction and calcium current in severely hypertrophied feline ventricular myocytes. *J Mol Cell Cardiol*. 1991;23:717-726.
- Kleiman RB, Houser SR. Outward currents in normal and hypertrophied feline ventricular myocytes. *Am J Physiol*. 1989;256: H1450-H1461.
- Hartmann HA, Mazzocca NJ, Kleiman RB, Houser SR. Effects of phenylephrine on calcium current and contractility of feline ventricular myocytes. *Am J Physiol*. 1988;255:H1173-H1180.
- Hirano Y, Fozzard HA, January CT. Characteristics of L- and T-type Ca^{2+} currents in canine cardiac Purkinje cells. *Am J Physiol*. 1989;256:H1478-H1492.
- Bean BP. Two kinds of calcium channels in canine atrial cells. *J Gen Physiol*. 1985;86:1-30.
- Niluis B, Hess P, Lansman JB, Tsien RW. A novel type of cardiac calcium channel in ventricular cells. *Nature*. 1985;316:443-446.
- Kawano S, DeHaan RL. Low-threshold current is major calcium current in chick ventricle cells. *Am J Physiol*. 1989;256:H1505-H1508.
- Gonoi T, Hasegawa S. Post-natal disappearance of transient calcium channels in mouse skeletal muscle: effects of denervation and culture. *J Physiol (Lond)*. 1988;401:617-637.
- Beam KG, Knudson CM. Effect of postnatal development on calcium currents and slow charge movement in mammalian skeletal muscle. *J Gen Physiol*. 1988;91:799-815.
- Swynghedauw B. Remodeling of the heart in chronic pressure overload. *Basic Res Cardiol*. 1993;86(suppl 1):99-105.
- Izumo S, Nadal-Ginard B, Mahdavi V. Protooncogene induction and reprogramming of cardiac gene expression produced by pressure overload. *Proc Natl Acad Sci U S A*. 1988;85:339-343.

19. Cooper G IV, Tomanek RJ, Ehrhardt JC, Marcus ML. Chronic progressive pressure overload of the cat right ventricle. *Circ Res*. 1992;71:488-497.
20. Silver LH, Hemwall EL, Marino TA, Houser SR. Isolation and morphology of calcium-tolerant feline ventricular myocytes. *Am J Physiol*. 1983;245:H891-H896.
21. Hamill OP, Marty A, Neher E, Sakmann B, Sigworth FJ. Improved patch-clamp techniques for high-resolution current recording from cells and cell-free membrane patches. *Pflügers Arch*. 1981;391:43-55.
22. Finkel AS, Redman S. Theory and operation of a single micro-electrode voltage clamp. *J Neurosci Methods*. 1984;11:101-127.
23. Jones SW. Sodium currents in dissociated bull-frog sympathetic neurones. *J Physiol (Lond)*. 1987;389:605-627.
24. Fox AP, Nowicky MC, Tsien RW. Kinetic and pharmacological properties distinguishing three types of calcium currents in chick sensory neurones. *J Physiol (Lond)*. 1987;394:149-172.
25. Tseng GN, Boyden PA. Different effects of intracellular Ca and protein kinase C on cardiac T and L Ca currents. *Am J Physiol*. 1991;261:H364-H379.
26. Balke CW, Rose WC, Marban E, Wier WG. Macroscopic and unitary properties of physiological ion flux through T-type Ca^{2+} channels in guinea-pig heart cells. *J Physiol (Lond)*. 1992;456:247-265.
27. Bahinski A, Kleiman RB, Hartmann HA, Houser SR. Two TTX-insensitive inward currents in feline ventricular myocytes. *Biophys J*. 1987;51:114a. Abstract.
28. Furukawa T, Ito H, Nitta J, Tsujino M, Adachi S, Hiroe M, Marumo F, Sawanobori T, Hiraoka M. Endothelin-1 enhances calcium entry through T-type calcium channels in cultured neonatal rat ventricular myocytes. *Circ Res*. 1992;71:1242-1253.
29. Hagiwara N, Irisawa H, Kameyama M. Contribution of two type of calcium currents to the pacemaker potentials of rabbit sino-atrial node cells. *J Physiol (Lond)*. 1988;395:233-253.
30. Xu X, Best PM. Increase in T-type calcium current in atrial myocytes from adult rats with growth hormone-secreting tumors. *Proc Natl Acad Sci U S A*. 1990;87:4655-4659.
31. Marban E, Koretsune Y. Cell calcium, oncogenes, and hypertrophy. *Hypertension*. 1993;15:652-658.
32. Izumo S, Lompre A-M, Matsuoka R, Koren G, Schwartz K, Nadal-Ginard B, Mahdavi V. Myosin heavy chain messenger RNA and protein isoform transitions during cardiac hypertrophy. *J Clin Invest*. 1987;79:970-977.
33. Lompre A-M, Schwartz K, d'Albis A, Lacombe G, Van Thiem N, Swynghedauw B. Myosin isoenzyme redistribution in chronic heart overload. *Nature*. 1979;282:105-107.
34. Mercadier J-J, Lompre A-M, Wisnewsky C, Samuel J-L, Bercovici J, Swynghedauw B, Schwartz K. Myosin isoenzymic changes in several models of rat cardiac hypertrophy. *Circ Res*. 1981;49:525-532.
35. Chizzonite RA, Zak R. Regulation of myosin isoenzyme composition in fetal and neonatal rat ventricle by endogenous thyroid hormone. *J Biol Chem*. 1984;259:12628-12632.
36. Ito H, Hirata Y, Hiroe M, Tsujino M, Adachi S, Takamoto T, Nitta M, Taniguchi K, Marumo F. Endothelin-1 induces hypertrophy with enhanced expression of muscle-specific genes in cultured neonatal rat cardiomyocytes. *Circ Res*. 1991;69:209-215.

Properties
paration of
e from rat
2:710:154-

R.K. Smith
e UI. Lior-
AS: Trans-
induction
and stimu-
Proc Natl

David A. Self
Ka Bian
Santosh K. Mishra
Kent Hermsmeyer

LM, de
ces in the
ig growth
-1045.
own AM.
Masuko
rotein in
ogenesis.

Oregon Regional Primate Research Center
and Departments of Medicine and Cell
Biology and Anatomy, Oregon Health
Sciences University, Beaverton, Oreg., USA

Growth
sive and
3:1404-

derived
iveness
l 1986:

tal JR:
lism in
ii:348-

macro-
.. Am J

Robin-
sterol-
cteris-
J Pa-

, Pic-
es to
pri-

Key Words

Ca²⁺ channels
Hypertension
Membranes
L- and T-type channels
Inactivation recovery

Stroke-Prone SHR Vascular Muscle Ca²⁺ Current Amplitudes Correlate with Lethal Increases in Blood Pressure

Abstract

Studies on the possible causal relationship between the Ca²⁺ channel current density in the vascular muscle cell (VMC) and increases in blood pressure were extended by a comparison of stroke-prone spontaneously hypertensive rats (SP-SHR) with N/nih outbred normotensive rats. Maximal amplitudes of both L-type and T-type Ca²⁺ channel currents were significantly increased in SP-SHR without a difference in cell capacitance. SP-SHR peak current amplitudes in 20 mM Ba²⁺ averaged 446 ± 64 pA while N/nih averaged 156 ± 25 pA (clearly separated statistically). Both L-type and T-type Ba²⁺ currents (I_{Ba}) were significantly increased in SP-SHR, shown also by peak current frequency distributions. There was a significant shift to the left of both activation (7 mV) and inactivation (15 mV) current-voltage (I-V) plots. SP-SHR I_{Ba} recovery from inactivation was significantly slower (103 versus 61 ms) than in N/nih VMC. The increases in SP-SHR I_{Ba} amplitude under maximized conditions correlated with increases in blood pressure. Together with earlier observations of increased vascular muscle Ca²⁺ current density coexistent with blood pressure elevation in Kyoto-Wistar SHR, these data provide evidence for altered function of Ca²⁺ channels as a fundamental component of hypertension. Since the Ca²⁺ channel alterations exist in venous VMCs of newborn SP-SHR rats (in a low pressure blood vessel and at a time when increased Ca²⁺ current density could not be an effect of increased blood pressure), our results add to the growing evidence of Ca²⁺ channel abnormalities as a cause of genetic hypertension.

Introduction

Ca²⁺ channel current density due to dihydropyridine-sensitive L-type Ca²⁺ channels is greater in vascular muscle cells (VMC) of hypertensives than normotensives [1-4], and these increases may at least partly account for increased contraction in hypertension [5]. Increases in Ca²⁺ entry [6, 7] closely correlate with the exaggerated Ca²⁺ currents (I_{Ca}) leading to increased intracellular ionized Ca²⁺ [5, 8, 9]. The strong correlation of increased Ca²⁺ channel function and blood pressure has been formulated as a hypothesis, the Ca²⁺ channel hypothesis of hypertension (CCHH), to postulate a causal relationship between the increase in Ca²⁺ channel function and blood pressure in genetic hypertension [1, 10].

Independent support for increased I_{Ca} in newborn SHR has recently been published by Ohya et al. [11]. In addition, there is indirect evidence for increased I_{Ca} from SHR experiments using the Ca²⁺ agonist, Bay k8644, which had greater actions on hypertensives than normotensives [12, 13]. In numerous reviews, the correlation of factors that imply exaggerated Ca²⁺ channel function with genetic hypertension in SHR and humans has been pointed out [8, 14-21].

An extreme example of increased blood pressure is the stroke-prone spontaneously hypertensive rat (SP-SHR), developed by selection of rats based on blood pressures by Aoki [22] Okamoto and Aoki [23] and Okamoto et al. [24]. In these exceptionally hypertensive animals, a life span limited to 3-6 months is common because of the

This research was supported by National Institutes of Health grants HL38537, HL38645, NRSA HL08101 (to D.A.S.), and Fogarty International Fellowship TW04553 (to S.K.M.). ORPRC publication No. 1937.

Received:
April 1, 1994
Accepted after revision:
June 9, 1994

Dr. Kent Hermsmeyer
Oregon Regional Primate Research Center
505 NW 185th Avenue
Beaverton, OR 97006 (USA)

© 1994 S. Karger AG, Basel

sequelae, mainly stroke, of blood pressures of 200–300 mm Hg [25]. Abnormalities in vascular muscle that allow such lethal blood pressures are likely to be especially apparent in this animal model.

We have chosen SP-SHR to test the CCHH, which would predict an increased I_{Ca} beyond that in genetically SHR that show less severe blood pressure elevation [1, 10, 26]. We have constrained conditions to 2–4 days after cell isolation in a 20-mM Ba^{2+} external solution, a design which we have determined favors large current amplitudes. If I_{Ca} increases are a contributor to the genesis of hypertension, SP-SHR should have the largest Ca^{2+} channel current amplitudes. However, if there were no correlation of Ca^{2+} channel currents with the further increase in blood pressure, the hypothesis would fail this test.

Materials and Methods

Animals

SP-SHR obtained from the University of Iowa were raised in the SP-SHR colony in Oregon, along with N/nih normotensive rats obtained from the National Institutes of Health. Systolic blood pressures of the SP-SHR were in excess of 200 mm Hg by age 12 weeks and continued to climb to above 280 mm Hg in surviving rats by age 26 weeks. The N/nih represents a panel of outbred strains in which Wistar and seven other laboratory rat types commonly used as controls are combined to produce a normotensive reference. Tail cuff blood pressure measurements on 8- to 12-week-old females revealed average systolic blood pressures of 196 ± 11 mm Hg for SP-SHR ($n = 28$) and 122 ± 8 for the N/nih ($n = 37$). The animals were fed standard rat chow and had free access to tap water.

Single Cell Dispersion

VMC were isolated by enzymatic treatment of the more gentle type as used for preparation of cell cultures [27]. These experiments were carried out on VMC from azygous veins of neonatal rats because this preparation has the virtues of being both on the venous side of the circulation and from animals from which even the arterial blood pressure is below 100 mm Hg due to the early developmental state. Azygous veins were surgically isolated from SP-SHR or N/nih and placed in 25°C CV3M solution. CV3M consists of 85% minimum essential medium (MEM) and 15% horse serum (vol/vol) to which is added 4 mM *L*-glutamine, 20 mM HEPES at pH 7.3, 4 mM $NaHCO_3$, and 20 μ g/ml gentamicin. This solution serves both as the initial rinsing solution and also as the final nutrient solution for the VMCs. After the rinse in CV3M, tissue was soaked for 10 min in KG solution, consisting of (mM): 140 K-glutamate; 25 HEPES (final pH 7.3); 0.5 NaH_2PO_4 ; 4 $NaHCO_3$; 5.5 glucose, and 0.014 phenol red. KG served as the cell isolation solution, designed to avoid overloading the cells during enzyme exposure with Na^+ , Ca^{2+} , or Cl^- by reduction or elimination of these three ions. Pieces of azygous vein from all the pups of 1 litter were minced into about 1 mm (maximum dimension) pieces using fine dissecting scissors, and incubated at 37°C for 30 min in collagenase (30 mg in 10 ml KG solution containing 0.1 μ M Ca^{2+}). After 30 min, the collagenase supernatant was dis-

carded and sediment sequentially exposed to 3–4 incubations of 1 mg/ml trypsin in KG solution for 15 min. After each incubation in trypsin, supernatant was removed and placed in 25 ml of CV3M on ice. Supernatants were centrifuged at 200 g and 4°C for 15 min and the pellet resuspended in 10 ml of ice-cold CV3M, which was further centrifuged (always at 4°C) for 10 min at 200 g. After the supernatant had been removed, the remaining cells were resuspended in 10 ml of 37°C CV3M and transferred to a T25 Falcon plastic tissue culture flask for 1 h of sedimentation of fibroblasts at 37°C. Non-attached VMCs were transferred to centrifuge tubes, spun at 200 g, resuspended in CV3M plus 250 μ M bromodeoxyuridine (BrdU), diluted to a density of about 70,000 cells/ml, and plated on clean, 9 × 22 mm glass coverslips (in 35-mm sterile Petri plastic tissue culture dishes). VMCs were kept in 95% air, 5% CO_2 at 95–98% relative humidity, and 37°C for 2–4 days. The limited time after isolation helped to maximize both L- and T-type Ca^{2+} current amplitudes. BrdU and gentamicin were always removed at least 24 h before contracting VMCs were used for electrophysiological experiments.

Voltage-Clamp Recordings of Membrane Currents

Glass coverslips with attached VMCs were studied in 300 μ l laminar flow LF922 chambers [28] on the stage of a Zeiss Axiovert microscope. VMCs were perfused at room temperature (23°C) with ionic solution flow of 0.6 ml/min. Patch pipettes were pulled from thin-walled Corning 7052 glass using a Brown-Flaming micropipette puller (P87 Sutter Instruments Co.). Heat-polished pipettes with tip resistances of 2.5–4 M Ω were used in whole cell voltage-clamp configuration [29]. Currents were acquired by a high speed/low noise current-to-voltage amplifier mounted on a three-dimensional hydraulic micromanipulator. The reference potential of the pipette was set to 0, and a Gigaseal (about 10 G Ω) was established. Holding potential (V_H) was set to –60 mV and breakthrough by gentle suction gave intracellular access to the pipette.

Membrane currents were amplified by an Axopatch amplifier (Axon Instruments), low pass Bessel filtered at 1 kHz, monitored on a Tektronix 5031 two-channel storage oscilloscope, and digitized using a TL-1 A-D interface at 10 kHz sampling frequency with p-Clamp 5.5.1 software (Axon Instruments) controlled by a Hewlett-Packard computer [30]. After the first 2 min at $V_H = -60$ mV, V_H was made –80 mV, which served as the potential at all times except during the V_H or test potential (V_T) protocols, as specifically defined in the Results.

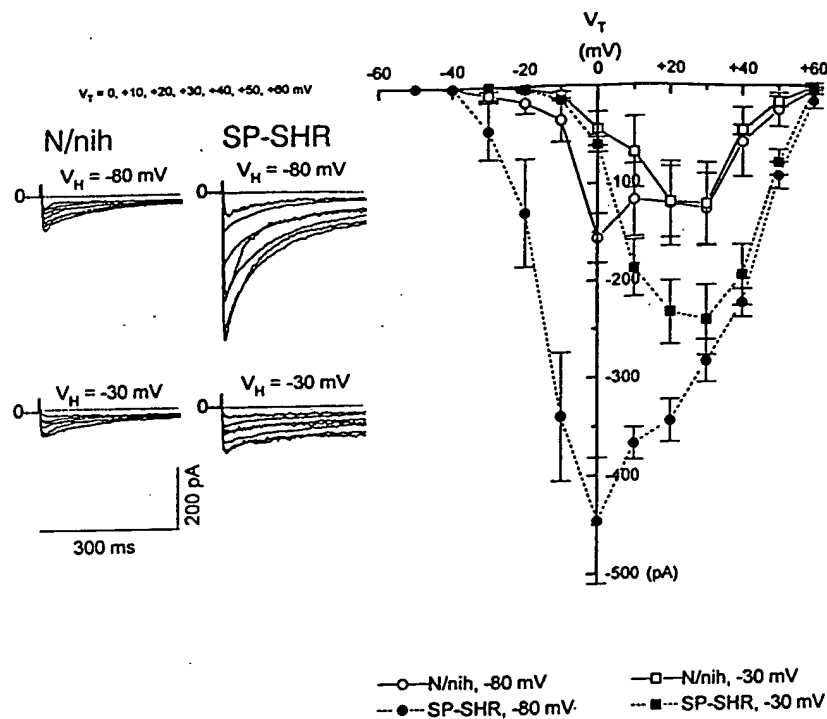
Solutions

The external solution for voltage-clamp experiments consisted of (mM): 20 $BaCl_2$; 125 TEA; 15 HEPES; 1 $MgCl_2$, and 5.5 glucose (pH 7.35). The pipette solution was (mM): 140 Cs-glutamate; 1 $MgCl_2$; 10 HEPES; 3.4 EGTA; 0.5 ATK-diK salt, and 0.5 GTP-Tris salt (pH 7.2).

Data Analysis

To determine current density, peak amplitudes were digitally measured and normalized by cell capacitance. Current densities were then plotted against corresponding V_T or V_H for the appropriate analyses. For the activation analysis, peak currents were plotted against corresponding V_T from V_H of –30 or –80 mV in two separate data sets to allow separation of T-type from L-type currents. For the inactivation analysis, peak currents were plotted against the V_H while V_T was held constant. Steady-state inactivation was obtained by a two-step protocol using conditioning potentials for 5 s, then stepping

Fig. 1. Activation of I_{Ba} in SP-SHR and N/nih VMC. Depolarizations from both -80 and -30 mV V_H activated significantly greater currents in SP-SHR than N/nih VMCs at every point from -20 to $+50$ mV for both V_H . These increased current densities, which were clearest in the V_T from 0 to 60 mV shown, were not due to increased cell surface area, as the cell capacitances were not significantly different in the cell averages and were 27 ± 8 pF for the N/nih VMCs and 26 ± 7 pF for the SP-SHR VMCs shown in this figure. Current voltage (I - V) activation curves from $V_H = -80$ mV show the significantly greater maximized peak I_{Ba} at $V_T = 0$ mV of SP-SHR (446 ± 64 pA) than of N/nih (156 ± 25 pA) VMCs (all SP-SHR versus N/nih V_T comparisons from -20 to $+50$ mV showed more negative, inward, values for SP-SHR at the 0.05 confidence level). I - V curves from $V_H = -30$ mV also showed larger peak I_{Ba} for SP-SHR at V_T from $+10$ to $+50$ mV (with the maximum SP-SHR peak of 243 ± 36 pA and N/nih peak of 123 ± 43 pA at $V_T = +30$ mV). The I - V curves are based on values averaged from 7 SP-SHR and 6 N/nih VMCs.



immediately to the V_T of $+20$ mV. The membrane potential was clamped at -80 mV between trials. Fits were made using Origin (MicroCal Software, Inc.) to the Boltzmann equation:

$$I = 1/[1 + \exp[(V - V_{1/2})/k]],$$

where I is the relative current, V is the command potential, $V_{1/2}$ is the potential at which 50% of the maximum current occurs, and k is the Boltzmann coefficient. Conductance (g) was calculated from:

$$g = \frac{I}{\bar{g}(V_m - V_{rev})},$$

where g is the normalized conductance (0–1), I is the peak current amplitude, \bar{g} is the maximum conductance, V_m is the membrane potential, and V_{rev} is the reversal potential (taken to be $+60$ mV for these calculations).

Fitting the data to each equation was performed using nonlinear least squares. Data are expressed as mean \pm standard error of the mean, with statistical significance determined by an analysis of variance followed by a multiple comparison test (Scheffé test), with a significance criterion of 0.05.

Results

Comparison of Ca^{2+} Currents

Voltage-dependent Ca^{2+} channel currents were recorded with whole cell voltage clamps using 20 mM Ba^{2+} in the bathing solution (replacement of NaCl by tetraethylam-

monium) with a Cs-glutamate pipette solution to eliminate or minimize Na^+ , K^+ , and Cl^- currents. Figure 1 shows Ba^{2+} currents (I_{Ba}) and the activation current-voltage relationships for both T- and L-type I_{Ba} in SP-SHR and N/nih. By studying the conditions for maximum I_{Ba} density, we determined that 2–4 days after isolation, with minimized exposure to dispersion enzymes and in the absence of BrdU and gentamicin, produced the largest I_{Ba} in the external solution containing 20 mM Ba^{2+} for both SHR and N/nih VMCs, and limited our studies to these conditions. No other selection of cells on the basis of amounts of T- or L-type Ca^{2+} current was made for this comparison so that the data would reflect the distribution of the two types of Ca^{2+} channels in the SP-SHR and N/nih VMC populations. Using current family traces and I - V plots, figure 1 shows that there was an increase in the average maximum L-type I_{Ba} (which was the result of depolarizations from the $V_H = -30$ mV), and a much larger increase in SP-SHR average maximum combined L + T currents (which resulted from depolarizations from $V_H = -80$ mV). SP-SHR maximum I_{Ba} peaks averaged 446 ± 64 pA from $V_H = -80$ mV at $V_T = 0$ mV and 243 ± 36 pA from $V_H = -30$ mV at $V_T = +30$ mV, while N/nih averaged 156 ± 25 pA from $V_H = -80$ mV at $V_T = 0$ mV and 123 ± 43 pA from $V_H = -30$ mV at $V_T = +30$ mV ($n = 7$

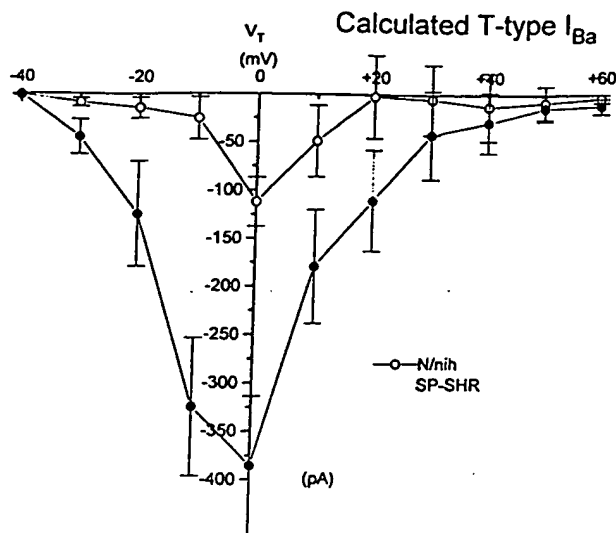


Fig. 2. T currents were larger in SP-SHR than in N/nih cells, as shown by digitally subtracted data from the same cells in figure 1. For this comparison, L-type I_{Ba} (defined by depolarizations from $V_H = -30$ mV) were subtracted from corresponding currents from $V_H = -80$ mV at each V_T value. The $V_H = -30$ mV inactivates T-type Ca^{2+} channels, leaving a virtually pure L-type I_{Ba} , which can then be subtracted to determine the T-type I_{Ba} remaining. At V_T less than +30 mV, there was a large and significant increase in the amplitude of I_{Ba} in SP-SHR versus N/nih VMCs, as shown. Peak of the T-channel currents was at 0 mV for both, with averages of 385 ± 71 for SP-SHR and 112 ± 25 for N/nih, making T-type I_{Ba} clearly a dependent variable.

for SP-SHR and $n = 6$ for N/nih). I_{Ba} were significantly increased at all V_T between -20 and $+50$ mV. In a larger group of VMC, there was no significant difference in cell capacitance, which averaged 26 ± 3 pF for SP-SHR and 24 ± 2 pF for N/nih ($n = 40$ for both SP-SHR and N/nih). The larger maximum current densities for both the L-type I_{Ba} and the combined I_{Ba} in SP-SHR were significant at the 5% criterion, using analysis of variance (ANOVA) and a Scheffé test.

The larger increases in average I_{Ba} peaks at $V_H = -80$ mV were further analyzed to isolate the T-type components. Using digitally stored current records, determination of the T-type I_{Ba} component was made by subtraction of the L-type I_{Ba} (obtained from $V_H = -30$ mV) from the total current (obtained from $V_H = -80$ mV) at each V_T between -30 and $+60$ mV (fig. 2). There were large increases in the average maximum T-type I_{Ba} density at all points between -30 mV and $+20$ mV (the entire T-type Ca^{2+} channel voltage domain) in the SP-SHR cells, which were significant at or beyond the 5% level.

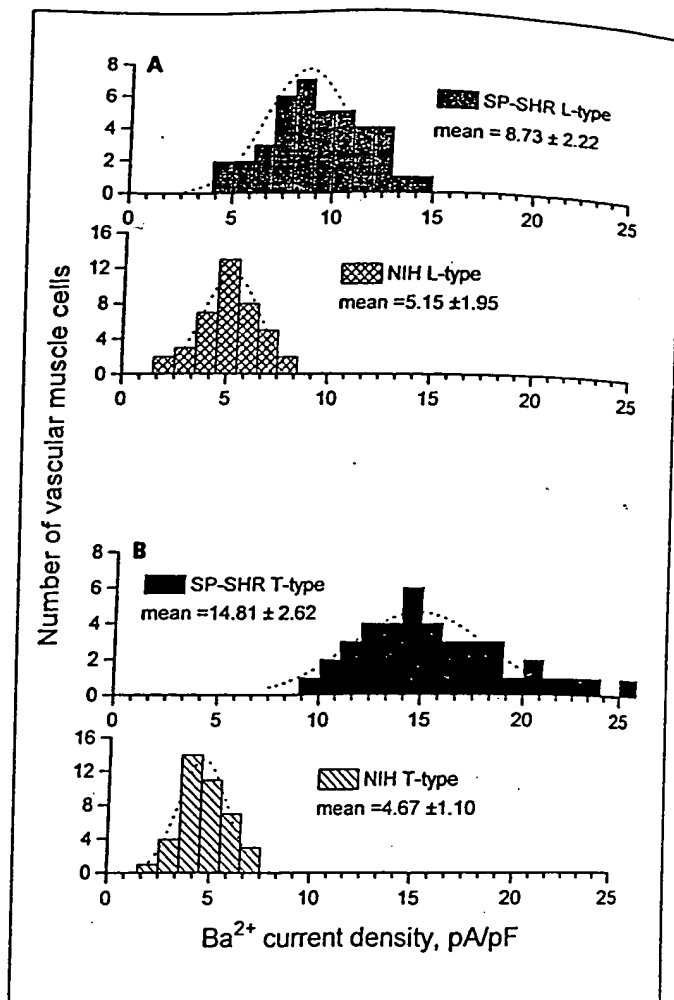


Fig. 3. Peak current frequency distributions from an abbreviated 3-step protocol for L- and T-type Ca^{2+} currents (A and B, respectively) from SP-SHR and N/nih show the dramatic shift to greater amplitudes in the extremely hypertensives, compared with outbred controls. A L-type peaks were determined by $V_H = -80$ mV to $V_T = -30$ mV steps, while in B T-type peaks were from digitally subtracted $V_H = -80$ to $V_T = 0$ mV steps minus $V_H = -30$ mV to $V_T = 0$ mV. Values are expressed as pA/pF after normalization for cell capacitance. The dotted lines show the fit of a Gaussian curve to the data by least squares determinations. Both L- and T-type I_{Ba} amplitudes were significantly greater in SP-SHR, and there was no overlap in B of T-type amplitudes ($n = 40$ for each type).

Another comparison of the I_{Ba} peak density is presented as frequency histograms of calculated average maximum L- and T-type amplitudes of 40 of each cell type in figure 3. A 3-step (abbreviated) protocol was used to isolate individual components. L-type current maximums were from $V_H = -30$ mV to $V_T = +30$ mV transitions and T-type were from $V_H = -80$ mV to $V_T = 0$ mV transitions

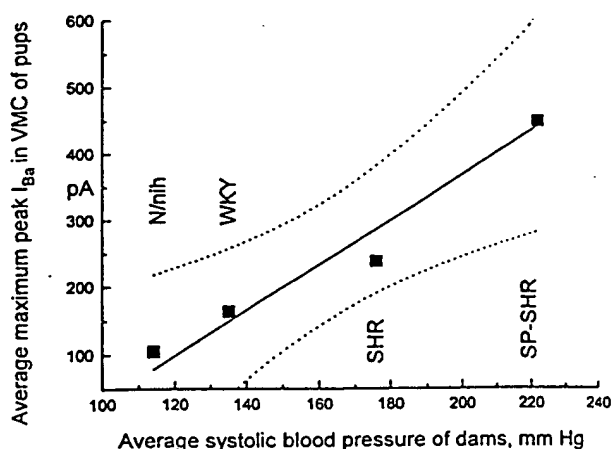


Fig. 4. Plots of blood pressure averages of dams versus pup VMC Ca^{2+} channel maximum current densities (as maximum peaks from $V_H = -80$ mV to $V_T = +20$ mV) for SP-SHR, N/nih, SHR, and WKY (with SHR and WKY data taken from our earlier report [4]). These data are not intended to represent a strict gene test, as would be provided in co-segregation experiments in F_2 (which require chromosomal markers); rather, the correlation between Ca^{2+} current density and blood pressure in these related animals, even though years intervened between the studies, is noteworthy. The positive 0.98 correlation coefficient (r) between Ca^{2+} channel current density and blood pressure for the composite of the four types of rats represented in this diagram might suggest a causal relationship. The correlation was significant beyond the 0.05 confidence level.

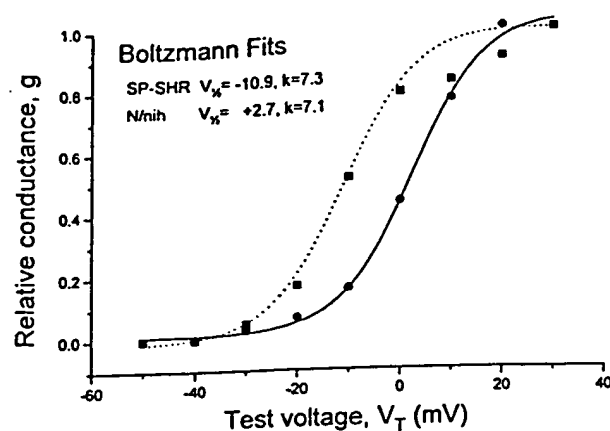


Fig. 5. Boltzmann equation fits to the activation I-V curves for total (composite of L- and T-type) I_{Ba} from $V_H = -80$ mV show a significant 7-mV shift to the left of the L-type activation curve in SP-SHR. The inset legend shows the parameters for the Boltzmann fits (dotted lines) which differed in $V_{1/2}$ ($V_{1/2} = -10.9$ versus $+2.7$ mV) but not the slope k (7.3 versus 7.1) for $n = 6$ for SP-SHR and N/nih, respectively.

blood pressures. The correlation value ($r = 0.98$) was statistically significant ($p \leq 0.05$).

Parameters of individual activation curves were determined by nonlinear least-squares fits to the Boltzmann equation for the composite of L-type and T-type Ca^{2+} currents, and the averages are shown in figure 5. There was a small, but significant, 7-mV shift to the left of the L-type activation curve in SP-SHR compared to N/nih. Based on 6 SP-SHR cells and 6 N/nih cells, mean values for voltage of half-maximum ($V_{1/2}$) were -10.9 ± 1 mV for SP-SHR and $+2.7 \pm 1$ mV for N/nih (significantly different). The slope values were 7.3 ± 1 and 7.1 ± 1 mV, respectively.

Analysis of the steady-state inactivation curves also showed significant differences between stroke-prone hypertensives and normotensives (fig. 6). Best fits to averaged Boltzmann curves (dotted lines) for steady-state inactivation gave mean values for SP-SHR that were significantly shifted to the left from the N/nih controls. Figure 6 shows that, in 6 cells each, $V_{1/2}$ was -36.1 ± 1.5 mV for SP-SHR versus -20.9 ± 1.1 mV for N/nih with $k = 9.6 \pm 0.5$ and $k = 12.2 \pm 0.5$ mV, respectively. $V_{1/2}$ was left-shifted, and there was a smaller slope in SP-SHR that were both statistically significant.

To separate differences in SP-SHR and N/nih Ca^{2+} channels further, we studied recovery from inactivation,

abbreviated
respective-
water ampli-
fied con-
V to $V_T =$
subtracted
 $V_T = 0$ mV.
cell capaci-
the data by
tudes were
ap in B of

present-
ge maxi-
l type in
d to iso-
ximums
ions and
nsitions

tension

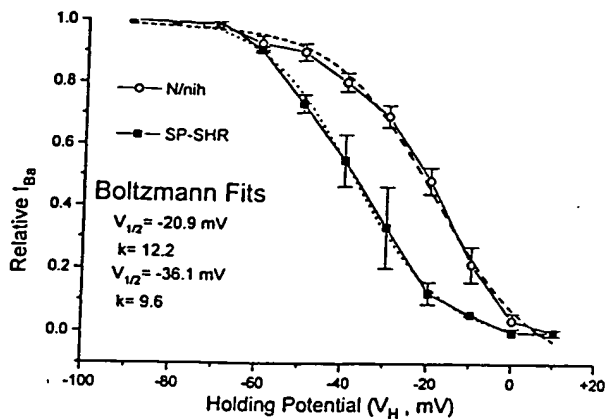


Fig. 6. Boltzmann fits to steady-state inactivation I - V curves showed that SP-SHR I_{Ba} were shifted to the left by 15 mV. SP-SHR were inactivated at significantly more negative membrane potentials ($V_{1/2} = -36.1 \pm 1.5$ mV) than were N/nih ($V_{1/2} = -20.9 \pm 1.1$ mV). These comparisons are based on 6 cells of each SP-SHR and N/nih, and there was a significant difference between the slope k values (9.6 ± 1 versus 12.2 ± 1 , respectively).

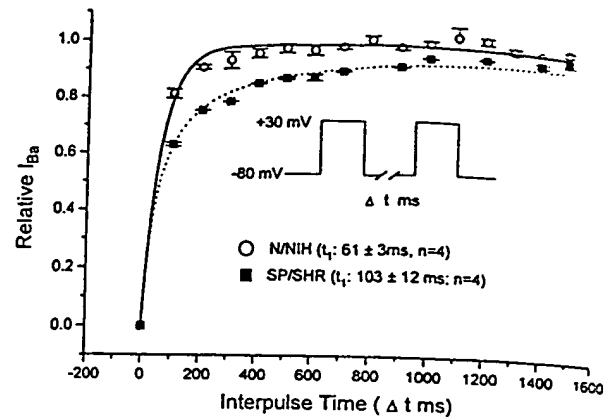


Fig. 7. Recovery from inactivation was slower in SP-SHR than in N/nih VMCs. Current amplitude increased as the step from $V_H = -80$ mV to $V_T = +30$ mV interpulse interval was increased, more slowly reaching a maximum for SP-SHR than for N/nih. These records from individual VMCs are representative of four experiments carried out for each rat strain. Time constants determined from the recovery showed an average of 103 ± 12 ms for SP-SHR, which was significantly greater than 61 ± 3 ms for N/nih.

using a series of variably delayed repeat depolarization pulses that extend from 100 to 1,500 ms (in a series of 15 increasing delays progressively 100 ms longer than the preceding pulse interval). Figure 7 shows the relative I_{Ba} as a function of interpulse interval (in milliseconds), with the voltage protocol from -80 to $+30$ mV with a variable delay until the next voltage command shown as an inset. SP-SHR had a significantly longer time for recovery than N/nih. This was an apparently independent difference in Ca^{2+} channel function, which would tend to reduce (rather than increase) Ca^{2+} channel currents. Curves were fit to a double exponential, as at least two time constants were apparent in the plotted recovery curves. Using the faster time constants (t_1) for each, SP-SHR had a mean of 103 ± 12 ms and N/nih had a t_1 of 61 ± 3 ms ($n = 4$ for each type), which were significantly different.

Discussion

The most important conclusion of this study is that the vascular muscle Ca^{2+} channel current densities under maximized conditions closely correlate with extremely high blood pressures, as would be predicted for a causal role by the CCHH [1]. This study extends observations of increased L-type Ca^{2+} currents [2, 4, 10, 11, 26] in genetical-

ly less hypertensive rats (SHR) with new data from extremely hypertensive SP-SHRs. Comparing SP-SHR, SHR, N/nih, and WKY data from this laboratory, the increased Ca^{2+} current density appears to be proportional to the increase in maternal blood pressure (fig. 4). Since all of these Ca^{2+} currents were measured from VMCs of azygous veins from newborn rats, there would not have been any opportunity for increased arterial blood pressure to develop and, even if it were argued that small increases in perinatal arterial blood pressure in SP-SHR versus N/nih might be significant, the much lower venous blood pressures would surely not be expected to induce changes in vascular muscle Ca^{2+} channels.

Additional insight into the possible roles of the two types of VMC Ca^{2+} channels can be inferred from this study. These data show evidence for increased T-type I_{Ba} and a significant shift of I_{Ba} to more negative potentials in SP-SHR VMCs. Earlier experiments suggested that there was no significant difference in T-type vascular muscle Ca^{2+} channels in SHRs [2]. These T-type Ca^{2+} channels have been found primarily in VMCs from embryonic or neonatal animals [5]. However, the exaggerated contribution of T-type Ca^{2+} channels to the much larger increases in I_{Ba} found in SP-SHR made them easier to detect. The exaggerated amplitude of T-type I_{Ca} is surprising in that it has been difficult to find cells with predominantly T-type

I_{Ca} . Although we and others earlier suggested that T-type Ca^{2+} current may be functioning primarily as a pacemaker current [2, 4, 30–32], it now appears that another important function for T-type Ca^{2+} currents might involve regulation of proliferation [33]. Proliferation and consequently decreased artery lumen diameter from increases in Ca^{2+} currents (including T-type, if they play a role in arterial VMC) may also importantly contribute to the greatly increased incidence of cardiovascular death in SP-SHR.

In an earlier report, we used the amplitude of T-type currents as a reference for comparison of L-type current amplitudes [2, 26]. However, it is clear from the present data (fig. 1, 2) that T-type current amplitude can also be exaggerated in hypertension. The basis for use of T-type currents as the frame of reference was their apparent equivalence in the first SHR and WKY experiments, the correlation of T-type currents with high quality recordings (current amplitudes, stability, and duration of recording), and the apparent insensitivity of T-type currents to drugs and intracellular modulators of Ca^{2+} current [29, 34]. Recently, we discovered that T-type Ca^{2+} currents can also be selectively inhibited by a new Ca^{2+} antagonist [35], which emphasizes the possibility for pharmacological manipulation of T-type Ca^{2+} currents. Thus, we have changed to normalization of I_{Ba} based on cell capacitance, which is probably the best available indicator of cell membrane surface area. The most useful comparisons appear to be maximum (composite) I_{Ba} amplitudes measured at $V_H = -80$ to $V_T = +20$ mV and normalized by membrane capacitance. The large amplitude of the T-type I_{Ba} in SP-SHR is all the more remarkable because the Ba/Ca permeability is nearly 1:1 [30]. Since both T- and L-type currents can be inhibited or possibly enhanced, and in light of the correlation of L- and T-type current amplitudes with blood pressure, it is important to continue studies of both types of Ca^{2+} channels in VMC from different types of hypertension in various blood vessels and at different ages.

If Ca^{2+} channel function were to be a cause of increased blood pressure, it might be predicted that increased Ca^{2+} channel function would be found not only in young hypertensives, but also in adults leading to fatal stroke. Mesenteric arteries from adult SHRs did show increased Ca^{2+} channel activity [26]. SP-SHR on a diet from Funabashi Farms and 1% NaCl drinking water all died by age 180 days from stroke [25, fig. 1]. However, Ohya et al. [11] reported that I_{Ba} amplitude increases were found only in VMCs from the mesenteric arteries of young, but not adult, SHR versus WKY normotensives, and also that

binding of the dihydropyridine, nicardipine, to VMC Ca^{2+} channels was only different in a comparison of adult rat cells (not young rat cells) in the inactivated state. Since it is likely that Ca^{2+} channels are multiply regulated, probably by redundant intracellular systems (e.g., intracellular Ca^{2+} , protein kinase C, phosphorylation, phosphatases, intracellular Mg^{2+} , high energy phosphates, and perhaps other so far unidentified factors), it is entirely possible that increased Ca^{2+} channel function might participate in the development of increased blood pressure and yet not be evident under certain experimental conditions (i.e., if other factors predominate). This may explain why SHR current density decreased from young to adult stages and WKY densities were high in the data by Ohya et al. [11]. Another possibility is that the lack of inactivation shown in figure 3B of Ohya et al. [11] may indicate that under their conditions (without inclusion in the pipette of GTP, without an excess of ATP over Mg^{2+} , and with the extra prepulse return to -80 mV before the depolarizing test pulse), Ca^{2+} channel differences may have been hidden.

Analysis of the voltage domains for both activation and inactivation I–V relationships (fig. 5, 6) in this report show changes in both. While the activation parameter is shifted to the left by 7 mV in SP-SHR, which would favor a greater Ca^{2+} current at a given resting membrane potential, this activation factor may well be less important than the left-shifted inactivation factor because the activation process only allows Ca^{2+} to enter for a matter of milliseconds, whereas the inactivation process extends over many seconds. To increase I_{Ca} , a shift to the right of the SP-SHR inactivation parameter would have been expected. The 15-mV shift to the left of the SP-SHR curve is therefore not a direct explanation for increased Ca^{2+} influx. What is more likely is that the left shift results from a more predominantly T-type Ca^{2+} current, as shown in figure 1 and 2, and reflected by the more negative voltage domain of the largest currents in the I–V curve for SP-SHR (fig. 1, 6, 7). Furthermore, both the inactivation and activation $V_{1/2}$ are useful to establish voltage domains, but do not increase in amplitude of currents, which are significantly greater in SP-SHR. Thus, it is possible for the SP-SHR VMC to show a left shift in the inactivation I–V curve (voltage domain) while still having increased amplitudes of long duration Ca^{2+} current, perhaps due to an increase in the number of Ca^{2+} channels. Modulation of the number of available Ca^{2+} channels by intracellular and extracellular chemical modulators, in addition to membrane voltage, is likely to be most important in the explanation of the increased Ca^{2+} currents found in these SP-SHR as well as in previous studies [2, 4, 11].

In any event, it is clear that in SP-SHR striking differences in voltage-dependent Ca^{2+} channels exist. The inactivation-state-recovery time course also showed that SP-SHR were significantly different from N/nih, but paradoxically, one would have anticipated quicker recovery from inactivation, which could hypothetically lead to increased current density in SP-SHR (because the Ca^{2+} channels would more quickly return to a state ready for activation). The slower recovery from inactivation may be a consequence of increased Ca^{2+} entry and a prolonged

Ca^{2+} -dependent inactivation, but this is a question that needs further exploration.

In summary, we have shown a striking correlation between increases in VMC Ca^{2+} channel function and blood pressure in SP-SHR, an extremely hypertensive genetic model, as compared to an outbred normotensive control (N/nih). The evidence presented here suggests that alterations in VMC Ca^{2+} channel function are causally linked with development of increased blood pressure, with both T-type Ca^{2+} channels and L-type Ca^{2+} channels involved.

References

- 1 Hermsmeyer K, Bian K: Calcium channel hypothesis in hypertension. *J Vasc Med Biol* 1991;3:219-222.
- 2 Rusch NJ, Hermsmeyer K: Calcium currents are altered in the vascular muscle cell membranes of spontaneously hypertensive rats. *Circ Res* 1988;63:997-1002.
- 3 Hermsmeyer K: Cellular calcium control in hypertension. *J Cardiovasc Pharmacol* 1988;12(suppl 6):8-9.
- 4 Hermsmeyer K, Rusch NJ: Calcium channel alteration in genetic hypertension. *Hypertension* 1989;14:453-456.
- 5 Rusch NJ, Hermsmeyer K: Vascular muscle calcium channels in hypertension: in Coca A, Garay RP (eds): *Ion Transport in Hypertension: New Perspectives*. Boca Raton, CRC Press, 1994, pp 197-227.
- 6 Erne P, Hermsmeyer K: Intracellular vascular muscle calcium modulation in genetic hypertension. *Hypertension* 1989;14:145-151.
- 7 Hermsmeyer K, Erne P: Cellular calcium regulation in hypertension. *Am J Hypertens* 1989;2:655-658.
- 8 Hermsmeyer K, Erne P: Vascular muscle electrophysiology and platelet calcium in hypertension: in Laragh JH, Brenner BM (eds): *Hypertension: Pathophysiology, Diagnosis, and Management*. New York, Raven Press, 1990, pp 661-666.
- 9 Oshima T, Young EW, Hermsmeyer K, McCarron DA: Modification of platelet and lymphocyte calcium handling and blood pressure by dietary sodium and calcium in genetically hypertensive rats. *J Lab Clin Med* 1992;119:151-158.
- 10 Hermsmeyer K: Calcium channel function in hypertension. *J Hum Hypertens* 1993;7:173-176.
- 11 Ohya Y, Abe I, Fuji K, Takata Y, Fujishima M: Voltage-dependent Ca^{2+} channels in resistance arteries from spontaneously hypertensive rats. *Circ Res* 1993;73:1090-1099.
- 12 Aoki K, Asano M: Effects of Bay K 8644 and nifedipine on femoral arteries of spontaneously hypertensive rats. *Br J Pharmacol* 1986;88:221-230.
- 13 Bruner CA, Webb RC: Increased vascular reactivity to Bay K 8644 in genetic hypertension. *Pharmacology* 1990;41:24-35.
- 14 Aoki K: The calcium membrane theory of essential hypertension: in Aoki K, Frohlich ED (eds): *Calcium in Essential Hypertension*. New York, Academic Press, 1989, pp 623-655.
- 15 Bohr DF, Webb R: Vascular smooth muscle membrane in hypertension. *Annu Rev Pharmacol Toxicol* 1988;28:389-409.
- 16 Bohr DF: Cell membrane in hypertension. *NIPS* 1989;4:85-88.
- 17 Bruner CA, Webb RC, Bohr DF: Vascular reactivity and membrane stabilizing effect of calcium in spontaneously hypertensive rats: in Aoki K, Frohlich ED (eds): *Calcium in Essential Hypertension*. New York, Academic Press, 1989, pp 275-306.
- 18 Bohr DF, Dominiczak AF: Experimental hypertension. *Hypertension* 1991;17(suppl 1):39-44.
- 19 Cauvin C, Johns A, Yamamoto MK, et al: Ca^{2+} movements in vascular smooth muscle and their alterations in hypertension: in Kwan CY (ed): *Membrane Abnormalities in Hypertension*. Boca Raton, CRC Press, 1989, pp 145-179.
- 20 Kwan C-Y, Daniel EE: Calcium handling by membranes isolated from vascular smooth muscle in hypertension: in Aoki K, Frohlich ED (eds): *Calcium in Essential Hypertension*. New York, Academic Press, 1989, pp 201-230.
- 21 Postnov YV, Orlov N: Cell membrane alterations as a source of primary hypertension. *J Hypertens* 1984;2:1-6.
- 22 Aoki K: Calcium membrane theory of essential hypertension: in Aoki K (ed): *Essential Hypertension*. New York, Springer, 1986, pp 223-242.
- 23 Okamoto K, Aoki K: Development of a strain of spontaneously hypertensive rats. *Jpn Circ J* 1963;27:282-293.
- 24 Okamoto K, Yamori Y, Nagaoka A: Establishment of a strain of stroke-prone SHR. *Circ Res* 1974;34/35:143-153.
- 25 Sadoshima S, Busija D, Brody M, Heistad D: Sympathetic nerves protect against stroke in stroke-prone hypertensive rats. *Hypertension* 1981;3(suppl 1):124-127.
- 26 Hermsmeyer K: Differences of calcium channels in vascular muscle in hypertension. *Am J Hypertens* 1991;4(suppl):412-415.
- 27 Hermsmeyer K, Mason R: Norepinephrine sensitivity and desensitization of cultured single vascular muscle cells. *Circ Res* 1982;50:627-632.
- 28 Hermsmeyer K, Robinson RB: High sensitivity of cultured cardiac muscle cells to autonomic agents. *Am J Physiol* 1977;233:C172-C179.
- 29 Bean BP, Sturek M, Puga A, Hermsmeyer K: Calcium channels in vascular muscle cells isolated from rat mesenteric arteries: Modulation by dihydropyridine drugs. *Circ Res* 1986;59:229-235.
- 30 Sturek M, Hermsmeyer K: Calcium and sodium channels in spontaneously contracting vascular muscle cells. *Science* 1986;233:475-478.
- 31 Bean BP: Classes of calcium channels in vertebrate cells. *Annu Rev Physiol* 1989;51:367-384.
- 32 Tsien RW, Ellinor PT, Horne WA: Molecular diversity of voltage-dependent Ca^{2+} channels. *Trends Pharmacol Sci* 1991;12:349-354.
- 33 Nuss HB, Houser SR: T-type Ca^{2+} current is expressed in hypertrophied adult feline left ventricular myocytes. *Circ Res* 1993;73:777-782.
- 34 Tsien RW, Lipscombe D, Madison DV, Bley KR, Fox AP: Multiple types of neuronal calcium channels and their selective modulation. *Trends Neurosci* 1988;11:431-438.
- 35 Mishra SK, Hermsmeyer K: Selective inhibition of T-type Ca^{2+} channels by Ro 40-5967. *Circ Res* 1994;75:143-148.

LOW-THRESHOLD CALCIUM CURRENTS IN CENTRAL NERVOUS SYSTEM NEURONS

J. R. Huguenard

Department of Neurology and Neurological Sciences, Stanford University School of Medicine, Stanford, California 94305

KEY WORDS: LVA current, T current, low-threshold spike, calcium-dependent burst firing, oscillations

ABSTRACT

The low-threshold calcium current, or T current, has recently been demonstrated with voltage-clamp recordings in a variety of central nervous system (CNS) neurons. It is especially prominent in the soma and dendrites of neurons with robust calcium-dependent burst firing behaviors such as thalamic relay neurons and cerebellar Purkinje cells. Single-channel and macroscopic current behavior have been carefully investigated and kinetic schemes devised to completely describe the activation and inactivation processes. The kinetic properties of T current lead to activation of low-threshold spikes subsequent to transient membrane hyperpolarizations. Putative functional roles for T current include generation of low-threshold spikes that lead to burst firing, promotion of intrinsic oscillatory behavior, boosting of calcium entry, and synaptic potentiation.

INTRODUCTION AND HISTORY

In an elegant series of in vitro intracellular studies in cat thalamus, Eccles and collaborators (3) discovered that some central neurons displayed a form of paradoxical excitation. In contrast to the typical responses in most cells where depolarized membrane potentials are normally associated with enhanced excitability, hyperpolarizations such as those produced by inhibitory synaptic potentials resulted in increased responsiveness. This period of enhanced excitability following membrane hyperpolarizations was termed post-anodal excitation. Llinás and colleagues carefully examined this property using intracellular recordings with in vitro slice preparations of inferior olive (65, 66) and thalamus (55, 56, 64). They noted that intracellular current injections, which hyperpolarized the membrane to levels more negative than rest (around

Table 1 Voltage-dependent kinetics for T current in a variety of neurons

Cell Type	Charge Carrier	Inactivation				Activation			Reference
		$V_{1/2}^a$	k^b	τ_h^c	$\tau_{recovery}^c$	$V_{1/2}^a$	k^b	τ_m^c	
Isolated hippocampal L-M cells	2 Ca	-94	6.3	25-10	~90 ms/-100 mV	-47	6	ttp	(35)
Isolated rat VB	3 Ca	-81	4.0	130-30	250 ms/-100mV	-57	6	15-2	(51, 52)
Isolated rat nRt	3 Ca	-80	5.3	100-80	500ms/-100mV	-50	7	11-3	(52)
Isolated rat dLGN	5 Ca	-64	7.8	70-20	750ms/-98mV	-45	6	ttp	(43)
Cat and rat dLGN in slice	1 Ca	-87	3.9	100-25	~300ms/-95mV	-60	2		(24)
Rat spinal dorsal horn in slice	2 Ba	-86	8.0	80-10		-45	7		(86)
Isolated rat basal forebrain	2.5 Ca	-49	3.9	82-16		-40	4.8	ttp	(2)
Isolated rat lateral habenula	3 Ca	-81	4.4	150, 50-30 ^d	510ms/-90mV	-58	3.4	8-2	(50)
Isolated rat dorsal horn neurons	5 Ca	-82	3.7	43-16		-50	6		(49)
Isolated rat neostriatum	5 Ca	-88	6.1		288ms/-100mV	-53	6	ttp	(48)
Isolated rat Purkinje cells	5 Ba	-93	8.2	100-25		-46	9		(84)
<i>Xenopus</i> neurons in culture	2 Ca	-79	6.9	55-20		-49	6	ttp	(40)
Neuroblastoma	50 Ba	-51	4.0	400-20	~150ms/-80mV	-20	11	8-2	(110)
GH3 cells	10 Ca	-71		100-20	250, 1000ms ^d /-100mV	-33	7	10-2	(44)
Chick drg	10 Ca	-78	5.0	50-20		-51	7	tp	(32)

Charge carrier concentrations are in mM. ^a: half-activation or inactivation voltage; ^b: slope of activation/inactivation curve, mV/efold; ^c: all values for τ (time constant) in ms. $\tau_{recovery}$ is the time constant for recovery at the indicated potential; ^d: Two exponential components; ttp: time to peak is voltage dependent.

potential sufficiently negative that $h_o \approx 0$, g' is determined primarily by m_∞ . From Ohm's law $g = I/E$; therefore, g_i can be obtained by dividing the current by the driving force ($E - E_{Cl}$) or by the constant field equation (21, 44, 46, 51). Relative values for m_∞ at a series of command potentials can then be obtained. Alternatively, activation can be approximated by measuring tail current amplitudes after a brief activating voltage step (e.g. 50-52, 84, 104). If an appropriate step duration is chosen, activation will be nearly complete while inactivation has not yet become significant. Thus tail current amplitude will closely reflect the maximum activation $[(m_\infty)^n]$ and has the advantage that the driving force is the same for each step.

Under physiological recording conditions, the apparent activation threshold for I_T is near resting membrane potential, -50 to -60 mV, with activation normally complete at -20 to -30 mV. Activation is relatively gradual in most cases, with an e-fold increase in conductance normally requiring about 6-7 mV depolarization (Table 1). Exceptions include cat and rat thalamic relay (24) and rat lateral habenular cells (50), which have very steep activation curves (2-3.4 mV/efold) that would promote rapid regenerative Ca^{2+} -dependent responses. However, one of these studies was performed in slices where neurons retain extensive dendritic trees, and as indicated by the authors, voltage-clamp control was probably compromised (24). Thus T current activation slope is probably a relatively constant feature in neurons from several brain areas. The voltage at which I_T is half-activated ($V_{1/2}$) is also comparable in many cell types, with values ranging between -45 and -60 mV in most cases. The differences in half-activation voltage between cell types (Table 1) cannot be completely explained by methodological differences. In a few experiments, direct comparison of activation properties between cell types was obtained with the same recording conditions (50, 52). In these cases, clear differences in $V_{1/2}$ were obtained, with thalamic reticular neurons showing half-activation 9 mV more depolarized than thalamic relay cells or lateral habenular neurons.

The rate of I_T activation is highly voltage dependent. In every case where it has been measured (Table 1), the time to peak (ttp) current becomes shorter with depolarization. Furthermore, the time constant of activation (τ_m) has been directly measured in many cases by fitting Equation 1 to whole-cell current traces. At threshold, τ_m is relatively slow (84-15 ms) and decreases to around 2 ms at maximal activation (Table 1). Comparison between cell types reveals that differences in the rate of activation are largely accounted for by shifts in the voltage dependence. For example, the relationship between τ_m and voltage is similar for thalamic relay and reticular neurons, but it is shifted about 20 mV in the positive direction for the latter (52). Functionally this means that at LTS threshold, ~-50 mV, the rate of onset of T current is approximately twice as fast in relay cells compared with reticular cells. This slow onset of

Table 2 Blockade of T current by Cd^{2+} and Ni^{2+}

Cell type	Charge carrier	Ni^{2+}	Cd^{2+}	Reference
Rat hippocampal L-M	2 Ca	400	260	(35)
Rat Purkinje	10 Ca	110	70	(58)
Rat Purkinje	5 Ba	52		(84)
Rat amygdala	10 Ca	30	650	(57)
Rat frontal cortex pyramids	10 Ca	260	15	(109)
Rat CA1 pyramids	10 Ca	230	80	(97)
Rat dorsal horn	5 Ca	230	240	(49)
Neuroblastoma	50 Ba	47	160	(77)
GH3	10 Ca	777	188	(44)

Charge carrier concentrations are in mM. Values for Ni^{2+} and Cd^{2+} are EC_{50} in μM .

hippocampal CA1 neurons (97), cerebellar Purkinje cells (58), amygdaloid neurons (57), and in mouse sensory neurons (85). Other organic Ca^{2+} channel antagonists, including D-600 and diltiazem, block I_T at 100-fold higher concentrations (57, 58). An experimental diphenylmethylpiperazine derivative, U-92032, has recently been shown to be a more potent blocker of I_T than flunarizine and is ineffective in reducing HVA in a neuronal cell line (54).

Succinimides and related compounds include a class of antiepileptic drugs that are specifically effective in the treatment of absence-type epilepsy (19). Ethosuximide, or 2-ethyl-2-methylsuccinimide, effectively controls absence seizures when blood levels are between 200 and 700 μM . In this same concentration range, ethosuximide reduces I_T in thalamic relay (19, 20, 53) and reticular (53) neurons, without having any effect on activation or inactivation kinetics. At these concentrations, ethosuximide has no effect on HVA (19, 20) or on other voltage-dependent conductances (53). Two related compounds, methyl-phenylsuccinimide and dimethadione (active metabolites of anti-absences drug methsuximide and tridione), also reduce I_T in thalamic neurons (19, 22), but these drugs are not as selective as ethosuximide in that they also reduce HVA current. Furthermore, the unsubstituted succinimide ring compound is not active in either I_T current blockade or absence seizure reduction. The mechanism of block by methylphenylsuccinimide, as tested by nonstationary fluctuation analysis methods, was a reduction in the number of channels without a change in single-channel conductance (23), which suggests that succinimides block I_T channels without affecting their gating or permeation. Taken together, these results indicate that T current blockade in thalamic neurons is a likely mechanism for the antiepileptic action of this class of drugs. Consistent with this theory is the finding that in an animal model of absence

epilepsy the amplitude of I_T in thalamic reticular neurons is increased compared with that in nonepileptic controls (103). Additionally, an unrelated antiabsence compound, valproic acid, has also been shown to exert weak antagonistic effects on I_T (61).

Amiloride is a relatively specific blocker of I_T in neuroblastoma cells (101), with an EC_{50} of ~50 μM . In central neurons, however, the effects are highly variable. For example, in hippocampal CA1 cells, 300 μM amiloride reduces I_T by ~40% but also significantly reduces some components of HVA (99). In other studies of hippocampal cells, the EC_{50} s were ~250–500 μM (60, 102). By contrast, in amphibian spinal (40) and basal forebrain (2) neurons, the EC_{50} was ~100 μM , whereas in rat spinal motoneurons, 1 mM amiloride produced only 27% block (104). Ocitanol has been reported to be a specific antagonist of I_T (92). In cultured rat sensory neurons, 1 μM 1-ocitanol strongly inhibits I_T without affecting HVA (90). However, in hippocampal neurons, 300 μM ocitanol reduced all components of Ca^{2+} current (99), and in GH3 cells, the EC_{50} for I_T reduction was ~250 μM (44). Volatile anesthetics (45, 100) and neuroleptics (81) have all been shown to reduce the amplitude of I_T in various preparations.

Modulators

A prominent and common difference between I_T and HVA Ca^{2+} currents is metabolic stability. In contrast to HVA currents, I_T is stable during whole-cell dialysis (6, 13, 21, 29, 32, 35, 77, 82), persists with intracellular F^- (13, 35, 44, 98) or Ca^{2+} (13, 52) perfusion, without intracellular ATP or GTP (29), and in cell-free patches (14, 63). Given the relatively stable metabolic state of I_T channels, this may explain why there are fewer reports of I_T modulation than for HVA currents.

Examples of modulatory actions include cholinergic and serotonergic increases, as well as baclofen-dependent blockade, of I_T in hippocampal interneurons (35). Muscarinic and carbachol, but not the β -adrenergic agonist isoproterenol, increase channel open probability in cell-attached patch recordings of hippocampal CA3 neurons (30). Substance P enhances I_T in dorsal horn neurons (86). Dopamine and norepinephrine slightly decrease I_T in chick sensory and sympathetic neurons (70). Angiotensin II causes a small (20%) depression of I_T in a neuronal cell line through a G protein-dependent process (10, 11). An activator of protein kinase C (1-oleoyl-2-acetyl-sn-glycerol, OAG) reduces both I_T and HVA currents in GH3 cells, with half-maximal effects near 25 μM (69). In sensory neurons, I_T is selectively downregulated by another protein kinase C activator, phorbol 12-myristate-13-acetate (88), but only at temperatures of 29°C and higher, whereas I_T and the inactivating components of HVA are both reduced by opiates acting at the μ receptor (89). The general

rule in each of these cases of T current modulation is a reduction in peak current with little effect on kinetics. One possible explanation for this result is that modulation alters the number of available channels but does not affect their time- and voltage-dependent gating.

LOCALIZATION

The specific location of I_T channels within the somadendritic membrane has significant influence on neuronal function. As far as LTS generation in thalamic relay neurons is concerned, it is clear that I_T channels are present in the somatic membrane at high density because large T currents are recorded in acutely isolated relay cells that have had most of their dendritic tree truncated (21, 43, 96). By contrast, thalamic reticular cells are capable of generating robust LTSs in vitro (53) and in vivo (75), yet only a relatively small conductance is observed in isolated and truncated neurons (52). This is consistent with a putative concentration of I_T channels in dendrites of thalamic reticular cells (75, 91). Dendritic localization in hippocampal CA1 cells has recently been directly demonstrated by dendrite-attached recordings up to 300 μm from the soma (68). Furthermore, a calcium-imaging study demonstrated that spike trains produced a Ni^{2+} -sensitive increase in $[\text{Ca}^{2+}]_i$ that was more pronounced in dendritic than somatic regions, which indicates that I_T channels may be somewhat restricted to dendritic membranes (17). Recordings of Ca^{2+} current from intact hippocampal CA1 neurons in slices demonstrated a transient Ca^{2+} current that resembles I_T , but the voltage-dependence of steady-state inactivation was very hyperpolarized with a $V_{1/2}$ value around -106 mV (60). This was interpreted as being the result of dendritic I_T channels that could not be adequately voltage clamped from a somatic site. In support of this idea was the finding that the amplitude of I_T became progressively smaller with cuts that removed increasing amounts of the apical dendritic tree. Intracellular recording of rat cerebellar Purkinje cells in culture reveal a low-threshold, inactivating Ca^{2+} current present at moderate densities (7).

FUNCTION

Besides promoting Ca^{2+} -dependent burst firing, several additional functional roles for I_T have been proposed. These include intrinsic neuronal oscillations, promotion of Ca^{2+} entry, boosting of synaptic signals, and lowering threshold for high-threshold spike generation. By contrast, one role for T channels that appears unlikely is Ca^{2+} entry at synaptic terminals leading to synaptic release. A voltage-clamp study of excitatory synaptic connections in cultured thalamic neurons demonstrated that Cd^{2+} -dependent block of excitatory synapses was correlated with the level of HVA current blockade (83). For example, 10 μM

Cd^{2+} reduced HVA and evoked synaptic currents by greater than 60%, but only reduced I_T by 20%. Furthermore, 50 μM Cd^{2+} completely blocked synaptic transmission and HVA currents while leaving more than 50% of I_T unblocked. It appears that I_T channels cannot by themselves support excitatory neurotransmission, at least in thalamic cells.

Perhaps the most obvious functional role of T channels is to promote LTS generation, which can lead to burst firing in several cell types that include thalamic reticular (75) and relay cells (25, 64), inferior olive cells (65), hippocampal interneurons (35), lateral habenular neurons (107), a subpopulation of pontine reticular formation cells (37), and neocortical neurons (36). Within the neocortex, T channels seem to be found mainly in pyramidal neurons but not in interneurons (38, 42).

Several biophysical features of T current kinetics promote regenerative LTSs. Activation of I_T begins approximately at rest, around -65 mV and more positive, so that brief hyperpolarizing sojourns can result in return of the membrane potential to the activation range. The relatively hyperpolarized activation region for this current means that when I_T is deactivated, the threshold for regenerative responses becomes much closer to the resting potential (~ -60 mV), compared with the normal threshold for Na^+ -spike generation (~ -45 mV). Another feature is the voltage-dependent activation rate (Table 1) that contributes to robust regenerative responses in a manner similar to, but slower than, that which occurs with fast Na^+ spikes. When the threshold for LTS generation is crossed, the activation rate is slow but becomes progressively faster, leading to more and more depolarization (21).

Inactivation in general, and specifically a voltage-dependent inactivation rate, leads to a LTS that is self-limiting in time (21). During the LTS, the rate of macroscopic inactivation becomes progressively faster, largely as a result of shortening of the time to first opening. Thus a separate repolarization mechanism may not be necessary for the LTS. This explains why LTS duration is not affected by Ba^{2+} substitution for Ca^{2+} (55). An exception occurs in thalamic reticular neurons (52), where the rate of inactivation is relatively slow and not very dependent on voltage. Along with dendritic localization of I_T , this may be one factor that promotes relatively long duration bursts in nRt cells (75, 91).

The steady-state inactivation function will determine the necessary hyperpolarization for repriming or deinactivation of sufficient I_T channels to lead to subsequent activation of an LTS. Given the variability in the position and sleepiness of this function among different cell types (Table 1), it appears that some neurons are poised to fire LTSs with minimal provocation, whereas others require substantial hyperpolarization. Interestingly, thalamic neurons have a large reserve of T channels, more than would be necessary to produce a full-fledged LTS. Specific blockade of approximately 40% of T channels by

- their functional organization. *J. Physiol.* 174:370-59.
4. Avanzini G, de Curtis M, Panzica F, Spreafico R. 1989. Intrinsic properties of nucleus reticularis thalami neurons of the rat studied in vitro. *J. Physiol.* 416:111-22.
5. Bal T, McCormick DA. 1993. Mechanisms of oscillatory activity in guinea-pig nucleus reticularis thalami in vitro: a mammalian pacemaker. *J. Physiol.* 468:669-91.
6. Berger AJ, Takahashi T. 1990. Serotonin enhances a low-voltage-activated calcium current in rat spinal motoneurons. *J. Neurosci.* 10:1922-28.
7. Bostu JL, Dupont JL, Feltz A. 1989. Calcium currents in rat cerebellar Purkinje cells maintained in culture. *Neuroscience* 30:605-17.
8. Bostu JL, Fagni L, Feltz A. 1989. Voltage-activated calcium channels in rat Purkinje cells maintained in culture. *Pflügers Arch.* 414:92-94.
9. Bostu JL, Feltz A, Thomann JM. 1985. Depolarization elicits two distinct calcium currents in vertebrate sensory neurons. *Pflügers Arch.* 403:360-68.
10. Buisson B, Bostu SP, de Gasparo M, Gallo-Payel N, Payet MD. 1992. The angiotensin AT2 receptor modulates T-type calcium current in non-differentiated NG108-15 cells. *FEBS Lett.* 309:161-64.
11. Buisson B, Lafamme L, Bostu SP, de Gasparo M, Gallo-Payel N, Payet MD. 1993. A G protein is involved in the angiotensin AT2 receptor inhibition of the T-type calcium current in non-differentiated NG108-15 cells. *J. Biol. Chem.* 270:1670-74.
12. Carbone E, Lux HD. 1984. A low voltage-activated, fully inactivating Ca channel in vertebrate sensory neurons. *Neuron* 3:10501-2.
13. Carbone E, Lux HD. 1987. Kinetics and selectivity of a low-voltage-activated calcium current in chick and rat sensory neurons. *J. Physiol.* 386:547-70.
14. Carbone E, Lux HD. 1987. Single low-voltage-activated calcium channels in chick and rat sensory neurons. *J. Physiol.* 386:571-601.
15. Catterall WA. 1991. Functional subunit structure of voltage-gated calcium channels. *Science* 253:1499-500.
16. Chen CP, Hess P. 1990. Mechanism of gating of T-type calcium channels. *J. Gen. Physiol.* 96:603-30.
17. Christie BR, Elliot LS, Ito K-I, Miyakawa H, Johnston D. 1995. Different Ca^{2+} channels in soma and dendrites of hippocampal pyramidal neurons mediate spike-induced Ca^{2+} influx. *J. Neurophysiol.* 73:2353-57.
18. Chung JM, Huguenard JR, Prince DA. 1993. Transient enhancement of low-threshold calcium current in thalamic relay neurons after corticectomy. *J. Neurophysiol.* 70:20-27.
19. Coulter DA, Huguenard JR, Prince DA. 1989. Characterization of ethosuximide reduction of low-threshold calcium current in thalamic neurons. *Ann. Neurol.* 25:582-93.
20. Coulter DA, Huguenard JR, Prince DA. 1989. Specific petit mal anticonvulsants reduce calcium currents in thalamic neurons. *Neurosci. Lett.* 98:74-78.
21. Coulter DA, Huguenard JR, Prince DA. 1989. Calcium currents in rat thalamocortical relay neurons: kinetic properties of the transient, low-threshold current. *J. Physiol.* 414:587-604.
22. Coulter DA, Huguenard JR, Prince DA. 1990. Differential effects of petit mal anticonvulsants and convulsants on thalamic neurons: calcium current reduction. *Br. J. Pharmacol.* 100:800-6.
23. Coulter DA, Huguenard JR, Prince DA. 1991. Mechanism of block of thalamic "T"-type Ca^{2+} channels by petit mal anticonvulsants. *Exp. Brain Res.* 20:201-4.
24. Cramell V, Lightowler S, Pollard CE. 1989. A T-type Ca^{2+} current underlies low-threshold Ca^{2+} potentials in cells of the cat and rat lateral geniculate nucleus. *J. Physiol.* 413:543-61.
25. Deschênes M, Roy JP, Stenise M. 1982. Thalamic bursting mechanism: an inward slow current revealed by membrane hyperpolarization. *Brain Res.* 239:289-93.
26. Donich L, Oskson G, Stenise M. 1986. Thalamic burst patterns in the naturally sleeping cat: a comparison between cortically projecting and reticularis neurons. *J. Physiol.* 379:429-49.
27. Elliot LS, Johnston D. 1994. Multiple components of calcium current in acutely dissociated dentate gyrus granule neurons. *J. Neurophysiol.* 72:762-77.
28. Ertel EA, Warren VA, Adams ME, Griffin PR, Cohen CJ, Smith MM. 1994. Type III omega-agatoxin: a family of probes for similar binding sites on L- and N-type calcium channels. *Biochemistry* 33:5098-108.
29. Fedulova SA, Kostyuk PG, Veselovsky NS. 1985. Two types of calcium channels in the somatic membrane of newborn rat dorsal root ganglion neurons. *J. Physiol.* 359:431-46.
30. Fisher R, Johnston D. 1990. Differential modulation of single voltage-gated calcium channels by cholinergic and adrenergic agonists in adult hippocampal neurons. *J. Neurophysiol.* 64:1291-302.
31. Fisher RE, Gray R, Johnston D. 1990. Properties and distribution of single voltage-gated calcium channels in adult hippocampal neurons. *J. Neurophysiol.* 64:91-104.
32. Fox AP, Newkety MC, Tsien RW. 1987. Kinetic and pharmacological properties distinguishing three types of calcium currents in chick sensory neurons. *J. Physiol.* 394:149-72.
33. Fox AP, Newkety MC, Tsien RW. 1987. Single-channel recordings of three types of calcium channels in chick sensory neurons. *J. Physiol.* 394:173-200.
34. Franzenhauser B, Hodgkin AL. 1957. The action of calcium on the electrical properties of squid axons. *J. Physiol.* 137:218-44.
35. Fraser DD, MacVicar BA. 1991. Low-threshold transient calcium current in rat hippocampal lacunosum-moleculare interneurons: kinetics and modulation by neurotransmitters. *J. Neurosci.* 11:2812-20.
36. Friedman A, Guinick MJ. 1987. Low-threshold calcium electrogenesis in neocortical neurons. *Neurosci. Lett.* 81:117-22.
37. Garber U, Greene RW, McCarley RW. 1989. Repetitive firing properties of medial pontine reticular formation neurons of the rat recorded in vitro. *J. Physiol.* 410:553-60.
38. Griffin K, Solomon JS, Burchhalter A, Nertonne JM. 1991. Differential expression of voltage-gated calcium channels in identified visual cortical neurons. *Neuron* 6:321-32.
39. Griffith WH, Taylor L, Davis MJ. 1994. Whole-cell and single-channel calcium currents in guinea pig basal forebrain neurons. *J. Neurophysiol.* 71:2359-76.
40. Gu X, Spitzer NC. 1993. Low-threshold Ca^{2+} current and its role in spontaneous elevations of intracellular Ca^{2+} in developing *Xenopus* neurons. *J. Neurosci.* 13:4936-48.
41. Guinick MJ, Yarom Y. 1989. Low threshold calcium spikes, intrinsic neuronal oscillation and rhythm generation in the CNS. *J. Neurosci. Methods* 28:93-99.
42. Hamill OP, Huguenard JR, Prince DA. 1991. Patch-clamp studies of voltage-gated currents in identified neurons of the rat cerebral cortex. *Cereb. Cortex* 1:48-61.
43. Hernandez-Cruz A, Pape HC. 1989. Identification of two calcium currents in acutely dissociated neurons from the rat lateral geniculate nucleus. *J. Neurophysiol.* 61:1270-83.
44. Herrington J, Linggle CJ. 1992. Kinetic and pharmacological properties of low voltage-activated Ca^{2+} current in rat clonal (GH3) pituitary cells. *J. Neurophysiol.* 68:213-32.
45. Herrington J, Stem RC, Evans AS, Linggle CJ. 1991. Halothane inhibits two components of calcium current in clonal (GH3) pituitary cells. *J. Neurosci.* 11:2226-40.
46. Hille B. 1992. *Ion Channels of Excitable Membranes*. Sunderland, MA: Sinauer, 607 pp.
47. Hodgkin AL, Huxley AF. 1952. A quantitative description of membrane current and its application to conduction and excitation in nerve. *J. Physiol.* 117:500-44.
48. Hoehn K, Watson TWJ, MacVicar BA. 1993. Multiple types of calcium channels in acutely isolated rat neocortical neurons. *J. Neurosci.* 13:1244-57.
49. Huang L-YM. 1989. Calcium channels in isolated rat dorsal horn neurons, including labelled spinolaminar and nigrothalamic cells. *J. Physiol.* 411:161-77.
50. Huguenard JR, Guinick MJ, Prince DA. 1993. Transient Ca^{2+} currents in neurons isolated from rat lateral habenula. *J. Neurophysiol.* 70:158-66.
51. Huguenard JR, McCormick DA. 1992. Stimulation of the currents involved in rhythmic oscillations in thalamic relay neurons. *J. Neurophysiol.* 68:1372-83.
52. Huguenard JR, Prince DA. 1992. A novel T-type current underlies prolonged Ca^{2+} -dependent burst firing in GABAergic neurons of rat thalamic reticular nucleus. *J. Neurosci.* 12:3804-17.
53. Huguenard JR, Prince DA. 1994. Intrathalamic rhythmically studied in vitro: nominal T current modulation causes robust anti-oscillatory effects. *J. Neurosci.* 14:5485-502.
54. Ito C, Im WB, Takagi H, Takahashi M, Tsubaki K, et al. 1994. U-92032, a T-type Ca^{2+} channel blocker and antioxidant, reduces neuronal ischemic injuries. *Eur. J. Pharmacol.* 257:203-10.
55. Jahnson H, Llinás R. 1984. Ionic basis for the electro-responses and oscillatory properties of guinea-pig thalamic neurons in vitro. *J. Physiol.* 349:227-47.
56. Jahnson H, Llinás R. 1984. Electrophysiological properties of guinea-pig thalamic neurons: an in vitro study. *J. Physiol.* 349:205-26.
57. Kaneda M, Aitaki N. 1989. The low-threshold Ca current in isolated amy-

- study by the mystatin perforated patch technique. *Brain Res.* 606:111-17.
110. Yoshii M, Tsunoo A, Narahashi T. 1988. Gating and permeation properties of two types of calcium channels in neuroblastoma cells. *Biophys. J.* 54:885-95.
111. Zhang L, Valiante TA, Carlen PL. 1993. Contribution of the low-threshold T-type calcium current in generating the post-spike depolarizing afterpotential in dentate granule neurons of immature rats. *J. Neurophysiol.* 70:223-31.

PERSISTENT SODIUM CURRENT IN MAMMALIAN CENTRAL NEURONS

Wayne E. Crill

Department of Physiology and Biophysics, University of Washington, Seattle, Washington 98195

KEY WORDS: sodium channels, persistent sodium current, neurons

ABSTRACT

Neurons from the mammalian CNS have a noninactivating component of the tetrodotoxin-sensitive sodium current (I_{NaP}). Although its magnitude is <1% of the transient sodium current, I_{NaP} has functional significance because it is activated about 10 mV negative to the transient sodium current, where few voltage-gated channels are activated and neuron input resistance is high. I_{NaP} adds to synaptic current, and evidence indicates that it is present in dendrites where relatively small depolarizations will activate I_{NaP} , thereby increasing effectiveness of distal depolarizing synaptic activity. The mechanism for I_{NaP} is not known. Research in striated muscle and neurons suggests a modal change in gating of conventional sodium channels, but it is also possible that I_{NaP} flow through a distinct subtype of noninactivating sodium channels. Modulation of I_{NaP} could have a significant effect on the transduction of synaptic currents by neurons.

INTRODUCTION

The ionic model proposed in 1952 by Hodgkin & Huxley (31) continue to serve as the foundation for our understanding of excitability. Depolarization evokes all-or-nothing action potentials by activating the voltage-dependent opening of sodium channels. With maintained polarization, the sodium conductance inactivates within a millisecond or so and this, together with activation of potassium conductances, leads to rapid repolarization of the action potentials in neurons. The Hodgkin-Huxley model (31) also explains the voltage-dependent inactivation of sodium channels causes spike threshold accommodation and anodal break excitation. At present, biophysicists are designing experiments to understand the molecular mechanism for select

Selective Increase in T-Type Calcium Conductance of Reticular Thalamic Neurons in a Rat Model of Absence Epilepsy

Evdoxia Tsakiridou,¹ Laura Bertollini,² Marco de Curtis,² Giuliano Avanzini,² and Hans-Christian Pape^{1,3}

¹Abteilung für Neurophysiologie, Medizinische Fakultät, Ruhr-Universität, D-44780 Bochum, Germany, ²Dipartimento di Neurofisiologia, Istituto Nazionale Neurologico "Carlo Besta," I-20133 Milano, Italy, and ³Institut für Physiologie, Medizinische Fakultät, Otto-von-Guericke-Universität, D-39120 Magdeburg, Germany

The properties of voltage-dependent calcium currents were compared in thalamic neurons acutely dissociated from a rat model of absence epilepsy, designated as Genetic Absence Epilepsy Rat from Strasbourg (GAERS), and from a Nonepileptic Control strain (NEC). Two populations of neurons were isolated: thalamocortical relay neurons of the nucleus ventrobasis (VB) and neurons of the nucleus reticularis (RT) of the thalamus. Whole-cell patch-clamp analysis demonstrated an increase in the amplitude of the calcium (Ca^{2+}) current with a low threshold of activation (I_T) in RT neurons of GAERS in comparison to that of the seizure-free rat strain (-198 ± 19 pA and -128 ± 14 pA, respectively), whereas the sustained component (I_L) was not significantly different. The kinetic properties, voltage dependence, and basic pharmacological sensitivity of the Ca^{2+} conductances were similar in the two populations of neurons. The amplitude of both I_T and I_L in RT neurons increased after birth, and differences in I_T between GAERS and NEC attained significance after postnatal day 11. At corresponding ages, the Ca^{2+} currents in VB thalamocortical relay neurons were not altered in GAERS in comparison to those in NEC.

We conclude that the selective increase in I_T of RT neurons enhances the probability of recurrent intrathalamic burst activity, thereby strengthening the synchronizing mechanisms in thalamocortical systems, and, as such, represents a possible primary neuronal dysfunction that relates to the pathological increase in synchronization underlying the generation of bilateral and synchronous spike and wave discharges (SWDs) in an established genetic model of generalized epilepsy.

[Key words: thalamus, calcium currents, synchronization, spike and wave discharges, absence epilepsy, genetic model]

Received Aug. 1, 1994; revised Oct. 26, 1994; accepted Nov. 2, 1994.

We thank Drs. C. Marescaux and M. Vergnes for letting us use the genetic absence epilepsy model GAERS, and Dr. Z. F. Kisvárdy, Mrs. E. Tóth, and Mrs. U. Neubacher for help with immunohistochemical techniques. L.B. and M.d.C. are grateful to Dr. E. Wanke for making a recording setup available; E.T. and H.-C.P. acknowledge the generous support by Dr. U. T. Eysel. This research was supported by a grant from the Deutsche Forschungsgemeinschaft to H.-C.P. (Ey 8/17-3; Ey 8/17-4) and a European Neuroscience Program Grant to H.-C.P. and M.d.C. (No. 24).

Correspondence should be addressed to Hans-Christian Pape, Institut für Physiologie, Universitätsklinikum Otto-von-Guericke, Leipziger Strasse 44, D-39120 Magdeburg, Germany.

Copyright © 1995 Society for Neuroscience 0270-6474/95/153110-08\$05.00/0

Idiopathic generalized epilepsies in humans are characterized by the spontaneous occurrence of convulsive or nonconvulsive seizures that correlate with the abrupt appearance of bilateral synchronous spike and wave discharges (SWDs) on the electroencephalogram (EEG). Rhythmic SWDs that involve the entire cortical mantle from the very onset of the seizure are observed in the prototypical form of idiopathic epilepsy, the absence epilepsy, a presumably genetically determined disease (Metrakos and Metrakos, 1961; Roger et al., 1985; Berkovic et al., 1987; Commission on Classification and Terminology of the International League Against Epilepsy, 1989). The abrupt initiation and cessation of EEG discharges in generalized epilepsy suggested the hypothesis that a centrencephalic pacemaker structure projecting diffusely to the cortex could be responsible for bilateral and synchronous SWDs (Jasper and Kershman, 1941). Since the demonstration that SWDs in humans originate from the thalamus (Spiegel et al., 1951; Williams, 1953), the hypothesis that the mechanisms of thalamocortical synchronization could be implicated in the generation of spontaneous SWDs has been extensively investigated (Jasper and Droogelever-Fortuyn, 1946; Avoli and Gloor, 1982; Gloor and Fariello, 1988; Avoli et al., 1990).

It is widely recognized that the thalamus is intimately involved in cortical rhythmogenesis. During the transition toward quiescent sleep (from a desynchronized to a synchronized EEG state), thalamic nuclei generate rhythmic oscillations that progressively entrain the entire thalamocortical system to produce synchronous rhythmic activity termed spindling (Jahnsen and Llinás, 1984; Steriade and Deschenes, 1984; Steriade and Llinás, 1988; McCormick, 1992; Steriade et al., 1993). Important elements during the transition from desynchronized to synchronized states of the EEG are represented by the neurons of the nucleus reticularis thalami (RT). The RT is a shell-shaped nucleus formed by GABAergic neurons that project to the dorsal thalamus and receive axon collaterals from both corticothalamic and thalamocortical fibers (Jones, 1985). Spindle activity is produced in the RT by the peculiar interplay between the intrinsic membrane properties, in particular, a Ca^{2+} conductance with low threshold of activation and Ca^{2+} -dependent potassium or cationic currents (Avanzini et al., 1989; Huguenard and Prince, 1992; Bal and McCormick, 1993), and by the arrangement of RT synaptic interactions within the thalamocortical network (Steriade et al., 1986, 1987; Spreafico et al., 1991; von Krosigk et al., 1993). The potential role of RT neurons in sustaining the pathological synchronization underlying SWDs has been studied in a genetically based animal model that mimics the characteristics of human absence epilepsy, designated as Genetic Absence

Epilepsy Rat from Strasbourg (GAERS; Marescaux et al., 1992). Absence-like seizures in GAERS occur spontaneously and are characterized by behavioral arrest, staring, and clonic twitching of the vibrissae, associated with high-amplitude SWDs at 7–11 Hz. As for human generalized primary idiopathic epilepsies, in GAERS (1) the SWD trait is inherited, (2) the onset of seizures is age dependent, (3) seizure occurrence increases during phases of transition between sleep and wakefulness, (4) SWDs are suppressed by drugs effective against human absence epilepsy, (5) intercritical EEG activity is normal, and (6) there are no signs of neurological deficits or intercritical behavioral impairment. In agreement with a possible pathogenic role of the thalamus and, in particular, of the RT in the expression of absence seizures, SWDs in GAERS were demonstrated to originate from the lateral thalamic nuclei (Vergnes et al., 1987), and were abolished by local infusion of Ca^{2+} antagonists into the RT (Avanzini et al., 1993).

In order to gain insights into the cellular mechanisms that may be involved in the generation of SWDs, we analyzed voltage-dependent Ca^{2+} currents in thalamocortical relay neurons and in RT neurons acutely isolated from GAERS and from a selected 100% seizure-free rat strain (nonepileptic controls, NEC).

Materials and Methods

Acutely isolated neurons were prepared from coronal slices (400 μm), including the RT and the ventrobasal complex of the thalamus (VB) cut by vibratome or tissue chopper from 7–20-d-old GAERS and NEC after halothane anesthesia. Under a stereoscopic microscope, the RT was isolated from the adjacent VB by a cut along the external medullary lamina. The cellular content of the isolated tissue was verified with standard GABA or glutamic acid decarboxylase (GAD) immunostaining (Pape et al., 1994); tissue sections including RT contained a high concentration of immunopositive neurons, whereas GABAergic cells were extremely rare in VB tissue slices. RT cells and relay VB neurons from the same animal were separately dissociated using standard enzymatic/mechanical procedures (Kay and Wong, 1986; Budde et al., 1992). Thalamic slices were incubated in oxygenated medium containing either trypsin (Sigma type XI; 1–4 mg/ml, 60–90 min at room temperature) or papain (Worthington; 14 U/ml, 10–20 min at 36°C), bovine serum albumin (0.5 mg/ml) and (in mM) 120 NaCl, 5 KCl, 1 MgCl_2 , 1 CaCl_2 , 20 PIPES, 25 dextrose (pH 7.35). After washing with enzyme-free medium, the neurons were mechanically dissociated by trituration. Neurons acutely dissociated from the VB were characterized by a large, multipolar, and GABA-negative soma, whereas RT neurons showed a fusiform soma intensely stained by GABA, giving rise to two major dendrites at opposite poles (see also Huguenard and Prince, 1992). Intracellular recordings were performed at room temperature from isolated neurons using the whole-cell variant of the patch-clamp technique (Hamill et al., 1981). Patch electrodes had an access resistance of 4–8 M Ω . Series resistance compensation > 50% was routinely utilized. Records were low-pass filtered at 2.5 kHz (3–8 pole Bessel filter), and a P/4 pulse protocol (pCLAMP; Axon Instruments, USA) was used to remove leak and capacitive current interferences (see Budde et al., 1992). Two different extracellular solution perfused continuously at 0.1–1 ml/min were utilized in the two laboratories to isolate Ca^{2+} currents. The solution used in the Bochum laboratory was (in mM) 120 NaCl, 1 KCl, 10 D-mannitol, 2 CaCl_2 , 1 MgCl_2 , 20 TEA-Cl, 6 4-AP, 10 HEPES, and 1.5 μM TTX. The solution in Milano laboratory was (in mM) 80 choline-Cl, 3 KCl, 24 glucose, 5 CaCl_2 , 1 MgCl_2 , 50 TEA-Cl, 8 4-AP, 10 HEPES. The solution in the pipette contained (in mM) 128 *N*-methyl-D-glucamine, 10 NaCl, 1 CaCl_2 , 2 MgCl_2 , 11 EGTA, 5 Na_2ATP , 0.5 Na_2GTP , and 20 TEA-Cl (pH 7.35); or (in mM) 110 Tris- PO_4 dibasic, 28 Tris-base, 2 MgCl_2 , 0.5 CaCl_2 , 11 EGTA, 2 MgATP , 0.2 Tris-GTP, 20 creatine-phosphate, and 50 U/ml creatine-phosphokinase (pH 7.4), in the Bochum and Milano laboratories, respectively.

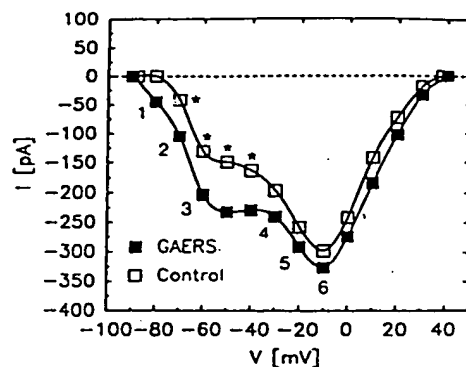
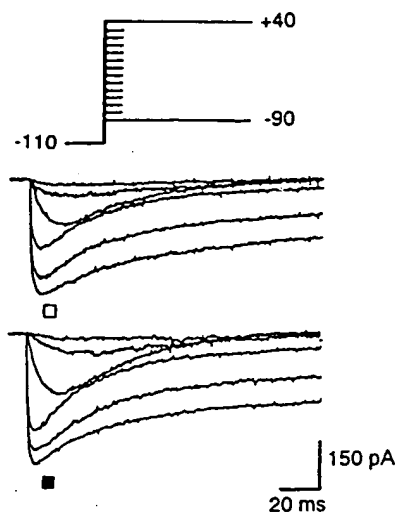
Results

Whole-cell voltage-clamp experiments were performed in acutely dissociated neurons under conditions where Ca^{2+} currents are

isolated. Depolarization of the membrane in the range between -80 and -40 mV from a holding potential of -110 mV evoked a transient Ca^{2+} inward current (I_T), whose amplitude increased with membrane depolarization (Fig. 1A). Positive to -40 mV, a more sustained Ca^{2+} current (I_L) was additionally evoked, confirming the existence in RT neurons of two Ca^{2+} conductances with different activation threshold and kinetics (Huguenard and Prince, 1992). By comparing the basic characteristics of Ca^{2+} currents in RT neurons from GAERS and NEC, a striking difference in the amplitude of I_T was observed. As illustrated in Figure 1, depolarizing steps from a holding potential of -110 mV evoked much larger transient I_T currents in RT neurons from GAERS than in NEC, whereas the amplitude of the sustained I_L component was similar in the two groups of neurons. Current-voltage relationships (I/V histograms in Fig. 1A), constructed from a larger sample of neurons, demonstrated a significant increase in peak current amplitude at potential values negative to -30 mV in GAERS ($n = 16$) compared with that in NEC ($n = 18$), with no obvious shift in the peak current-voltage relationship. The sensitivity toward inorganic Ca^{2+} channel antagonists was not significantly different in RT neurons from the two groups of rats (data not shown). Nickel (50 μM) reduced I_T by $54.0 \pm 21.4\%$ ($n = 9$) and by $37.7 \pm 8.8\%$ ($n = 7$), and I_L by $30.0 \pm 14.0\%$ ($n = 6$) and by $33.1 \pm 7.6\%$ ($n = 7$) in RT neurons from GAERS and NEC, respectively. Cadmium (50 μM) reduced I_T by $32.3 \pm 23.0\%$ ($n = 7$) in GAERS and by $57.1 \pm 23.2\%$ ($n = 6$) in NEC, while I_L was completely abolished in RT neurons from both groups of animals ($n = 10$ and $n = 8$, respectively). Ethosuccinimide, at a saturating concentration (5 mM; Coulter et al., 1989b), reduced I_T by $18.3 \pm 6.9\%$ ($n = 7$) and by $19.5 \pm 2.9\%$ ($n = 3$) in GAERS and in the control group, similar to the reduction observed for the L-type current in the two populations of neurons ($18.1 \pm 6.3\%$, $n = 5$; $22.6 \pm 6.7\%$, $n = 7$). Replacement of Ca^{2+} by barium ions (2 mM) resulted in an increase in amplitude of both I_T ($23.2 \pm 6.3\%$, $n = 7$ GAERS; $18.1 \pm 3.4\%$, $n = 7$ NEC) and I_L ($43.4 \pm 13.4\%$, $n = 6$ GAERS; $20.8 \pm 10.5\%$, $n = 3$ NEC), as previously reported (Huguenard and Prince, 1992).

The transient and sustained Ca^{2+} current components were separated using a conditioning pulse protocol. A 100 msec prepulse to -50 mV between the holding potential (-110 mV) and the depolarizing voltage steps inactivated I_T . The I_L current activated at membrane potentials positive to approximately -40 mV, and the amplitude was not significantly different in RT neurons from GAERS and NEC (Fig. 1B). The I_T current was isolated by digital subtraction of the records obtained without and with the conditioning prepulse (Fig. 1C). In both groups of RT neurons, I_T was rapidly activated through depolarizing voltage steps and peaked at around -50 mV. The average peak amplitude at -50 mV was significantly larger in GAERS [-198 ± 19 pA (mean \pm SEM; $n = 16$)] than in NEC [-128 ± 14 pA; $n = 17$] ($p < 0.005$). The amplitude of the T-type Ca^{2+} current in thalamic neurons increases significantly during postnatal development (see Fig. 3; see also Pirchio et al., 1990). The I_T amplitude differences observed in the present study are not related to development, since the two populations of RT neurons were isolated at the same postnatal age (postnatal days: 15.6 ± 0.6 , $n = 16$ GAERS; 15.6 ± 0.6 , $n = 18$ NEC). The possibility that the differences in I_T amplitude resulted from differences in cell size could be largely ruled out by using the whole-cell capacitance as an index of membrane surface area, and which was

A



B

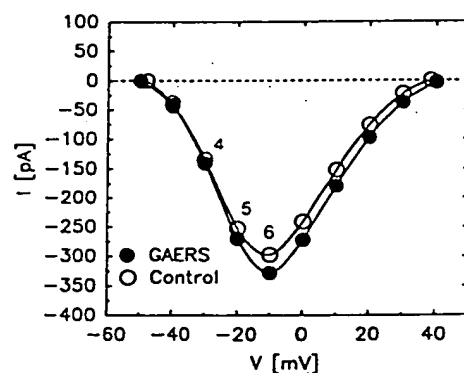
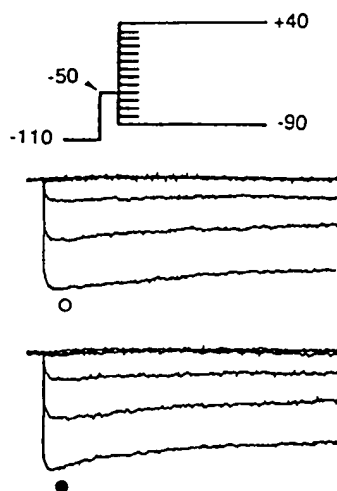
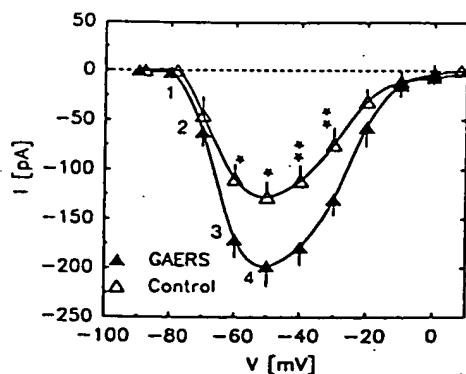
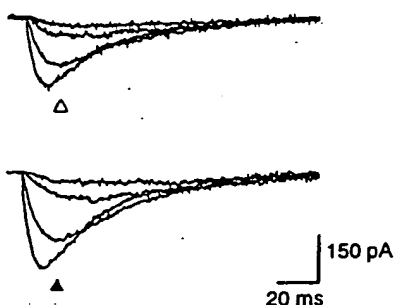


Figure 1. Whole-cell Ca^{2+} currents in RT neurons isolated from GAERS (closed symbols) and NEC (control; open symbols). **A**, Depolarizing voltage steps from -110 mV evoke a transient Ca^{2+} current, I_T , followed by a sustained component, I_L , at more positive potentials. Note the increase in the transient component in GAERS, which is also indicated by the increase in the typical shoulder separating the two current components with different activation threshold in the I/V relationship. **B**, A conditioning prepulse to -50 mV (duration 100 msec) inactivates I_T , and the remaining I_L is very similar in RT neurons from GAERS and NEC. **C**, Digital subtraction of I_L (from experiments in **B**) from the total Ca^{2+} current (from **A**) isolates I_T , whose amplitude is significantly increased in GAERS. I/V relationships of peak currents are averaged from recordings in $n = 16$ and $n = 18$ RT neurons from GAERS and from NEC, respectively; numbers indicate examples shown as original traces; bars in **C** represent SEM, asterisks mark significant differences (**, $p < 0.001$; *, $p < 0.005$; two-tailed t test) between GAERS and NEC. Neurons from both groups of animals were dissociated at postnatal day 16.

C

Difference, A-B



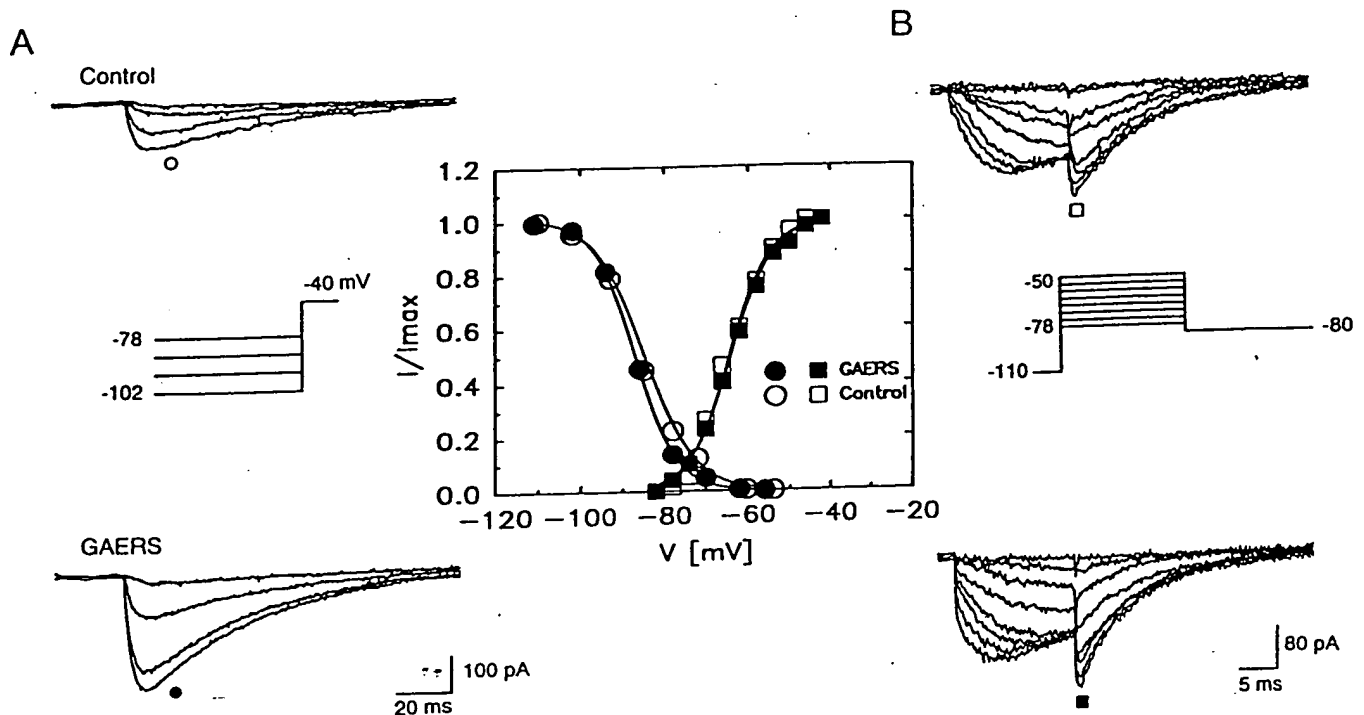


Figure 2. Similar voltage-dependent properties of I_T in RT neurons from GAERS (closed symbols) and NEC (control; open symbols). **A**, Steady-state inactivation of I_T , as determined by varying a prepulse of 2 sec duration between -110 and -54 mV before stepping to -40 mV. The amplitude of I_T decreases with more positive values of the prepulse, indicating inactivation of the underlying conductance. **B**, Analysis of tail amplitude of I_T decreases with more positive values of the prepulse, indicating inactivation of the underlying conductance. **C**, The inactivation (circles) and activation curve (squares) of I_T , as obtained from normalized peak currents (experiments in **A**) and tail current amplitudes (**B**), are not significantly different for the two groups of cells. Histogram represents averaged data ($n = 10$ – 15); continuous curves are Boltzmann fits.

not significantly different in the two groups of neurons (16.3 ± 0.8 pF, $n = 13$ GAERS; 15.7 ± 1.2 pF, $n = 11$ NEC).

A possible explanation for the altered expression of I_T in RT neurons may relate to changes in the voltage-dependent properties of the underlying conductance, for example, a shift in the inactivation and activation curves, or an alteration in the kinetics of the current. Since the time constant of activation of I_T could not be reliably determined, due to the relatively small amplitude of the current, the time-to-peak values were used as an approximation of the activation kinetics. The time-to-peak of I_T decreased with more positive membrane potentials: averaged values in the voltage range between -70 and -40 mV were between 21.2 ± 1.6 msec and 5.1 ± 0.5 msec in GAERS ($n = 11$) and between 17.8 ± 1.6 msec and 6.6 ± 1.7 msec in NEC ($n = 10$). The difference did not attain statistical significance (data not shown). The I_T currents inactivated completely with sustained depolarization, and they could not be elicited from holding potentials positive to -60 mV. The time course of current decay was well fitted by a single exponential function of the form $I = A_0 + A_1 \exp(-t/\tau)$, where I is the amplitude of the membrane current at the time t , A_0 and A_1 are the amplitude coefficients, and τ is the time constant. The time constant displayed very little voltage dependence, averaging 37.1 ± 2.9 and 25.3 ± 0.9 msec in GAERS ($n = 15$), 37.4 ± 3.0 and 26.5 ± 2.6 msec in NEC ($n = 14$) for depolarizations to -70 and -30 mV, respectively (data not shown).

Figure 2A illustrates samples of current records used to determine the voltage dependence of steady-state inactivation of the conductance underlying I_T . A 2 sec prepulse was incre-

mented between -110 and -54 mV with 8 mV steps, before delivering a constant test pulse at -40 mV, subthreshold for I_L and near maximal for I_T activation. The peak current progressively reduced as the prepulse potential became less negative, indicating an increased level of inactivation. The normalized peak amplitudes of the currents were averaged and plotted against the prepulse potential (circles in histogram of Fig. 2). Approximation of a Boltzmann function¹ to the data points indicated a range of steady-state inactivation of I_T that was largely overlapping in the two groups of RT neurons. The I_T current was completely inactivated positive to -60 mV; the values of half inactivation (at -87.0 ± 0.8 and -84.8 ± 1.3 mV) and the slope of the curves (4.9 ± 0.4 and 6.0 ± 0.6 mV⁻¹) were not significantly different in GAERS ($n = 15$) and NEC ($n = 12$). The time course of recovery from inactivation of I_T was approximated best by a single exponential function (data not illustrated). The average time constant in RT neurons from GAERS (278.1 ± 20.4 msec; $n = 13$) was unaltered compared with that in NEC (274.9 ± 13.7 msec; $n = 14$). To study the activation range of I_T , tail currents were analyzed, obtained by repolarizing the membrane to -80 mV following 15 msec depolarizing commands (4 mV increments) from a holding potential of -110 mV. The most depolarized command steps evoked nearly overlapping tail currents, indicating near-maximal activation of I_T . With fur-

¹ The equation for the Boltzmann function was $I/I_{\max} = [1 + \exp((V - V_{1/2})/k)]^{-1}$, where $V_{1/2}$ is the potential of the half-(in)activation and k is the slope factor indicating the steepness of the calculated curve. The equation applies to inactivation and activation curves, k assuming a positive and negative value, and V representing the prepulse potential and the command potential, respectively.

ther depolarization, tail currents were contaminated by I_L . The duration of the depolarizing commands was set to values near peak current activation, and the tail currents evoked by repolarization to potentials outside the range of I_T activation can be assumed to reflect the T-channels activated during the depolarizing command. Since the repolarizing potential is fixed, tail currents can be normalized and plotted against the command potential to produce an activation curve.

The normalized amplitudes of the tail currents were averaged, plotted against the command step, and a Boltzmann function was approximated to the data points (squares in histogram of Fig. 2). The activation curves of I_T were nearly identical in RT neurons from GAERS ($n = 13$) and NEC ($n = 10$). Activation started at around -80 mV and was almost complete at -40 mV; the values of half-activation (-64.0 ± 1.2 and -64.4 ± 1.8 mV) and slope (-4.9 ± 0.3 and -4.7 ± 0.4 mV $^{-1}$) were not significantly different in GAERS and NEC neurons.

As shown in Figure 3, the amplitude of I_T and I_L increased substantially after birth in RT neurons, and differences in I_T amplitude between GAERS and NEC attained significance after postnatal day 11. At the same postnatal age, the I_T current in thalamocortical relay neurons isolated from VB was not significantly altered in GAERS in comparison to NEC (see also Guyon et al., 1993).

Discussion

The choice of the experimental model

The study of the mechanisms underlying epileptic discharges in primary generalized epilepsies requires the utilization of appropriate experimental models, which have to fulfill the criteria described by the terms idiopathic and generalized (Commission on Classification and Terminology of the International League Against Epilepsy, 1989). The strain of Wistar rats with genetically determined seizures designated as GAERS present spontaneous absences correlated with high-amplitude SWDs occurring abruptly on a normal intercritical EEG activity. Neurophysiological, behavioral, genetic, and pharmacological studies carried out in the past 10 years demonstrated that SWDs in GAERS fulfill the requirements for an experimental model of absence epilepsy (Marescaux et al., 1992). The SWD genetic trait in GAERS is inherited, and the onset of seizures is age dependent, starting after 1 month of postnatal life (Vergnes et al., 1986; Marescaux et al., 1992). As for spindles and human generalized SWDs (Kellaway, 1985), seizure occurrence in GAERS increases during phases of transition between arousal and sleep, although the frequency of SWDs in GAERS at 7–11 Hz (Marescaux et al., 1992) is higher than that (2–4 Hz) seen in the EEG of petit mal patients (Kellaway, 1985) and in animal experiments using the penicillin model of generalized epilepsy (Gloor and Fariello, 1988) or the cortically or thalamically induced seizure activity in acute and chronic preparations (cf. Avoli et al., 1990). This heterogeneity of SWDs may indicate that multiple mechanisms may be involved in the genesis of different forms of SWDs (cf. Steriade et al., 1993; von Krosigk et al., 1993). In any case, *in vivo* recordings from the thalamus and cortex in GAERS demonstrated that SWDs were abolished ipsilaterally by a large lesion of the lateral thalamus after a complete callosotomy (Vergnes et al., 1987; Vergnes and Marescaux, 1992). Moreover, Avanzini et al. (1993) demonstrated that SWDs in GAERS are disrupted ipsilaterally to selective lesions of RT induced by stereotaxic injections of the excitotoxin ibotenic acid in previously callosotomized animals. Similarly, in-

organic Ca^{2+} antagonists suppressed SWDs when locally infused in RT and only reduced their expression when injected in the lateral thalamic relay nuclei (Vergnes et al., 1987; Avanzini et al., 1993). These data strongly suggested that Ca^{2+} -dependent processes in RT are determinant in the regulation of SWDs in GAERS, and they achieve particular relevance in light of the demonstration in isolated thalamic neurons that the transient calcium current I_T , critical for the generation of oscillatory behavior, is reduced by antiepileptic drugs effective on absence seizures and on GAERS SWDs, like ethosuccimide (Marescaux et al., 1984; Coulter et al., 1989b, 1990; Huguenard and Prince, 1992, 1994a).

Selective I_T increase in RT

The present study demonstrates that in GAERS the transient Ca^{2+} conductance I_T is selectively augmented in neurons of the RT after the second postnatal week. This alteration seems to be selective in terms of the type of Ca^{2+} conductance and the type of thalamic neuron that are affected, since the L-type current component was not affected in the same sample of RT neurons, and Ca^{2+} currents were not significantly different in thalamocortical relay neurons isolated from the VB complex of the same animals. The latter result confirms the observation by Guyon et al. (1993) of unaltered Ca^{2+} currents in VB slices obtained from adult GAERS. The observed enhancement of I_T amplitude is not due to differences in membrane surface area or postnatal age of the two populations of RT neurons that were studied, and it is not likely to result from an alteration in the gating properties of the underlying conductance, since activation and inactivation curves and the kinetics of the current were similar in neurons dissociated from NEC and GAERS. Following from this, the augmented I_T current in RT neurons from GAERS seems to reflect an increase in the number of available T-type Ca^{2+} channels or an increase in single channel conductance, thereby resembling the transient enhancement of I_T demonstrated in relay neurons after cortical lesions (Chung et al., 1993).

A transient Ca^{2+} current with a nearly voltage-independent, slow rate of inactivation and a rather positive range of activation ($V_h = -49$ mV), designed as I_T , has been demonstrated by Huguenard and Prince (1992) in neurons isolated predominantly from the most anterior section of the thalamus. The neurons from the dorsal, VB-related portion of the RT studied in the two laboratories participating in the present study (see Materials and Methods) possessed a more rapidly inactivating I_T with negative range of activation ($V_h = -64$ mV). This heterogeneity suggests that the I_T may be selectively segregated in neurons of the most anterior portion of RT, where neurons also present morphological features different from those of the more caudal RT (Scheibel and Scheibel, 1972; Spreafico et al., 1991; Lübke, 1993), or that two classes of neurons possessing distinctive electrophysiological properties may exist in the RT nucleus (Contreras et al., 1992).

Increased synchronization and SWDs

Several lines of evidence summarized in the introduction indicate that common circuitry and intrinsic mechanisms in the thalamus, of which reciprocal intrathalamic connections and burst firing dependent on the T-type Ca^{2+} conductance represent two important variables, underlie spindle rhythm and SWDs of absence epilepsy. We suggest that the selective, presumably genetically determined, increase in the conductance underlying I_T in RT neurons enhance the propensity for burst firing, thereby

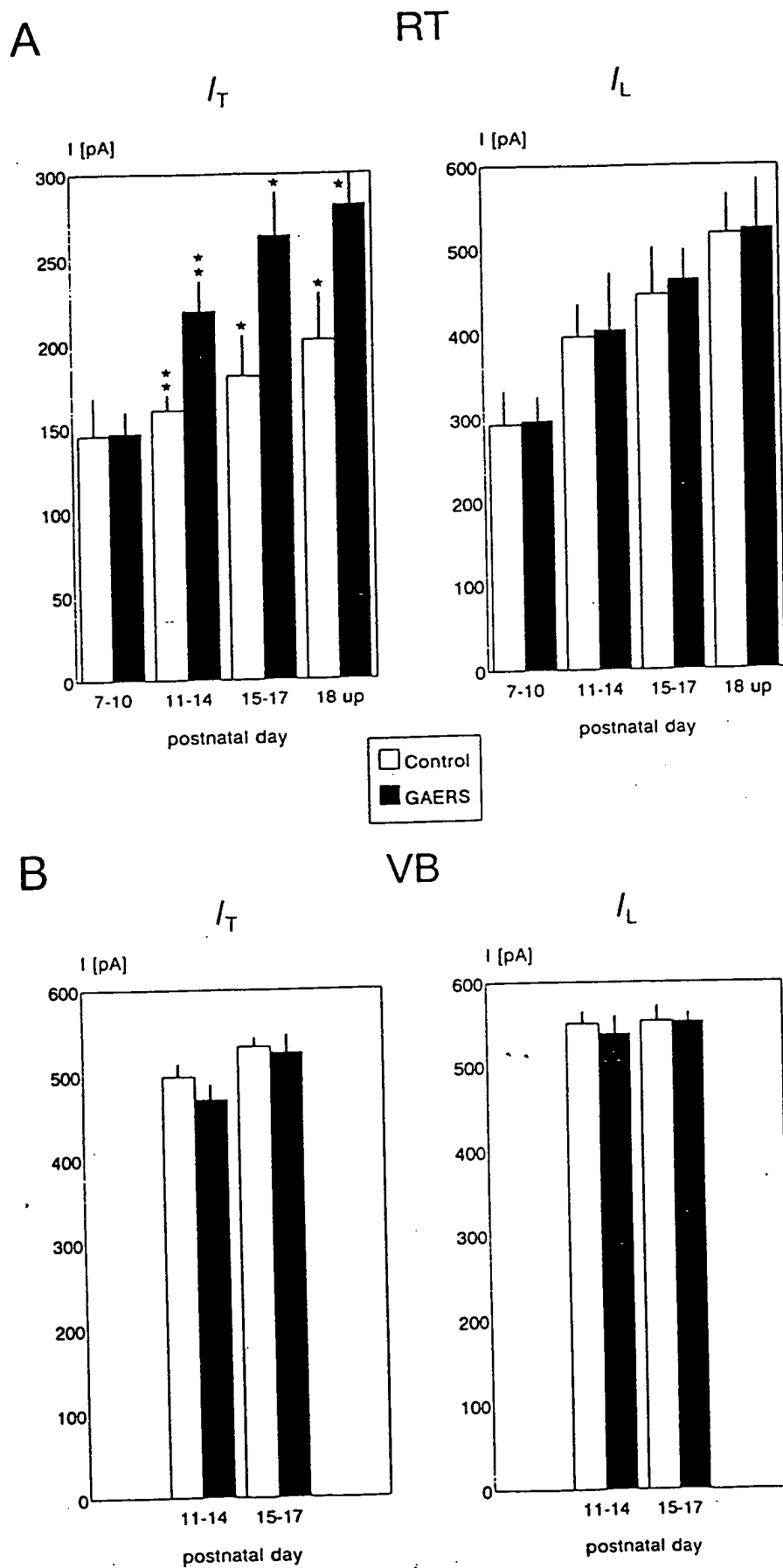


Figure 3. Age-dependent and selective increase of I_T in RT neurons from GAERS. Mean maximal amplitudes of I_T and I_L in RT neurons (A) and relay neurons from VB (B) acutely dissociated from GAERS (closed bars) and NEC (control; open bars) at different postnatal ages. Note the selective increase in I_T in GAERS starting at postnatal days 11–14. Bars represent averaged data (\pm SEM); significant differences between GAERS and NEC are indicated by asterisks (**, $p < 0.01$; *, $p < 0.05$; two-tailed t test). To account for possible differences in cell size at different postnatal days, current amplitudes were normalized to a membrane surface area corresponding to an input capacitance of 20 pF.

entraining recurrent burst activity and contributing to the pathological increase in synchronization underlying SWDs in GAERS. In line with this hypothesis is the recent observation in thalamic slice preparations that the decrease (30–40%) in I_T conductance by succinimides resulted in a dramatic reduction in intrathalamic oscillations through a slight decrease in burst probability of thalamic neurons (Huguenard and Prince, 1994b). The Ca^{2+} currents in thalamocortical relay neurons in VB and possibly in other thalamic nuclei are not affected in GAERS, but relay cells can be assumed to be secondarily recruited by the rhythmic discharges generated in RT. In addition, an increase in GABA_B receptor-mediated responsiveness (Snead, 1992; Horsford et al., 1992) and resulting increase in deactivation of I_T in relay cells may act to reinforce recurrent rhythmic discharges into pathological forms of synchronization on the level of the relay nuclei (Von Krosigk et al., 1993).

The fact that seizures and SWDs in human absence epilepsy and in genetic animal models are age dependent and are usually absent at birth suggests that the pathological expressivity of the original defect (or defects) depends on the complete maturation of neuronal elements and synaptic circuitry in the thalamocortical system. In GAERS, both the increase in I_T amplitude and the appearance of SWDs are absent at early postnatal stages. Their later developmental course diverges considerably, since I_T augmented with respect to controls 11 d after birth, whereas SWDs are undetectable before the end of the first month of postnatal life. It is conceivable that, as for the physiological thalamocortical synchronizing patterns (Jouvet-Mourner et al., 1970), SWD expression in GAERS requires the complete maturation of the thalamocorticothalamic synaptic network to become fully expressed. It is known that maturation of thalamic and cortical connections in rats is completed within 2 weeks of postnatal age (Jones, 1985). By comparison, other processes such as synaptogenesis and spine formation, which control post-synaptic potential generation in the thalamus and cortex and which are probably needed to express functionally mature rhythmic and synchronous thalamocortical oscillations, are modified during later phases of development and do not reach near-adult stages before the fourth postnatal week (Cragg, 1975; Daniels et al., 1975; Wise et al., 1978; Jones, 1985; for a review see Shatz, 1990).

Changes in the quantitative expression of a single current or membrane receptor during the thalamocortical developmental time table paced by a programmed sequence of gene expression (Desarmenian et al., 1992; Spitzer et al., 1994) may significantly modify the synaptic arrangement and the weight of synapses in a developing network. The possibility that such a process is active in the ontogenesis of SWD generation is strengthened by the notion that synaptic activity and rhythmic oscillations play an important role in organizing synaptic connectivity (Changeaux and Danchin, 1976; Provine and Rogers, 1977; Llinás, 1984; Llinás, 1988; Shatz, 1990; Kalb and Hockfield, 1992; Sillar, 1994). It is known from these studies that during development, neurons produce electrical autorhythmicity, which can entrain homogeneous populations of neurons to oscillate. Network oscillations lead to a dynamic linkage between different brain areas and may reinforce synaptic interactions. Oscillatory rhythmic activity at various frequencies, whose relevance in normal physiological conditions can be easily appreciated by looking at the EEG of an infant, may be an important factor in determining the strength and the ontogenic organization of synaptic connectivity that are necessary to regulate a complex func-

tion. The abnormal thalamic oscillatory activity generated in juvenile GAERS by the augmented I_T in RT neurons could, in principle, consolidate excitatory synapses and influence the plastic properties of developing thalamic and cortical neurons toward a persistent state of hyperexcitation, which is expressed by SWDs.

The selective increase in I_T conductance in RT neurons is the first demonstration of a primary neuronal dysfunction suspected to relate to seizure generation in an established animal model of genetic epilepsy and represents a potentially important step in the attempt to identify markers for genetic linkage studies in human epilepsies.

References

- Avanzini G, de Curtis M, Spreafico R (1989) Intrinsic properties of nucleus reticularis neurons of the rat studied *in vitro*. *J Physiol (Lond)* 416:111–122.
- Avanzini G, Vergnes M, Spreafico R, Marescaux C (1993) Calcium-dependent regulation of genetically determined spike and waves by the RTN of rats. *Epilepsia* 34:1–7.
- Avoli M, Gloor P (1982) Role of thalamus in generalized penicillin epilepsy: observations on decorticated cats. *Exp Neurol* 77:386–402.
- Avoli M, Gloor P, Kostopoulos G, Naquet R (1990) Generalized epilepsy: neurobiological approaches. Boston: Birkhauser.
- Bal T, McCormick DA (1993) Mechanisms of oscillatory activity in guinea pig nucleus RT *in vitro*: a mammalian pacemaker. *J Physiol (Lond)* 468:669–691.
- Berkovic JC, Andermann F, Andermann E, Gloor P (1987) Concepts of absence epilepsies: discrete syndromes or biological continuum? *Neurology* 37:993–1000.
- Budde T, Mager R, Pape H-C (1992) Different types of potassium outward current in relay neurons acutely isolated from the rat lateral geniculate nucleus. *Eur J Neurosci* 4:708–722.
- Changeaux JP, Danchin A (1976) Selective stabilization of developing synapses as a mechanism for the specification of neuronal networks. *Nature* 264:705–712.
- Chung J-M, Huguenard JR, Prince DA (1993) Transient enhancement of low-threshold calcium current in thalamic relay neurons after corticectomy. *J Neurophysiol* 70:20–27.
- Commission on Classification and Terminology of the International League Against Epilepsy (1989) Proposal for revised classification of epilepsies and epileptic syndromes. *Epilepsia* 30:389–399.
- Contreras D, Currló Dossi R, Steriade M (1992) Bursting and tonic discharges in two classes of reticular thalamic neurons. *J Neurophysiol* 68:973–977.
- Coulter DA, Huguenard JR, Prince DA (1989a) Calcium currents in rat thalamocortical relay neurons: kinetic properties of the transient, low-threshold current. *J Physiol (Lond)* 414:587–604.
- Coulter DA, Huguenard JR, Prince DA (1989b) Characterization of ethosuximide reduction of low-threshold calcium current in thalamic neurons. *Ann Neurol* 25:582–593.
- Coulter DA, Huguenard JR, Prince DA (1990) Differential effect of petit mal anticonvulsants and convulsants on thalamic neurons: calcium current reduction. *Br J Pharmacol* 100:800–806.
- Cragg BG (1975) Development of synapses in the visual system of the cat. *J Comp Neurol* 160:147–166.
- Crunelli V, Lightowler S, Pollard CE (1989) A T-type calcium current underlies low threshold calcium potentials in cells of the cat and rat lateral geniculate nucleus. *J Physiol (Lond)* 413:543–561.
- Daniels JD, Pettigrew JD, Norman JL (1978) Development of single unit responses in kitten's LGN. *J Neurophysiol* 41:1373–1393.
- Gloor P, Fariello RG (1988) Generalized epilepsy: some of its cellular mechanisms differ from those of focal epilepsy. *Trends Neurosci* 11:63–68.
- Guyon M, Vergnes M, Leresche N (1993) Thalamic low threshold calcium current in a genetic model of absence epilepsy. *Neuroreport* 4:1231–1235.
- Hamill OP, Marty A, Neher E, Sakmann B, Sigworth FJ (1981) Improved patch clamp techniques for high resolution current recordings from cells and cell-free membrane patches. *Pflügers Arch* 391:85–100.
- Hernández-Crus A, Pape H-C (1989) Identification of two calcium cur-

- rents in acutely dissociated neurons from the rat geniculate nucleus. *J Neurophysiol* 61:1270-1283.
- Hosford DA, Clark S, Cao Z, Wilson WA, Lin F-H, Morrisett RA, Huin A (1992) The role of GABA_A receptor activation in absence seizures of lethargic (*lh/lh*) mice. *Science* 257:398-401.
- Huguenard JR, Prince DA (1992) A novel T-type current underlies prolonged calcium-dependent burst firing in GABAergic neurons of rat RT. *J Neurosci* 12:3804-3821.
- Huguenard JR, Prince DA (1994a) Clonazepam suppresses GABA_A-mediated inhibition in thalamic relay neurons through effects in nucleus reticularis. *J Neurophysiol* 71:2576-2581.
- Huguenard JR, Prince DA (1994b) Intrathalamic rhythmicity studied *in vitro*: nominal T current modulation causes robust anti-oscillatory effects. *J Neurosci* 14:5485-5502.
- Inoue M, Duysens J, Vossen JMH, Coenen AML (1993) Thalamic multiple unit activity underlying SWD in anesthetized rats. *Brain Res* 612:35-40.
- Jahnsen H, Llinás RR (1984) Ionic basis for the electroresponsiveness and oscillatory properties of guinea pig thalamic neurons *in vitro*. *J Physiol (Lond)* 349:227-247.
- Jasper HH, Droogleever-Fortuyn J (1946) Experimental studies of the functional anatomy of the petit mal epilepsy. *Res Publ Assoc Res Nerv Ment Disord* 26:272-290.
- Jasper HH, Kershman J (1941) Electroencephalographic classification of the epilepsies. *Arc Neurol Psychiatry* 45:903-943.
- Jones EG (1985) The thalamus. New York: Plenum.
- Jouvet-Mormier D, Astic L, Lacote M (1970) Ontogenesis of the states of sleep in rat, cat and guinea pig during the first postnatal month. *Dev Psychobiol* 2:216-239.
- Kalb RG, Hockfield S (1986) Activity dependent development of spinal chord motor neurons. *Brain Res Rev* 17:283-289.
- Kay AR, Wong RKS (1986) Isolation of neurons suitable for patch-clamping from adult mammalian central nervous system. *J Neurosci Methods* 16:227-238.
- Kellaway P (1985) Sleep and epilepsy. *Epilepsia* 26:S15-S30.
- Liu Z, Vergnes M, Depaulis A, Marescaux C (1992) Involvement of intrathalamic GABA_B neurotransmission in the control of absence seizures in the rat. *Neuroscience* 51:87-93.
- Llinás RR (1984) Possible role of tremor in the organization of the nervous system. In: *Movement disorders: tremor* (Findley LJ, Capildeo R, eds), pp 473-478. London: Macmillan.
- Llinás RR (1988) The intrinsic electrophysiological properties of mammalian neurons: insight into the central nervous system functions. *Science* 242:1654-1664.
- Lübke J (1993) Morphology of neurons in the thalamic reticular nucleus (TRN) of mammals revealed by intracellular injections into fixed brain slices. *J Comp Neurol* 329:458-471.
- Marescaux C, Vergnes M, Micheletti G (1984) Antiepileptic drug evaluation in a new animal model: spontaneous petit mal epilepsy in the rat. *Fed Proc* 43:280-281.
- Marescaux C, Vergnes M, Depaulis A (1992) Genetic absence epilepsy in rats from Strasbourg—a review. *J Neural Transm* 35:37-69.
- McCormick DA (1992) Neurotransmitter actions in the thalamus and cerebral cortex and their role in neuromodulation of thalamocortical activity. *Prog Neurobiol* 39:337-388.
- Metrakos K, Metrakos J (1961) Genetic of convulsive disorders. II. Genetic and EEG studies in centrencephalic epilepsy. *Neurology* 11:474-483.
- Pape H-C, Budde T, Mager R, Kisvárdy ZF (1994) Prevention of Ca²⁺-mediated action potentials in GABAergic local circuit neurons of the rat thalamus by a transient K⁺ current. *J Physiol (Lond)* 478:403-422.
- Pirchio M, Lightowler S, Crunelli V (1990) Postnatal development of the T-calcium current in cat thalamocortical cells. *Neuroscience* 38:39-45.
- Prince DA, Farrel D (1969) Centrencephalic SWD following parenteral penicillin injection in the cat. *Neurology* 19:309-310.
- Provine RR, Rogers L (1977) Development of spinal chord bioelectrical activity in spinal chick embryos and its behavioural implications. *J Neurobiol* 8:217-228.
- Roger J, Dravet C, Bureau M (1985) Epileptic syndromes in infancy, childhood and adolescence. London: Libbey.
- Scheibel ME, Scheibel AB (1972) Specialized organizational patterns within the RT nucleus of the cat. *Exp Neurol* 34:316-322.
- Shatz CJ (1990) Impulse activity and the patterning of connections during CNS development. *Neuron* 5:745-756.
- Sillar KT (1994) Synaptic specificity: development of locomotor rhythmicity. *Curr Opin Neurosci* 4:101-107.
- Snead OC (1992) Evidence for GABA_B-mediated mechanisms in experimental generalized absence seizures. *Eur J Pharmacol* 213:343-349.
- Spiegel EA, Wycis HT (1950) Thalamic recordings in man with special reference to seizure discharges. *EEG Clin Neurophysiol* 2:23-27.
- Spreafico R, Battaglia G, Frassonni C (1991) The RT nucleus of the rat: cytoarchitecture, Golgi, immunocytochemical and -HRP study. *J Comp Neurol* 304:478-490.
- Steriade M, Deschenes M (1984) The thalamus as a neuronal oscillator. *Brain Res Rev* 8:1-31.
- Steriade M, Llinás RR (1988) The functional states of the thalamus and the associated neuronal interplay. *Physiol Rev* 68:649-742.
- Steriade M, Domich L, Oakson G (1986) Reticularis thalami neurons revisited: activity changes during shifts in states of vigilance. *J Neurosci* 6:68-81.
- Steriade M, Domich L, Oakson G (1987) The deafferented reticular thalamic nucleus generates spindle rhythmicity. *J Neurophysiol* 57:260-273.
- Steriade M, McCormick DA, Sejnowski TJ (1993) Thalamocortical oscillations in the sleeping and aroused brain. *Science* 262:679-685.
- Vergnes M, Marescaux C (1992) Cortical and thalamic lesions in rats with genetic absence epilepsy. *J Neural Transm* 35:71-83.
- Vergnes M, Marescaux C, Depaulis A, Micheletti G, Warter JM (1986) Ontogeny of spontaneous petit mal-like seizures in Wistar rats. *Dev Brain Res* 30:85-87.
- Vergnes M, Marescaux C, Depaulis A, Micheletti G, Warter JM (1987) Spontaneous SWD in thalamus and cortex in a rat model of genetic petit mal epilepsy. *Exp Neurol* 96:127-136.
- von Krosigk M, Bal M, McCormick DA (1993) Cellular mechanisms of a synchronized oscillation in the thalamus. *Science* 261:361-364.
- Williams D (1953) Study of thalamic and cortical rhythms in petit mal. *Brain* 76:50-69.
- Wise SP, Fleshman J Jr, Jones EG (1978) Developmental study of thalamocortical and commissural connections in the rat somatic sensory cortex. *J Comp Neurol* 178:187-208.

Differential effects of petit mal anticonvulsants and convulsants on thalamic neurones: calcium current reduction

¹Douglas A. Coulter, John R. Huguenard & David A. Prince

Department of Neurology and Neurological Sciences, Rm M016, Stanford University Medical Center, Stanford, CA 94305, U.S.A.

1 Succinimide derivatives can be either convulsant (tetramethylsuccinimide (TMS)), or anticonvulsant (ethosuximide (ES); α -methyl- α -phenylsuccinimide (MPS)). ES, an anticonvulsant succinimide, has previously been shown to block calcium currents of thalamic neurones, while the convulsant succinimide TMS blocks γ -aminobutyric acid (GABA) responses in a similar fashion to the convulsant pentylenetetrazol (PTZ).

2 Using voltage-clamp techniques, we analysed the effects of the anticonvulsant succinimides ES and MPS and the convulsants TMS and PTZ on calcium currents of acutely isolated thalamic relay neurones of the rat.

3 MPS and ES reduced low-threshold calcium current (LTCC) in a voltage-dependent manner, without affecting steady-state inactivation. MPS was less potent than ES (IC_{50} of 1100 vs 200 μ M) but greater in efficacy (100% maximal reduction vs 40% for ES).

4 PTZ had no effect on calcium currents, and TMS only reduced LTCC at very high concentrations, and did not occlude MPS effects when applied concurrently.

5 These results, which demonstrate that anticonvulsant, but not convulsant, succinimides block LTCC, provide additional support for the hypothesis that LTCC reduction is a mechanism of action of the anticonvulsant succinimides related to their effects in petit mal epilepsy.

Introduction

Spike-wave discharges, the electroencephalographic hallmark of petit mal seizures, are thought to result from an underlying oscillatory interaction between reciprocally connected thalamic and cortical neuronal populations in both animal models of petit mal (Avoli *et al.*, 1983; Gloor & Fariello, 1988; Vergnes *et al.*, 1987), and in man with this form of epilepsy (Williams, 1953). Virtually all thalamic neurones are endowed with a prominent low-threshold calcium conductance that is of sufficient magnitude to generate a low-threshold calcium spike (Deschênes *et al.*, 1984; Jahnsen & Llinás, 1984a,b; Coulter *et al.*, 1989c). This conductance is important in the generation of normal thalamocortical oscillations such as sleep spindles (reviewed in Steriade & Llinás, 1988), and may also play a key role in the development of spike-wave discharges of petit mal (see Coulter *et al.*, 1989b for review). We have proposed that reductions in this calcium current in thalamic neurones might be one mechanism by which the thalamocortical oscillatory interaction underlying petit mal epilepsy could be dampened or blocked by anticonvulsant drugs (Coulter *et al.*, 1989a,b). Ethosuximide (ES; structure illustrated in Figure 1) is an agent widely used in treatment of petit mal (Browne *et al.*, 1975). Previous results from this laboratory have shown that ES, but not succinimide, the unsubstituted, clinically inactive ring base of ES (Ferrendelli & Kupferberg, 1980), specifically reduces the low-threshold calcium current (LTCC) underlying the low-threshold calcium spike in thalamic neurones (Coulter *et al.*, 1989a,b). A structurally similar petit mal anticonvulsant, dimethadione (DMD), also reduced LTCC in thalamic neurones when applied in clinically relevant concentrations (Coulter *et al.*, 1989a,b; Figure 1).

The reduction of LTCC in thalamic neurones may thus be a cellular mechanism by which ES and DMD control petit mal seizures. In order to test this hypothesis further, we have examined the actions of ES, two other succinimides (α -methyl- α -phenyl succinimide, an anticonvulsant, MPS; Figure 1), tetramethylsuccinimide (TMS, a convulsant; Figure 1) and the

convulsant pentylenetetrazol (PTZ) on calcium currents and, in an accompanying paper (Coulter *et al.*, 1990), on γ -aminobutyric acid (GABA)ergic responsiveness of thalamic neurones. The convulsant action of the α -, β -substituted succinimide, TMS (Klunk *et al.*, 1982c), may be due to its reduction of GABAergic responsiveness in cortical neurones (Barnes & Dichter, 1984). A similar mechanism may be responsible for the convulsant action of PTZ (Nicoll & Padjen, 1976; Macdonald & Barker, 1977). PTZ-induced convulsions are a commonly utilized animal model of epilepsy against which drugs are tested for potential petit mal anticonvulsant activity. Many drugs effective in the control of petit mal are also effective against PTZ seizures, including ES, MPS, and DMD. However, some drugs which are ineffective in petit mal (e.g. phenobarbitone and primidone) are of equal or greater potency in blocking PTZ seizures than petit mal

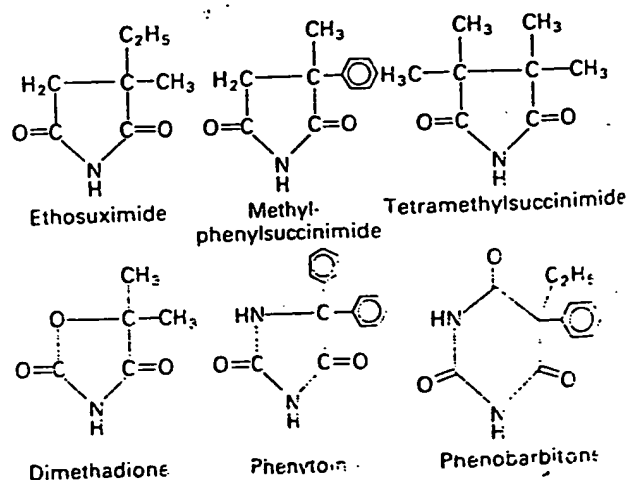


Figure 1 Structures of anticonvulsant and convulsant drugs discussed in the text. Top row: three succinimide drugs: two anticonvulsants (ethosuximide and methyl-phenyl succinimide) and one convulsant (tetramethylsuccinimide). Bottom row: three anticonvulsant drugs (dimethadione, phenytoin, and phenobarbitone).

rents and
0). on y
thalamic
tuted suc-
ue to its
neurones
may be
Nicoll &
uced con-
of epilepsy
anticon-
d of petit
ding ES.
neffective
of equal
petit mal

13
—CH₃
=O
inimide
2H₂
O
1000
rugs dr-
we anti-
and on-
ce anti-
arbitone
Isants

anticonvulsants (Löscher & Schmidt, 1988). We were therefore interested in the effects and interactions of petit mal anticonvulsants on calcium currents and on GABA responses of thalamic neurones (Coulter *et al.*, 1990).

We hypothesized that TMS and PTZ should exhibit low potency in reducing LTCC (a proposed petit mal anticonvulsant action) and higher potency in blocking GABAergic responsiveness (a proposed convulsant action), while MPS should reduce LTCC in clinically relevant concentrations (as does ES), and exhibit lower potency as a blocker of GABAergic responsiveness (as should ES). These spectra of action are supported by the results presented here, and in the accompanying paper (Coulter *et al.*, 1990). In addition, we found that the block of LTCC produced by MPS had many similarities to that produced by ES. The implication of these findings with respect to the potential link between LTCC reduction and petit mal anticonvulsant action is discussed, as is the structure-activity relationship of the LTCC-blocking receptor.

Methods

Dissociation

All experiments were performed on thalamic neurones isolated from the ventrobasal nucleus of young rats (age 1–15 days) with methods described by Kay & Wong (1986), modified as described in Coulter *et al.* (1989c). Animals were anaesthetized with pentobarbitone, decapitated, and a block of brain containing the ventrobasal nucleus of the thalamus was removed. This tissue block was glued to the stage of a vibratome (Lancaster, St. Louis, MO, U.S.A.) and sliced into 500 μ m sections. Slices were then placed into oxygenated, piperazine-N, N'-bis(2-ethanesulphonic acid) (PIPES)-buffered solution containing trypsin (0.8 mg ml⁻¹, Sigma, St. Louis, MO, U.S.A.) for 45–100 min. The PIPES solution contained (in mM): NaCl 120, KCl 5, CaCl₂ 1, MgCl₂ 1, D-glucose 25, PIPES 20 (pH 7.0). Slices were then removed from the enzyme solution, rinsed, cut into chunks, and triturated with fire-polished Pasteur pipettes. Cells were plated onto culture dishes (Lux, E & K Scientific, Saratoga, CA, U.S.A.), and stored in an oxygenated chamber for 0.5–12 h before use.

Voltage-clamp recording

Whole-cell voltage-clamp recordings of calcium currents were made with the method described by Hamill *et al.* (1981). The intracellular (pipette) solution contained (in mM): Trizma phosphate (dibasic) 110, Trizma base 28, ethylene glycol bis-(β -aminoethylether)-N,N,N',N'-tetraacetic acid 11, MgCl₂ 2, CaCl₂ 0.5 and Na₂-ATP 4; pH 7.35. The pipette solution also contained an intracellular ATP reconstitution system consisting of creatine phosphokinase 50 μ mol l⁻¹, and phosphocreatine 22 mM (Forscher & Oxford, 1985; Mody *et al.*, 1988). This maintenance solution was used to fill the shank of the electrode, but was omitted from the solution which was used to back-fill the tip of the electrode, because it was found that gigaohm seals were difficult to obtain with protein in the tip solution. The external solution contained (in mM): NaCl 155, KCl 3, MgCl₂ 1, CaCl₂ 3, HEPES-Na⁺ 10 and tetrodotoxin 0.0005; pH 7.4. All recordings were obtained at room temperature (20–22°C). Patch electrodes were pulled on a List L7M-3P-A puller by a two-stage pull, and had resistances of 6–8 M Ω . Currents were monitored with an Axopatch 1A amplifier (Axon Instruments, Burlingame, CA, U.S.A.) and filtered at 5 kHz with an 8-pole Bessel filter before digitization. All data were stored and analysed by a DEC PDP 11/73 computer, with a Cheshire data interface (Indec, Sunnyvale, CA, U.S.A.). Leak and capacitive currents were subtracted from active currents in all figures (Coulter *et al.*, 1989c).

Drug concentrations and method of application

MPS is an N-demethylated active metabolite of methsuximide (Celontin, Parke Davis) (Strong *et al.*, 1974; Porter *et al.*, 1979) that is effective in the control of petit mal epilepsy. It is more toxic than ES (Chen *et al.*, 1963), but has a broader spectrum of action, being also effective against complex partial seizures (Wilder & Buchanan, 1981; Browne *et al.*, 1983). Clinically relevant free serum concentrations of MPS are in the range of 50–250 μ M (Strong *et al.*, 1974; Porter *et al.*, 1979), while those for ES have been found to be 250–750 μ M (Browne *et al.*, 1975). We applied MPS (Sigma, St. Louis, MO, U.S.A.) and ES (a gift of Parke Davis, Ann Arbor, MI, U.S.A.) in a concentration range of 10 μ M to 10 mM to explore fully the dose-dependence of the LTCC reduction by these agents. TMS (ICN Biomedicals, Inc. Cleveland, OH, U.S.A.) free serum concentrations in man are obviously unavailable. However, TMS reduces GABAergic responses by 60–80% at 0.5–1 mM in cultured cortical neurones (Barnes & Dichter, 1984), and therefore we applied the drug concentrations of 10 μ M to 10 mM. ES and TMS were readily soluble in the perfusion medium. MPS often required sonication to speed solubilization. All drugs were bath applied.

Results

Calcium currents

Under voltage-clamp conditions, with internal and external ionic composition designed to isolate calcium currents (see Methods), depolarizing voltage commands elicit at least two distinct calcium currents in thalamic neurones, which differ both in their kinetics, and sensitivity to pharmacological blockers (Coulter *et al.*, 1989c). Small depolarizing commands from a holding potential of –100 mV evoked a transient, fully inactivating current that could be seen in isolation (e.g. Figure 2a). This current had a threshold of approximately –65 mV. Larger amplitude depolarizing commands elicited a high-threshold, sustained component of calcium current (HTCC), with a threshold of approximately –30 mV (Figure 2b). The HTCC peaked in amplitude during step commands to 0 mV (e.g. Figure 2b and c), and varied little in magnitude when evoked from holding potentials of –100 mV or –30 mV (see Coulter *et al.*, 1989c). By contrast, the low threshold, transient calcium current (LTCC) showed complete steady-state inactivation at potentials of –65 mV or more depolarized, and was half-inactivated at –83 mV, on average (Coulter *et al.*, 1989c). As in other neurones (Fox *et al.*, 1987; Narahashi *et al.*, 1987), the LTCC and HTCC were differentially blocked by divalent cations, with the LTCC being more sensitive to Ni²⁺, and the HTCC to Cd²⁺ (Coulter *et al.*, 1989c). Therefore, the LTCC appears analogous to the 'T' current (Fox *et al.*, 1987), 'type I' current (Narahashi *et al.*, 1987) or the 'l.v.a.' current (Carbone & Lux, 1984) described by others while the HTCC has properties similar to the 'L' current (Fox *et al.*, 1987), 'type II' current (Narahashi *et al.*, 1987), or the 'h.v.a.' current (Carbone & Lux, 1984).

Drug effects on calcium currents

The actions of drugs on calcium currents were examined in 77 neurones. MPS (20 μ M–20 mM) reduced the LTCC in all neurones to which it was applied ($n = 55$). In higher concentrations ($\geq 500 \mu$ M), it reduced the high threshold calcium current (HTCC) as well. Figure 2 illustrates the selective reduction of LTCC (a) without effects of the sustained HTCC (b) in response to bath application of 200 μ M MPS. In Figure 2c, amplitudes of the transient and sustained calcium currents are plotted vs command potential eliciting the current in control, MPS 200 μ M, and wash conditions, to show the reversibility of the drug action, and its selectivity for the LTCC at this con-

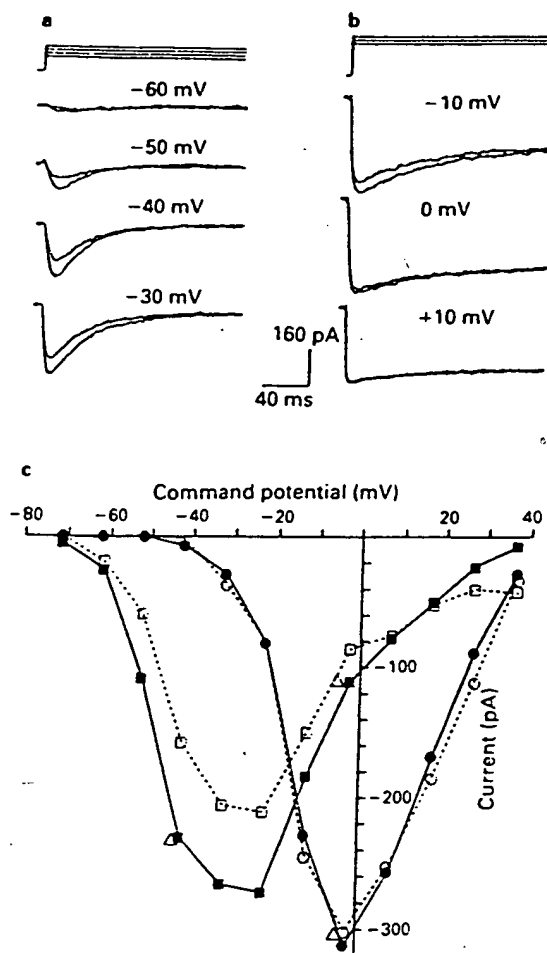


Figure 2 Effects of methylphenylsuccinimide (MPS, 200 μ M) on calcium currents in a thalamic neurone. (a,b) Two superimposed traces at various depolarizing command potentials, from a holding potential of -100 mV, show the effects of MPS on the transient low-threshold calcium current (LTCC) and the sustained high-threshold calcium current (HTCC). The larger peak current in each case is the control. This concentration of MPS specifically reduces the LTCC. (c) Plot of voltage command potential vs transient and sustained calcium current amplitude, under control, MPS-exposed (200 μ M), and wash conditions for the cell of (a). Transient current was defined as the portion of current that decayed during the 200 ms duration of the step command, and the sustained current was defined as the portion of current which remained at the end of the 200 ms step command. At this concentration, MPS specifically reduced the transient, low-threshold calcium current over the full activation range of this current, and this effect was fully reversible. (■) Control transient current, (□) transient current in presence of 200 μ M MPS; (●) control sustained current, (○) sustained current in the presence of 200 μ M MPS; Δ recovery.

centration. Figure 3 illustrates the effects of bath application of 800 μ M MPS on calcium currents in another neurone. At this concentration, MPS reduced both the LTCC (Figure 3a) and the HTCC (Figure 3b). This effect is also shown graphically in Figure 3c. The traces of Figures 2 and 3 show that this reduction of calcium current occurred without effects on the time-course of the current. A concentration-response relationship for the effects of MPS on LTCC was plotted (semilogarithmically) in Figure 4. The resulting data plot can be fitted with a function that assumes a bimolecular interaction between drug and receptor, a maximal effect of 100%, and an IC_{50} of 1100 μ M. The corresponding Hill plot of Figure 4b is best fitted by a linear regression with a slope of 0.79 ± 0.05 ($r = 0.98$), also supporting a bimolecular interaction between MPS and its receptor. Co-operative binding of more than one molecule of MPS to the LTCC-reducing receptor would result in a Hill plot with a slope of > 1 .

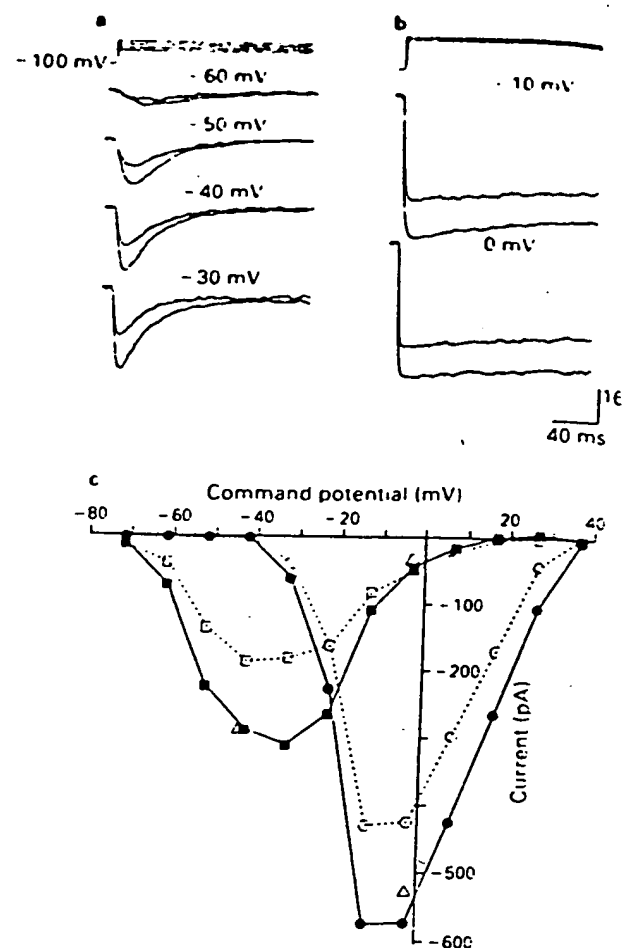


Figure 3 Effects of methylphenylsuccinimide (MPS, 800 μ M) on calcium currents in a thalamic neurone. (a,b) Sweeps as described in the legend of Figure 2. The larger peak current in each case is control. Depolarizing command level eliciting the current accompanies each trace. MPS, at this concentration, reduced both the transient low-threshold calcium current (LTCC) and the sustained high-threshold calcium current (HTCC). (c) Plot of voltage command potential vs transient and sustained calcium current amplitude, under control (■, ●) and sustained (□, ○) calcium current amplitude, under control (■, ●), MPS (800 μ M)-exposed (□, ○), wash (Δ) conditions for the cell of (a). Transient and sustained currents are defined as in the legend of Figure 2. MPS, at this high concentration, reduced both the transient, low-threshold calcium current and the high threshold, sustained calcium current over the activation range of these currents in a completely reversible manner.

The reductions of LTCC produced by MPS were strongly influenced by the command potential used to elicit current. This voltage-dependence is illustrated in Figure 5. Figure 5a shows the reduction of LTCC elicited in response to varying voltage commands from -70 to -35 mV (holding potential = -102 mV) in a cell exposed to 800 μ M MPS. LTCC was elicited in isolation over this range of voltage commands (Figures 2 and 3; see also Coulter *et al.*, 1989c). Fractional MPS reduction of the LTCC was maximal for currents evoked by less depolarized command potentials. For example, MPS (800 μ M) blocked 88% of the LTCC evoked by a step to -65 mV, while only 42% reduction occurred when the LTCC was elicited by a command step to -35 mV. Figure 5b shows a plot of the percentage reduction of LTCC vs. command potential used to elicit the LTCC for the cell of Figure 5a. With lower, clinically relevant concentrations of MPS (2-250 μ M) the voltage-dependence of reduction was also pronounced. For example, in 5 cells, MPS (250 μ M) was significantly more effective in blocking the LTCC-elicited by a step to -60 mV ($22.2 \pm 2.8\%$ reduction, mean \pm s.d.) than LTCC elicited by a step to -30 mV ($7.4 \pm 3.9\%$ reduction, t test, $P < 0.0001$, $t = 6.90$, degrees of freedom = 8). Figure

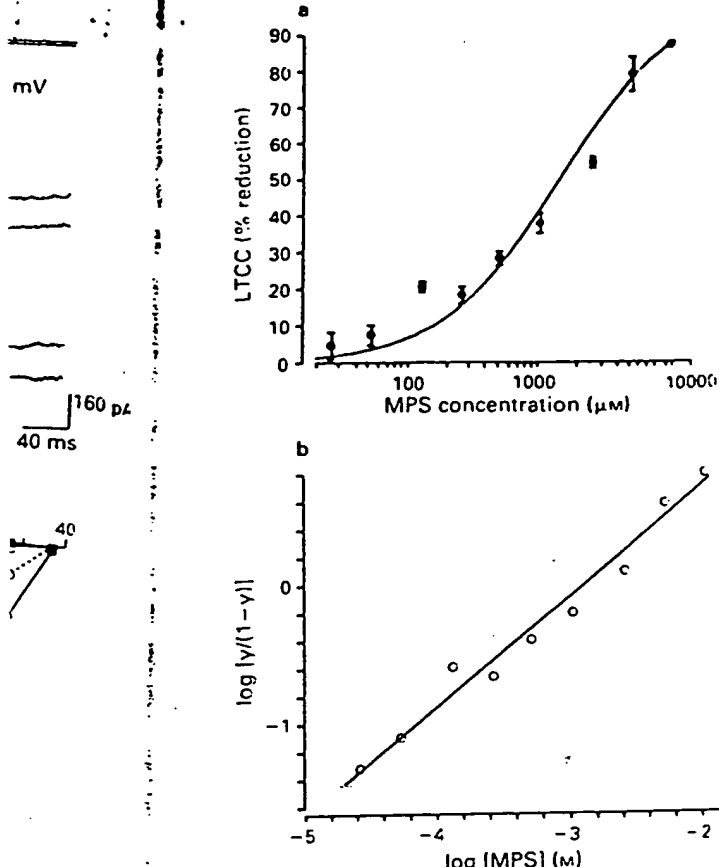


Figure 4 (a) Plot of methylphenylsuccinimide (MPS) bath concentration (logarithmic scale) vs % reduction of low-threshold calcium current (LTCC) ($V_{\text{hold}} = -100 \text{ mV}$, command potential = -40 mV) for 31 thalamic neurones (symbols show mean and vertical lines s.e. mean for 3–10 cells per point). The curve, which was fitted to the data by eye, was constructed from the equation: $\text{effect} = \text{maximal effect} \times \text{MPS concentration} / (\text{MPS concentration} + \text{IC}_{50})$. An IC_{50} estimate of $1100 \mu\text{M}$ was used, and a maximal effect estimate of 100%. (b) Hill plot of log MPS concentration vs $\log[\text{effect}/(1 - \text{effect})]$. The line was fitted to the data by linear regression, and has a slope of 0.79 ($r = 0.98$). Both the equation of (a), and the slope of the line in (b) support a bimolecular interaction between drug and receptor.

and d illustrate the voltage-dependent reduction of LTCC in response to $200 \mu\text{M}$ MPS.

One mechanism for reductions in LTCC by MPS might be an effect on the voltage-dependent steady-state inactivation of this current. This possibility was examined by evoking the LTCC by a depolarizing step to -42 mV from different holding potentials as shown in Figure 6a. MPS exposure did not alter the voltage-dependence of steady-state inactivation, although it reduced the peak amplitude of the LTCC. Figure 6b illustrates a plot of the average fraction of LTCC available to be activated (relative to the maximal LTCC under control and drug-exposed conditions) vs the holding potential from which the LTCC was evoked, for 4 cells to which MPS ($800 \mu\text{M}$) was bath applied, and shows that drug application had no effect on steady-state inactivation of the LTCC relative to control. In addition, lower, clinically relevant concentrations of MPS were also without effect (not shown).

Many aspects of MPS reduction of LTCC are similar to those previously demonstrated for ES (Coulter *et al.*, 1989b). We therefore compared the effects of these two agents (in equivalent concentrations) on calcium currents in 6 cells. In this group of neurones, $500 \mu\text{M}$ ES or MPS reduced LTCC by $23.4 \pm 2.7\%$ and $27.6 \pm 3.6\%$, respectively. By contrast in 14 cells, the convulsant succinimide TMS had little effect on LTCC at concentrations of 1 mM or less (0% reduction at $100 \mu\text{M}$, $4.4 \pm 2.0\%$ reduction at 1 mM , in 4 cells to which concentrations of $100 \mu\text{M}$, 1 mM , and 10 mM TMS were applied).

Figure 7 illustrates the effect of 1 mM MPS and TMS, on LTCC in the same neurone. MPS clearly reduced the LTCC in a reversible manner, while TMS had little or no effect on the LTCC at 1 mM . In addition, Figure 7 shows that TMS, when applied together with MPS in equivalent concentrations, had no influence on MPS effects. Reductions in LTCC elicited by 1 mM MPS were similar to those produced by perfusion with 1 mM MPS and 1 mM TMS. This finding suggests that TMS does not antagonize MPS LTCC-reducing effects by binding to the LTCC-reducing receptor without activity. At very high concentrations (10 mM), TMS did reduce LTCC (by $30.3 \pm 4.0\%$, $n = 4$). The characteristics of this LTCC block by high concentrations of TMS appeared similar to those elicited by ES and MPS, including similar voltage-dependence (not shown). PTZ had no effect on LTCC in concentrations from $100 \mu\text{M}$ to 10 mM ($n = 8$, not shown).

Discussion

We previously demonstrated that both ES and DMD, structurally similar petit mal anticonvulsants (Figure 1), reduce LTCC in thalamic neurones when applied in clinically relevant concentrations (Coulter *et al.*, 1989a,b). The clinically inactive ring base of ES, succinimide, had no effect on the LTCC at equivalent concentrations (Coulter *et al.*, 1989a). The results of the experiments described here show that another anticonvulsant succinimide, MPS, also reduces LTCC in these cells, while a convulsant succinimide, TMS, only reduces LTCC when applied in very high concentrations. PTZ, a convulsant commonly utilized to screen drugs for potential petit mal anticonvulsant activity, did not affect calcium currents in concentrations up to 10 mM .

Thalamic neurones are thought to participate in the oscillatory thalamocortical discharge underlying the 3 Hz spike-wave rhythms of petit mal. The low-threshold calcium spike, which is generated by the LTCC (Coulter *et al.*, 1989c) and is ubiquitous in thalamic neurones, has been implicated as important in the generation and maintenance of thalamocortical oscillatory interactions (reviewed in Steriade & Llinás, 1988). The reduction in LTCC produced by ES, MPS, and DMD therefore appears compatible with the anticonvulsant activity of these compounds (i.e. they may depress the pathological thalamocortical rhythm underlying the spike-wave discharges through their effects on LTCC). The lack of effect of the inactive and convulsant succinimides, succinimide and TMS, on LTCC also appears consistent with this conclusion.

MPS-induced reduction of LTCC is similar in many respects to ES reduction of the same conductance. Like ES, MPS reduces LTCC without affecting the time course of the current (Coulter *et al.*, 1989b), suggesting that the LTCC reduction is accomplished without either slowing activation or speeding inactivation (Figure 2a,b). The actions of MPS and ES occur without effects on the voltage-dependence of steady-state inactivation (Figure 6; Coulter *et al.*, 1989b), and both agents reduce LTCC in a similar voltage-dependent manner, with maximal effects at the voltage threshold for eliciting the current (Figure 5; Coulter *et al.*, 1989b). Such voltage-dependence would increase the effectiveness of these drugs *in vivo*, by reducing the LTCC maximally when it is elicited by small depolarizations, as would occur at the onset of spindle waves (Steriade & Llinás, 1988) and probably during spike wave discharges (SWD). In a positive feedback circuit such as the thalamocortical loop underlying the spike-and-wave discharge of petit mal, this kind of action would be very effective either at blocking the onset of the discharge, or severely curtailing the full expression of the oscillations responsible for the epileptic attack.

There were also some interesting differences between the actions of ES and MPS. ES reduced LTCC with greater potency, but lower efficacy than MPS (the IC_{50} for ES was $200 \mu\text{M}$ vs $1100 \mu\text{M}$ for MPS and the maximal effects were 40% and 100% reductions for ES and MPS, respectively (Coulter *et al.*, 1989b; Figure 2c)). MPS was also less specific than ES

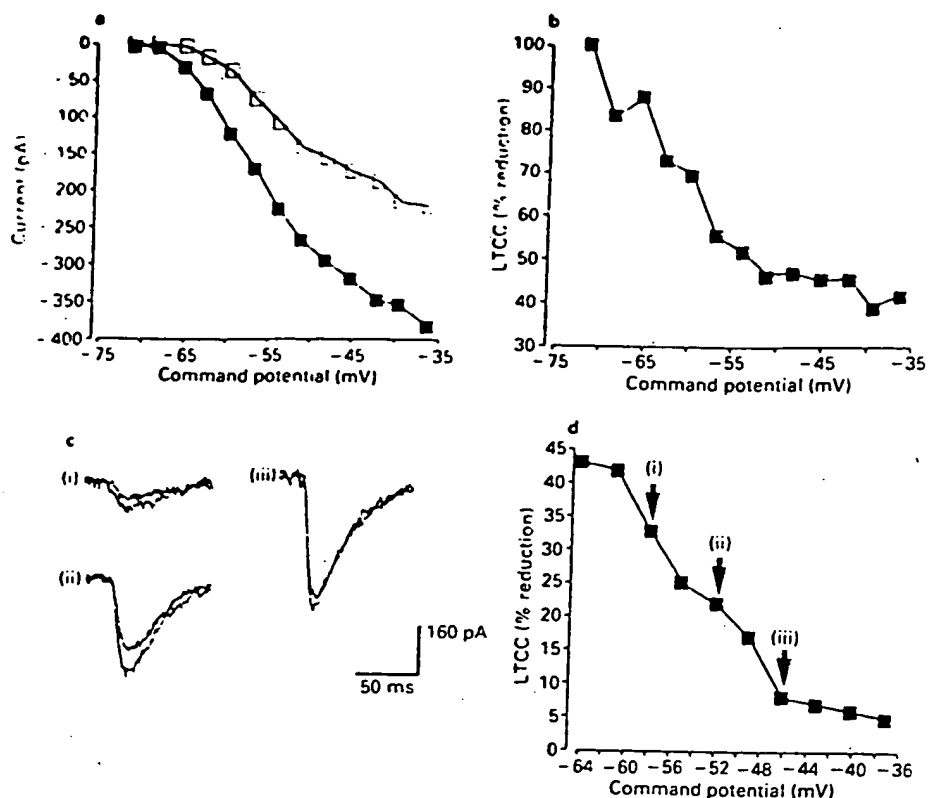


Figure 5 Voltage-dependence of methylphenylsuccinimide (MPS)-induced reduction of the low-threshold calcium current (LTCC). (a) Plot of amplitude of calcium current vs command potential in the potential range where the LTCC is elicited in isolation, under control (■) and MPS (800 μ M)-exposed (□) conditions. There is a pronounced voltage-dependence to MPS reduction of the LTCC; proportionally larger reductions of LTCC occurred when the current was elicited near threshold than at more depolarized command potentials. (b) Plot of percentage reduction of LTCC by MPS (800 μ M) vs command potential for the same cell as in (a). (c) Effects of MPS (200 μ M) on LTCC evoked by 3 different command potentials (i) = -58 mV, (ii) = -52 mV, (iii) = -46 mV in a different cell from that in (a) and (b). Control and MPS-exposed traces are superimposed. MPS produced a proportionately greater reduction of LTCC at less depolarized step commands. (d) Plot of amplitude of calcium current vs command potential in the potential range where the LTCC was elicited in isolation, under control and MPS (200 μ M)-exposed conditions for the same cell as in (c). At this concentration, the voltage-dependence of LTCC reduction was qualitatively similar but quantitatively smaller than that obtained when 800 μ M MPS was applied (a and b). The potentials corresponding to the traces in (c) are indicated by arrows.

in reducing calcium currents. ES selectively reduced LTCC, rarely affecting the HTCC at any concentration (Coulter *et al.*, 1989a,b), while MPS had a selective action on LTCC at clinically relevant concentrations (200 μ M or less, Figure 3a,b) but reduced the HTCC as well at higher concentrations (Figure 3c). This effect of higher concentrations of MPS was similar to that of DMD (Coulter *et al.*, 1989a,b). This decreased specificity of MPS and DMD for the LTCC might contribute to their increased clinical toxicity relative to ES. The HTCC-reducing effects of MPS and DMD are probably not related to their petit mal anticonvulsant effectiveness, since clinically relevant concentrations of MPS block only LTCC. Also, ES, which is clinically selective for petit mal, does not reduce HTCC.

Evidence from these experiments and other studies provides insight into the structural aspects of the receptor that mediates LTCC reduction. ES and MPS (both α -substituted succinimides, Figure 1) reduce LTCC at concentrations less than 1 mM, while succinimide (the unsubstituted ring base of ES and MPS) does not (Coulter *et al.*, 1989a), suggesting that some alkyl substitutions are necessary for activity at this receptor. TMS, an α - and β -substituted succinimide, does not reduce LTCC to any significant extent unless applied at high concentrations (≥ 1 mM), and does not occlude MPS responses when applied at 1 mM. This suggests that TMS binds with very low affinity (relative to ES and MPS) to the LTCC-reducing receptor. Furthermore, since TMS does not occlude MPS reduction of LTCC when applied concurrently (Figure 7), it is unlikely that TMS even binds to any significant degree to the receptor at 1 mM concentration. Therefore, α -substitution appears necessary for activity at the LTCC-

reducing receptor, while β -substitution reduces effectiveness. DMD and phenytoin also reduce the LTCC (Twombly *et al.* 1988; Coulter *et al.*, 1989a,b). These molecules are similar ES and MPS in that they are substituted 5-membered heterocyclic rings with two carbonyl carbons bordering a nitrogen but they differ in their ring closure (-N- for phenytoin, -O- for DMD, vs -CH₂- for the succinimides, Figure 1). This suggests that there is some nonselectivity on the part of the receptor in terms of the ring closure, and ring shape of agonists. One prediction from this is that certain barbiturates, including phenobarbital, which are structurally similar to the act succinimides (particularly to MPS, Figure 1) might be active at the LTCC-reducing site. This prediction is currently being tested.

Many characteristics of this LTCC-reducing receptor are similar to those of a receptor responsible for anticonvulsant activity described by Ferrendelli and colleagues (Klunk *et al.* 1982c). In their studies of alkyl-substituted butyrolactones and succinimides, these investigators showed that α -substitution alone resulted in significant anticonvulsant activity (Klunk *et al.* 1982b), while α - and β - or γ - (for the butyrolactones) substitution resulted in convulsant activity (Klunk *et al.* 1982). The order of potency of the various succinimides in reducing LTCC is ES > MPS > TMS, while the order of potency of these same compounds in reducing GABAergic responsiveness is TMS > ES > MPS (Coulter *et al.*, 1990). The receptor mediating the LTCC-reducing action (as discussed above) appears to be distinct from the picrotoxin receptor, hypothesized by Klunk *et al.* (1982c) to be responsible for the convulsant actions of TMS. PTZ, which shares the convulsant actions of TMS, perhaps inducing convulsions by a similar

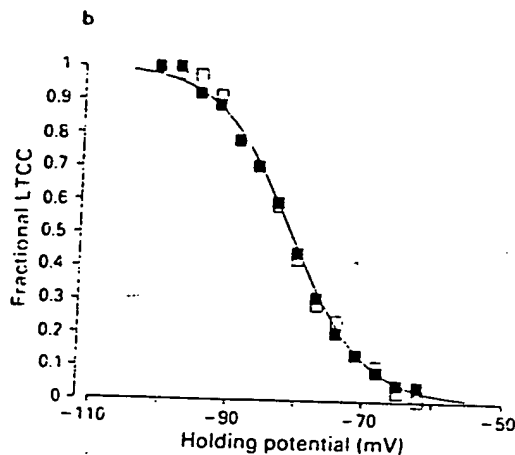
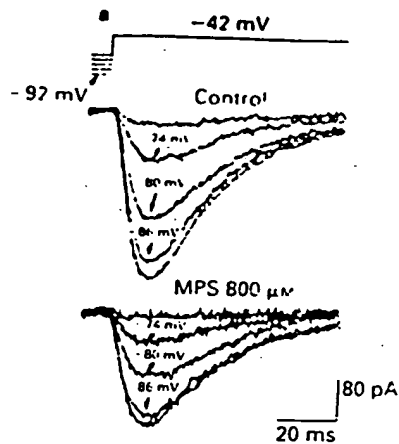


Figure 6 Steady-state inactivation of control and methylphenylsuccinimide (MPS)-reduced low-threshold calcium current (LTCC). (a) Superimposed sweeps of control (top) and MPS ($800 \mu\text{M}$)-exposed (bottom) LTCC, evoked by depolarizing commands to -42 mV from varying holding potentials (upper traces). Sweeps corresponding to holding potentials of -86 , -80 , and -74 mV , the steepest portion of the steady-state inactivation curve, are labelled under both conditions. MPS exposure did not alter the voltage-dependence of steady-state inactivation (although it reduced the peak amplitude of the LTCC), and the time-course of the LTCC was not affected by its amplitude. (b) Plot of holding potential vs mean fraction of LTCC available (relative to LTCC evoked from -112 mV) from 4 cells recorded under control (■) and MPS ($800 \mu\text{M}$)-exposed (□) conditions (includes the cell of (a)). MPS reduced LTCC without affecting the voltage-dependence of steady-state inactivation.

mechanism, GABAergic blockade (Nicol & Padjen, 1976; Macdonald & Barker, 1977), did not affect LTCC in concentrations up to 10 mM , and so its convulsant actions cannot be attributed even partially to actions on thalamic calcium cur-

rents. These findings have important implications related to the use of PTZ-induced seizures as a screen for testing potential petit mal anticonvulsants, and are further discussed in the succeeding paper (Coulter *et al.*, 1990).

The LTCC reducing effects of MPS do not explain its anti-convulsant spectrum of action, since this drug is effective against both petit mal and other seizure types, whereas ES, with essentially the same action on LTCC, is selectively effective in petit mal absence. MPS is structurally intermediate between ES and phenytoin in that it has both alkyl and phenyl substitutions at what corresponds to the α -position on a heterocyclic-5-membered ring (Figure 1). Phenytoin is known to reduce sustained repetitive firing (reviewed in Macdonald & McLean, 1986), and to shift steady-state inactivation of the sodium current (Willow *et al.*, 1985), actions which may underlie its anticonvulsant effects against partial complex and generalized motor seizures (Macdonald & McLean, 1986). These actions of phenytoin, together with the structural similarities between MPS and phenytoin, lead to the hypothesis that the broader spectrum of action of MPS versus ES might be due to effects of the former drug on sodium currents.

One interesting consequence of the hypothesis that thalamic low-threshold calcium spikes are involved in generation of spike-wave discharge is that drugs which specifically block the LTCC and cross the blood/brain barrier might be expected to exhibit petit mal anticonvulsant activity. Various alcohols, including menthol (Swandulla *et al.*, 1987), and octanol (Llinás & Yarom, 1986) have been shown to block LTCC in different neuronal preparations. However, this block is not specific, in that the HTCC is also reduced (Swandulla *et al.*, 1987; Twombly & Narahashi, 1989). It also remains to be determined whether these alcohols have added effects on other ion channels, and/or on membrane fluidity. Another interesting family of drugs which might have anticonvulsant activity are amiloride and related compounds. These agents specifically block LTCC in mouse neuroblastoma and chick dorsal root ganglion neurones (Tang *et al.*, 1988). However, other actions include inhibition of the Na^+/H^+ and $\text{Na}^+/\text{Ca}^{2+}$ exchange systems (Kinsella & Aronson, 1981; Schellenberg *et al.*, 1983), and blockade of the tetrodotoxin-insensitive Na^+ channel in epithelial cells (Palmer, 1984). Also, the positive charge on amiloride at physiological pH should prevent the drug from crossing the blood/brain barrier. It may be possible to develop analogues of amiloride, or entirely new compounds, which will cross the blood/brain barrier, block LTCC, and prove effective as anticonvulsants.

The finding that petit mal anticonvulsant succinimides ES and MPS, but not convulsant (TMS) and inactive succinimides (succinimide), reduce the LTCC in thalamic neurones in clinically relevant concentrations lends strong support to the idea that this cellular action is related to the clinical effectiveness of these agents as anticonvulsants. This idea is further supported by the finding that the convulsant PTZ was without effect on calcium currents in concentrations up to 10 mM .

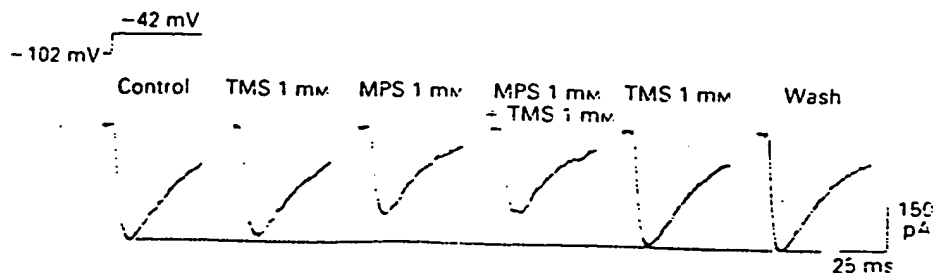


Figure 7 Effects of tetramethylsuccinimide (TMS), methylphenylsuccinimide (MPS) and MPS plus TMS on the low-threshold calcium current (LTCC) in one neurone. Sweeps illustrating the amplitude of LTCC in control, 1 mM TMS, 1 mM MPS, 1 mM TMS plus 1 mM MPS and 1 mM TMS again, and wash conditions. TMS had little or no effect on LTCC at 1 mM , and did not occlude MPS reductions of LTCC when applied concurrently. All currents were elicited by a step command to -42 mV from a holding potential of -102 mV . The dotted line is included to aid comparison between sweeps.

References

- AVOLI, M., GLOOR, P., KOSTOPOULOS, G. & GOTMAN, J. (1983). An analysis of penicillin-induced generalized spike and wave discharges using simultaneous recordings of cortical and thalamic single neurons. *J. Neurophysiol.*, **50**, 819-837.
- BARNES, D.M. & DICHTER, M.A. (1984). Effects of ethosuximide and tetramethylsuccinimide on cultured cortical neurones. *Neurology*, **34**, 620-625.
- BROWNE, T.R., DREIFUSS, F.E., DYKEN, P.R., GOODE, D.J., PENRY, J.K., PORTER, R.J., WHITE, B.G. & WHITE, P.T. (1975). Ethosuximide in the treatment of absence (petit mal) seizures. *Neurology*, **25**, 515-524.
- BROWNE, T.R., FELDMAN, R.G., BUCHANAN, R.A., ALLEN, N.C., FAWCETT-VICKERS, L., SZABO, G.K., MATTSON, G.F., NORMAN, S.E. & GREENBLATT, D.J. (1983). Methsuximide for complex partial seizures: efficacy, toxicity, clinical pharmacology, and drug interactions. *Neurology (Cleveland)*, **33**, 414-418.
- CARBONE, E. & LUX, H.D. (1984). A low voltage-activated, fully inactivating Ca channel in vertebrate sensory neurons. *Nature*, **310**, 501-502.
- CHEN, G., WESTON, J.K. & BRATTON, A.C. Jr. (1963). Anticonvulsant activity and toxicity of phensuximide, methsuximide and ethosuximide. *Epilepsia*, **4**, 66-76.
- COULTER, D.A., HUGUENARD, J.R. & PRINCE, D.A. (1989a). Specific petit mal anticonvulsants reduce calcium currents in thalamic neurons. *Neurosci. Lett.*, **98**, 74-78.
- COULTER, D.A., HUGUENARD, J.R. & PRINCE, D.A. (1989b). Characterization of ethosuximide reduction of low-threshold calcium current in thalamic neurons. *Ann. Neurol.*, **25**, 582-593.
- COULTER, D.A., HUGUENARD, J.R. & PRINCE, D.A. (1989c). Calcium currents in rat thalamocortical relay neurones: kinetic properties of the transient, low-threshold current. *J. Physiol.*, **414**, 587-604.
- COULTER, D.A., HUGUENARD, J.R. & PRINCE, D.A. (1990). Differential effects of petit mal anticonvulsant and convulsants on thalamic neurones: GABA current blockade. *Br. J. Pharmacol.*, **100**, 807-813.
- DESCHÊNES, M., PARADIS, M., ROY, J.P. & STERIADE, M. (1984). Electrophysiology of neurons of lateral thalamic nuclei in cat: resting properties and burst discharges. *J. Neurophysiol.*, **51**, 1196-1219.
- FERRENDELLI, J.A. & KUPFERBERG, H.J. (1980). Antiepileptic drugs. Succinimides. In *Antiepileptic Drugs: Mechanisms of Action*, ed. Glaser, G.H., Penry, J.K. & Woodbury, D.M. New York: Raven Press.
- FORSCHER, P. & OXFORD, G.S. (1985). Modulation of calcium channels by norepinephrine in internally dialyzed avian sensory neurons. *J. Gen. Physiol.*, **85**, 743-763.
- FOX, A.P., NOWYCKY, M.C. & TSIEN, R.W. (1987). Kinetic and pharmacological properties distinguishing three types of calcium currents in chick sensory neurons. *J. Physiol.*, **394**, 149-172.
- GLOOR, P. & FARIELLO, R.G. (1988). Generalized epilepsy: some of its cellular mechanisms differ from those of focal epilepsy. *TINS*, **11**, 63-68.
- HAMILL, O.P., MARTY, A., NEHER, E., SAKMANN, B. & SIGWORTH, F.J. (1981). Improved patch clamp technique for high resolution recordings from cells and cell-free membranes. *Pflügers Arch.*, **391**, 85-100.
- JAHNSEN, H. & LLINÁS, R. (1984a). Electrophysiological properties of guinea-pig thalamic neurons: an *in vitro* study. *J. Physiol.*, **349**, 205-226.
- JAHNSEN, H. & LLINÁS, R. (1984b). Ionic basis for the electroresponsiveness and oscillatory properties of guinea-pig thalamic neurons *in vitro*. *J. Physiol.*, **349**, 227-247.
- KAY, A.R. & WONG, R.K.S. (1986). Isolation of neurons suitable for patch-clamping from adult mammalian nervous system. *J. Neurosci. Meth.*, **16**, 227-238.
- KINSELLA, J.L. & ARONSON, P.S. (1981). Amiloride inhibition of the Na⁺-H⁺ exchanger in renal microvillus membrane vesicles. *Am. J. Physiol.*, **241**, F374-379.
- KLUNK, W.E., COVEY, D.F. & FERRENDELLI, J.A. (1982a). Correlation of epileptogenic properties of unsubstituted and β -alkylated γ -butyrolactones. *Mol. Pharmacol.*, **22**, 431-437.
- KLUNK, W.E., COVEY, D.F. & FERRENDELLI, J.A. (1982b). Convulsant properties of α -, γ -, and α - γ -substituted butyrolactones. *Mol. Pharmacol.*, **22**, 438-443.
- KLUNK, W.E., COVEY, D.F. & FERRENDELLI, J.A. (1982c). Structure-activity relationships of alkyl-substituted γ -butyrolactone succinimides. *Mol. Pharmacol.*, **22**, 444-450.
- LLINÁS, R. & YAROM, Y. (1986). Specific blockage of the low threshold calcium channel by high molecular weight alcohols. *Soc. Neurosci. Abstr.*, **16**, 174.
- MACDONALD, R.L. & BARKER, J.L. (1977). Pentylentetrazol penicillin are selective antagonists of GABA-mediated synaptic inhibition in cultured mammalian neurones. *Nature*, **270**, 720-721.
- MACDONALD, R.L. & McLEAN, M.J. (1986). Anticonvulsant mechanisms of action. *Adv. Neurol.*, **44**, 713-736.
- MODY, I., SALTER, M.W. & MACDONALD, J.F. (1988). Requirement for NMDA receptor/channels for intracellular high-energy phosphate and the extent of intraneuronal calcium buffering in cultured mouse hippocampal neurons. *Neurosci. Lett.*, **93**, 73-78.
- NARAHASHI, T., TSUNOO, A. & YOSHII, M. (1987). Characterization of two types of calcium channels in mouse neuroblastoma cell. *Physiol.*, **383**, 231-249.
- NICOLL, R.A. & PADJEN, A. (1976). Pentylentetrazol: An antagonist on GABA at primary afferents of the frog isolated spinal cord. *Neuropharmacol.*, **15**, 69-71.
- PALMER, L. (1984). Voltage-dependent block by amiloride and monovalent cations of apical Na channels in the toad urinary bladder. *J. Membr. Biol.*, **80**, 153-165.
- PORTER, R.J., PENRY, J.K., LACY, J.R., NEWMARK, M.E. & KUPFERBERG, H.J. (1979). Plasma concentrations of phensuximide, methsuximide, and their metabolites in relation to clinical efficacy. *Neurology (NY)*, **29**, 1509-1513.
- SCHULLENBERG, G.D., ANDERSON, L. & SWANSON, P. (1983). Inhibition of Na⁺-Ca²⁺ exchange in rat brain by amiloride. *Mol. Pharmacol.*, **24**, 251-258.
- STERIADE, M. & LLINÁS, R.R. (1988). The functional states of the lamus and the associated neuronal interplay. *Physiol. Rev.*, **68**, 649-742.
- STRONG, J.M., ABE, T., GIBBS, E.L. & ATKINSON, A.J. Jr. (1985). Plasma levels of methsuximide and N-desmethylethosuximide during methsuximide therapy. *Neurology (Minneapolis)*, **24**, 250-252.
- SWANDULLA, D., CARBONE, E., SCHÄFER, K. & LUX, H.D. (1985). Effect of menthol on two types of Ca currents in cultured sensory neurons of vertebrates. *Pflügers Arch.*, **409**, 52-59.
- TANG, C.-M., PRESSER, F. & MORAD, M. (1988). Amiloride selectively blocks the low threshold (T) calcium channel. *Science*, **240**, 215.
- TWOMBLY, D.A. & NARAHASHI, T. (1989). Calcium channel block actions of octanol. *Soc. Neurosci. Abstr.*, **15**, 355.
- TWOMBLY, D.A., YOSHII, M. & NARAHASHI, T. (1988). Mechanism of calcium channel block by phenytoin. *J. Pharmacol. Exp. Ther.*, **249**, 189-195.
- VERGNES, M., MARESCAUX, C., DEPAULIS, A., MICHELETTI, G. & WARTER, J.M. (1987). Spontaneous spike-and-wave discharges: thalamus and cortex in a rat model of genetic petit mal-like seizures. *Exp. Neurol.*, **96**, 127-136.
- WILDER, B.J. & BUCHANAN, R.A. (1981). Methsuximide for refractory complex partial seizures. *Neurology*, **31**, 741-744.
- WILLIAMS, D. (1953). A study of thalamic and cortical rhythms in petit mal. *Brain*, **76**, 50-69.
- WILLOW, M., GONOI, T. & CATTERALL, W.A. (1985). Voltage clamp analysis of the inhibitory actions of diphenylhydantoin and carbamazepine on voltage-sensitive sodium channels in neuroblastoma cells. *Mol. Pharmacol.*, **27**, 549-558.

Received November 16, 1990

Revised February 12, 1991

Accepted March 19, 1991

Distinct Functions of T- and L-Type Calcium Channels during Activation of Bovine Adrenal Glomerulosa Cells*

MICHEL F. ROSSIER†, MURIEL M. BURNAY, MICHEL B. VALLOTTON, AND ALESSANDRO M. CAPPONI

Division of Endocrinology and Diabetology, University Hospital, Geneva, Switzerland

ABSTRACT

Calcium influx into adrenal glomerulosa cells is a key event during the stimulation of aldosterone secretion by physiological increases in extracellular potassium concentrations. Two types of voltage-operated calcium channels, T- and L-types, are present on bovine glomerulosa cells, but their respective functions are not yet clearly defined. Using the patch-clamp method in the perforated patch configuration combined with microfluorimetry of cytosolic calcium, we demonstrate that L-type channels are exclusively responsible for the sustained elevation of cytosolic calcium observed upon stimulation with extracellular potassium, even at low, physiological concentrations of this agonist. In contrast, aldosterone secretion appears

closely related to T-type channel activity. Moreover, when the activity of each channel type is selectively modulated by pharmacological agents, such as dihydropyridines or zonisamide, the cytosolic calcium response can be clearly dissociated from the steroidogenic response. Similarly, modulation of T channel activation by protein kinase C results in a parallel inhibition of aldosterone secretion, without any effect on the levels of cytosolic free calcium. This direct functional link between T-type calcium channel activity and steroidogenesis suggests a model in which calcium entering the cell through these channels bypasses the cytosol to activate intramitochondrial steps of aldosterone biosynthesis. (*Endocrinology* 137: 4817–4826, 1996)

THE STIMULATION of aldosterone synthesis in adrenal glomerulosa cells by angiotensin II (AngII) or potassium ion is maintained through a sustained influx of Ca^{2+} into the cell (1–3). Although a crucial role for Ca^{2+} entry has been recognized for many years (4), the nature of the pathways allowing extracellular Ca^{2+} to reach its intracellular target sites, such as the mitochondria, where the cation can control key steps of steroidogenesis, was only recently determined.

A biphasic response of the cytosolic free Ca^{2+} concentration ($[\text{Ca}^{2+}]_c$) can be clearly observed upon AngII stimulation; indeed, a first Ca^{2+} release phase from intracellular stores triggered by the formation of inositol 1,4,5-trisphosphate (5–7) is followed by a sustained Ca^{2+} influx. This second entry phase is mainly attributable to the activation of a capacitative influx resulting from the depletion of intracellular Ca^{2+} stores (8, 9); however, a component of this influx is also due to voltage-operated Ca^{2+} channels activated during AngII-induced cell depolarization.

In contrast, extracellular K^+ does not affect intracellular Ca^{2+} pools and, therefore, appears to exclusively activate voltage-operated Ca^{2+} channels as a consequence of its depolarizing action. However, both L- and T-type Ca^{2+} channels are expressed in bovine glomerulosa cells (10, 11), and which channel is involved in the activation of glomerulosa cells by KCl is still a matter of debate. Whereas the slow kinetics of L-type channel inactivation obviously favor a role

of these channels during long lasting stimulations of steroidogenesis by K^+ , the lower threshold of activation of T-type channels has been proposed to provide the cell with an exquisite sensitivity to low, physiological concentrations of extracellular K^+ . Moreover, the existence of a window of voltage, which is compatible with the membrane potential values reached during stimulation with physiological concentrations of extracellular K^+ and in which a statistical proportion of T-type channels can be maintained open (12, 13), supports the hypothesis of a role for the latter channels in cell activation.

Early pharmacological studies aiming at discriminating between T- and L-type channel function largely contributed to the present confusion, because of the low specificity and high concentrations of the agents used and the poor control of the action of these channel blockers on specific current amplitudes (2, 14). Additional problems could also originate from the fact that steroidogenesis and $[\text{Ca}^{2+}]_c$ were not always systematically measured under the same conditions, and both parameters were generally considered *a priori* as inextricably related.

Recently, Barrett *et al.* (15) used the spider toxin ω -agatoxin IIIA to specifically and completely block L-type Ca^{2+} channels in bovine glomerulosa cells. Under these conditions, the steroidogenic response to physiological concentrations of K^+ (7 mM) remained unaffected, suggesting that aldosterone secretion is primarily stimulated by Ca^{2+} entry through T-type Ca^{2+} channels. Moreover, upon activation with a much higher concentration of K^+ (60 mM), which is believed to efficiently open L-type channels, aldosterone production was even enhanced by ω -Aga IIIA and inhibited by the L-type channel activator BayK 8644, an observation that has also been reported in rat cells (16). A negative modulation of

Received April 19, 1996.

Address all correspondence and requests for reprints to: Dr. Michel F. Rossier, Division of Endocrinology and Diabetology, University Hospital, CH-1211 Geneva 14, Switzerland. E-mail: rossier@cmu.unige.ch.

* This work was supported by Swiss National Science Foundation Grants 32-39277.93 and 31-42178.94.

† Recipient of a grant from the Prof. Max Clœtta Foundation.

steroidogenesis by Ca^{2+} when entering the cell through L-type channels was, therefore, proposed (15).

In the present study, we examined the effects of various pharmacological agents, such as dihydropyridines and zonisamide, on both T- and L-type channel activities as well as on $[\text{Ca}^{2+}]_i$ and aldosterone production to determine which parameters are functionally linked upon stimulation with extracellular K^+ . We found that whereas L-type channels are mostly responsible for the variations in $[\text{Ca}^{2+}]_i$, T-type, but not L-type, channel activity is closely correlated with aldosterone biosynthesis.

Materials and Methods

Percoll was obtained from Pharmacia (Piscataway, NJ), and Cell-Tak from Inotech (Dottikon, Switzerland). Amphotericin B, nystatin, tetrodotoxin, sodium ATP, sodium GTP, ionomycin, EGTA, and nifedipine were purchased from Sigma (St. Louis, MO), and pluronic acid, fluo-3, and fura-2 acetoxymethyl esters were obtained from Molecular Probes (Eugene, OR). Phorbol 12-myristate 13-acetate (PMA) was purchased from LC Laboratories (Woburn, MA), and calciseptine was purchased from Latoxan (Rosans, France). BayK 8644 was kindly donated by Bayer (Leverkusen, Germany), and zonisamide was a generous gift from Dr. S. Kurooka, Dainippon Pharmaceutical Co. (Osaka, Japan).

Adrenal glomerulosa cell isolation and culture

Bovine adrenal glands were obtained from a local slaughterhouse, and glomerulosa cells were prepared by enzymatic dispersion, purified on a Percoll density gradient, and maintained in culture for 2–4 days, as described in detail previously (11). The relatively small size of glomerulosa cells compared to that of fasciculata cells, the presence of lipid droplets, as well as the responsiveness to AngII confirmed that more than 95% of the cell population was composed of glomerulosa cells.

Patch-clamp measurements

The activity of voltage-operated Ca^{2+} channels in bovine adrenal glomerulosa cells was recorded under voltage clamp either in the whole cell configuration of the patch clamp technique, as previously described (13), or in combination with $[\text{Ca}^{2+}]_i$ measurement with the fluorescent dye fluo-3 in the perforated patch configuration (17). In the latter case, the bath solution contained 117 mM tetraethylammonium chloride, 20 mM CaCl_2 , 0.5 mM MgCl_2 , 5 mM D-glucose, 32 mM sucrose, and 200 mM tetrodotoxin and was buffered to pH 7.5 with 10 mM HEPES- CsOH . The patch pipette (3–6 M Ω ; Clark 150T, Reading, UK) contained 130 mM CsCl , 5 mM MgCl_2 , and 1 mM CaCl_2 , and the pH was buffered to 7.2 with 20 mM HEPES- CsOH . The pipette solution also contained 0.2 mg/ml nystatin (17) or 0.24 mg/ml amphotericin B (18), but the tip of the pipette was filled with ionophore-free solution to allow formation of the seal. The access resistance was reduced to 10–30 M Ω in less than 15 min, and the process was slightly faster with amphotericin B than with nystatin. The reference electrode was placed in a KCl solution linked to the bath with an Agar bridge; the resulting liquid junction potential was smaller than 2 mV and has been neglected. The cell was voltage clamped (Axopatch 1D, Axon Instruments, Foster City, CA) at a holding potential of -90 mV and depolarized as indicated. The currents were filtered at 1–2 kHz and sampled at 6.2 kHz. Leak was subtracted either digitally after the experiment or automatically by a P/4 protocol (pclamp 6, Axon Instruments).

$[\text{Ca}^{2+}]_i$ measurements

$[\text{Ca}^{2+}]_i$ was determined either with fura-2 in populations of cells freshly isolated and purified on a Percoll density gradient, as previously described in detail (13), or in single voltage-clamped cells loaded with the probe fluo-3 in combination with the patch-clamp technique in the perforated patch configuration. For this purpose, bovine glomerulosa cells were plated on small glass coverslips coated with Cell-Tak and cultured for 2–4 days. The cells were then incubated for 45 min at 37°C in the presence of 8 μM fluo-3 acetoxymethyl ester and 6.25% (wt/vol)

pluronic acid, washed in bath solution, and immediately mounted in a home-made patch-clamp recording chamber maintained in the dark. Fluo-3 fluorescence (excitation at 470 nm and emission at 540 nm) was monitored on a Zeiss Axiovert 10 inverted microscope (Zeiss, New York, NY) equipped with a Bio-Rad CRS-400 microfluorimeter (Bio-Rad, Glattbrugg, Switzerland). The fluorescent signal was sampled at 2 Hz and recorded using the CRS-400 software (Bio-Rad).

Determination of aldosterone formation

Measurement of aldosterone production from freshly prepared or cultured glomerulosa cells was performed as described previously (8). Glomerulosa cells, when cultured for 3 days, were incubated at 37°C in multiwell plates containing a modified Krebs-Ringer medium and various concentrations of potassium and pharmacological inhibitors of Ca^{2+} channels. At the end of the incubation period, the aldosterone content of the medium was determined by direct RIA, using a commercially available kit (Diagnostic Systems Laboratories, Webster, TX).

Statistical analysis

When appropriate, statistical significance of differences was determined by paired Student's *t* test and corrected according to Bonferroni's method. A difference was considered statistically significant at a corrected *P* < 0.05.

Results

Contribution of T- and L-type Ca^{2+} channels to the depolarization-evoked cytosolic Ca^{2+} signal

To determine the role of T-type Ca^{2+} channels in the sustained $[\text{Ca}^{2+}]_i$ response to cell depolarization induced in bovine adrenal glomerulosa cells during stimulation by extracellular K^+ or AngII, Ca^{2+} currents and $[\text{Ca}^{2+}]_i$ variations were recorded in the same cell by combining the patch-clamp technique, in its perforated patch configuration, and the microfluorimetry of fluo-3. Cell depolarization to 0 mV, from a holding potential of -100 mV, induced a marked increase in $[\text{Ca}^{2+}]_i$, which rapidly returned to basal values upon cell repolarization, demonstrating the ability of the Ca^{2+} pumps to maintain a low $[\text{Ca}^{2+}]_i$ in the absence of stimulation (Fig. 1A). When the cell was gradually depolarized in a stepwise manner, no response was observed below -60 mV; $[\text{Ca}^{2+}]_i$ then rapidly rose to reach a maximum at -30 mV and slightly decreased at more positive potentials (Fig. 1, A and D). Once again, $[\text{Ca}^{2+}]_i$ returned to basal levels immediately after cell repolarization, and a novel response could be evoked by a large depolarization to 0 mV. The steady state current through T-type channels was also determined in the same cell, as described previously (13), by measuring slowly deactivating Ca^{2+} currents evoked upon repolarization at -65 mV (not shown). Analysis of tail currents allowed us to establish the activation and inactivation curves of T channels (Fig. 1C); the expected relative steady state current through these channels was calculated from Ohm's law and compared to the depolarization-evoked $[\text{Ca}^{2+}]_i$ response (Fig. 1D). A clear dissociation was observed between the sustained Ca^{2+} influx expected to occur through T channels (I_{ss}) and the measured $[\text{Ca}^{2+}]_i$ response (fluo-3 signal). Because this dissociation appeared much more pronounced at more positive voltages, a large participation of L-type channels to Ca^{2+} influx was hypothesized.

To reduce as much as possible the contribution of L-type channels, the cell was then exposed to highly specific inhibitors of L-type channels. As shown in Fig. 1B, the addition of

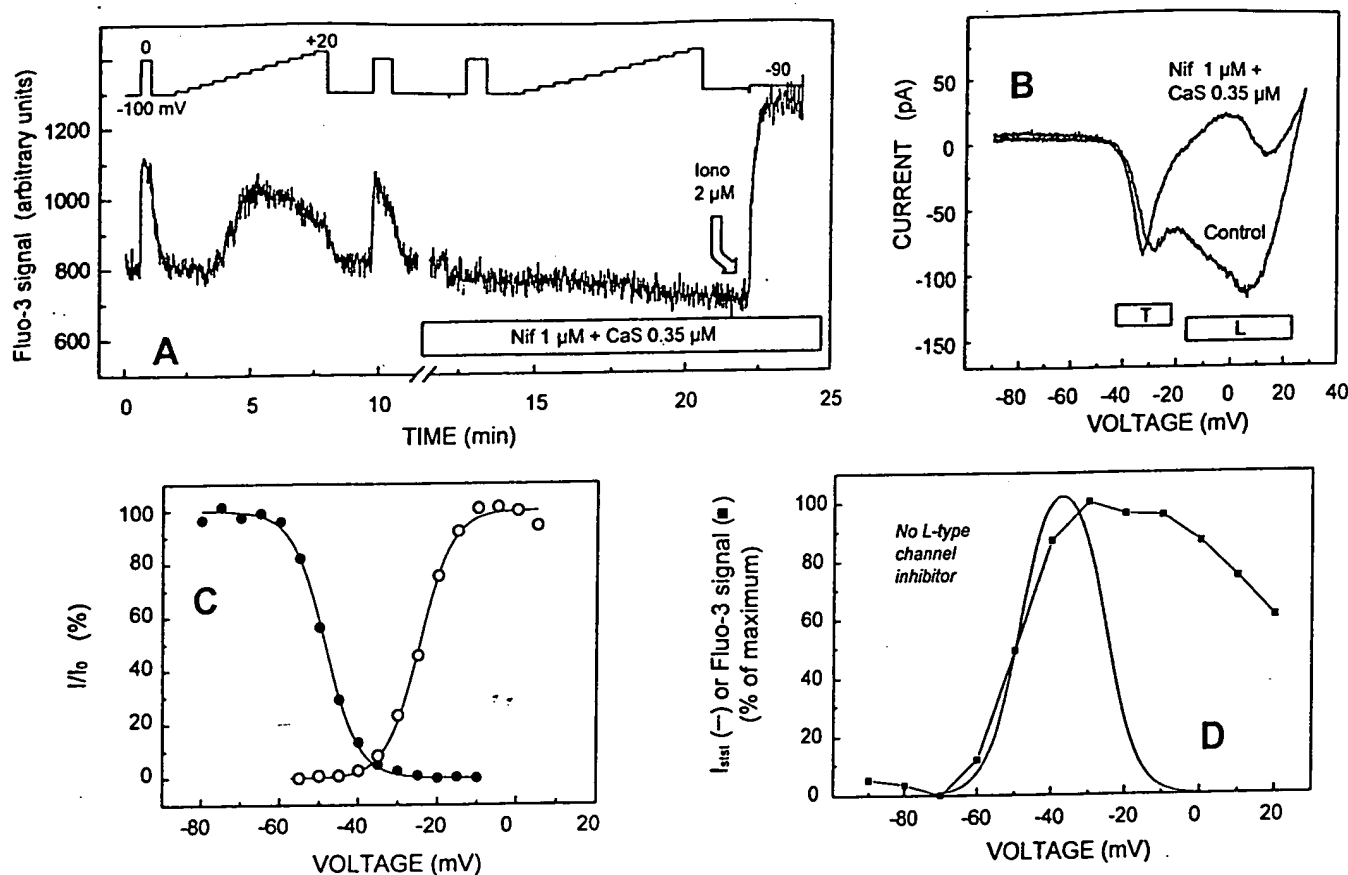


FIG. 1. Minor role of T-type calcium channels in depolarization-evoked cytosolic calcium response. A, Voltage-dependent cytosolic Ca^{2+} signal. A single fluo-3-loaded bovine adrenal glomerulosa cell was voltage clamped in the nystatin perforated patch configuration of the patch-clamp technique, as described in detail in *Materials and Methods*. Cytosolic Ca^{2+} -dependent fluorescence was recorded at a holding potential of -100 mV and upon various step depolarizations (the voltage protocol is indicated on the top of the trace). After 12 min of recording, nifedipine (1 μ M) and calciseptine (0.35 μ M) were added together to the medium, the protocol was repeated, and 2 μ M ionomycin was introduced at the end of the experiment to induce a maximal Ca^{2+} response. B, Selectivity of nifedipine and calciseptine for L-type channels. T- and L-type Ca^{2+} currents were evoked in the same cell as in A by ramp depolarization from -110 to $+40$ mV (duration, 1.8 sec), before the fluorescence recording (Control), and immediately after addition of Nif and CaS to the bath (during the gap of the time scale in A). Currents are expressed as a function of the voltage value reached during the ramp protocol (33). C, Activation and inactivation curves of slowly deactivating currents were measured in this same cell at the beginning of the experiment as described previously (13). Current amplitudes were plotted as a function of test voltage, fitted to Boltzman's equation, and normalized to the maximal current (I_0). $V_{1/2}$ values (the voltage corresponding to half the maximal effect) were -24.7 and -48.1 mV for activation and inactivation, respectively, in this particular cell. D, Comparison of steady state current through T channels and membrane potential-dependent $[Ca^{2+}]_c$ concentration. The theoretical steady state current (I_{ss}) was calculated from the activation and inactivation curves according to Ohm's equation as previously described (13) and expressed as a percentage of the maximal current as a function of voltage (smooth curve). The fluo-3 signal observed during the first gradual stepwise depolarization (A) was averaged for each potential value and normalized (\blacksquare). Similar results were obtained in each of five separate cells in which currents were recorded in combination with fluo-3 signal.

1 μ M nifedipine and 0.35 μ M calciseptine specifically decreased L current evoked by a ramp depolarization, but did not affect the lower threshold, transiently activated, T-type current. Surprisingly, the disappearance of L current was accompanied by complete abolition of the $[Ca^{2+}]_c$ response to cell depolarization, although a large entry of Ca^{2+} , induced by the Ca^{2+} ionophore ionomycin, was still detectable with fluo-3 (Fig. 1A).

These results, therefore, suggested that T channels play only a minor role in the elevation of $[Ca^{2+}]_c$ observed upon glomerulosa cell depolarization. This hypothesis was reinforced by the observation of a significant correlation of the maximal $[Ca^{2+}]_c$ increase elicited during a slow ramp depolarization (duration, 2 min), under various pharmacological conditions (Fig. 2B), with the maximal amplitude of L cur-

rents, but not with that of T currents, induced by a similar, but faster, depolarization (duration, 1.8 sec; Fig. 2A). Indeed, the amplitudes of T- and L-type currents could be independently manipulated in the same cell by adding consecutively to the bath: 1) 200 nM BayK 8644, an agonist of L-type channels; 2) 500 nM nifedipine, an antagonist of L-type channels; 3) 0.1 mM Ni^{2+} , an inorganic blocker of T-type channels; and finally, 4) 2 μ M nifedipine. In the presence of BayK 8644 alone, L current was predominant in this cell, and the maximal current amplitude was slightly shifted toward more negative potentials, partially overlapping T-type current (Fig. 2A-I). Analysis of the fluo-3 signal in response to cell depolarization (Fig. 2, B-I and C-I) showed that $[Ca^{2+}]_c$ was maximal between -45 and -15 mV and decreased thereafter. The addition of 500 nM Nif did not completely block

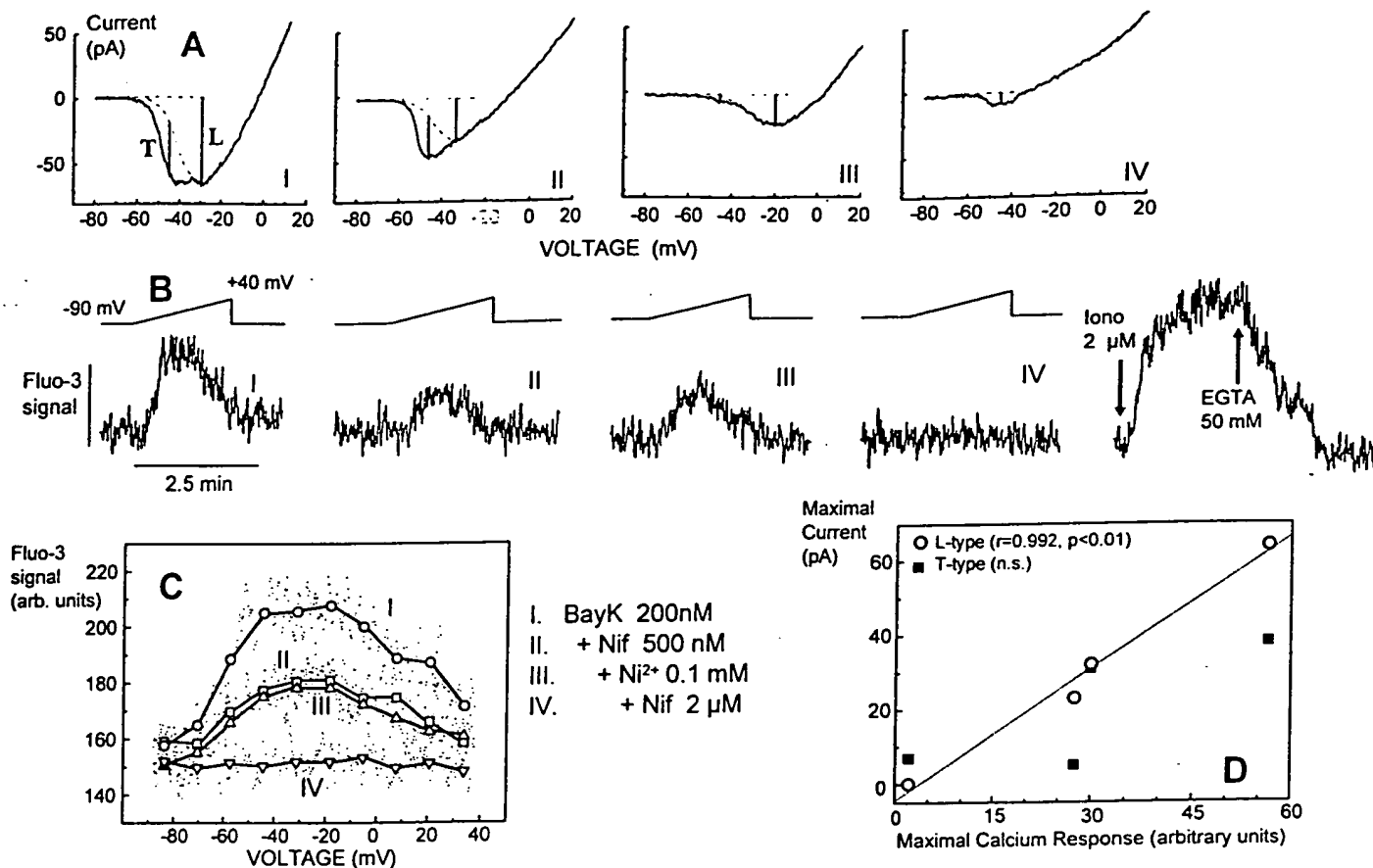


FIG. 2. Correlation between L-type calcium channel activity and depolarization-evoked cytosolic calcium response. Calcium currents (A) and fluo-3 signals (B) in response to a ramp depolarization were consecutively recorded in a single voltage-clamped glomerulosa cell maintained in the amphotericin B perforated patch configuration and in the presence of various pharmacological modulators of T- and L-type channels. Phase I, BayK (200 nM); phase II, BayK plus nifedipine (500 nM); phase III, BayK, Nif, and Ni^{2+} (0.1 mM); phase IV, BayK, Ni^{2+} , and Nif (2.5 μM). Calcium currents (A) were evoked at the beginning and end of each phase by cell depolarization from -110 to $+40$ mV (duration, 1.8 sec) and were averaged and expressed as a function of the instantaneous voltage, as described in Fig. 1B. The maximal amplitudes of T- and L-type currents were estimated to occur at -45 mV and approximately -30 mV, respectively. Calcium responses were recorded during the 2-min depolarization protocol indicated at the top of the traces (B), and ionomycin (2 μM) followed by EGTA (50 mM) were added at the end of the experiment to determine, respectively, the maximal and minimal signals of fluo-3. C, Fluo-3 signal during each phase was smoothed by averaging every 25 consecutive data points (the sampling rate during data acquisition was 2 Hz, corresponding to a point every 0.54 mV), and the results were expressed as a function of the mean voltage of the averaging domain. D, Correlation between L-type current and $[\text{Ca}^{2+}]_i$. The maximal T- and L-type currents estimated in A were compared to the maximal fluo-3 signal determined in C, and the correlation was assessed by least square linear regression analysis.

L-type channels, presumably because of the continuous presence of BayK, but reduced the maximal amplitude of L current by approximately 50% without significantly affecting that of T-type current (Fig. 2A-II). Concomitantly, fluo-3 signal amplitude was reduced by about half, without any apparent shift in its maximum (Fig. 2, B-II and C-II). In contrast, Ni^{2+} almost completely abolished T-type current (Fig. 2A-III), without modifying either L current or $[\text{Ca}^{2+}]_i$ (Fig. 2, B-III and C-III). Finally, complete inhibition of L-type channels with an excess of Nif resulted in complete inhibition of the $[\text{Ca}^{2+}]_i$ response to cell depolarization (Fig. 2, A-IV, B-IV, and C-IV), although the addition of a Ca^{2+} ionophore (ionomycin) and a Ca^{2+} chelator (EGTA) resulted in the expected variations in $[\text{Ca}^{2+}]_i$. When the maximal Ca^{2+} current amplitudes through each channel were compared to the maximal $[\text{Ca}^{2+}]_i$ responses (Fig. 2D), a significant correlation was observed only with L-type currents, suggesting that the ac-

tivation of L-type channels is principally responsible for the voltage-dependent variations of $[\text{Ca}^{2+}]_i$.

To demonstrate that L-type channels are involved in the $[\text{Ca}^{2+}]_i$ response to even low, physiological concentrations of extracellular potassium, fura-2-loaded cells in suspension were exposed to various pharmacological agents before being gradually depolarized by consecutive additions of KCl to the medium. Figure 3A shows that 100 nM BayK 8644, which by itself had only a minor effect on basal $[\text{Ca}^{2+}]_i$, markedly potentiated the response to KCl addition. When the mean $[\text{Ca}^{2+}]_i$ increase was determined and expressed as a function of the actual K^+ concentration in the medium (Fig. 3B), BayK 8644 (100 nM) appeared to considerably increase and Nif (50 nM) to reduce the $[\text{Ca}^{2+}]_i$ response at each KCl concentration tested, without shifting the maximum. To determine whether T-type channels could be primarily responsible for the $[\text{Ca}^{2+}]_i$ response to low K^+ concentrations, whereas L-type

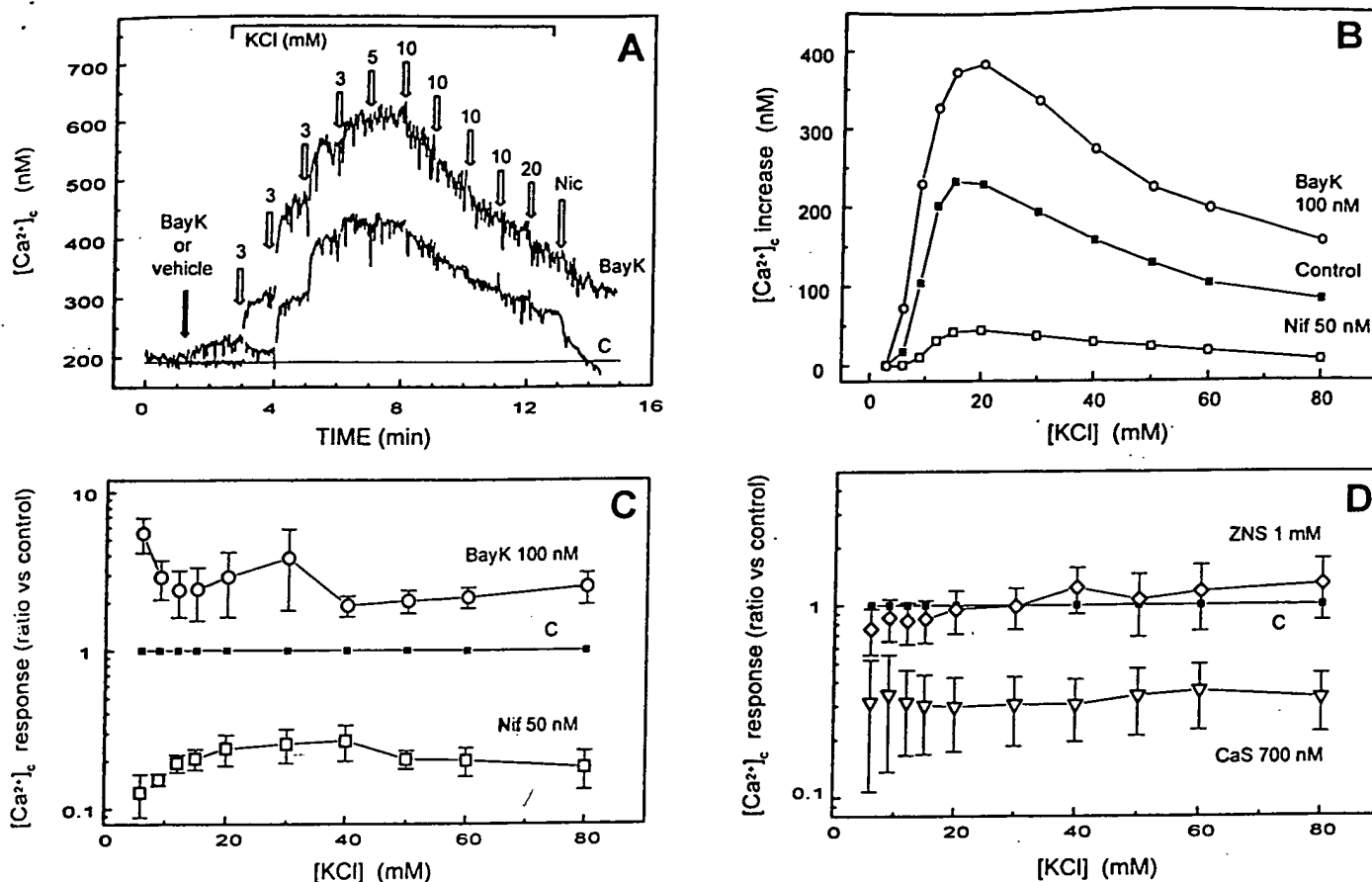


FIG. 3. Involvement of L-type channels in the cytosolic calcium response to physiological concentrations of potassium. A, Effect of BayK on the $[Ca^{2+}]_i$ response to extracellular K^+ . Freshly prepared glomerulosa cells were loaded with fura-2, as described in *Materials and Methods*, and exposed to increasing concentrations of extracellular K^+ (basal K^+ , 3 mM; arrows indicate the time and numbers the millimolar increases in K^+). One batch of cells was previously exposed (black arrow) to 100 nM BayK, whereas the control cells received dimethylsulfoxide only (C). Both groups were exposed to 2 μ M nifedipine at the end of the experiment. The dotted line represents basal $[Ca^{2+}]_i$. B, Modulation of the K^+ -dependent $[Ca^{2+}]_i$ signal by BayK and nifedipine. The same protocol as that described in A was performed with cells exposed to 50 nM nifedipine, 100 nM BayK, or dimethylsulfoxide, and the mean increase in $[Ca^{2+}]_i$ over basal was expressed as a function of the K^+ concentration. C and D, Efficacy of various Ca^{2+} channel modulators as a function of the extracellular K^+ concentration. At each extracellular K^+ concentration of the protocol described in A, the ratio between the $[Ca^{2+}]_i$ response measured in the presence and the absence of 100 nM BayK, 50 nM Nif, 1 mM zonisamide (ZNS), or 700 nM calciseptine (CaS) was calculated. Results are the mean \pm SEM from four to six experiments performed in duplicate.

channels would be only involved at higher, supraphysiological K^+ concentrations, the sensitivity of the response to dihydropyridines was analyzed as a function of the KCl concentration. For this purpose, the ratio of the response after treatment with each dihydropyridine over the response in control untreated cells was calculated (Fig. 3C). The cells did not appear to be less sensitive at lower K^+ concentrations, as would be the case if Ca^{2+} influx occurred through T-type channels under these conditions. Similarly, when L-type channels were specifically inhibited with 700 nM calciseptine (Fig. 3D), the $[Ca^{2+}]_i$ response was inhibited in the same proportion over the complete range of KCl concentrations tested. This demonstrates that the K^+ -induced Ca^{2+} signal is mediated by a single, pharmacologically homogeneous class of channel, highly sensitive to dihydropyridines and calciseptine. In contrast, treatment of the cells with 1 mM zonisamide, an antiepileptic agent with a low selectivity for T-type channels (19), had almost no effect on the $[Ca^{2+}]_i$ response (Fig. 3D).

It, therefore, appears that the cytosolic Ca^{2+} response to extracellular K^+ measured in bovine adrenal glomerulosa cells with fluorescent probes is principally, if not entirely, due to activation of dihydropyridine-sensitive L-type Ca^{2+} channels even at lower K^+ concentrations when the cells are only slightly depolarized. In contrast, the modulation of Ca^{2+} influx through T-type channels is not detectable in the cytosol (see *Discussion*).

Lack of correlation between cytosolic calcium and aldosterone secretion

The relationship between the levels of $[Ca^{2+}]_i$ maintained by K^+ and the activation of aldosterone secretion by the same agonist was investigated by modulating Ca^{2+} channel activity with nifedipine, BayK 8644, or zonisamide (Fig. 4). Increasing concentrations of Nif, between 1 nM and 3 μ M (Fig. 4, left panels), markedly and monotonously reduced $[Ca^{2+}]_i$ stimulated by 12 mM K^+ , even below resting levels, indicat-

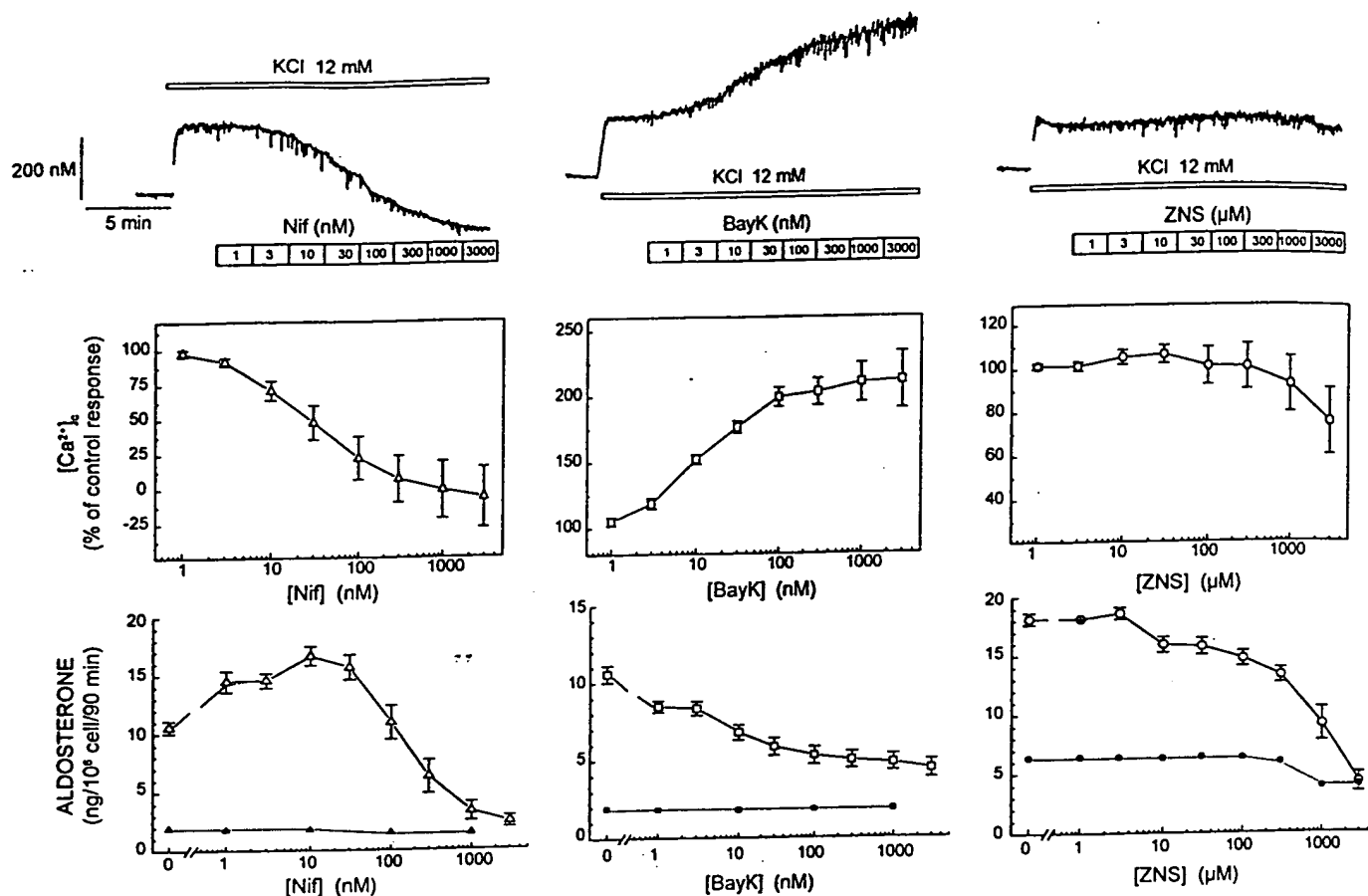


FIG. 4. Lack of correlation between the $[Ca^{2+}]_i$ and aldosterone responses to potassium. The effects of increasing concentrations of nifedipine, BayK 8644, and zonisamide on K^+ -induced $[Ca^{2+}]_i$ and steroidogenic responses were examined in freshly prepared bovine glomerulosa cells. Representative traces of $[Ca^{2+}]_i$ measured in cell populations with the fura-2 technique are shown in the top panels. Potassium and drug concentrations in the medium are indicated at the bottom or the top of each trace. Basal $[Ca^{2+}]_i$ (measured in a Krebs-Ringer medium containing 3 mM K^+) was 207 ± 5 nM (mean \pm SEM; $n = 9$). The effect of increasing concentrations of each drug on $[Ca^{2+}]_i$ stimulated by a 9-mM increase 3 mM K^+ was determined and expressed as a percentage of the response to KCl in the absence of the drug (center panels). Aldosterone secretion in KCl was determined and expressed as a percentage of the response to KCl in the absence of the drug (bottom panels). Aldosterone secretion (bottom panels) was measured in the medium, as described in Materials and Methods, after 90-min incubation of the cells in the presence of increasing concentrations of Nif, BayK, ZNS, and either low (3 mM; closed symbols) or high K^+ (12 mM; open symbols). Results are the mean \pm SEM from three to seven experiments, and aldosterone was measured in duplicate.

ing the presence of a small basal Ca^{2+} influx sensitive to dihydropyridines, as previously described in these cells (8). The effect of Nif on aldosterone secretion followed a different pattern. While concentrations of Nif above 100 nM efficiently inhibited K^+ -induced steroidogenesis, aldosterone output was significantly potentiated by the presence of the Ca^{2+} antagonist at concentrations between 1–30 nM. Basal aldosterone production was not affected by Nif.

As expected, the agonist BayK 8644 potentiated the $[Ca^{2+}]_i$ response to 12 mM K^+ , increasing the signal by approximately 110% at the maximal concentration; however, the same agent markedly reduced, in a concentration-dependent manner, aldosterone secretion sustained by high K^+ (12 mM) without affecting basal steroidogenesis (Fig. 4, middle panels).

Finally, zonisamide (right panels), the slightly selective inhibitor of T-type channels, only minimally affected K^+ -induced $[Ca^{2+}]_i$ compared to Nif or BayK 8644, but markedly decreased both stimulated and basal aldosterone secretion.

By using various pharmacological agents acting selectively on T- or L-type channels, it was, therefore, possible to illustrate the dissociation existing between the levels of bulk

$[Ca^{2+}]_i$, as measured with classical fluorescent probes, and aldosterone synthesis upon stimulation with high K^+ concentrations.

Correlation between T-type channel activity and potassium-stimulated aldosterone production

To determine the specificity of the Ca^{2+} channel-modulating agents employed in this study, it was necessary to examine the effects of various concentrations of these agents on T- and L-type channels. The upper panels of Fig. 5 show the pattern of Ba^{2+} currents recorded in the whole cell configuration of the patch-clamp technique and elicited by a gradual depolarization of the cells, as described in Figs. 1B and 2A. The size of the inward current with the lower threshold, peaking at about -30 mV, was systematically compared to the amplitude of the slowly deactivating current induced in the same cell (not shown), measured as described in detail previously (13). Both methods for isolating and measuring T-type channel activity were closely correlated ($r = 0.928$; $n = 48$; $P < 0.001$), demonstrating that the voltage ramp protocol

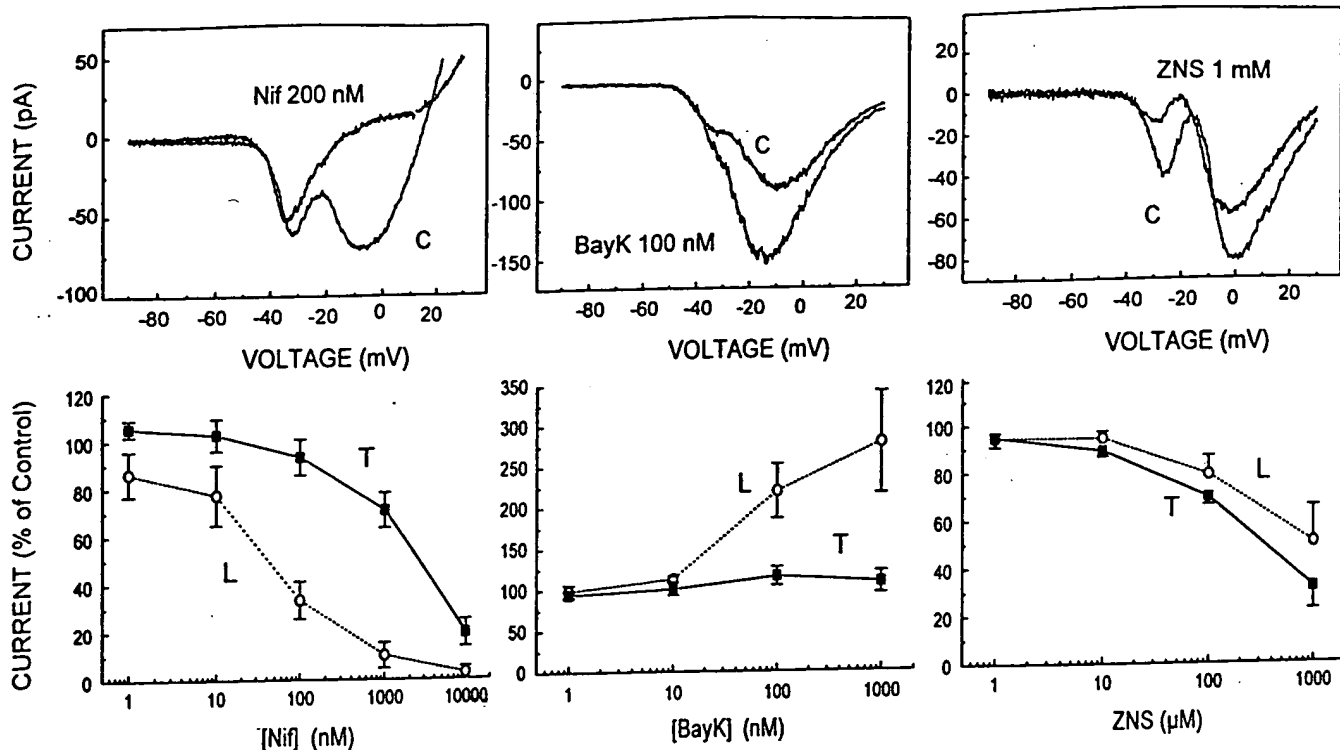


FIG. 5. Selectivity of nifedipine, BayK 8644, and zonisamide for T- and L-type calcium channels. T- and L-type Ba^{2+} currents were partially resolved by ramp depolarizations (from -110 up to $+40$ mV during 1.8 sec) in the whole cell configuration of the patch-clamp method. An example of the effect of 200 nM Nif, 100 nM BayK 8644, and 1 mM ZNS on Ba^{2+} currents is presented in the upper panels (C, control trace, recorded before drug addition). Concentration-dependent curves of inhibition or activation of each current by Nif, BayK, and ZNS were established by expressing the value of the specific peak current, measured after drug addition, as a percentage of the control current (lower panels). Data are the mean results obtained from 5–14 independent cells.

TABLE 1. Correlation between potassium-induced aldosterone secretion and T channel activity

Drug	Activity (% of control)			Cytosolic Ca^{2+}
	Aldosterone	T Channel	L Channel	
Nif (100 nM)	69.5 ± 13.4 (9)	93.2 ± 7.5 (7)	33.3 ± 7.8 (5)	21.5 ± 5.4 (8)
Nic (10 nM)	124.6 ± 13.5 (13)	131.4 ± 23.2 (5)	58.9 ± 13.2 (5)	26.8 ± 5.5 (5)
BayK (100 nM)	71.3 ± 7.3 (9)	115.5 ± 11.3 (10)	219.1 ± 33.3 (7)	224.6 ± 43.9 (7)
ZNS (100 μM)	87.3 ± 4.2 (10)	75.9 ± 3.8 (14)	79.2 ± 7.9 (7)	101.5 ± 8.5 (7)
TET (10 μM)	58.8 ± 5.1 (11)	51.9 ± 9.0 (13)	ND	ND

Aldosterone secretion from freshly prepared or cultured glomerulosa cells stimulated with 12 mM K^+ was determined in control (untreated) cells and in cells exposed to drugs at a concentration (100 nM nifedipine, 10 nM nicardipine, 100 nM BayK 8644, 100 μM zonisamide, or 10 μM tetrandrine) yielding optimal selectivity for L- or T-type channels. The effect of each drug on aldosterone production, expressed as a percentage \pm SEM of the control value, is compared to the effect of the same drug concentration on T and L channel activity, assessed as described in Fig. 5, and on $[\text{Ca}^{2+}]_i$, determined with fura-2. Least square linear regression analysis revealed a positive correlation between aldosterone secretion and T-type channel activity ($r = 0.69$) and between $[\text{Ca}^{2+}]_i$ and L-type channel activity ($r = 0.97$). No correlation was observed between any other groups. The values in parentheses indicate the number of independent determinations. ND, Not determined.

allows discrimination between T- and L-type currents. The ratio between L- and T-type currents under control conditions varied greatly from one cell to the other [see, for example, the control (C) traces in the upper panels of Fig. 5], and the effects of the drugs were, therefore, expressed as the amplitude of each current as a percentage of the corresponding control current measured before treatment (Fig. 5, lower panels).

Nifedipine inhibited both currents, but T-type channels were affected by approximately 100 times higher concentrations of the drug, showing that it is possible to substantially reduce L-type channel activity without markedly affecting

T-type channels at concentrations of Nif ranging from 100–1000 nM.

The effect of BayK 8644 on T- and L-type channels was even more contrasted, as this compound, at concentrations above 10 nM, considerably increased L-type current by up to 170%, whereas the current flowing through T-type channels was not significantly affected.

Finally, zonisamide was slightly more efficient in inhibiting T-type current compared to L-type current, although millimolar concentrations of this agent also markedly affected the latter.

The actions of these drugs on T- and L-type channel ac-

tivity as well as on $[Ca^{2+}]_c$ were then compared to their abilities to prevent aldosterone secretion upon stimulation with 12 mM K^+ (Table 1). Tetrandrine, an alkaloid relatively selective for T-type channels (11), and nifedipine, a dihydropyridine efficiently blocking both T- and L-type channels when used at micromolar concentrations (8), were also included in this comparison. The effect of each drug on potassium-induced steroidogenesis, when employed at a concentration providing an optimal selectivity for one type of Ca^{2+} channel, appeared to correlate much better with their actions on T channel ($r = 0.69$) than on L channel activity ($r = -0.37$). In contrast, $[Ca^{2+}]_c$ measured in the presence of the same drugs was more closely related to L-type currents ($r = 0.97$) than to T-type currents ($r = 0.03$), suggesting distinct cellular functions for these channels.

Phorbol ester inhibits Ca^{2+} influx through T-type channels as well as steroidogenesis without affecting $[Ca^{2+}]_c$ concentration

An additional illustration of the discrepancy between $[Ca^{2+}]_c$ on the one hand, and aldosterone synthesis and T channel activity, on the other hand, is provided by the action

of the phorbol ester, PMA. Through the direct activation of protein kinase C (PKC), PMA mimics some of the effects of AngII, among which is an inhibition of T-type channel activity (13). This inhibition is attributable to a significant shift ($P < 0.01$) in the activation curve of the channel by approximately 7 mV (at half-activation) toward more positive voltage values (Fig. 6A). In contrast, the inactivation of the channel is not affected by this treatment. As a consequence, the size of the permissive window of voltage is reduced, resulting in a substantial decrease in the expected steady state current through these channels (Fig. 6B). The reduction of Ca^{2+} influx resulting from T channel inhibition by PMA was not reflected by the levels of $[Ca^{2+}]_c$ as shown in Fig. 6C. In this experiment, fura-2-loaded cells were first stimulated with 9 mM KCl to maximally activate T- and L-type channels, and when the $[Ca^{2+}]_c$ response had reached a plateau, 500 nM PMA was added. No effect of PMA was observed, suggesting that this compound does not significantly affect L-type channels. However, upon stimulation with AngII, after a transient Ca^{2+} release phase mediated by inositol 1,4,5-trisphosphate, a marked reduction of $[Ca^{2+}]_c$ was induced, as previously described (13), possibly because L-type channels are con-

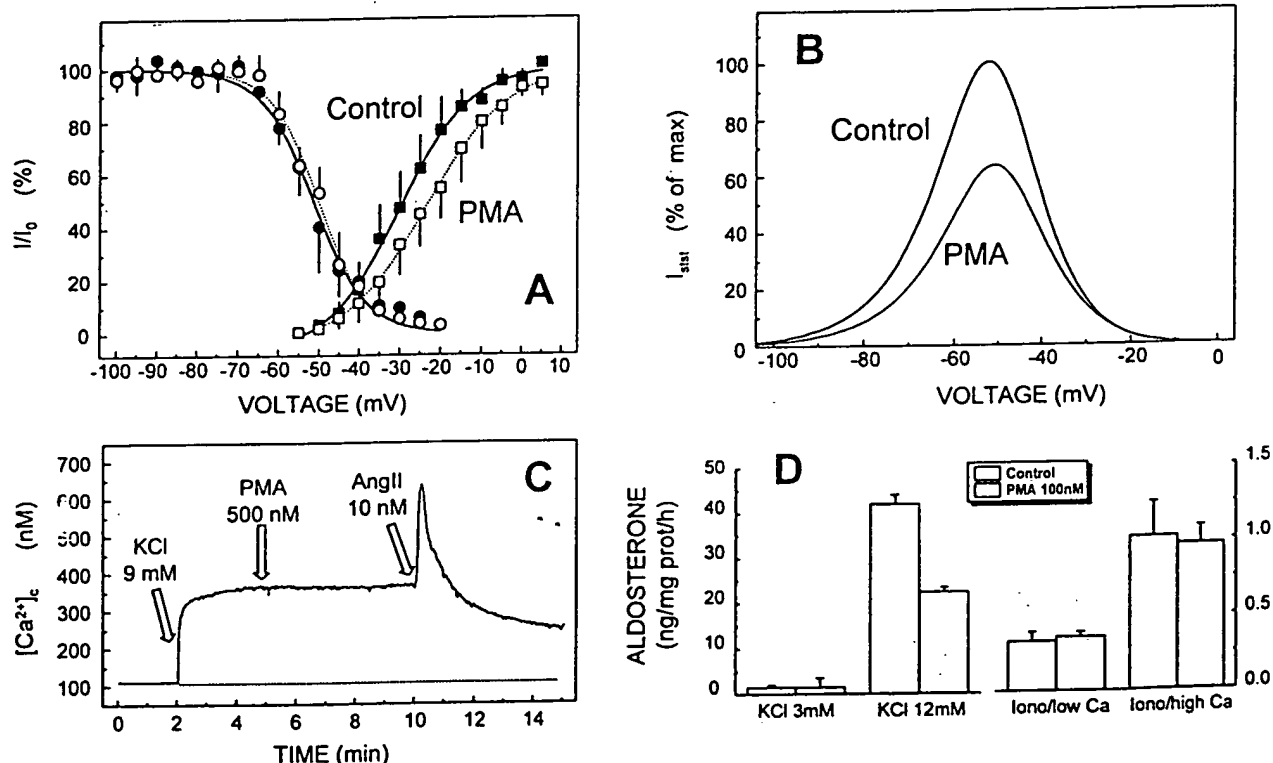


FIG. 6. Inhibition by PMA of T-type channel activity and potassium-stimulated aldosterone secretion, but not of the $[Ca^{2+}]_c$ response. A, PMA effect on the T channel activation curve. Glomerulosa cells were voltage clamped in the whole cell configuration, and Ba^{2+} currents were elicited as described in Fig. 1C, either before (Control) or 3 min after the addition of 500 nM PMA. Tail currents of T channels were analyzed for each cell separately; data were fitted to Boltzman's equation and normalized to I_0 (maximal current) before being averaged. Activation (■ and □) and inactivation (● and ○) curves were established, as described in Fig. 1, before (■ and ●) and after (□ and ○) exposure to PMA (mean \pm SEM; $n = 4$ cells). The mean $V_{1/2}$ for channel inactivation was -51.4 mV before and -50.1 mV after PMA application, whereas the $V_{1/2}$ for activation was shifted from -30.2 to -23.6 mV by the same treatment. B, Inhibition of the steady state current by PMA. The theoretical steady state current was calculated from Ohm's function, as described in Fig. 1D, before and after the addition of PMA. C, Lack of effect of PMA on $[Ca^{2+}]_c$. Fura-2-loaded cells were consecutively exposed to 9 mM KCl, 500 nM PMA, and 10 nM AngII, and $[Ca^{2+}]_c$ was monitored as described in Materials and Methods. The trace is representative of at least 10 independent observations from various cell preparations that gave similar results. D, Effect of PMA on calcium-induced aldosterone secretion. Aldosterone secretion was stimulated in the presence or absence of 100 nM PMA, either in intact cultured glomerulosa cells challenged with 12 mM K^+ (left ordinate) or in freshly prepared, ionomycin ($1 \mu M$)-treated cells (right ordinate) by increasing their $[Ca^{2+}]_c$ from 50 (low Ca) to 600 nM (high Ca).

trolled by AngII through a completely distinct mechanism, for example involving G proteins.

Despite the lack of effect of PMA on $[Ca^{2+}]_c$, KCl-stimulated aldosterone secretion was strongly inhibited (46%) by this agent (Fig. 6D), whereas basal aldosterone (at 3 mM K^+) was not affected. This inhibition did not appear to result from a direct action of PKC on the steroidogenic pathway, but, rather, from a reduction of Ca^{2+} influx into the cell, because when Ca^{2+} channels were bypassed with a Ca^{2+} ionophore such as ionomycin, the stimulation of steroidogenesis induced by increasing extracellular Ca^{2+} was insensitive to PMA (Fig. 6D).

Discussion

This study has allowed us to demonstrate that KCl-induced variations in $[Ca^{2+}]_c$ and aldosterone secretion in bovine adrenal glomerulosa cells can be dissociated with pharmacological agents possessing some specificity for T-type or L-type Ca^{2+} channels. Indeed, whereas $[Ca^{2+}]_c$ appeared to essentially reflect L-type channel activity, the steroidogenic response was closely related to T-type channels.

A sustained influx of Ca^{2+} through T-type channels upon physiological depolarization of the cell by extracellular K^+ is theoretically possible because of the overlap of the activation and steady state inactivation curves of the channel (12, 13). However, because of the low percentage (<1%) of T channels statistically open during a prolonged stimulation with K^+ , this current is expected to be very small. A raw estimation of the amplitude of this current by noise analysis revealed a sustained, nifedipine-resistant (500 nM) and Ni^{2+} -sensitive current of approximately 0.1 pA at -40 mV (data not shown). This very low amplitude of the steady state current through T-type channels certainly explains the lack of contribution of these channels to the cytosolic response, which is mainly maintained by the strong (at least 100-fold larger) Ca^{2+} current through L-type channels, but strikingly contrasts with its crucial role in the regulation of steroidogenesis.

One possible explanation for this paradox is the existence of a very efficient coupling between T-type channels and the Ca^{2+} target sites involved in the regulation of aldosterone formation. It is now well recognized that the mitochondria play a crucial role in this regulation (3), not only because these organelles contain the steroidogenic enzymes responsible for the early, rate-limiting, and late steps of aldosterone synthesis, but also because it has been shown that the stimulatory action of Ca^{2+} requires its entry into the mitochondrial matrix through the ruthenium red-sensitive uniporter (20). A close apposition of the mitochondria and of T-type channels or the existence of a sort of Ca^{2+} pipeline, possibly involving the endoplasmic reticulum and transporting Ca^{2+} from the mouth of the channel to the proximity of the mitochondrion with a very restricted passage of Ca^{2+} through the cytosol, could provide a functional link between Ca^{2+} influx through T-type channels and the activation of steroidogenesis.

In favor of this model is the observation that in some issues, basal and stimulated intramitochondrial $[Ca^{2+}]_m$, as assessed by targeted aequorin (21), are relatively high compared to the concentrations present in the bulk cytosol (22).

Although this gradient of $[Ca^{2+}]$ between the mitochondrial matrix and the cytosol could be partially due to the very negative potential of the inner mitochondrial membrane (23), the presence of mitochondria in some cellular microdomains with high $[Ca^{2+}]_c$ has been also demonstrated (22).

It, therefore, appears that T- and L-type channels might play distinct functional roles in glomerulosa cells. T-type channels are designed to conduct low amounts of Ca^{2+} directly to the mitochondria, where the cation can affect key steps of steroidogenesis, such as cholesterol transport to the inner membrane (24), whereas L-type channels are responsible for the entry of much larger amounts of Ca^{2+} , which spreads throughout the cytosol. The role of this cytosolic Ca^{2+} has not yet been clearly defined and could relate to more general cell functions, such as gene expression or cytoskeleton remodeling. However, an excess of cytosolic Ca^{2+} exerts a negative effect on aldosterone biosynthesis (15, 24), and this could explain the observed potentiation of the steroidogenic action of K^+ by low, L-type channel-specific concentrations of nifedipine as well as its inhibition by BayK 8644, as observed by others (15, 16, 25). Indeed, the inhibition of aldosterone by BayK 8644 was observed only at K^+ concentrations greater than 10 mM (not shown) and could, therefore, be only partially attributed to its known inhibitory action on T-type channels (26, 27).

A specific role for various types of channels has been clearly demonstrated in the central nervous system, where neurotransmitter release is attributed to presynaptic N- and P-type Ca^{2+} channel activation and is not affected by inhibition of L-type channels (28). This selectivity has been postulated to result from a privileged localization of some channels in the membrane, permitting a more efficient supply of Ca^{2+} to the secretory apparatus. This hypothesis has been recently reinforced by the observation that the N-type channel strongly binds, in a Ca^{2+} -dependent fashion, to syntaxin, a membrane protein allowing docking and fusion of synaptic vesicles during neurosecretion (29). Interestingly, syntaxin is able to modulate by itself the activity of N-type channels (30), suggesting considerable cross-talk between N-type channels and the synaptic core complex. The possibility of a similar interaction between glomerulosa cell T-type channels and some cellular proteins clearly requires further investigation.

What could be the advantage for glomerulosa cells of using specific Ca^{2+} pathways for triggering steroidogenesis? Firstly, because the main site of Ca^{2+} action is localized in the mitochondria, a small amount of Ca^{2+} entering the cell should be sufficient during activation, but this Ca^{2+} needs to reach its target with a minimal dispersion in the cytosol. Secondly, it is now widely admitted that the domain of Ca^{2+} action in the cytosol is restricted to very limited areas (31), its diffusion being prevented by its binding to slowly mobile or immobile buffers. Depending upon the distribution of the mitochondria within the cell, the presence of a Ca^{2+} pipeline might, therefore, be an absolute requirement. Finally, in contrast to L-type channels, T-type channels are not subject to down-regulation by Ca^{2+} (possibly because they are preserved during their relatively longer inactivation phase) and, therefore, can maintain a sustained stimulation of steroidogenesis during chronic elevation of extracellular potassium.

The inhibition of T channel activity and aldosterone se-

cretion observed upon treatment with phorbol ester is presumably due to activation of PKC. This action of PKC appears to be restricted to T-type channels, because $[Ca^{2+}]_i$ is not affected. However, a definitive proof would require a complete evaluation of PMA action on L-type channels. Interestingly, AngII, when added after PMA, markedly reduced $[Ca^{2+}]_i$, suggesting a PKC-independent regulation of L-type channels by the hormone, possibly through a GTP-binding protein. This confirms our previous observation that in adrenal glomerulosa cells, AngII action involves stimulatory as well as inhibitory pathways (13, 32, 34).

In conclusion, the demonstration that various Ca^{2+} channels may play distinct roles in the glomerulosa cell stresses the need for the development of more specific drugs to efficiently and selectively control individual channel functions. This approach should be particularly relevant in the treatment of hypertension, because the drugs classically used for preventing vasoconstriction, such as L-type channel-specific dihydropyridine antagonists, appear to potentiate, rather than inhibit, mineralocorticoid secretion.

Acknowledgments

We are grateful to Mrs. L. Bockhorn, G. Dorenter, W. Dimeck, and M. Lopez for their excellent technical assistance.

References

- Barrett PQ, Bollag WB, Isales CM, McCarthy RT, Rasmussen H 1989 Role of calcium in angiotensin II-mediated aldosterone secretion. *Endocr Rev* 10:496-518
- Spät A, Enyedi P, Hajnoczky G, Hunyady L 1991 Generation and role of calcium signal in adrenal glomerulosa cells. *Exp Physiol* 76:859-885
- Capponi AM, Python CP, Rossier MF 1994 Molecular basis of angiotensin II action on mineralocorticoid synthesis. *Endocrine* 2:579-586
- Fakunding JL, Chow R, Catt KJ 1979 The role of calcium in the stimulation of aldosterone production by adrenocorticotropin, angiotensin II, and potassium in isolated glomerulosa cells. *Endocrinology* 105:327-333
- Rossier MF, Krause K-H, Lew PD, Capponi AM, Vallotton MB 1987 Control of cytosolic free calcium by intracellular organelles in bovine adrenal glomerulosa cells: effects of sodium and inositol 1,4,5-trisphosphate. *J Biol Chem* 262:4053-4058
- Rossier MF, Capponi AM, Vallotton MB 1988 Inositol trisphosphate isomers in angiotensin II-stimulated adrenal glomerulosa cells. *Mol Cell Endocrinol* 57:163-168
- Balla T, Baukal AJ, Guillemette G, Morgan RO, Catt KJ 1986 Angiotensin-stimulated production of inositol trisphosphate isomers and rapid metabolism through inositol 4-monophosphate in adrenal glomerulosa cells. *Proc Natl Acad Sci USA* 83:9323-9327
- Burnay MM, Python CP, Vallotton MB, Capponi AM, Rossier MF 1994 Role of the capacitative calcium influx in the activation of steroidogenesis by angiotensin II in adrenal glomerulosa cells. *Endocrinology* 135:751-758
- Rohacs T, Bago A, Deak F, Hunyady L, Spät A 1994 Capacitative calcium influx in adrenal glomerulosa cells: possible role in angiotensin II response. *Am J Physiol* 267:C1246-C1252
- Matsunaga H, Yamashita N, Maruyama Y, Kojima I, Kurokawa K 1987 Evidence for two distinct voltage-gated calcium channel currents in bovine adrenal glomerulosa cells. *Biochem Biophys Res Commun* 149:1049-1054
- Rossier MF, Python CP, Capponi AM, Schlegel W, Kwan CY, Vallotton MB 1993 Blocking T-type calcium channels with tetrandrine inhibits steroidogenesis in bovine adrenal glomerulosa cells. *Endocrinology* 132:1035-1043
- Barrett PQ, Isales CM, Bollag WB, McCarthy RT 1991 Calcium channels and aldosterone secretion: modulation by potassium and atrial natriuretic peptide. *Am J Physiol* 261:F706-F719
- Rossier MF, Aptel HBC, Python CP, Burnay MM, Vallotton MB, Capponi AM 1995 Inhibition of low threshold calcium channels by angiotensin II in adrenal glomerulosa cells through activation of protein kinase C. *J Biol Chem* 270:15137-15142
- Rasmussen H, Isales CM, Calle R, Throckmorton D, Anderson M, Gasalla-Herraz J, McCarthy RT 1995 Diacylglycerol production, calcium influx, and protein kinase C activation in sustained cellular responses. *Endocr Rev* 16:649-681
- Barrett PQ, Ertel EA, Smith MM, Nee JJ, Cohen CJ 1995 Voltage-gated calcium currents have two opposing effects on the secretion of aldosterone. *Am J Physiol* 268:C985-C992
- Balla T, Varnai P, Hollo Z, Spät A 1990 Effects of high potassium concentration and dihydropyridine calcium channel agonists on cytoplasmic calcium and aldosterone production in rat adrenal glomerulosa cells. *Endocrinology* 127:815-822
- Horn R, Marty A 1988 Muscarinic activation of ionic current measured by a new whole cell recording method. *J Gen Physiol* 92:145-159
- Rae J, Cooper K, Gates P, Watsky M 1991 Low access resistance perforated patch recordings using amphotericin B. *J Neurosci Methods* 37:15-26
- Suzuki S, Kawakami K, Nishimura S, Watanabe Y, Yagi K, Seino M, Miyamoto K 1992 Zonisamide blocks T-type calcium channel in cultured neurons of rat cerebral cortex. *Epilepsy Res* 12:21-27
- Capponi AM, Rossier MF, Davies E, Vallotton MB 1988 Calcium stimulates steroidogenesis in permeabilized bovine adrenal cortical cells. *J Biol Chem* 263:16113-16117
- Rizzuto R, Simpson AWM, Brini M, Pozzan T 1992 Rapid changes of mitochondrial calcium revealed by specifically targeted recombinant aequorin. *Nature* 358:325-327
- Rizzuto R, Brini M, Murgia M, Pozzan T 1993 Microdomains with high calcium close to inositol trisphosphate-sensitive channels that are sensed by neighboring mitochondria. *Science* 262:744-747
- McCormack JG, Daniel RL, Osbaldeston NJ, Rutter GA, Denton RM 1992 Mitochondrial calcium transport and the role of matrix calcium in mammalian tissues. *Biochem Soc Trans* 20:153-159
- Python CP, Laban OP, Rossier MF, Vallotton MB, Capponi AM 1995 The site of action of calcium in the activation of steroidogenesis: studies in calcium-clamped bovine adrenal zona glomerulosa cells. *Biochem J* 305:569-576
- Fitzpatrick SC, McKenna TJ 1992 Evidence for a tonic inhibitory role of nifedipine-sensitive calcium channels in aldosterone biosynthesis. *J Steroid Biochem Mol Biol* 42:575-580
- Wu L, Wang R, Karpinski E, Pang PKT 1992 Bay K-8644 in different solvents acts as a transient calcium channel antagonist and a long-lasting calcium channel agonist. *J Pharmacol Exp Ther* 260:966-974
- Richard S, Diochot S, Nargeot J, Baldy-Moulinier M, Valmier J 1991 Inhibition of T-type calcium currents by dihydropyridines in mouse embryonic dorsal root ganglion neurons. *Neurosci Lett* 132:229-234
- Dunlap K, Luebke JI, Turner TJ 1995 Exocytotic calcium channels in mammalian central neurons. *Trends Neurosci* 18:89-98
- Sheng Z-H, Rettig J, Cook T, Catterall WA 1996 Calcium-dependent interaction of N-type calcium channels with the synaptic core complex. *Nature* 379:451-454
- Bezprozvanny I, Scheller RH, Tsien RW 1995 Functional impact of syntaxin on gating of N-type and Q-type calcium channels. *Nature* 378:623-626
- Allbritton NL, Meyer T, Stryer L 1992 Range of messenger action of calcium ion and inositol 1,4,5-trisphosphate. *Science* 258:1812-1815
- Capponi AM, Johnson EIM, Rossier MF, Lang U, Vallotton MB 1989 The calcium messenger system in angiotensin II-induced aldosterone production. In: Mantero F, Takeda R, Scoggins BA, Biglieri EG, Funder JW (ed) *The Adrenal and Hypertension: From Cloning to Clinic*. Raven Press, New York, vol 57:45-52
- Varnai P, Osipenko ON, Vizi ES, Spät A 1995 Activation of calcium current in voltage-clamped rat glomerulosa cells by potassium ions. *J Physiol* 483:67-78
- Aptel HB, Johnson EIM, Vallotton MB, Rossier MF, Capponi AM 1996 Demonstration of an angiotensin II-induced negative feedback effect on aldosterone synthesis in isolated rat adrenal zona glomerulosa cells. *Mol Cell Endocrinol* 119:105-111

Activation of mouse sperm T-type Ca^{2+} channels by adhesion to the egg zona pellucida

CHRISTOPHE ARNOULT*, RICHARD A. CARDULLO†, JOSE R. LEMOS‡, AND HARVEY M. FLORMAN*§

*Department of Anatomy and Cellular Biology, Tufts University School of Medicine, 136 Harrison Avenue, Boston, MA 02111; †Department of Biology, University of California, Riverside, CA 92521; and ‡Neurobiology Group, Worcester Foundation for Biomedical Research, Shrewsbury, MA 01545

Communicated by George E. Seidel, Jr., Colorado State University, Fort Collins, CO, August 30, 1996 (received for review July 17, 1996)

ABSTRACT The sperm acrosome reaction is a Ca^{2+} -dependent exocytotic event that is triggered by adhesion to the mammalian egg's zona pellucida. Previous studies using ion-selective fluorescent probes suggested a role of voltage-sensitive Ca^{2+} channels in acrosome reactions. Here, whole-cell patch clamp techniques are used to demonstrate the expression of functional T-type Ca^{2+} channels during mouse spermatogenesis. The germ cell T current is inhibited by antagonists of T-type channels (pimozide and amiloride) as well as by antagonists whose major site of action is the somatic cell L-type Ca^{2+} channel (1,4-dihydropyridines, arylalkylamines, benzothiazapines), as has also been reported for certain somatic cell T currents. In sperm, inhibition of T channels during gamete interaction inhibits zona pellucida-dependent Ca^{2+} elevations, as demonstrated by ion-selective fluorescent probes, and also inhibits acrosome reactions. These studies directly link sperm T-type Ca^{2+} channels to fertilization. In addition, the kinetics of channel inhibition by 1,4-dihydropyridines suggests a mechanism for the reported contraceptive effects of those compounds in human males.

The acrosome reaction, a Ca^{2+} -dependent exocytotic event in sperm, is an obligatory early step in the fertilization process that must be completed prior to fusion with eggs. In mammals, it is triggered by contact with the egg's extracellular matrix, or zona pellucida. The signal-transducing mechanisms that couple gamete adhesion to acrosome reactions play a central role in fertilization and also provide possible targets for contraceptive intervention (1).

Particular attention has focused on the control of sperm internal Ca^{2+} (Ca_i^{2+}) during fertilization. Zona pellucida adhesion elevates sperm Ca_i^{2+} , as reported by ion-selective fluorescent probes, yet the Ca^{2+} entry pathways have not been identified directly. In this regard, mammalian sperm have voltage-sensitive Ca^{2+} channels (2–4), and antagonists that act primarily at L-type Ca^{2+} channels inhibit both the zona pellucida-dependent Ca_i^{2+} elevation and the initiation of acrosome reactions (3, 5). Moreover, one class of L-type channel antagonists, the 1,4-dihydropyridines, have been reported to act as a human male contraceptive (6, 7). These observations suggest a role for a putative L-type channel of sperm during gamete interaction. Yet several features of the sperm Ca_i^{2+} regulatory pathway are inconsistent with the presence of L-type channels. (i) The selectivity of divalent metal cation block ($\text{Ni}^{2+} > \text{Cd}^{2+}$) is the reverse of that anticipated at L channels. (ii) Bay K8644, an agonist of somatic cell L-type channels, fails to affect sperm Ca^{2+} channel function or to bind to sperm membranes. (iii) The sperm pathway is inhibited by L channel antagonists, including arylalkylamines, benzothiazapines, and 1,4-dihydropyridines, but at 10- to 100-fold higher concentrations than typically observed at somatic cell L chan-

nels (see discussion in refs. 3 and 5). The nature of the zona pellucida-activated Ca^{2+} entry pathway is thus unresolved.

Here, we apply patch clamp methods to assess directly the expression of functional Ca^{2+} channels during spermatogenesis. The role of specific channels in fertilization is determined by using Ca^{2+} -selective fluorescent probes. These studies indicate that a T-type Ca^{2+} channel is present on male germ cells and can account for both the zona pellucida-induced Ca^{2+} influx during acrosome reactions and the reported antifertility effects of 1,4-dihydropyridines.

MATERIALS AND METHODS

Biological Preparations. Spermatogenic cells and sperm were obtained from CD-1 mice by manual trituration of testicular slices (8) and from caudae epididymides, respectively. Methods for sperm capacitation in a Hepes-buffered medium, for sperm–zona pellucida adhesion assays, and for determination of acrosome reactions by Coomassie blue staining have been described (3, 9–12). The fraction of motile sperm was determined by visual examination. Zonae pellucidae were isolated by manual dissection from germinal vesicle-intact, follicular oocytes. Soluble extracts were prepared in 5 mM NaH_2PO_4 (pH 2.5) and adjusted to pH 7.4 prior to use (13).

Electrophysiological Methods. Spermatogenic cells were immobilized on culture dishes coated with Cell-Tak (Collaborative Biomedical Products, Bedford, MA) and perfused with a bath solution containing (mM): NaCl (100), KCl (5), CaCl_2 (10), MgCl_2 (1), $\text{N}(\text{C}_2\text{H}_5)_4\text{Cl}$ (26), sodium lactate (6), Hepes (10, pH 7.4 with NaOH), and D-glucose (3.3).

Hard glass (Gardner #7052; 2–10 M Ω pipette resistance), Sylgard-coated pipettes were used to voltage clamp spermatogenic cells in the whole-cell configuration of the patch clamp method, as described by Hamill *et al.* (14). The pipette internal solution contained (mM): cesium glutamate (120), MgCl_2 (5), $\text{N}(\text{C}_2\text{H}_5)_4\text{Cl}$ (20), Mg_2ATP (3), CsEGTA (10), Hepes (10, pH 7.0 with CsOH), and D-glucose (5). Ca^{2+} currents were recorded using an Axopatch 1-D amplifier (Axon Instruments, Foster City, CA). Data were sampled at 10 kHz, filtered at 3 kHz, corrected for leakage and capacitance currents, and analyzed with BIOPATCH (Biologic, Grenoble, France).

High-resistance seals form readily on spermatogenic cells but are difficult to establish on sperm. Cell geometry is important, as seals can be formed on sperm with flattened, spatulate-shaped heads (bovine, ovine) more frequently than on sperm with crescent-shaped heads (mouse, hamster, guinea pig). In addition, the mouse sperm plasma membrane is relatively noncompliant, possibly due to interactions with the cytoskeleton, and fractures during attempts to form high-resistance seals. As a result, patch clamp techniques were applied only to spermatogenic cells and not to sperm.

Ca²⁺ Determinations. Sperm were incubated 0.25 hr with fura 2-AM (the acetoxymethyl ester) (1–3 μ M; Molecular Probes) and immobilized on Cell-Tak-coated glass coverslips. Extracellular fura 2 and fura 2-AM were removed by perfusion, cells were placed on a heated microscope stage, and fluorescent images were acquired, stored, and analyzed, as described previously (5, 15, 16). Data are expressed as the relative Ca²⁺ concentration and related to the internal ion concentration, [Ca²⁺]_i, by the relationship

$$Ca_i^{2+} = [Ca^{2+}]_i / K_d = [(R_{max} - R) / (R - R_{min})] \times B,$$

where R , R_{min} , and R_{max} are the emission ratios after sequential excitation at 340 and 380 nm in samples and in Ca²⁺-depleted and Ca²⁺-saturated solutions, respectively; B is a sensitivity factor; and K_d is the affinity of Ca²⁺-fura 2 complexes (17). Average cellular Ca²⁺ is derived by integration of local values. Rates ($\Delta Ca_i^{2+} / \text{min}$) are the slopes of regression lines calculated for the linear portions of Ca²⁺ time courses.

RESULTS

Ca²⁺ Channel Characterization. Whole-cell patch recordings of diploid (pachytene spermatocytes) and haploid (round and condensing spermatids) stages of the male mouse germ lineage reveal an inward Ca²⁺ current ($4.85 \pm 1.03 \mu\text{A}/\text{cm}^2$, $n = 57$) with an activation threshold at -60 mV and a peak current at -30 mV (Fig. 1A and B), similar to that reported in rat spermatogenic cells (8).

The mouse germ cell Ca²⁺ current has the anticipated characteristics of somatic cell T-type channels. (i) The current activates at low depolarizations with a threshold that is typical for only the T-type channel and inconsistent with the presence of high-voltage-activated channels such as the L-, N-, or P/Q-type channels (Fig. 1B). (ii) The voltage range for inactivation is also characteristic of T-type channels (Fig. 1C; refs. 18–20). (iii) Current is inhibited by amiloride ($IC_{50} \approx 245 \mu\text{M}$; Fig. 1D) and by pimozide ($IC_{50} \approx 0.47 \mu\text{M}$; Fig. 2A), antagonists of somatic cell T channels (20, 21). In contrast, spermatogenic cell Ca²⁺ currents are not affected by ethosuximide

(data not shown), an anticonvulsant that blocks only a restricted population of T channels (20, 22). (iv) The relative potency of metal cation inhibition of this current is Ni^{2+} ($IC_{50} \approx 34 \mu\text{M}$; Fig. 1E) $>$ Cd^{2+} ($IC_{50} \approx 285 \mu\text{M}$; data not shown), similar to that observed at somatic cell T-type channels and the reverse of that found for L-type channels. (v) Inward current in spermatogenic cells is not enhanced when Ba²⁺ replaces Ca²⁺ as the charge carrier ($I_{Ca} \approx I_{Ba}$). The biophysical and pharmacological properties of the spermatogenic cell Ca²⁺ current indicate that it is mediated by a T-type channel.

Any channels that are required by sperm must be synthesized during spermatogenesis, since sperm are transcriptionally and translationally inactive. Previously, examination of sperm Ca²⁺ using ion-selective fluorescent probes suggested that zona pellucida contact activates a putative L-type channel (3). Yet inspection of spermatogenic cell Ca²⁺ currents does not reveal the presence of an L-type component (Fig. 1A and B). L channels produce a high-voltage-activated, slowly inactivating current that would persist after inactivation of T channels during depolarization to positive membrane potentials. We attempted to detect L currents by recording Ba²⁺ currents in the presence of an L channel agonist, Bay K8644. Even though L channels conduct Ba²⁺ at 2- to 3-fold greater rates than Ca²⁺ (18, 20), we found no evidence for an L channel-mediated component of spermatogenic cell Ca²⁺ currents (data not shown).

Effects of L Channel Antagonists on Germ Cell T Channels. The dual observations that L channel antagonists inhibit the zona pellucida-dependent elevation of sperm Ca²⁺ (3, 5, 23) and that germ cells lack a detectable L current led us to examine the effects of these antagonists on the T current. The spermatogenic cell T channel is inhibited by several classes of L channel antagonists. PN200-110, the high-affinity, 1,4-dihydropyridine antagonist of somatic L channels (24), blocks approximately 50% of the spermatogenic cell T current ($IC_{50} \approx 39 \text{ nM}$; Fig. 2B). Inhibition is due to reduced peak Ca²⁺ current, without obvious effects on either activation or inactivation kinetics (Fig. 2C *Inset*). The effects of PN200-110 are not readily reversible, with no detectable recovery during

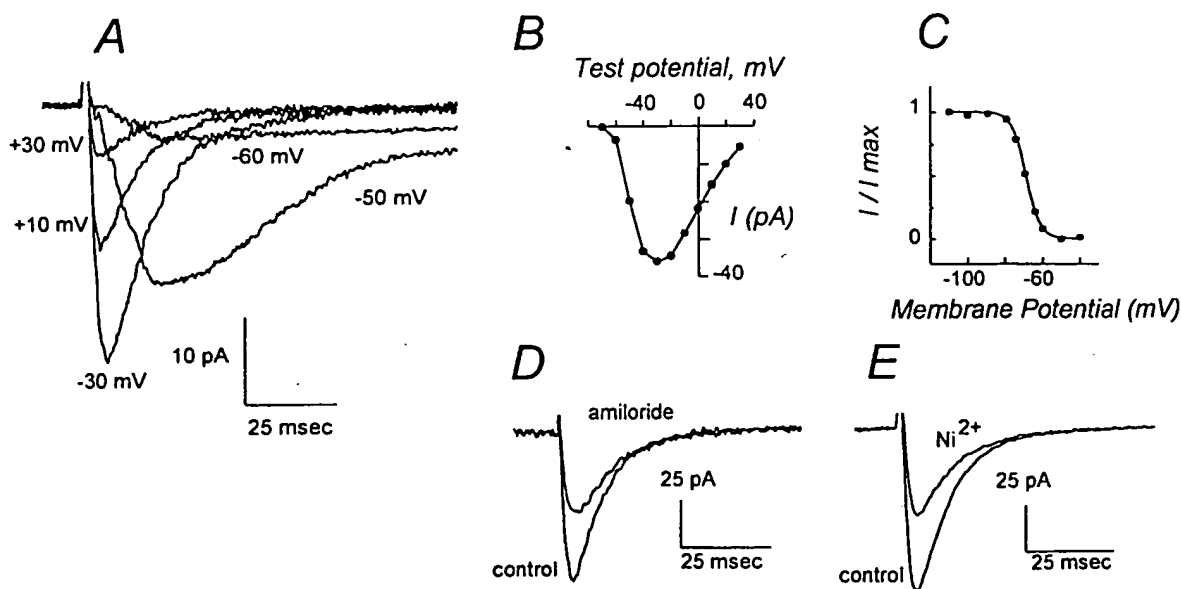


FIG. 1. Ca²⁺ currents of mouse spermatogenic cells are mediated by low-voltage-activated T channels. (A) Montage of whole-cell Ca²⁺ current traces after depolarizations of a round spermatid to the indicated membrane potentials from a holding potential of -90 mV. A slowly inactivating component of I_{Ca} after depolarization to positive potentials, diagnostic of L currents, is not apparent. (B) Current-voltage relationship for peak current amplitude elicited by depolarizations from a holding potential of -90 mV. (C) Voltage dependence of steady-state inactivation of round spermatid Ca²⁺ current. (D) Inhibition of peak Ca²⁺ current amplitude by amiloride. Traces show current elicited by depolarizations from -80 mV to -20 mV in a cell prior to (control) and after addition of $200 \mu\text{M}$ amiloride. (E) Inhibition of peak Ca²⁺ current amplitude by Ni^{2+} . Traces show current elicited by depolarizations from -80 mV to -20 mV in a cell prior to (control) and following addition of $50 \mu\text{M}$ Ni^{2+} . Current scales are indicated and differ between panels A, D, and E.

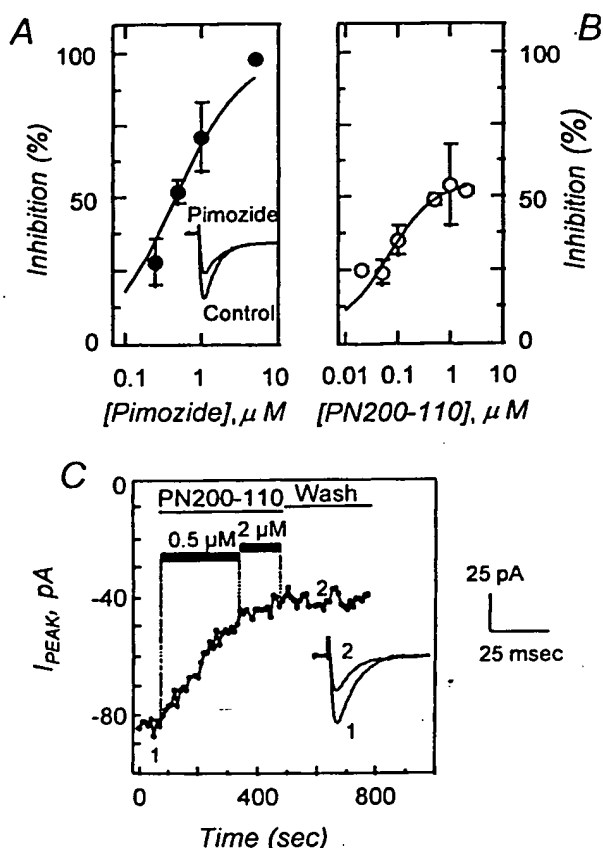


FIG. 2. Low-voltage-activated Ca²⁺ currents are inhibited by pimozone and by PN200-110. (A) Dose-response relationship showing the effects of pimozone (●) on the peak Ca²⁺ current density after depolarization to -20 mV from a holding potential of -80 mV. Data represent the mean (±SEM) response of five to eight cells and was fit to the relationship $D/D_{max} = (V/[C]) / (K_i + [C])$, where D/D_{max} is the proportion of current density remaining after pimozone treatment, $[C]$ is pimozone concentration, V is the maximum inhibition, and K_i is the inhibitory constant. In this data set V and K_i were determined to be 100% and 467 nM, respectively. (Inset) Comparison of control Ca²⁺ current and currents after treatment with 1 μM pimozone. (B) Dose-response relationship showing the effects of PN200-110 (○) on the peak Ca²⁺ current density, determined under conditions similar to those in A, with derived values of $V = 53\%$ and $K_i = 39$ nM. Data are obtained from one to six cells. (C) Peak Ca²⁺ current during repetitive depolarizations to -20 mV from a holding potential of -80 mV. Depolarizations (100 msec) were provided at a frequency of 0.2 Hz. Control currents were recorded, PN200-110 was introduced by perfusion (0.5 and 2 μM; solid bars), and peak currents were recorded for several minutes. Recovery was followed for 5 min after removal of PN200-110. Representative Ca²⁺ current traces are illustrated before (point 1) and after (point 2) PN200-110 treatment. Scale bars for current traces are shown on the right.

5-min wash periods (Fig. 2C). The spermatogenic cell T current is also inhibited by certain other L channel antagonists, including another 1,4-dihydropyridine (nifedipine), a benzothiazapine (diltiazem), and an arylalkylamine (verapamil; not shown). The inhibition of spermatogenic T-type channels by verapamil is reversible (50% recovery in ≈30 sec), unlike the effects of PN200-110. Certain other L channel ligands, such as Bay K8644, do not affect spermatogenic T channels (not shown). Thus, the spermatogenic cell T channel is similar to somatic cell T channels in its sensitivity to inhibition by some Ca²⁺ entry blockers that are generally believed to act as L channel antagonists, including the 1,4-dihydropyridines (25–27).

T Channel Activation During Sperm-Egg Interaction. The ability of antagonists that principally act at somatic cell L channels to inhibit the spermatogenic cell T channel, coupled

with the absence of detectable L channels in the germ cell lineage, suggests that the inhibitory effects of these agents on zona pellucida-dependent responses in sperm (3, 5, 23) may be mediated by T channels. This hypothesis was tested by examining the effects of specific T channel antagonists on sperm-egg interaction.

Zona pellucida glycoproteins promote sustained elevations of mouse sperm Ca²⁺ (Fig. 3A; ref. 27), as was also observed in bovine sperm (4, 5, 15). This response is inhibited by the same concentrations of pimozone and of amiloride (Fig. 3) that suppress spermatogenic cell T currents (Figs. 1D and 2A). The Ca²⁺ response is also inhibited by Ni²⁺ (44% ± 7% inhibition at 50 μM; $n = 3$) and by Cd²⁺ (59 ± 4% inhibition at 250 μM; $n = 3$) with potencies that correspond to the effects of these cations on the spermatogenic cell T current. These results suggest that the zona pellucida-induced Ca²⁺ elevation in mouse sperm is mediated by T channels.

The effects of T channel antagonists on the acrosome reaction were determined by examining sperm during adhesion to intact zonae pellucidae. Mouse sperm bind to the zona pellucida in the absence of inhibitors, and >80% complete the acrosome reaction (Fig. 4A and B), as described previously (28–30). Pimozone (1 μM) and amiloride (0.5 mM) had no apparent effect on sperm motility, on spontaneous rates of acrosome reaction, or on sperm-zona pellucida adhesion, but they greatly inhibited induction of acrosome reactions by zona pellucidae after sperm adhesion (Fig. 4A and C).

T channel antagonists also inhibit the acrosome reaction that is promoted by soluble extracts of zonae pellucidae. Incubation with zona pellucida glycoproteins for 20 min increased the fraction of acrosome reacted sperm from 19% ± 5% to 62% ± 6% ($n = 3$; >200 sperm assayed per sample), as reported previously (28, 29). This is a specific effect of the zona pellucida, and only 23% ± 8% of sperm were acrosome reacted after incubation with control glycoproteins (50 μg/ml transferrin or fetuin). As shown in Table 1, pimozone and amiloride

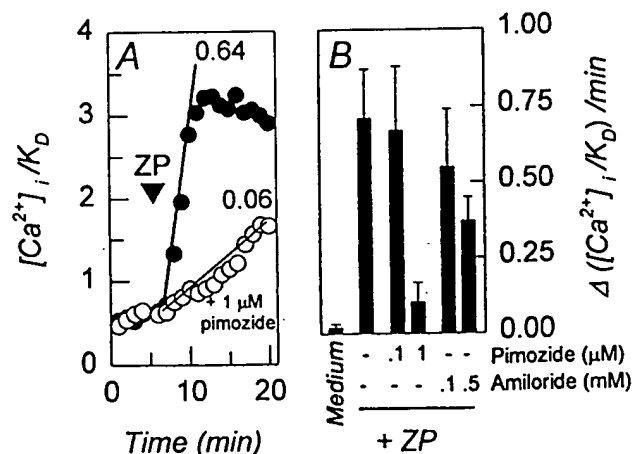


FIG. 3. T channel antagonists inhibit the zona pellucida-dependent increase in Ca²⁺. [Ca²⁺]_i/K_d values were determined from fluorescent emission of intracellular fura 2. (A) The effects of zona pellucida glycoproteins on [Ca²⁺]_i/K_d in representative sperm that were incubated in control medium (○) or in medium containing 1 μM pimozone (10-min preincubation; ●). Solubilized zona pellucida glycoproteins were added (ZP, ▽; 50 μg/ml) and rates were determined by regression analysis of the linear portions of the response time courses. Slopes of regression lines are indicated. (B) Rates of [Ca²⁺]_i/K_d responses obtained from experiments similar to that shown in A. Capacitated sperm were incubated for 10 min with indicated concentrations of pimozone or amiloride and then treated with solubilized zona pellucida glycoproteins (50 μg/ml). Control populations were treated with culture medium throughout. Data were obtained from four to six separate experiments, with 7–22 sperm observed per experiment. Average response rates were determined for each experiment and used to determine the indicated mean values (±SEM).

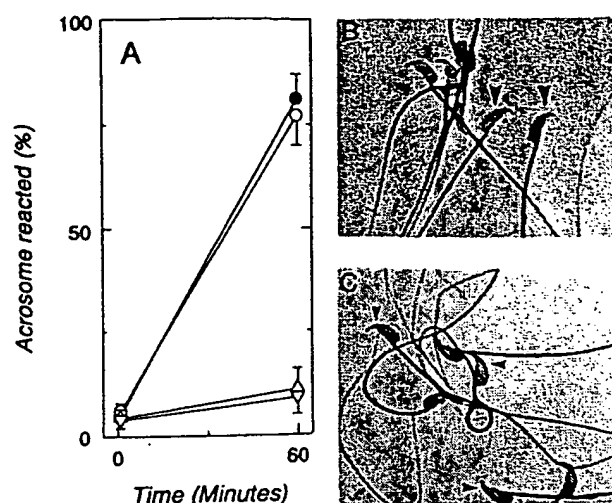


FIG. 4. Effects of T channel antagonists on sperm acrosome reactions. (A) Occurrence (%) of acrosome reactions following sperm adhesion to zonae pellucidae for 1 and 60 min in control medium (●) or in medium supplemented with D-glucose (1 mM; ○), amiloride (500 μ M; Δ), or pimoizide (0.5 μ M; ▽). Data represent the mean (\pm SEM) of four experiments using 72–135 zonae pellucidae for each experimental condition and with 29–34 sperm bound per zona pellucida in all treatments. (B) Sperm bound to zona pellucida in control medium for 60 min. ($\times 1000$; zona pellucida staining subtracted.) Most sperm are acrosome reacted and do not exhibit dark staining in the apical head (large arrowheads). (C) Sperm bound to zona pellucida for 60 min in the presence of 0.5 μ M pimoizide. Most sperm fail to acrosome react, as indicated by a stained region in the apical head (small arrowheads).

inhibit the zona pellucida-dependent acrosome reaction in a concentration-dependent fashion. Treatment with 1 μ M pimoizide or with 0.5 mM amiloride inhibited the secretory response to zonae pellucidae by 77% and by 72%, respectively, but had no significant effects on the incidence of acrosome reactions in populations treated with control glycoproteins. Yet sperm treated with T channel antagonists retain the ability to undergo acrosome reactions after addition of A23187 (5 μ M; 20 min). This Ca^{2+} -transporting ionophore induced acrosome reactions in $68\% \pm 7\%$ and in $74\% \pm 9\%$ of cells treated with

Table 1. Effects of T channel antagonists on the zona pellucida-induced acrosome reaction

Treatment	Conc.	Acrosome reacted, %	
		+ Control	+ ZP
Medium	—	23 \pm 8	62 \pm 6*
Pimoizide	0.1 μ M	21 \pm 3	49 \pm 5*
	1.0 μ M	18 \pm 6	27 \pm 4†
Amiloride	0.1 mM	17 \pm 4	54 \pm 7*
	0.5 mM	22 \pm 3	33 \pm 4*†

Capacitated mouse sperm were incubated for 10 min in culture medium or in medium supplemented with the indicated T channel antagonists. The fraction of acrosome reacted sperm in culture medium-treated populations was $19\% \pm 5\%$, and this background value was not altered significantly by treatment with T channel antagonists (range of means for pimoizide and amiloride, 16–20%). Sperm were incubated an additional 20 min after addition of control glycoproteins (+Control, 50 μ g/ml transferrin or fetuin) or soluble extracts of zonae pellucidae (+ZP, 50 μ g/ml) were added and acrosome reactions were assessed. The results are given as the mean (\pm SEM) of triplicate experiments, with triplicate samples obtained in each experiment and with 100–200 sperm assayed per sample.

*Sperm treated with zonae pellucidae differ from sperm treated with control glycoproteins ($P < 0.01$).

†Sperm treated with T channel antagonists differ from culture medium controls ($P < 0.01$).

pimoizide and amiloride. A similar response was observed in control populations that had not been treated with T channel antagonists ($77\% \pm 4\%$ acrosome reacted; duplicate experiments, > 250 assayed per treatment). These control experiments demonstrate that drug treatment does not alter the ability of sperm to acrosome react after Ca_i^{2+} elevations and are consistent with the suggestion that these agents act by inhibiting a zona pellucida-induced Ca^{2+} influx.

DISCUSSION

The results of this study strongly suggest that only T-type Ca^{2+} channels are present in mouse sperm and are activated by the zona pellucida during fertilization. Previously, we demonstrated a role for sperm voltage-sensitive Ca^{2+} channels in the initiation of acrosome reaction (3, 5). In somatic cells there is a large family of voltage-sensitive Ca^{2+} channels, including the high-voltage-activated L-, N-, and P/Q-types of channels as well as the R- and T-type channels that are activated by smaller depolarizations (30–32). However, the subtype of Ca^{2+} channel that is present in sperm and activated by the zona pellucida had not previously been determined.

The functional expression of T channels during mammalian spermatogenesis was demonstrated previously in the rat, on the basis of biophysical characteristics of a Ca^{2+} current (8). This conclusion is confirmed here by demonstrating that the major voltage-sensitive Ca^{2+} channel of mouse spermatogenic cells has the biophysical and pharmacological characteristics anticipated of a T channel. The channel can be detected in the early meiotic stage of spermatogenesis and is retained thereafter. However, it is still not certain whether T channels are active during germ cell differentiation or are stored in the membrane for a primary function during fertilization.

This study provides what is to our knowledge the first identification of a sperm Ca^{2+} channel subtype that is activated by sperm contact with the zona pellucida. Ca^{2+} channel function was examined in sperm by using ion-selective fluorescent probes. The zona pellucida-activated channel of sperm was inhibited by several distinct structural classes of Ca^{2+} entry antagonists (3, 5). A major site of action of these compounds in somatic cells is the L-type Ca^{2+} channel (30, 32). Yet other features of the sperm mechanism were inconsistent with the presence of L channels, including the low potency for inhibition by L channel antagonists, the failure of Bay K8644 to modulate sperm Ca_i^{2+} , and a selectivity for inhibition by divalent metal cations (3, 5).

Three aspects of the present study extend these earlier observations. First, the spermatogenic cell T channel accounts for all of the characteristics of zona pellucida-activated mechanism in sperm, including those that are inconsistent with the presence of an L channel. For example, similar concentrations of PN200-110 (0.039 and 0.07 μ M), Ni^{2+} (34 and 50 μ M), and Cd^{2+} (245 and 250–500 μ M) are required to inhibit T channels in spermatogenic cells and zona pellucida-activated Ca^{2+} channel function by 50% (present study; ref. 3). Given that T currents are monitored by electrophysiological methods while sperm Ca^{2+} channels are assessed by using fluorescent probes, the agreement between these effective inhibitory doses is quite close. The T current also is similar to the zona pellucida-regulated Ca^{2+} channel in that neither is modulated by Bay K8644.

Second, the zona pellucida-dependent activation of sperm Ca^{2+} channels and the initiation of acrosome reactions are inhibited by pimoizide and amiloride, antagonists that suppress somatic cell T currents (Figs. 3 and 4). These compounds also inhibit the spermatogenic cell Ca^{2+} current (Figs. 1 and 2). Pimoizide and amiloride can discriminate between T channels and other classes of voltage-sensitive Ca^{2+} channels (19–21), thereby further associating the T channel with zona pellucida-dependent responses. Although these compounds also act in

somatic cells at sites other than Ca^{2+} channels, such as the Na^+/H^+ exchange mechanism (33–35), these alternative targets do not appear to be present in mammalian sperm (16, 36). Third, we have confirmed that the T-type channel is the only voltage-sensitive Ca^{2+} channel that can be detected in mammalian spermatogenic cells (8). These observations strongly suggest that the spermatogenic cell T channel is retained by sperm after the completion of spermatogenesis and mediates the zona pellucida-dependent Ca^{2+} influx during initiation of acrosome reactions. It should be noted that the electrophysiological and pharmacological characteristics of the germ cell T channel are similar to those determined previously for these channels in somatic cells (18–21, 25–27).

T channels are present in a wide range of excitable cells, including neurons, skeletal muscle, cardiac muscle, smooth muscle, neuroendocrine cells, and endocrine cells (20, 32, 37, 38). Channel activity is typically associated with rhythmic burst activity, such as in the oscillations of thalamic reticular neurons (27) or in cardiac muscle, where T channels contribute to pacemaker current (26, 39). These channels also enhance synaptic transmission and lower threshold processes (27, 30). In contrast, T channels are not generally believed to participate in exocytosis, although some indirect evidence supports an undefined role in certain somatic cell secretory systems (refs. 40 and 41, but also see ref. 42). In this regard, the present study demonstrates that sperm T channel function is essential for acrosomal exocytosis.

The specific role of T channel-mediated Ca^{2+} influx in zona pellucida-dependent signal transduction has not been determined. Zona pellucida signals produce sustained elevations of sperm Ca_i^{2+} that are required for the acrosome reaction (4, 5, 15, 43). In contrast, T-type channels mediate small, transient Ca^{2+} fluxes as a consequence of their rapid inactivation (Fig. 1; refs. 18–20). While the Ca^{2+} buffering and efflux mechanisms of sperm are not well understood (44, 45), it is unlikely that such processes could permit T channels to produce sustained Ca_i^{2+} responses. Alternatively, a transient Ca^{2+} influx through zona pellucida-activated T channels may activate Ca^{2+} -dependent Ca_i^{2+} elevation. In this regard, recent studies show that mammalian sperm contain sequestered Ca^{2+} pools, and thapsigargin-induced emptying of these pools results in acrosome reactions (46, 47). Moreover, *inositol trisphosphate* (IP3) receptors are present in acrosomal membranes, and Ca^{2+} efflux from internal pools of permeabilized sperm occurs through an IP3-sensitive pathway (47). Conductance through the IP3 receptor/ Ca^{2+} release pathway is positively modulated by Ca_i^{2+} (48) and provides a likely amplification mechanism for Ca^{2+} entering sperm through any pathway, including through zona pellucida-activated T-type channels.

In this model T channels would generate a triggering pulse of Ca^{2+} that is necessary for sustained Ca_i^{2+} elevations and for acrosome reactions. Other zona pellucida-dependent responses, such as a transient elevation of internal pH (4, 15) and the production of IP3 (49), can act in concert with T currents to regulate Ca^{2+} release from acrosomal stores, although Ca^{2+} influx through T channels is essential for this mechanism (Figs. 3 and 4). This complex regulatory system is consistent with previous observations that sperm membrane potential and internal pH act synergistically to promote sustained elevations of Ca_i^{2+} (2–4, 15). This mechanism permits stringent control of exocytosis in sperm, which have a single secretory vesicle and must strictly coordinate exocytosis with egg contact (1).

These results may also account for the reported contraceptive action of 1,4-dihydropyridines in human males (6, 7). The principal somatic cell target of the 1,4-dihydropyridines is the L-type voltage-sensitive Ca^{2+} channel, where these drugs act as reversible antagonists and produce an antihypertensive effect. Therapeutic doses of 1,4-dihydropyridines maintained in males should not inhibit sperm Ca^{2+} channel function

during fertilization if the drug target were acting at an L channel, since the several hours required in the female reproductive tract for sperm capacitation and transport to the site of fertilization (1) will permit dissociation of bound drug from sperm receptors. The observation that 1,4-dihydropyridines are potent and poorly reversible inhibitors of T channels in male germ cells (Fig. 2) provides a new mechanism of contraceptive action. In contrast, arylalkylamine and benzothiazapine compounds inhibit spermatogenic T currents reversibly and provide strategies for dissecting antihypertensive and contraceptive effects.

Note Added in Proof. While this manuscript was in review, we became aware of the recent study of Lievano *et al.* (50), in which they report the presence of a 1,4-dihydropyridine-sensitive T-type Ca^{2+} channel on mouse spermatogenic cells.

We give special thanks to Qin Chen, Michelle Gonzales, Eric Reese, and Esther Valdez for technical assistance and to Vince Coccia for help with illustrations. Our work was supported by grants from the Philippe Foundation, the Bushrod H. Campbell and Adah F. Hall Charity Fund (C.A.), the Whitaker Foundation (R.A.C.), and the National Institutes of Health (R.A.C., HD27244; H.M.F., HD32177).

1. Yanagimachi, R. (1994) in *The Physiology of Reproduction*, eds. Knobil, E. & Neill, J. D. (Raven, New York), pp. 189–317.
2. Babcock, D. F. & Pfeiffer, D. R. (1987) *J. Biol. Chem.* **262**, 15041–15047.
3. Florman, H. M., Corron, M. E., Kim, T. D.-H. & Babcock, D. F. (1992) *Dev. Biol.* **152**, 304–314.
4. Arnoult, C., Zeng, Y. & Florman, H. M. (1996) *J. Cell Biol.* **134**, 637–645.
5. Florman, H. M. (1994) *Dev. Biol.* **165**, 152–164.
6. Benoff, S., Cooper, G. W., Hurley, I., Mandel, F. S., Rosenfeld, D. L., Scholl, G. M., Gilbert, B. P. & Hershlag, A. (1994) *Fertil. Steril.* **62**, 606–617.
7. Hershlag, A., Cooper, G. W. & Benoff, S. (1995) *Hum. Reprod.* **10**, 599–606.
8. Hagiwara, S. & Kawa, K. (1984) *J. Physiol. (London)* **356**, 135–149.
9. Florman, H. M., Bechtol, K. B. & Wassarman, P. M. (1984) *Dev. Biol.* **106**, 243–255.
10. Florman, H. M. & Wassarman, P. M. (1985) *Cell* **41**, 313–324.
11. Moller, C. C., Bleil, J. D., Kinloch, R. A. & Wassarman, P. M. (1990) *Dev. Biol.* **137**, 276–286.
12. Thaler, C. D. & Cardullo, R. A. (1995) *Biochemistry* **34**, 7788–7795.
13. Bleil, J. D. & Wassarman, P. M. (1980) *Dev. Biol.* **76**, 185–202.
14. Hamill, O. P., Marty, A., Neher, E., Sakmann, B. & Sigworth, F. J. (1981) *Pflügers Arch.* **391**, 85–100.
15. Florman, H. M., Tombes, R. M., First, N. L. & Babcock, D. F. (1989) *Dev. Biol.* **135**, 133–146.
16. Zeng, Y., Oberdorf, J. A. & Florman, H. M. (1996) *Dev. Biol.* **173**, 510–520.
17. Gryniewicz, G., Poenie, M. & Tsien, R. Y. (1985) *J. Biol. Chem.* **260**, 3440–3450.
18. Fox, A. P., Nowicky, M. C. & Tsien, R. W. (1987) *J. Physiol. (London)* **394**, 149–172.
19. Tsien, R. W., Lipscombe, D., Madison, D. V., Bley, K. R. & Fox, A. P. (1988) *Trends Neurosci.* **11**, 431–438.
20. Herrington, J. C. & Lingle, J. (1992) *J. Neurophysiol.* **68**, 213–232.
21. Tang, C.-M., Presser, F. & Morad, M. (1988) *Science* **240**, 213–215.
22. Coulter, D. A., Huguenard, J. R. & Prince, D. A. (1989) *Ann. Neurol.* **25**, 582–593.
23. Clark, E. N., Corron, M. E. & Florman, H. M. (1993) *J. Biol. Chem.* **268**, 5309–5316.
24. Janis, R. A., Silver, P. J. & Triggle, D. J. (1987) *Adv. Drug Res.* **116**, 309–591.
25. Akaike, N., Kostyuk, P. G. & Osipchuk, Y. V. (1989) *J. Physiol. (London)* **412**, 181–195.
26. McDonald, T. F., Pelzer, S., Trautwein, W. & Pelzer, D. J. (1994) *Physiol. Rev.* **74**, 365–507.
27. Huguenard, J. R. (1996) *Annu. Rev. Physiol.* **58**, 329–348.
28. Florman, H. M. & Storey, B. T. (1982) *Dev. Biol.* **91**, 121–130.
29. Bleil, J. D. & Wassarman, P. M. (1983) *Dev. Biol.* **95**, 317–324.

30. Hille, B. (1992) *Ionic Channels of Excitable Membranes* (Sinauer, Sunderland, MA).
31. Clapham, D. E. (1995) *Cell* 80, 259–268.
32. Tsien, R. W., Lipscombe, D., Madison, D., Bley, K. & Fox, A. (1995) *Trends Neurosci.* 18, 52–54.
33. Kleyman, T. R. & Cragoe, E. J. (1988) *J. Membr. Biol.* 105, 1–21.
34. Enyeart, J. J., Biagi, B. A., Day, R. N., Sheu, S.-S. & Maurer, R. A. (1990) *J. Biol. Chem.* 265, 16373–16379.
35. Hamill, O. P., Lane, J. W. & McBride, D. W. (1992) *Trends Pharmacol. Sci.* 13, 373–376.
36. Babcock, D. F., Rufo, G. A. & Lardy, H. A. (1983) *Proc. Natl. Acad. Sci. USA* 80, 1327–1331.
37. Bean, B. P. (1989) *Annu. Rev. Physiol.* 51, 367–384.
38. Tsien, R. W. & Tsien, R. Y. (1990) *Annu. Rev. Cell Biol.* 6, 715–760.
39. Hagiwara, N., Irisawa, H. & Kameyama, M. (1988) *J. Physiol. (London)* 395, 233–253.
40. Enyeart, J. J., Mlinar, B. & Enyeart, J. A. (1993) *Mol. Endocrinol.* 7, 1031–1040.
41. McCarthy, R. T., Isales, C. & Rasmussen, H. (1993) *Proc. Natl. Acad. Sci. USA* 90, 3260–3264.
42. Coyne, M. D. & Pinkney, L. (1991) *Endocrinology* 129, 263–269.
43. Bailey, J. L. & Storey, B. T. (1994) *Mol. Reprod. Dev.* 39, 297–308.
44. Noland, T. D., Olson, G. E. & Garbers, D. L. (1983) *Biol. Reprod.* 29, 987–998.
45. Meizel, S. (1984) *Biol. Rev.* 59, 125–157.
46. Blackmore, P. F. (1993) *Cell Calcium* 14, 53–60.
47. Walensky, L. D. & Snyder, S. H. (1995) *J. Cell Biol.* 130, 857–869.
48. Bezprozvanny, I., Watras, J. & Ehrlich, B. E. (1991) *Nature (London)* 351, 751–754.
49. Tomes, C. N., McMaster, C. R. & Saling, P. M. (1996) *Mol. Reprod. Dev.* 43, 196–204.
50. Lievano, A., Santi, C. M., Serrano, J., Trevino, C. L., Bellve, A. R., Hernandez-Cruz, A. & Darszon, A. (1996) *FEBS Lett.* 388, 150–154.

fairness of the result we reach. As noted earlier, the court limited the initial trial in this litigation to six trade secrets. The court did not, however, select which trade secrets would be tried. Instead, it permitted plaintiff to select four of the secrets and defendant to select (from plaintiff's then current list) the remaining two. While the court urged counsel, when making their selections, to consider the possible preclusive effects of the initial trial on other aspects of this litigation, as well as the effects the first trial might have on subsequent settlement negotiations, the court imposed no limits or restraints at all on the choices made by the parties. In this setting, it would be surprising, to understate the matter, if all four of the trade secrets picked by plaintiff for the trial were at the margins of the case, as plaintiff perceived it. Rather, one would expect plaintiff to have chosen at least one or two secrets which plaintiff perceived as in some sense representative of other, related claims and as vehicles for plaintiff to make as strong a case of misappropriation as possible. In other words, it seems fair to assume that plaintiff would have chosen trade secrets whose misappropriation would have represented a serious, material breach of the relationship of trust and confidentiality that it once had with defendants Pless and Sweeney. Our confidence that this assumption is fair is increased by the fact that the four alleged trade secrets selected by plaintiff obviously are related to others on plaintiff's list.²³ The fact that plaintiff was given an unfettered opportunity to select four trade secrets for the initial trial, coupled with the apparent connection between those trade secrets and others on plaintiff's list, reduces substantially the likelihood that a breach that consisted of misappropriation of these trade secrets would have been perceived by plaintiff in early 1986 as immaterial or inconsequential, and thus reduces substantially the likelihood that applying the rule we announce today to plaintiff is unfair.

V.

PLAINTIFF'S COUNTERMOTION

Plaintiff's counter-motion, being supported only by a non-sequitur, is DENIED.

²³ See, e.g., Olson Dec. re October 16, 1991 Trade Secret Listing at ¶ 8, filed Nov. 19, 1991, where counsel for Intermedics describes some of the ways trade secrets 4, 5, 6, 7 and 39 are related. There also are language-apparent connections between alleged trade secrets 22, 23, 24, 25, 26, 27, 28, 29 and 36, as well as between numbers 30-35.

VI.

SUMMARY OF RULINGS

The court hereby ORDERS entry of SUMMARY JUDGMENT in favor of defendants PLESS and SWEENEY on *all* of the claims in the instant action that arise out of or depend on alleged misappropriation of *any* of plaintiff's alleged trade secrets or confidential information, including the causes of action that sound in misappropriation (under Texas or California law), breach of contract, breach of fiduciary duty, and civil conspiracy.

The court further ORDERS entry of SUMMARY JUDGMENT in favor of defendant VENTRITEX on *all* of the claims in the instant action that arise out of or depend on alleged misappropriation of *any* of plaintiff's alleged trade secrets or confidential information, including the causes of action that sound in misappropriation (under Texas or California law), unfair competition, inducement to misappropriate, inducement to breach contractual obligations, inducement to breach fiduciary obligations, and civil conspiracy.

IT IS SO ORDERED.

U.S. Patent and Trademark Office
Board of Patent Appeals and Interferences

Ex parte Maizel

No. 91-2301

Decided May 27, 1992

On Reconsideration October 19, 1992

Released April 23, 1993

PATENTS

1. Patentability/Validity — Specification — Enablement (§115.1105)

Reasonable correlation must exist between scope of exclusive right granted to patent applicant and scope of enablement set forth in patent application; thus, claims for recombinant human B-cell growth factor were properly rejected under 35 USC 112 on ground that claims are broader than what is enabled by specification, since claims are not limited to a DNA which encodes solely protein described by amino acid sequence set forth, but rather include such language as "biologically functional equivalent thereof," which covers any conceivable means that achieves stated biological result, while specification only discloses, at most, specific DNA sequence known to inventor.

Mec
Office
in spec
errors
be est
or not
sequen
ted de
signifi
matter
in spec

2. Patentability/Validity — Specification — In general (§115.1101)

Mechanism within Patent and Trademark Office for correcting DNA sequencing errors in specification is highly desirable, since such errors may well arise, but no general rule can be established because question of whether or not change in chemical structure of DNA sequence set forth in specification is permitted depends upon facts of each case and significance of modification to both subject matter claimed and subject matter described in specification.

3. Patentability/Validity — Anticipation — Prior art (§115.0703)

Patentability/Validity — Obviousness — Relevant prior art — In general (§115.0903.01)

Burden of proof shifts to applicant, when examiner obtains product of prior art which reasonably appears to fall within scope of that which is claimed by applicant, to provide evidence showing that such product does not fall within scope of applicants' claims.

4. Patentability/Validity — Obviousness — Relevant prior art — Particular inventions (§115.0903.03)

Examiner's rejection of claims for recombinant human B-cell growth factor as obvious in view of prior art, which examiner asserted described protein whose existence would have motivated one skilled in art to isolate protein, sequence it, construct synthetic DNA probes, utilize probes to isolate messenger RNA, synthesize cDNA, and produce additional protein, reflects "obviousness to try" approach of "armchair" chemist, and must be reversed.

5. Patentability/Validity — Specification — Written description (§115.1103)

Deposit of specific plasmid in American Type Culture Collection does not satisfy written description requirement of 35 USC 112 for either BCGF-type DNA being claimed, or protein produced thereby, since there is no evidence that those skilled in art who have such deposited material would have been aware of BCGF DNA structure and protein encoded thereby, or would have been able to accurately determine said DNA structure and protein sequence without undue experimentation.

6. Patentability/Validity — Date of invention — In general (§115.0401)

Patentability/Validity — Specification — In general (§115.1101)

"New matter" prohibition of 35 USC 112 plays important role in establishing filing

date of application as prima facie date of invention, and thus it cannot be said that no harm is done to public when badly mis-sequenced DNA is properly sequenced in specification prior to issue date of patent; patent laws do not permit insertion of additional descriptive matter subsequent to filing date in order to complete disclosure so as to conform specification's description of invention to statutory standard.

Appeal from final rejection of claims (C. Low, examiner, Elizabeth C. Weimar, supervisory patent examiner).

Application for patent filed April 27, 1987, by Abby Maizel, Surendra Sharma, and Shashikant Mehta, serial no. 043,119, which is a continuation-in-part of application serial no. 828,388, filed Feb. 11, 1986, now abandoned, which is a continuation-in-part of application serial no. 944,905, filed Jan. 5, 1987, now abandoned (recombinant human B-cell growth factor). From examiner's final rejection of claims, applicants appeal. Affirmed; request for reconsideration granted, but modification of decision denied.

David L. Parker, of Arnold, White & Durkee, Houston, Texas, for appellants.

Before Goolkasian, Kimlin, and Garris, examiners-in-chief.

Goolkasian, examiner-in-chief.

This is an appeal from the examiner's final rejection of claims 1, 3 through 8, 12, 14 and 18, which are all the claims remaining in the application.

Claim 1 is illustrative of the invention and reads as follows:

1. A recombinant DNA vector comprising a DNA sequence which encodes a protein exhibiting a molecular weight between about 8 and about 14 kilodaltons upon gel exclusion chromatography, said protein having an amino acid sequence which includes the non-B-galactosidase-derived sequence of amino acids displayed in Figure 4, or a biologically functional equivalent thereof, and having a BCGF biological activity characterized by an ability to stimulate the incorporation of thymidine into DNA of BCGF-dependent

B-cells, or an ability to stimulate the comitogenesis of anti-u activated B-cells, when said protein is cocultured in effective concentrations with said respective B-cells *in vitro*.

The references relied on by the examiner are:

Okano et al. (Okano) (Japan) 60-232091 Nov. 18, 1985

Maizel et al. (Maizel), *Proc. Natl. Acad. Sci. USA*, "Long-term growth of human B cells and their use in a microassay for B-cell growth factor," Vol. 80, August 1983, pages 5047-5051.

Beaucage et al. (Beaucage), *Tetrahedron Letters*, "Deoxynucleoside Phosphoramidites — A New Class Of Key Intermediates For Deoxypolynucleotide Synthesis," Vol. 22, No. 20, 1981, pages 1859-1862.

Freeman et al. (Freeman), *Proc. Natl. Acad. Sci. USA*, "Sequential expression of new gene programs in inducer T-cell clones," Vol. 80, July 1983, pages 4094-4098.

Clark et al. (Clark), *Proc. Natl. Acad. Sci. USA*, "Human T-cell growth factor: Partial amino acid sequence, DNA cloning and organization and expression in normal and leukemic cells," Vol. 81, April 1984, pages 2543-2547.

Mehtat et al. (Mehta), *Federation Proceedings*, "Expression Of Human B Cell Growth Factor In *Escherichia Coli*, Vol. 44, No. 4, S5123, March 5, 1985, page 1287.

Appellants' invention concerns a protein molecule or "factor" which has the ability to maintain the growth of B-cells in a culture medium. Appellants do not claim the protein as such but, rather, claim recombinant vectors¹ containing a DNA sequence which encodes the protein or an equivalent thereof and causes a recombinant cell containing said DNA sequence to produce said protein or its equivalent. Claims 1 and 3 are directed to recombinant DNA vectors containing the requisite DNA sequence. Claims 4 and 8 are directed to recombinant cells bearing the recombinant DNA vector. Claim 5 is directed to a cell which produces the desired protein but is not limited with regard to the DNA encoding the protein. Claims 12 and 14 claim the recombinant DNA sequence itself and claim 18 is directed to a method of

utilizing recombinant cells to produce the B-cell growth factor (BCGF) protein.

Appellants do not argue the separate patentability of the various independent and dependent claims. Accordingly all claims stand or fall together. *In re Nielson*, 816 F.2d 1567, 2 USPQ2d 1525 (Fed. Cir. 1987); *In re Kroekel*, 803 F.2d 705, 231 USPQ 640 (Fed. Cir. 1986).

Appellants' claims stand rejected as follows:

(a) Claims 1, 3 through 8, 12, 14 and 18 stand rejected under 35 U.S.C. § 112, first paragraph, as being directed to subject matter not described in the specification as filed. This is a "new matter" rejection.

(b) Claims 1, 4, 5, 7, 12, 14 and 18 stand rejected under 35 U.S.C. § 112, first paragraph, as being broader than the enabling disclosure.

(c) Claim 1, 3 through 8, 12, 14 and 18 stand rejected under 35 U.S.C. § 102(a) or, alternatively, under 35 U.S.C. § 103 over Okano.

(d) Claims 1, 3 through 8, 12, 14 and 18 stand rejected under 35 U.S.C. § 103 as being unpatentable over Clark or Freeman, each in view of Beaucage and Maizel.

Before considering the propriety of the examiner's rejections, it is helpful to consider the scope of appellants' claims. To do so, every limitation positively recited in a claim must be given effect in order to determine what subject matter that claim defines. *In re Wilder*, 429 F.2d 447, 166 USPQ 545 (CCPA 1970). We are mindful that during prosecution the claims are given their broadest reasonable interpretation in light of the specification. *In re Yamamoto*, 740 F.2d 1569, 1571, 222 USPQ 934, 936 (Fed. Cir. 1984).

Claim 1 herein describes a recombinant DNA vector which comprises any DNA sequence which encodes a protein characterized as (a) exhibiting a molecular weight within a defined range, (b) having an amino acid sequence² which includes the sequence of amino acids displayed in Figure 4, and (c) having BCGF biological activity as measured by two specific and alternative tests set forth in the claims. Importantly, appellants' claims are not limited to a DNA which encodes solely the protein described by the amino acid sequence set forth in Figure 4 but, rather, include language such as "or a biologically functional equivalent thereof" or "corresponds biologically to" which

¹ A vector is a carrier molecule to which a desired segment of DNA is linked. The vector serves to incorporate foreign DNA into host cells. The vector exemplified by appellants is a plasmid. Viruses may also serve as vectors.

² The protein itself is not claimed; the claims are directed to the DNA sequence which encodes the protein.

broadens the claims such that the claims encompass any recombinant DNA, vector or cell which encodes any protein having sufficient BCGF biological activity such that it may properly be considered a "biologically functional equivalent" of the protein having the amino acid sequence displayed in Figure 4.

Appellants have attempted to relate, and thereby limit, the phrase "biologically functional equivalent" to proteins having amino acid substitutions wherein the substituted acids have similar hydrophobicity and charge characteristics such that the substitutions are "conservative" and do not modify the basic functional characteristics of the BCGF protein. However, as defined in appellants' specification at page 26, lines 24 through 28, the phrase "biological functional equivalent" is so broad as to encompass any protein regardless of structure that is "functionally equivalent to BCGF in terms of biological activity." Such a protein may be a highly truncated protein comprising mainly the active site of the BCGF protein. Other cells or DNA's encoding proteins having dissimilar structural configurations but similar biological functionality would fall within the scope of appellants' claims. Appellants' Brief, pages 18 through 20, describes several proteins including TCGF which exhibit B cell activity quite similar to the BCGF activity exhibited by the presently claimed factor. Such materials would reasonably be considered to fall within the scope of appellants' "biologically functional equivalent" language.

[1] We consider first the rejection of claims 1, 4, 5, 7, 12, 14 and 18 under 35 U.S.C. § 112 on the ground that the claims are far broader than what is enabled by appellants' specification. We affirm the rejection. Appellants have not chosen to claim the DNA by what it is but, rather, by what it does, i.e., encoding either a protein exhibiting certain characteristics, or a biologically functional equivalent thereof. Appellants' claims might be analogized to a single means claim of the type disparaged by the Court of Customs and Patent Appeals in *In re Hyatt*, 708 F.2d 712, 218 USPQ 195 (Fed. Cir. 1983). The problem with the phrase "biologically functional equivalent thereof" is that it covers any conceivable means, i.e., cell or DNA, which achieves the stated biological result while the specification discloses, at most, only a specific DNA segment known to the inventor.³ Clearly the disclosure is not

commensurate in scope with the claims. The following passage from the Supreme Court's opinion in *O'Riley v. Morse*, 56 U.S., (15 How) 62, 14 L.Ed 601 (1854) is appropriate here:

If this claim can be maintained, it matters not by what process or machinery the result is accomplished. For aught that we now know some future inventor, in the onward march of science, may discover a mode of writing or printing at a distance by means of the electric or galvanic current, without using any part of the process or combination set forth in a plaintiff's specification. His invention may be less complicated — less liable to get out of order — less expensive in construction, and in its operation. But yet if it is covered by this patent the inventor could not use it, nor the public have the benefit of it without the permission of this patentee.

It is well established that there must be a reasonable correlation between the scope of the exclusive right granted to a patent applicant and the scope of enablement set forth in the patent application. *In re Fisher*, 427 F.2d 833, 839, 166 USPQ 18, 24 (CCPA 1970). On the facts before us, we are in full agreement with the examiner that the scope of the exclusive right sought by appellants is far in excess of that warranted by the scope of enablement set forth in the specification.

We consider next the examiner's rejection of claims 1, 3 through 8, 12, 14 and 18 under 35 U.S.C. § 112, first paragraph, on the ground that the subject matter now claimed is not described in the specification as filed. This is a "new matter" rejection.

During prosecution appellants advised the examiner that the DNA coding sequence set forth in the specification and drawings was erroneous. It appears that appellants' original sequencing of the DNA contained three errors at nucleotide positions +128, +185 and +196, the latter two errors concerned

9). At page 10 thereof it is stated that applicants' cloning procedure is directed toward identifying clones expressing proteins having a "particular biological activity" and that the claims are phrased in terms of such biological activity rather than a particular DNA sequence *per se*. At page 9 of the same response, it is stated that one skilled in the art would be enabled to isolate a DNA sequence which encodes a protein exhibiting a molecular weight of between about 8 and about 14 kilodaltons wherein the protein exhibits a BCGF biological activity. The scope of such proteins is intended to encompass any of the "multiple BCGF species" which had not been isolated at that time.

³ The broad scope of appellants' claims is evidenced by certain statements made in the response submitted January 9, 1990 (Paper No.

the presence of "C" and "A" residues, respectively, which should have been deleted. The presence or absence of a nucleotide in a sequence shifts the reading frame such that the amino acid content of the protein differs dramatically. Appellants also noted that the errors resulted in a frame shift in the predicted N-terminal portion of the BCGF amino acid sequence thus changing the identity of all N-terminal residues up to the point of the third error. Thus, rather than the BCGF N-terminus beginning at the ATG (MET codon) at nucleotide positions +76 to +78, it now begins at the ATG start codon at positions +86 to +88.⁴

We have carefully considered the declaration of Surendra Sharma identified as Exhibit H and all of the arguments set forth in appellants' Brief and Reply Brief. Nevertheless, we are unpersuaded of error in the examiner's rejection and, accordingly, we affirm the rejection.

The examiner has criticized the Sharma declaration for a number of reasons specifically set forth on pages 8 and 9 of the Answer. As best we understand the examiner's position, the declaration is considered deficient because it (1) does not indicate that the plasmid newly sequenced is from the cells actually deposited in the ATCC, (2) does not indicate the protocols used in the original and re-sequencing experiments, and (3) does not adequately explain the changes in the protein sequence, especially the start position for the protein.⁵ Appellants' Brief and Reply Brief do not explain the lack of specific information.

It appears to be recognized in the art that single amino acid substitutions usually do not significantly alter the biological activity of proteins. The textbooks indicate that generally amino acid replacements in many parts of a polypeptide chain may be made without seriously modifying the activity of the polypeptide. See, e.g., Watson et al., *Molecular Biology of the Gene* (1987), pages 226-227. As noted by the examiner, however, it is also recognized that additions or deletions of nucleotides in a DNA sequence can have drastic consequences be-

cause the addition or deletion affects the reading frame such that the amino acid sequence of the protein coded by the DNA is drastically altered. Watson, et al., *supra*, pages 228-229.⁶

[2] We recognize that errors may well arise in the sequencing of DNA and that a mechanism for correcting such errors in the Patent and Trademark Office is highly desirable. Appellants have urged this Board to establish general rules and guidelines to be followed. Unfortunately, no general rule can be established because the question of whether or not a change in the chemical structure of a DNA sequence set forth in the specification is permitted depends on the facts of each case and the significance of the modification to both the subject matter claimed, i.e., the invention, and the subject matter described in the specification.

Appellants urge that the specification "fully described and enables the claimed material" (Brief, page 8). Appellants note that *E. coli* cells bearing the recombinant plasmid pARJ43 were deposited with the American Type Culture Collection and assigned the ATCC accession number 67099. It is urged that *Ex parte Marsili*, 214 USPQ 904 (Bd.App. 1979) permits the correction of the structural formula of the protein because the claimed DNA material was described.⁷

We are cognizant of the position of this Board in *Ex parte Marsili*, *supra*. Nevertheless, we are of the opinion that the *Marsili* case may be distinguished on its facts. In *Marsili*, the invention involved a chemical compound and its method of preparation. Claims to the method of preparation had been allowed but claims to the compound were on appeal because *Marsili* had advised the PTO of an error in the structural formula of a single ring moiety of a complex compound and had modified the ring structure of the claims to eliminate the error. (The error was minor in nature reflecting the difference in an aromatic vs. non aromatic heterocyclic ring structure.) *Marsili* provided analytical data and literature references to support the propriety and scientific desirability of the changes. Indeed, the *Marsili* board noted that the original description of the compound in the specification included "sufficient characteristics to distinguish" the claimed com-

⁴ The relationship between the sequencing errors and the change in the N-terminus from the ATG MET codon at position +76 to position +88 has not been explained.

⁵ With regard to the start position for the protein, appellants' specification, page 25, lines 27 through 31, indicates the start sequence for the protein is at the zero point. The Sharma declaration, without explanation, places the N-terminal (start sequence) at position 82.

⁶ Copies of the Watson et al. pages are attached hereto.

⁷ Appellants are not specific regarding whether the specification or the deposit of the cell line constitutes the "description" of the claimed invention.

pound. The adding characterized but structural fo

The issue and any other of the claim disclosure is guish the cl than, 328 F. 1964).

Appellants major in nature by the art as quences on protein ded provided no the invention includes su guish the ir

A review reveals that the DNA sequence the biological for, its presence pARJ45, the ATCC in rough estimate the active pARJ45. that the DNA differed conducted true mature BCGF not purified by described the being produced by plasmid and appellants' Reply are numerous BCGF claims do rather, in amino acid appellants' description of the material molecule describe the appellants in

Appellants limited to one of the contain DNA BCGF accession number 67099 which were cells. The "description" matter sequence amino acid

pound. There was no question of *Marsili's* adding characteristics not previously mentioned but only a question of error in a structural formula.

The issue that must be broached in this and any other case is whether the description of the claimed compound in the original disclosure is adequate to identify and distinguish the claimed subject matter. *In re Nathan*, 328 F.2d 1005, 140 USPQ 601 (CCPA 1964).

Appellants' change, unlike *Marsili's*, is major in nature and of the type recognized by the art as having potentially drastic consequences on the properties of the DNA and protein deduced therefrom. Appellants have provided no evidence that the description of the invention set forth in the specification includes sufficient characteristics to distinguish the invention set forth in the claims.

A review of appellants' specification reveals that there is little or no description of the DNA sequence of the claims other than the biological activity of the protein it codes for, its presence in the plasmids pARJ43 and pARJ45, the former being on deposit in the ATCC in the form of *E. coli* cells, and a rough estimate of the molecular weights of the active DNAs spliced into pARJ43 and pARJ45. Appellants' specification admits that the DNA of the pARJ43 and pARJ45 differed considerably and that each produced truncated proteins as compared to mature BCGF. Importantly, appellants did not purify and sequence the protein produced by the cloned plasmids and have described the protein only by its capability of being produced by *E. coli* containing the plasmid and by its biological activity. Appellants' Reply Brief, page 7, admits that "there are numerous molecules known to have BCGF activity (even TCGF)." Appellants' claims do not describe the DNA directly but, rather, in terms of the protein and/or its amino acid sequence. As we view it, appellants' description of the protein solely in terms of its biological function, and approximate molecular weight, is insufficient to describe the protein and, thereby, place appellants in "possession" thereof.

Appellants' deposit in the ATCC was limited to a single cell line containing only one of the two plasmids (vectors) said to contain DNA coding for a protein exhibiting BCGF activity. At best, appellants' specification may be said to "describe" the deposited 67099 cell line and the plasmid pARJ43 which was incorporated in the deposited cells. The specification can not be said to "describe" the protein or the *broad* subject matter set forth in claims 1 and 5 because the amino acid sequence set forth as a descrip-

tive parameter in the original specification was erroneously deduced and the protein was not purified and/or isolated. In other words, the specification does not "convey with reasonable clarity to those skilled in the art that, as of the filing date . . . [appellants were] . . . in possession of the invention," i.e., "whatever is now claimed." See *Vas-Cath, Inc. v. Mahurkar*, 935 F.2d 1555, 19 USPQ2d 1111, 1117 (Fed. Cir. 1991).

We consider next the examiner's rejection of claims 1, 3 through 8, 12, 14 and 18 under 35 U.S.C. § 102(a) or, alternatively, under 35 U.S.C. § 103 over Okano. We affirm the rejection.

Appellants strongly urge that Okano's work was directed to a different BCGF molecule than that claimed herein. We are unpersuaded by this argument for two reasons. First, appellants do not claim a BCGF molecule of any sort. Rather, appellants claim a DNA which produces a protein which exhibits a certain molecular weight, and has certain biological activity. Moreover, appellants' claims extend to "biologically functional equivalents thereof." We have carefully reviewed the Okano reference and find nothing therein which reveals that the BCGF gene developed by Okano differs at all from that claimed herein even if one were to exclude the "biological equivalents" language of the claims. Okano's process of producing the DNA is virtually the same as that utilized by appellants. Okano isolated a mRNA fraction and utilizing reverse transcriptase produced a cDNA library that corresponds to BCGF mRNA. Okano teaches that the preferred mRNA fraction is that which corresponds to a molecular weight between the precipitation constants 15s and 21s in sucrose density gradient centrifugation. Appellants utilized a fraction having a molecular weight corresponding to 16s-18s which is approximately the same fraction preferred by Okano. Okano prepared a recombinant DNA and inserted the DNA into vector host microorganisms. The mRNA utilized tested positively by the same assay utilized by appellants (see page 9 of the translation). There is no reason to believe that the cDNA synthesized from the mRNA would not correspond to the claimed DNA and produce the necessary protein when inserted into an appropriate vector. We are in complete agreement with the examiner that the DNA produced by Okano either anticipates or makes obvious the subject matter claimed herein.

[3] When an examiner obtains a product which reasonably appears to fall within the scope of that which is claimed by a patent applicant, it is reasonable to shift the burden

to the applicant to provide evidence showing that the product of the prior art does not fall within the scope of applicants' claims. See *In re Swinehart*, 439 F.2d 210, 169 USPQ 226 (CCPA 1971); *In re Best*, 562 F.2d 1252, 195 USPQ 430 (CCPA 1977) and *In re Fitzgerald*, 619 F.2d 67, 205 USPQ 594 (CCPA 1980).

We consider next the examiner's rejection of claims 1, 3 through 8, 12, 14 and 18 under 35 U.S.C. § 103 over each of Clark and Freeman, each in view of Beaucage and Maizel.

[4] It is the examiner's position that BCGF is described as a protein useful in bolstering the immune response and the knowledge of the existence of this protein would have motivated one of skill in the art to utilize recombinant DNA protocols to (1) isolate the protein, (2) sequence the protein, (3) construct synthetic DNA probes from the proteins, (4) utilize the probes to isolate messenger RNA, (5) synthesize a cDNA, and (6) produce additional protein. We reverse the rejection.

The examiner's position reflects the "obviousness to try" approach of the "armchair" chemist. As noted by appellants there is nothing in the references which indicates that BCGF is a protein, ordinarily produced in such great amounts that one skilled in the art would have no trouble isolating and sequencing the protein. In the absence of being able to isolate substantial quantities of the protein to purity, it would be virtually impossible to produce probes insofar as sequencing the proteins would be disrupted by the presence of significant portions of other proteins. Appellants' specification indicates that the BCGF protein had not been isolated to sufficient purity and sufficient quantity for confirmation of its identity as of the time the application was filed. The examiner has not taken issue with this position and none of the references cited by the examiner reveals the sequence of the protein. Appellants' specification also reveals (pages 12 through 14) that the kinetics of accumulation of BCGF activity is such that a maximum yield occurs from 48 to 72 hours of culture and that a special procedure had to be developed to separate BCGF from TCGF. We are in complete agreement with appellants that the protocol set forth by the examiner would not have been enabling to one of skill in the art and, accordingly, we reverse the rejection.

The examiner's rejections of the claims under 35 U.S.C. § 112, first paragraph, for new matter and lack of enablement are affirmed. The examiner's rejection of the claims under 35 U.S.C. §§ 102/103 over Okano is also affirmed. The examiner's re-

jection of the claim under 35 U.S.C. § 103 over Clark et al. is reversed.

Our review of this specification reveals that there is no statement of utility for the BCGF protein and no indication in the specification of "how to use" the BCGF protein which is produced by the recombinant DNA vectors and cell lines of the claims. Appellants' specification clearly states that as of its filing date, the actual function of BCGF protein was unknown (specification, page 3, lines 19 through 28). Should this application be prosecuted further we urge the examiner to specifically consider whether or not the application complies with the utility requirements of 35 U.S.C. § 112 and to note his or her consideration on the record. In this regard, *In re Hafner*, 410 F.2d 1403, 161 USPQ 783 (CCPA 1969), may be of interest insofar as some later dated publications of appellants and others may constitute prior art if the examiner were to hold the application originally filed by the appellants did not comply with the utility requirements of 35 U.S.C. § 112.

No time period for taking any subsequent action in connection with this appeal may be extended under 37 CFR 1.136(a). See the final rule notice, 54 F.R. 29548 (July 13, 1989), 1105 O.G. 5 (August 1, 1989).

AFFIRMED

**ON REQUEST FOR
RECONSIDERATION
October 19, 1992**

Appellants request reconsideration of our decision mailed May 27, 1992, in particular that portion of our decision in which we affirmed the examiner's rejection of claims 1, 3 through 8, 12, 14 and 18 under 35 U.S.C. § 112 as being directed to subject matter not described in the specification as filed, i.e., the "new matter" rejection.

We have carefully considered all the arguments set forth in appellants' request but are unpersuaded of error in our decision and decline to modify the decision.

Appellants assert that because the specification (including the ATCC deposit) is *enabling* for pARJ43, the specification inherently enables the sequence contained on pARJ43 and, accordingly, satisfies the *description* requirement for the claimed subject matter.

We are unpersuaded by this line of argument for two reasons. First, though often intertwined, enablement and description are separate and distinct requirements of 35

U.S.C. § 112. Note the following comment of the court in *Vas-Cath Inc. v. Mahurkar*, 935 F.2d 1555, 1563, 19 USPQ2d 1111, 1117 (Fed. Cir. 1991):

... we hereby reaffirm, that 35 U.S.C. 112, first paragraph, requires a 'written description of the invention' which is separate and distinct from the enablement requirement. The purpose of the 'written description' requirement is broader than to merely explain how to 'make and use'; the applicant must also convey with reasonable clarity to those skilled in the art that, as of the filing date sought, he or she was in possession of the invention. The invention is, for purposes of the 'written description' inquiry, *whatever is now claimed* (citations omitted).

Second, the invention claimed herein is not the specific plasmid pARJ43 but, rather, a generic invention directed to DNA which produces either a protein molecule of specified amino acid sequence or, importantly, a biological equivalent of that protein.

We discuss first the effect of appellants' ATC deposit on the description requirement.

Appellants assert that they have satisfied the description requirement of 35 U.S.C. § 112 by depositing the pARJ43 plasmid in the American Type Culture Collection. This is not necessarily the case.

[5] We recognize that a patent applicant's deposit of a biological material in a public depository effectively incorporates the deposited material, by reference, into the patent application. It is analogous to a cross-reference to an earlier filed patent application for a description of the preparation of a starting material. See *Ex parte Schmidt-Kastner*, 153 USPQ 473 (Bd.App. 1963). In this case, however, the deposit does not satisfy the description requirement for either the BCGF type DNA being claimed or the protein produced thereby because there is no evidence of record that those skilled in the art having the deposited material would have been aware of the BCGF DNA structure and the protein encoded thereby or would have been able to accurately determine said DNA structure and protein sequence without undue experimentation. Indeed, in this case the evidence is to the contrary because appellants who are skilled in the art were unable to accurately sequence the DNA and protein until subsequent to the filing date of the application.

As noted in our decision, the structures of DNA now claimed¹ and the protein pro-

duced thereby are not effectively described in the specification itself. Indeed, they are badly misdescribed. Stripped of accurate DNA and protein sequences, the description of DNA which remains in the specification is limited to molecular weight, biological activity and method of preparation. In this case it is insufficient.

In *Amgen Inc. v. Chugai Pharmaceutical Co.*, 927 F.2d 1200, 18 USPQ2d 1016 (1991), the Federal Circuit set forth practical guidelines for determining "conception." These guidelines are applicable to the specifications of patent applications directed to biological subject matter. The court stated:

A gene is a chemical compound, albeit a complex one, and it is well established in our law that conception of a chemical compound requires that the inventor be able to define it so as to distinguish it from other materials, and to describe how to obtain it. ... Conception does not occur unless one has a mental picture of the structure of the chemical, or is able to define it by its method of preparation, its physical or chemical properties, or whatever characteristics sufficiently distinguish it. *It is not sufficient to define it solely by its principal biological property, e.g., encoding human erythropoietin, because an alleged conception having no more specificity than that is simply a wish to know the identity of any material with that biological property.* (Emphasis added). 927 F.2d at 1206, 18 USPQ2d at 1021.

We note that in this case the molecular biological property of interest is not peculiar to BCGF proteins but is also possessed by TCGF proteins (specification, page 3). Moreover many proteins would have the same molecular weight. There remains only the method of making the plasmid as a mechanism for describing the DNA.

Appellants' specification does set forth a procedure for preparing plasmids containing cDNA capable of translating an active protein. However, the plasmids described by appellants did not contain full length inserts of the BCGF gene. Moreover, out of 700 clones which contained cDNA inserts only two, pARJ43 and pARJ45, included inserts which coded for a biologically active protein. These cDNA inserts differed considerably in

¹Both appellants and the examiner have treated the claims as if appellants' proposed amendments to Figure 4 have been entered. The

examiner's Final Rejection and Examiner's Answer both indicate the amendments have not been entered. In the interest of efficiency, we have treated the claims as if the amendment to the figures had been entered.

molecular size. Were one to reproduce the experiments set forth in the specification by appellants, there is no guarantee that plasmid pARJ43 would be reproduced. Accordingly, from a description viewpoint, appellants' specification with its misstated DNA sequence does not of itself include enough information to otherwise satisfy the description requirement.

We discuss next the scope of appellants' claims *vis-a-vis* the scope of the description in the specification.

As noted in our decision of May 27, 1992, all of appellants' claims are generic claims directed to recombinant vectors or cells comprising DNA sequences encoding for a specific protein as set forth in the figures or a "biologically functional equivalent thereof." Appellants' claims do not describe² the DNA by what it is (an assemblage of nucleotides) but by the protein it encodes for. Appellants did not directly sequence the protein encoded by the BCGF DNA but, rather, deduced the protein sequence from the structure of the missequenced DNA. The deduced sequence misidentified the protein. Importantly, absent an accurate description of the protein sequence, one cannot describe or envisage the "biological equivalents thereof." On this point we note that appellants' theory of conservative replacement of amino acids based on hydropathic index (specification, pages 26 and 27) is *in this case* mere verbiage because the basic amino acid sequence was misdescribed at the time this application was filed.

[6] Appellants may be of the view that no harm is done to the public when a badly missequenced DNA is properly sequenced prior to the issue date of the patent. This is not always the case. The "new matter" prohibition of section 112 plays an important role in establishing the filing date of an application as the *prima facie* date of invention. *In re Hawkins*, 486 F.2d 569, 179 USPQ 157 (CCPA 1973). On this point the *Hawkins* court quoted the concurring opinion in *In re Argoudelis*, 434 F.2d 1390, 1395, 168 USPQ 99, 104 (CCPA 1970) as follows:

[I]t is essential that there be no question that, at the time an application for patent is filed, the invention claimed therein is fully capable of being reduced to practice

(i.e., that no technological problems, the resolution of which would require more than ordinary skill and reasonable time, remain in order to obtain an operative, useful embodiment).

Surely at the time of filing the instant application one of skill in the art, lacking a description of the amino acid structure of the protein, would have been unable to envisage and/or reduce to practice any "biologically functional" equivalent of the protein or the DNA coding for the equivalent. Accordingly, from a "scope of claim" viewpoint, appellants' description of the invention at the time of filing the instant application, fell far short of what is now claimed.

It would appear that appellants did not comply with the patent statutes and filed the instant application prematurely, without adequate descriptive support. The patent laws do not permit insertion of additional descriptive matter subsequent to an applicant's filing date in order to complete its disclosure so as to conform the specification's description of the invention to the statutory standard.

Appellants urge that the examiner and this board have accused the Sharma declaration of being "untruthful." This is not the case. We have again reviewed the examiner's discussion of the Sharma declaration, which discussion appears on pages 8 through 10 of the Answer. We are in agreement with the examiner's positions and comments as set forth therein. The examiner's questions regarding how the error was discovered and how the resequencing was accomplished appear to reflect a desire to know whether the error would have been readily and easily detected by one skilled in the art. With regard to the source of the sample of pARJ43 which was resequenced, the examiner rightly appears to be taking the position that a chain of evidence has been broken. Appellants' only description of the DNA set forth in Figure 4 is the material on deposit in the ATCC depository. Accordingly, proof of the accurate DNA sequence should include resequencing of either the material on deposit or a laboratory colony of pARJ43 material proven to be identical to that which was deposited in the ATCC.

We remain somewhat confused by appellants' explanation of the zero point and the discussion of the errors in DNA sequencing and their effect on the protein structure as set forth in paragraph 5 of the Sharma Declaration. As we read appellants' specification, everything after the zero point of Figure 4 constitutes BCGF DNA sequences whereas everything which precedes the zero point constitutes the B-galactosidase struc-

²We recognize that appellants take issue with our indicating that the claims define the DNA by "describing" the DNA in terms of the protein it codes for. Similar language was apparently considered appropriate and utilized by the court in *In re Johnson*, 558 F.2d 1008, 194 USPQ 187, 194 (CCPA 1977). We consider it appropriate here

tural gene. There is nothing in appellants' original specification which describes the first amino acid of BCGF as being encoded by the codon starting at position +1 to +79 or at +82. Additionally, there is nothing in the specification which describes the amino acid sequence from +1 to +79 as corresponding to a "quite apparent" leader sequence of the BCGF molecule as now alleged by appellants (Request, page 8). Indeed, appellants' specification, page 24, unequivocally states that "there is no leader sequence" in the vectors pARJ43 and pARJ45. Moreover, because it is known that proteins are synthesized in the amino-to-carboxyl direction (left to right in Fig. 4), we are unable to understand Sharma's comments that deletion "frame shifting" at codons +185 and +196 caused the BCGF N-terminus codon (which is "left" of the 185 codon) to shift from +76 to +86.

Appellants' request for reconsideration is granted to the extent we have reconsidered and clarified our decision but is denied to the extent it seeks modification thereof.

DENIED.

Court of Appeals, Federal Circuit

BIC Leisure Products Inc. v. Windsurfing International Inc.

Nos. 92-1106, -1107

Decided August 4, 1993

REMEDIES

1. Monetary — Damages — Patents — In general (§510.0507.01)

Amount of damages to be awarded for patent infringement is question of fact on which patent owner bears burden of proof; amount of damages fixed by federal district court is reviewed on appeal under clearly erroneous standard of Fed.R.Civ.P. 52(a).

2. Monetary — Damages — Patents — Lost profits (§510.0507.05)

Federal district court erred by awarding plaintiff lost profits for infringement of its sailboard patent equal to plaintiff's pro rata market share of defendant's sales, since at least 14 manufacturers competed in market, since plaintiff's sailboards sold for 60-80 percent more than defendant's boards, since defendant's customers demonstrated preference for sailboards of different design at lower end of price spectrum and would likely have sought boards in same price range had

defendant been absent from market, since plaintiff's sales continued to decline after district court enjoined defendant's infringement, and since plaintiff therefore failed to show with reasonable probability that defendant's customers would have purchased from plaintiff in proportion to plaintiff's market share if defendant's boards had been unavailable.

3. Monetary — Damages — Patents — Lost profits (§510.0507.05)

Test for lost profits set out in *Panduit Corp. v. Stahl Brothers Fibre Works Inc.*, 197 USPQ 726, operates under inherent assumption that patent owner and infringer sell products sufficiently similar to compete against each other in same market segment; if patentee's and infringer's products are not substitutes in competitive market, then first two factors of that test—demand for patented product and absence of acceptable, non-infringing alternatives—do not meet "but for" prerequisite for lost profits.

4. Monetary — Damages — Patents — Lost profits (§510.0507.05)

Federal district court properly found that evidence was too speculative to support award of lost profits due to price erosion, since record shows that other, newer sailboard designs replaced that of plaintiff's boards as choice of many buyers, since plaintiff licensed its sailboard patent to many competitors who produced boards at lower cost, and since plaintiff therefore lowered its prices in response to market forces other than defendant's infringement.

PATENTS

5. Infringement — Defenses — In general (§120.1101)

Patent infringement defendant properly raised defense of absolute intervening rights at damages stage of trial, since defense addresses question of which sales of infringing products properly serve as measure of damages, and thus did not become issue until plaintiff secured liability judgment; evidence of such defense was properly admitted under Fed.R.Civ.P. 15(b), even though defendant did not raise such defense in pleadings, nor was consideration of defense precluded by prior decision in litigation which involved defendant's waiver of equitable intervening rights defense to injunction